



FIGHTING VEHICLE ARMOR AND

ANTIARMOR MUNITIONS

April 2023



PREPARED BY:
Graham F. Silsby
Dr. Andrew Dietrich

DISTRIBUTION STATEMENT A
Approved for public release:
distribution unlimited.

REPORT DOCUMENTATION PAGE

Form Approved
OMB No. 0704-0188

Public reporting burden for this collection of information is estimated to average 1 hour per response, including the time for reviewing instructions, searching existing data sources, gathering and maintaining the data needed, and completing and reviewing this collection of information. Send comments regarding this burden estimate or any other aspect of this collection of information, including suggestions for reducing this burden to Department of Defense, Washington Headquarters Services, Directorate for Information Operations and Reports (0704-0188), 1215 Jefferson Davis Highway, Suite 1204, Arlington, VA 22202-4302. Respondents should be aware that notwithstanding any other provision of law, no person shall be subject to any penalty for failing to comply with a collection of information if it does not display a currently valid OMB control number.

PLEASE DO NOT RETURN YOUR FORM TO THE ABOVE ADDRESS.

1. REPORT DATE (DD-MM-YYYY) February 2021		2. REPORT TYPE Technical Monograph		3. DATES COVERED (From - To)	
4. TITLE AND SUBTITLE Fighting Vehicle Armor and Antiarmor Munitions				5a. CONTRACT NUMBER FA8075-14-D-0001	
				5b. GRANT NUMBER	
				5c. PROGRAM ELEMENT NUMBER	
6. AUTHOR(S) Graham Silsby and Dr. Andrew Dietrich				5d. PROJECT NUMBER	
				5e. TASK NUMBER	
				5f. WORK UNIT NUMBER	
7. PERFORMING ORGANIZATION NAME(S) AND ADDRESS(ES) AND ADDRESS(ES) Defense Systems Information Analysis Center (DSIAC) SURVICE Engineering Company 4695 Millennium Drive Belcamp, MD 21017-1505				8. PERFORMING ORGANIZATION REPORT NUMBER	
9. SPONSORING / MONITORING AGENCY NAME(S) AND ADDRESS(ES) Defense Technical Information Center (DTIC) 8725 John J. Kingman Rd. Ft. Belvoir, VA 22060-6218				10. SPONSOR/MONITOR'S ACRONYM(S)	
				11. SPONSOR/MONITOR'S REPORT	
12. DISTRIBUTION / AVAILABILITY STATEMENT Distribution A: Approved for public release; distribution is unlimited.					
13. SUPPLEMENTARY NOTES					
14. ABSTRACT This monograph examines the mechanics and physics behind current vehicular armor technologies and the threat munitions they face, to the extent that the technology is unclassified and widely disseminated. The discussion begins with fundamentals and then delves more deeply into details. In the early days of antiarmor munitions, the kinetic energy of hardened metal projectiles caused them to push through tough steel armor plate. The first advancement was the higher-velocity, subcaliber penetrator in the so-called hypervelocity armor-piercing shot design. Its decreased-diameter, higher-density penetrator core and higher striking velocity resulted in higher impact pressures and evolved into the long rod penetrator. Increased striking velocities increased their depth of penetration and, as in the shaped-charge jet, erosion of the penetrator became the norm. At the same time, weight-efficient spaced armors and then reactive armors were developed. Separately, the highly lethal shaped charge and other lined-cavity charge warhead designs evolved, particularly the explosively formed penetrator and the hemispherical liner geometry. These advances were made easier by the development of the Gurney and the Taylor models of metal-explosive sandwich behavior, which also drove advances in fragmenting warhead design. The important safety issues involved with working with energetic materials are also discussed as are the recommended qualifications of personnel who work with these materials. Finally, a historical overview of fighting vehicle armor and antiarmor technology is included as an appendix.					
15. SUBJECT TERMS armor, antiarmor munition, kinetic energy penetration, KE penetration, shaped charge, armor obliquity, vehicle armor, log rod penetrator, armor material, fragmenting warhead, yaw					
16. SECURITY CLASSIFICATION OF: U			17. LIMITATION OF ABSTRACT U	18. NUMBER OF PAGES 160	19a. NAME OF RESPONSIBLE PERSON Ted Welsh, DSIAC Director
a. REPORT U	b. ABSTRACT U	c. THIS PAGE U			19b. TELEPHONE NUMBER (include area code) 443-360-4600
Standard Form 298 (Rev. 8-98) Prescribed by ANSI Std. Z39.18			ON THE COVER A M2 Bradley Fighting Vehicle (U.S. Army photo by Spc. Zachary Bouvier)		

ABSTRACT

This monograph examines the mechanics and physics behind current vehicular armor technologies and the threat munitions they face, to the extent that the technology is unclassified and widely disseminated. The subject is examined from a number of perspectives. It begins with fundamentals and then delves more deeply into details.

In the early days of antiarmor munitions, the kinetic energy of hardened metal projectiles caused them to push through tough steel armor plate. The first advancement was the higher-velocity, subcaliber penetrator in the so-called hypervelocity armor-piercing shot design. Its decreased-diameter, higher-density penetrator core and higher striking velocity resulted in higher impact pressures and evolved into the long rod penetrator. Increased striking velocities increased their depth of penetration and, as in the shaped-charge jet, erosion of the penetrator became the norm. At the same time, weight-efficient spaced armors and then reactive armors were developed.

Separately, the highly lethal shaped charge and other lined-cavity charge warhead designs evolved, particularly the explosively formed penetrator and the hemispherical liner geometry. These advances were made easier by the development of the Gurney and the Taylor models of metal-explosive sandwich behavior, which also drove advances in fragmenting warhead design.

The important safety issues involved with working with energetic materials are also discussed as are the recommended qualifications of personnel who work with these materials. Finally, a historical overview of fighting vehicle armor and antiarmor technology is included as an appendix.

FOREWORD

When I started my career as an eager, young engineer at the U.S. Army Ballistic Research Laboratory (BRL) in 1985, I did not arrive with a background in penetration mechanics and terminal ballistics from my college coursework. I therefore relied heavily on the advice and guidance of the folks who were already experienced in the ballistics field.

Graham Silsby and Drew Dietrich were already well-established fixtures at BRL when I arrived. Their careers began in the 1960s during the Vietnam War and extended through the first Gulf War and into the early 21st century. These were times of rapid evolution and innovation in armor and antiarmor technology, and both of these men were at the forefront of these changes. New and improved armor materials were becoming available in conjunction with increased understanding of mechanisms and advancements in modeling and simulation.

Drew Dietrich was the respected chief of the Impact Physics Branch and had an extensive background in chemical energy munitions (shaped charges and explosively formed penetrators). In this role, he guided much of the evolution of these technologies at the BRL. Despite his leadership duties, Drew would always make time to help a ballistics neophyte with questions and **concerns. If he didn't know the answer, he always knew who did.** His attitude percolated down to all of his employees in that branch, which made collaborative work a pleasure.

Graham Silsby was an accomplished terminal ballisticians in the Penetration Mechanics Branch when I met him. While I was approaching a technical issue from the armor side, he was approaching it from the antiarmor side, and this different perspective was often very instructive. He was always willing to answer questions, provide advice, and take the time to thoroughly discuss any issue with a

new employee. In the early 1990s, I had the privilege of working with him in developing a smoothbore, high-velocity, 40mm laboratory gun system, which is still in use at several experimental facilities at the BRL and at sister labs.

Over the years, as BRL morphed into the U.S. Army Research Laboratory, Drew and Graham were always there to lend an ear and provide useful advice to me, other researchers, and Army leadership. This monograph captures a great deal of their sage instruction in a handy, printed reference. This collection of fundamental concepts (along with citations and bibliography) provides a good, single introductory source to assist the next generation of ballistics researchers in learning their trade.

Matthew Burkins

*Leader of the Tactical Systems Protection Team
Armor Branch, Terminal Effects Division
Weapons and Materials Research Directorate
U.S. Army Research Laboratory
(Retired January 2018)*

PREFACE

This monograph is published under the auspices of the Defense Systems Information Analysis Center (DSIAC). DSIAC is a Department of Defense (DoD) Information Analysis Center (IAC) operated by the SURVICE Engineering Company and a team of subcontractors under Contract FA8075-D-14-001. The center was established on 1 January 2014 and is the consolidation of six legacy DoD IACs: AMMTIAC, CPIAC, RIAC, SENSIAC, SURVIAC, and WSTIAC. The DoD IAC Enterprise is a component of the DoD's Scientific and Technical Information Program (STIP) prescribed by DoD Manual 3200.14. Government oversight of DSIAC is provided by the IAC Program Management Office, DTIC-I, 8725 John J. Kingman Road, Suite 0944, Fort Belvoir, VA, 22060-6218, and an appointed Contracting Officer's Representative (COR) and **Assistant Contracting Officer's Representative** (ACOR). All questions and comments regarding the content of this monograph may be directed to the following:

SURVICE Engineering Company
Aberdeen Area Operation
ATTN: Mr. Brian Benesch
4695 Millennium Drive
Belcamp, MD 21017-1505
410-273-7722
brian.benesch@survice.com

A Technical Monograph is a one-volume work of research or literature on a single subject that is intended to capture unique (and potentially perishable) technical information, insights, and experiences from senior-level personnel and make them available to other community practitioners for personnel/community development, technical training, and/or information archiving. As such, Technical Monographs are often broader in scope and applicability, more detailed in content, and/or more closely reviewed/refereed than typical technical reports.

ABOUT THIS MONOGRAPH

This monograph presents the physics of the interaction of antiarmor munitions and their target, fighting vehicle armor. The first armor was intended to protect against small-arms bullets, and of necessity, antiarmor munitions were then introduced. Both armor and antiarmor munitions continue to evolve apace. There are two types of antiarmor munitions: kinetic-energy (KE) penetrators, intended to push through armor by virtue of their KE, and explosive warheads, the most significant of which in terms of heavy fighting vehicle armor is the shaped-charge warhead.

This work is necessarily based on the authors' perspectives, both life-long researchers in their respective areas of KE and shaped-charge penetration and the respective heavy armors. It starts aimed at the beginner and ends at the journeyman's level.

In this material, you will not learn about the performance of specific ammunition but rather the process of armor penetration, so as to be able to improve your ability to design and to analyze the performance of antiarmor munitions and to understand how vehicles are armored against them. The material presented here is primarily from observation rather than theory, and practical and factual rather than speculative, so it should complement whatever background you have. After reading this material, a technician involved in testing should be able to tell if the shot went as expected. The engineer should be able to predict gross results in advance and draw reasonably sound inferences from the signature that a penetrator leaves on a target. Using penetration versus velocity data gleaned from the literature or developed in-house and the simple assumptions discussed, the analyst or program manager should be able to tell if particular performance claims are realistic. To avoid confusing the reader, where possible, figures are shown such that the motion of the projectile is from left to right, a commonly accepted convention in ballistics.

This monograph will not address weapons of mass destruction on the mega scale or the terminal ballistics of small-arms projectiles on the mini scale. The performance of the latter seems to be closely linked to the exact design of each model of ammunition, as well as the gun from which it is fired, the target impacted, and other complicating factors. In particular, the very complex topics of wound ballistics and protection against small arms will not be addressed.

The KE penetrator material in this monograph expands on three editions of Mr. Silsby's self-published monograph, *Penetration Mechanics of Anti-Armor Kinetic Energy Penetrators*, © 1987, 2004, and 2010 [1] used as a hand-out in lectures on the subject, primarily for Baldini Resource Associates, and on material prepared as handouts for a course on armored fighting vehicles presented in 2007. The material on KE penetration was derived from extensive experience in the field. The shaped-charge discussion is from Dr. Dietrich's Baldini Resource Associates lecture material [2], presented over roughly the same time span as Mr. Silsby's lectures, on the effects of jets from lined-cavity charges, the design of shaped-charge warheads, and on survivability and lethality modeling.

DEVELOPMENT OF ANTIARMOR MUNITIONS

An unattributed "In Brief" summary of an article entitled "The Most Invasive Species of All," by Curtis W. Marean in *Scientific American* (2015) is telling.

Of all the human species that have lived on earth, only *Homo sapiens* managed to colonize the entire globe. Scientists have long puzzled over how our species alone managed to disperse so far and wide. A new hypothesis holds that two innovations unique to *H. sapiens* primed it for world domination: a genetically determined

propensity for cooperation with unrelated individuals and advanced projectile weapons [3].

This monograph addresses a subclass of the latter subject.

It is a sad state of affairs that in the approximately 300,000 years since *H. sapiens* diverged from earlier ancestors (already adept at hafting a worked stone point to a wooden spear shaft) [4], we are now capable of the complete destruction of our species. Regardless of how peace-loving a people may be, faced with a seemingly uninterrupted chain of adversaries intent on dominating others by force, it is necessary to study war. We use the scientific method to uncover more and more knowledge, and then apply it to build automatic weapons, mount multiple, independently targeted thermonuclear warheads on a single ballistic missile, produce 70-ton tanks with a succeeding design under contemplation, and design hand-held, tank-destroying weapons that can be made with simple tools.

Over the recent decades, the nature of the threat to the United States has evolved from a global war against determined conventional forces to a prolonged series of wars against a number of loosely affiliated insurgents. The M1 main battle tank as a shock weapon had proven quite superior to the opposing tank forces which we encountered through the Korean War but is useless per se in taking and holding ground against insurgent forces. The focus on armored vehicle design has shifted to protection against ambush with antiarmor, rocket-propelled grenades and improvised explosive devices employed as buried and off-road mines. The last of the individuals involved in the introduction of the M1 tank and its ammunition and their subsequent improvements, including the authors, are retiring, often for the second or third time, hence this monograph.

Most antiarmor munitions defeat the target by perforation, so much of this work involves penetration mechanics. However, the mechanics of moving metal with high explosives is also important to understanding how fragments are thrown from a high-explosive warhead, how the shaped-charge's liner is collapsed and spit out as a very high-velocity coherent jet, and how to increase the effectiveness of individual armor plates by throwing them with explosives in explosive reactive armor.

There is no magic material just waiting to be discovered that will "bust through anything." Unlike exterior ballistics, terminal ballistics is a very messy discipline. The three approaches to advancing the understanding of terminal ballistics are analytical modeling, computational modeling, and experimentation. The subject of terminal ballistics is sorely lacking in physics-based models with simple equations that can be used to predict behavior. The few existing models will be discussed. Computational modeling is now quite sophisticated and provides solid insights into behavior. Unfortunately, we are not in a position to provide useful insight into current computational abilities in ballistics. This would be a very good subject for a review article or a monograph by someone skilled in that art. Still, experimentation is always needed to verify computational results and to surface unexpected behaviors.

The knowledge that allows understanding and exploitation of a new technology comes in three stages, which is a process that is often continued in a design spiral. First, the effect is observed or inferred from current knowledge. Second, a period of detailed analysis and experimentation then leads to understanding the physics and mechanics involved. Third, this knowledge is then exploited in sophisticated designs that maximize the performance of the hardware. In this phase, a good grasp of solid mechanics becomes necessary.

An example of this knowledge development is shaped-charge technology, as related by Walters in 1991 [5]. Von Forester in Germany in 1883 and Munroe in the U.S. in 1888 observed that when an explosive charge was detonated in contact with a heavy metal plate, a cavity in that charge produced a distinct additional depth of the depression made on the target material. Once this phenomenon was discovered, the study of it spread, people wondered what the cause was, and in the process discovered that an inert liner on the hollow cavity greatly enhanced the effect. This effect was used to defeat armor in WWII even without a clear understanding of the physics. Improvements in instrumentation in the form of flash x-rays (flash radiography), more precise instrumentation, clever experimental design, and computational modeling resulted in great advances in understanding, and finally, various people worked out the physics. The resulting mathematical models were then exploited to gain significant increases in performance from existing launch platforms.

In interpreting the results of both computational and experimental work, keep in mind that everything is constrained by physical law, particularly conservation of mass, momentum, and energy; Newton's laws of motion; and the complex relationship between stress and strain in elastic and plastic deformation and fracture. Mechanical deformation processes such as those found in forging, metal forming, and machining can be observed. Results vary in smooth and continuous ways with changes in striking conditions. While sometimes a sudden change in behavior is noted, it is usually a result of changes to a variable unknown to the experimenter, or of changes to the process crossing from one regime into another. Typical of the latter would be rod deceleration during penetration halting erosion under some conditions, but not under others. Even fracture-related phenomena are remarkably repeatable.

Ultimately, the terminal ballisticians will need to be well-versed in a number of topics. I highly recommend

reading a current textbook on materials and manufacturing practices, getting as much hands-on experience as possible with machining and machine tools, and keeping up with advances in materials and fabrication. Take the ASM International short course titled Elements of Metallurgy or Metallurgy for the Non-Metallurgist™ (Trademark, ASM International – The Materials Information Society). This is a serious, week-long, short course with exams and a certificate at the end that you can be proud of. It is also offered as an on-line course and a self-paced course. If you are a mechanical engineer and did not take a course in solid mechanics, consider taking one as part of your continuing education. Also, the civil engineering courses of structural analysis and structural design provide a deep understanding of stress and strain, while the portions on reinforced concrete are applicable to any composite design. A course on fatigue and fracture mechanics is also highly recommended. Understand the difference between commercial and specialty materials and how specifications and standards are written and interpreted.

THE AUTHORS

After long careers there, Mr. Graham Silsby and Dr. Andrew Dietrich both retired from the U.S. Army Research Laboratory's (ARL's) Weapons and Materials Research Directorate (WMRD), the successor in business to the U.S. Army Ballistic Research Laboratory (BRL), at Aberdeen Proving Ground (APG), Maryland.

Mr. Silsby, the primary author, has both a BSME specializing in engineering science and a BSCE specializing in structures. He retired from ARL in 2005 as a senior research mechanical engineer. He was then employed part time in a similar capacity at SURVICE Engineering Company, Belcamp, MD, retiring again in December of 2017. SURVICE was founded in 1981 to provide expertise in survivability and lethality modeling and assessment and has expanded to provide a broad range of engineering services to both the military and civilian sectors.

Mr. Silsby has over 40 years' experience in research and development engineering, the last 35 of which were spent in penetration mechanics work first in the ARL's Armor Branch and then ARL's Lethal Mechanisms Branch, Terminal Ballistics Division. One of the main focuses of the work over that time span was the development and improvement of the armor on the M1 tank and the Bradley fighting vehicle, as well as improvement of their antiarmor ammunition. Mr. Silsby has an experimental rather than theoretical inclination and enjoys design and development of unique items.

He has extensive firing-range experience, both at large-caliber and at reduced scale. Most of his experimental firings have been done using smoothbore laboratory powder guns for ordnance velocity work (1–2 km/s or 3,000–6,000 ft/s). The reduced-scale work was primarily phenomenological, while the large-caliber work was primarily developmental. He has worked extensively with a 50mm high-pressure powder gun, which was

designed many years ago for BRL by associates of Hal Swift at the University of Dayton Research Institute. It can deliver useful masses up to about 2.5 km/s. He has overseen high-velocity KE penetrator shots using two-stage light gas guns at other installations, at striking velocities up to 4.5 km/s with typical 100–200-gm laboratory long-rod penetrators.

Dr. Dietrich, recently deceased, received his bachelor's (1965), master's, and Ph.D. degrees (1968) in physics from the Johns Hopkins University's Department of Mechanics. His graduate research involved modeling penetration in hypervelocity impact for BRL under the well-respected Robert B. "Robby" Pond and Coy Glass. He began his career at BRL in 1968 as a research physicist, working there in increasingly responsible positions primarily involving research and development of shaped-charge warheads and armor. He also received a second master's degree from the Armed Forces Industrial College. **He retired as Chief of ARL's Impact Physics Branch in WMRD in 2002.** Upon retiring, he returned to ARL as a civilian contractor, retiring again in 2007, for a total of over 40 years' experience.

ACKNOWLEDGMENTS

This work is dedicated to our wives, Louise Silsby and Priscilla Dietrich. They tolerated many weeks and even months of separation while we were away at remote test venues, without serious complaint, because they understood the need. Without their understanding support, this work would not be possible.

That you are reading this work is really because of many people in the ballistics research, development, test, and evaluation community who were always free in sharing ideas about what they thought was happening when presented with unexplained phenomena and quick with advice about how to get things done. There are far too many people who have helped us over the years to acknowledge them all without forgetting many more, so thanks to you all. You know who you are. This monograph is also dedicated to the personnel of the U.S. Army Ballistics Research Laboratory and its successor in business, the Weapons and Materials Research Directorate of the U.S. Army Research Laboratory, a great group of people with which to work, as well as to the management of SURVICE Engineering Company who promoted this project to DSIAC while facing the usual fits and starts of funding over the years.

We dedicate this work in particular to the late John Kineke, a wise mentor and coworker; the late Allen **Murray, a consummate manager from below ("Nothing moves unless you push it!");** to Dr. Fred Malinowski, a mathematician who derived some particularly difficult penetration modeling equations in closed form; and to Walter Rowe, who while partnered with Mr. Silsby, fired many quarter-scale KE penetrator phenomenology shots.

Finally, the reader should be aware of the extensive amount of work done by various reviewers during the iterative process of authorship. Without their candid input after each successive rewrite, refining the organization and clearing up questions, this monograph

would be a lot less readable. The anonymous process allowed them to be critical, but at the same time their comments attempted to force us to cut out the fat and focus the narrative. Thank you, each anonymous reviewer, whoever you are.

A number of persons contributed significantly to this work. Our former supervisor at SURVICE Engineering, Dyrck Van Dusen, made us aware of the monograph as a way of preserving institutional knowledge and helped to initiate the process and keep it going over a number of years. Thanks to Eric Edwards who served as primary editor over a number of cycles of writing, reviewing, and rewriting the manuscript. When Eric Edwards was unavailable, Frank Gostomski helped as a point of contact with the publishing staff. Former co-worker Matthew Burkins, now retired and heading Burkins Armor Consulting, did the final outside review of the manuscript. He gave it a thorough scrub and caught a number of errors and loose ends that had slipped through. I owe Matt a lot for his extensive work. Brian Benesch, as head of DSIAC at SURVICE took over the job of shepherding the process along in the final iteration. Finally, Janine Gettier of SURVICE did the final formal edit and did a lot to make the product easier to read and understand. Thanks again.

TABLE OF CONTENTS

ABSTRACT	III
FOREWORD	IV
PREFACE	V
About This Monograph.....	v
Development of Antiarmor Munitions	vi
THE AUTHORS	IX
ACKNOWLEDGMENTS	X
1. TERMINAL BALLISTICS.....	1-1
1.1 KE Penetration.....	1-1
1.2 Accurate Penetration Measurement	1-2
1.3 Armor.....	1-3
1.4 Penetrator Materials	1-4
2. EVOLUTION OF CURRENT ANTIARMOR THREATS	2-1
2.1 KE Penetrators	2-1
2.2 Lethal Mechanism of KE Penetration in Chemical Energy (CE) Warheads.....	2-3
2.3 The SC Warhead.....	2-4
2.4 Other Lined-Cavity Charges.....	2-6
2.5 The Importance of Increased KE Projectile Striking Velocity	2-7
2.6 Advantages and Disadvantages of KE vs. SC Ammunition.....	2-8
2.6.1 KE Ammunition Advantages	2-8
2.6.2 KE Ammunition Disadvantages.....	2-8
3. NORMAL INCIDENCE SEMI-INFINITE PENETRATION: DATA	3-1
3.1 Experimentation and Data Interpretation.....	3-1
3.2 Effect of Rod Length on Depth of Penetration	3-3
3.3 Effect of Penetrator Density on Penetration	3-3
3.4 Effect of Penetrator and Target Strengths on Penetration	3-4
3.4.1 Strain Rate Effects on Material Strength	3-5
3.4.2 Temperature Effects on Material Strength.....	3-5
3.4.3 Penetrator Strength	3-5

3.4.4 Target Strength.....	3-5
3.5 Penetration Hole Diameter	3-6
3.6 Penetration Hole Volume	3-7
3.7 The L/D Effect	3-7
3.7.1 Normalizing L/D Data.....	3-8
3.7.2 Exploiting the L/D Effect	3-8
3.8 More Material Properties Important in Semi-infinite Penetration.....	3-9
3.9 Effect of Size (Geometric Scale)	3-10
4. NORMAL INCIDENCE SEMI-INFINITE PENETRATION: MECHANICS	4-1
4.1 The Reaction of Penetrator Material Upon Penetration	4-1
4.2 The Reaction of Target Material Upon Penetration.....	4-2
4.3 Simple Physical Relationships.....	4-3
4.4 Derivation of Interface Velocity, U	4-4
4.5 Derivation of the Density Law.....	4-4
4.6 The Influence of Penetrator Strength at Higher Velocities.....	4-6
4.7 Unbalanced Unsteady State Effects.....	4-7
4.8 Summary	4-8
5. NORMAL INCIDENCE PERFORATION	5-1
5.1 Perforation vs. Penetration.....	5-1
5.2 Wave Mechanics.....	5-1
5.3 Limit Measures: V_L , V_{50} , θ_{50} , and $V_S - V_R$	5-3
5.3.1 V_L – Ballistic Limit	5-4
5.3.2 V_{50} – Ballistic Limit Velocity	5-4
5.3.3 θ_{50} – Ballistic Limit Obliquity	5-4
5.3.4 $V_S - V_R$ – Striking Velocity vs. Residual Velocity	5-4
5.3.5 Advantages and Disadvantages of Limit Velocities	5-5
5.3.6 Reliability of Limit Velocities.....	5-5
5.3.7 The Other Performance Measure: The Witness Plate.....	5-6
5.3.8 Relationship of Perforation to Penetration	5-7
5.4 Vehicle Armor Obliquity and Line-of-Sight Thickness.....	5-8
6. EFFECTS OF OBLIQUITY, SPACING, AND LAMINATION	6-1
6.1 Obliquity.....	6-1
6.2 Natural Coordinate System for Oblique Impact.....	6-1
6.3 Oblique Armor	6-2

6.3.1	Armor Will Usually not be Struck at Normal Incidence	6-2
6.3.2	Features in Oblique Perforation of a Thick Target	6-3
6.3.3	Measuring Penetration in an Oblique Impact	6-5
6.3.4	Oblique Perforation of a Thin Target.....	6-6
6.3.5	Penetrator Design Considerations for Attacking Oblique Armor	6-6
6.4	Spaced Armors.....	6-7
6.5	Laminated Target Elements.....	6-9
7.	UNFAIR HITS	7-1
7.1	Free Surface Effects	7-1
7.2	Yaw	7-2
8.	ARMOR AND PENETRATOR DESIGN AND MATERIALS	8-1
8.1	Armor vs. Armor Plate	8-1
8.2	Armor is a Combination of Geometries and Materials	8-1
8.3	Areal Density is the Most Important Characteristic in Fighting Vehicle Armor	8-2
8.4	Comparing Real Armor Designs to Monolithic RHA.....	8-2
8.5	Defeat Mechanisms.....	8-3
8.6	Materials in Ballistics.....	8-4
8.6.1	Armor Materials	8-5
8.6.1.1	Armor Steel Alloys.....	8-5
8.6.1.2.	Other Metallic Armors.....	8-9
8.6.1.3	Composite and Ceramic Armors	8-11
8.6.2	Other Penetration-Resistant Materials	8-12
8.6.3	Penetrator Materials	8-12
8.7	The Penetrator Must Be Designed with the Sabot and Propelling Charge for Maximum Launch Velocity	8-14
8.7.1	LRP Round Design	8-15
8.8	Toxicity of Tungsten.....	8-17
8.9	Using the Kinematic Empirical Model.....	8-17
9.	MOVING METAL WITH EXPLOSIVES	9-1
9.1	Introduction	9-1
9.2	Fundamentals of Explosives	9-1
9.3	Detonation vs. Deflagration.....	9-2
9.4	Forest-Fire Model of Detonation Propagation	9-4
9.5	Sensitivity and Power	9-5
9.6	Failure Thickness and Confinement	9-7

9.7 High Detonation Velocities Mean Timing Is Critical	9-8
9.8 Fabrication: Cast, Pressed, or Molded: Sheet, Plastic, and Polymer Bonded	9-8
9.9 Projecting Metal with Explosives	9-9
9.9.1 Predicting Speed: The Gurney Equations	9-9
9.9.2 Predicting Trajectory: The Taylor Angle	9-11
9.9.3 Improvements to the Gurney and Taylor Models	9-12
10. FRAGMENTING WARHEAD DESIGN	10-1
10.1 The Fragment Threat is Ubiquitous on the Battlefield	10-1
10.2 Estimating Armor Requirements Requires Knowing Fragment Characteristics	10-1
10.3 Fragmenting Warhead Technology is Mature	10-2
10.4 Warhead Design Process	10-2
11. NONJETTING LINED-CAVITY CHARGE DESIGN	11-1
11.1 Introduction	11-1
11.2 EFPs	11-1
11.3 Hemispherical Liner Warhead	11-2
12. JETTING WARHEADS: THE SHAPED-CHARGE	12-1
12.1 Introduction	12-1
12.2 Jet Formation, Stretching, and Particulation	12-1
12.3 Portraying the Jet: The x-t Plot	12-2
12.4 Deviations from the Density Law	12-3
12.5 Regimes of Jet Penetration, Standoff Curves, and Effective Jet Length	12-4
12.6 Formation of the Jet	12-5
12.7 Attached vs. Detached Shock	12-7
12.8 Tailoring the Liner Collapse	12-8
12.9 Collapse Symmetry Critical to Performance	12-11
12.10 SC Defeating Armors and Their Influence on Warhead Design	12-11
12.11 Fuzing and Other Considerations for Maximum Performance	12-12
12.12 Computational Design Tools	12-13
12.13 Specific Safety Issues	12-15
13. ENERGETIC MATERIALS: SOME SAFETY ISSUES	13-1
13.1 Explosives <i>are</i> Dangerous Goods	13-1
13.2 Insults and Incidents	13-2
13.3 Personnel Qualifications	13-4
14. CONCLUSION	14-1

15. REFERENCES	15-1
16. BIBLIOGRAPHY	16-1
APPENDIX A. HISTORICAL OVERVIEW OF FIGHTING VEHICLE ARMOR AND ANTIARMOR TECHNOLOGY	A-1
A.1 Early Evolution of the Tank and Antitank (AT) Weapons	A-2
A.1.1 The Tank as Mobile Machine-Gun Nest	A-3
A.1.2 AT Guns	A-3
A.1.3 The Tank as AT Weapon	A-3
A.1.4 Armor-Piercing (AP) Shot and the Towed AT Gun	A-4
A.2 The Development of Heavy Frontal Armor and the SC	A-5
A.3 The High-Explosive Plastic (HEP) Round	A-6
A.4 The Hypervelocity Armor-Piercing (HVAP) Round and the LRP	A-7
A.5 Weight-Efficient Tank Armor	A-8
A.5.1 Weight-Efficient Frontal Armor	A-8
A.5.2 The Skirting Plate as Weight-Efficient Armor	A-9
A.6 The Evolution of the SC	A-9
A.6.1 Eliminating SC Performance Degradation	A-9
A.6.2 Threats to Technological Leads	A-10
A.6.3 Evolution vs. Revolution	A-11
A.7 Armor Evolution	A-11
A.8 RA	A-12
A.9 The Tandem SC	A-14
A.10 Other Armor Concepts	A-14
A.11 Other Ammunition Concepts	A-15
A.12 Conclusion	A-15
A.13 Appendix A References	A-16
APPENDIX B. ACRONYMS AND ABBREVIATIONS	B-1

LIST OF TABLES

Table 7-1. Fraction of Rod Length Clearing Hole	7-2
Table 8-1. Rod and Target Defeat Mechanisms	8-3
Table 8-2. Aluminum Alloys Used as Armor and Their Military Specifications	8-10
Table 8-3. Three Common Armor Ceramics as of 2007	8-11
Table 13-1. Exposure Threats to Energetic Materials	13-3
Table 13-2. The Human Element: Typical Accidents and Lessons Learned	13-4

LIST OF FIGURES

Figure 1-1. Generic KE Penetration.....	1-2
Figure 1-2. Computation from HELP Code and Radiograph	1-2
Figure 1-3. Measuring Penetration Depth.....	1-3
Figure 1-4. Measuring Penetration in a Laminated Target	1-3
Figure 2-1. Evolution of Antitank KE Penetrators.....	2-1
Figure 2-2. Cross-Section of an Earlier SC Warhead	2-4
Figure 2-3. Typical SC and LRP Rounds for the 120mm M256 Tank Cannon	2-4
Figure 2-4. SC Jet Formation.....	2-5
Figure 2-5. Typical Penetration-Standoff Curve.....	2-5
Figure 2-6. Typical SC Penetration of Armor Plate.....	2-6
Figure 2-7. Penetrator from SC with Hemispherical Liner	2-6
Figure 2-8. EFP Smart Munitions	2-7
Figure 2-9. Typical P/L vs. Velocity Data for Tungsten Long-Rod Penetrators vs. RHA	2-8
Figure 3-1. Penetration vs. Velocity for Three Rod Lengths.....	3-1
Figure 3-2. Another Interpretation of the Same Data Set as Shown in Figure 3-1.....	3-2
Figure 3-3. Normalizing Penetration by Rod Length Simplifies the Data	3-2
Figure 3-4. Effect of Penetrator Density on Penetration	3-4
Figure 3-5. Normalized Density Curves.....	3-4
Figure 3-6. Effect of Target Strength on Penetration Depth	3-5
Figure 3-7. Hole Diameter vs. Velocity at Ordnance Velocities	3-6
Figure 3-8. Hole Volumes are not Entirely Proportional to Striking Energy	3-7
Figure 3-9. P/L vs. Velocity as a Function of L/D.....	3-8
Figure 3-10. Normalization by L/D.....	3-8
Figure 3-11. Exploiting the L/D Effect.....	3-9
Figure 3-12. Steel and Ceramic Ball Targets.....	3-9
Figure 3-13. The Effect of the Geometric Scale of the Experiment	3-11
Figure 3-14. Geometric Modeling of a Penetrator as Scale Factor Decreases	3-12
Figure 4-1. Penetrator Eversion During Penetration	4-1
Figure 4-2. Target Material Displacement After Penetration	4-2
Figure 4-3. Everting Penetrator.....	4-3
Figure 4-4. Simple Mathematical Relationships Yield Value for U	4-4
Figure 4-5. Streams of Equal Area but Different Densities Impinging on Each Other Coaxially	4-4
Figure 4-6. Tungsten on Steel Long-Rod Penetration Data with the Hydrodynamic Limit Superimposed.	4-5
Figure 4-7. Small Penetrator Diameter, Large Target but Different Densities on Each Other Coaxially	4-5
Figure 4-8. Deep Penetration.....	4-6
Figure 4-9. Target Hole Growth due to Target Material Inertia	4-7
Figure 4-10. Secondary Target Penetration Caused by Forward-Moving Penetrator Residue.....	4-7
Figure 4-11. Interface Velocity and Relative Velocity Between Penetrator and Target vs. Striking Velocity	4-7
Figure 4-12. Segmented Penetrator.....	4-8
Figure 5-1. Normal Incidence Perforation.....	5-2

Figure 5-2. Target Deformation from Bulge to Perforation	5-2
Figure 5-3. Sectioned Perforated Target	5-3
Figure 5-4. Residual Penetrator and Target Plug	5-3
Figure 5-5. V_{50} Curve.....	5-4
Figure 5-6. V_s - V_r Curve.....	5-5
Figure 5-7. Aluminum Witness Plate for Aluminum Slug Residuals, 10 Shots.....	5-6
Figure 5-8. Witness Plate Stack for Diagnostics Involving Deep Penetration.....	5-7
Figure 5-9. Speculation Leads to Inaccurate Breakout Allowance Measurement.....	5-7
Figure 5-10. One Case in Which Limit Velocities Fall on the P/L Curve	5-8
Figure 5-11. Ductility Could Just Offset Plugging to Explain Figure 5-10	5-8
Figure 6-1. Obliquity in Armor Design	6-1
Figure 6-2. Natural Coordinate System for Describing Striking Obliquity	6-1
Figure 6-3. Relationship Between Vehicle Armor Geometry, Attack Geometry, and True Striking Obliquity	6-2
Figure 6-4. Detail of Figure 6-3 Relationships	6-2
Figure 6-5. Oblique Perforation of a Thick Target	6-3
Figure 6-6. Behind-Armor Debris Classes.....	6-5
Figure 6-7. Incorrect Measure of Depth of Penetration.....	6-5
Figure 6-8. Effective Interface Path Length Depends on T and D	6-5
Figure 6-9. Examples of Thin Target Plate Orientations and a Resulting Perforation	6-6
Figure 6-10. Perforation of a T/D 1 Plate at 60° Obliquity.....	6-6
Figure 6-11. Effects of an Oblique Target on the Penetrator. Imagine the effect of several spaced elements.....	6-7
Figure 6-12. The Effect of Several Spaced Elements on the Penetrator.....	6-7
Figure 6-13. Spaced Armor: Skirting Plates on Israeli Merkava Mk I Tank	6-7
Figure 6-14. Spaced Armor Array	6-8
Figure 6-15. Corrugated Appliqué Over Plate Armor on the USMC AAV7A1	6-8
Figure 6-16. Erosion Budget for a Long Rod Perforating a Thin, Oblique Plate	6-9
Figure 6-17. Typical Rod Breakup on Spaced Oblique Targets.....	6-9
Figure 6-18. Effect of Lamination on Target Performance	6-10
Figure 7-1. Centered vs. Uncentered Normal Incidence Penetration on Thick Square Target	7-1
Figure 7-2. Yawed Rod Impact Geometry	7-2
Figure 7-3. Yawed Rod Penetration at Normal Incidence	7-2
Figure 7-4. Yawed and Pitched Impact on an Oblique Plate Target.....	7-3
Figure 7-5. Yawed Rod Penetration in an Oblique Target.....	7-3
Figure 7-6. Example Curves Comparing the Effect of Pitch on Penetration for a Monolithic and a Laminated Oblique Target.....	7-4
Figure 7-7. Inclined Interface Path in Yawed Normal Incidence Impact.....	7-4
Figure 7-8. Inclined Path Changes the Effective Target Line of Sight Traversed in Oblique Impacts	7-4
Figure 8-1. Real Armors are Combinations of Geometry and Materials.....	8-1
Figure 8-2. Determining Mass Efficiency of an Armor (left) or Appliqué (right) Design	8-2
Figure 8-3. Determining the Space Efficiency of an Armor Design	8-2
Figure 8-4. (Coiled) Cable Shock Isolators.....	8-4

Figure 8-5. Army Armor Steel Specifications	8-7
Figure 8-6. Process Schematic of Explosively Welded Metallic Sandwich	8-9
Figure 8-7. Surface Cut Through Explosively Welded Metallic Sandwich	8-9
Figure 8-8. Comparison of Penetrator Failure Modes	8-13
Figure 8-9. Comparison of Residual Penetrators.....	8-14
Figure 8-10. Comparison of Residual Rods After RHA Perforation.....	8-14
Figure 8-11. Comparison of Penetration Channels as a Function of Velocity.....	8-14
Figure 8-12. DU Long Rod Eroded into Shear Chips as it Perforates a 70.5° Steel Plate Target.....	8-14
Figure 8-13. The Russian Bm15 LRP and Sabot.....	8-15
Figure 8-14. M735 Flight Body and Sabot.....	8-16
Figure 8-15. M829 Family of LRP Ammunition	8-16
Figure 8-16. Estimating Relative Penetrator and Target Erosion.....	8-18
Figure 9-1. Forest-Fire Model of Detonation	9-4
Figure 9-2. Derivation of the Gurney Equation.....	9-10
Figure 9-3. Other Flyer Plate Curves.....	9-11
Figure 9-4. Gurney Flat Plate Curve.....	9-11
Figure 9-5. Tamping	9-11
Figure 9-6. Taylor Model for Throw-off Angle	9-11
Figure 9-7. Comparison of the Fluid Model and the Elastic-Plastic with Gas Leakage Model to the Gurney and Taylor Models	9-12
Figure 10-1. The Ubiquitous HE Round.....	10-1
Figure 10-2. Results of Adding a Fragmentation Sleeve to a Hellfire Missile.....	10-3
Figure 10-3. Fragment Production Techniques	10-4
Figure 10-4. Add Projectile Velocity to Calculate Correct Fragment Velocities	10-5
Figure 11-1. EFP Munition Concepts.....	11-2
Figure 11-2. U.S. Antitank HE M75 Mine.....	11-2
Figure 11-3. Casspir APC Hull Attacked by the TMRP-6 Antitank Mine.....	11-2
Figure 11-4. Mechem Appliqué on Casspir Hull – Details.....	11-3
Figure 11-5. Collapse of a Hemispherical Liner.....	11-4
Figure 12-1. The SC Warhead Initiation and Penetration	12-1
Figure 12-2. Collapse of the Liner, and Jet Formation, Stretching, and Particulation	12-2
Figure 12-3. Radiograph of a Particulated Jet.....	12-2
Figure 12-4. Typical x-t Plot	12-2
Figure 12-5. Virtual Origin.....	12-3
Figure 12-6. Features in the x-t Plot	12-3
Figure 12-7. Target Penetration and the x-t Plot.....	12-3
Figure 12-8. The Effect of Target Compressibility.....	12-4
Figure 12-9. Particulated Jet Misalignment.....	12-4
Figure 12-10. Penetration vs. Various Standoff Distances.....	12-5
Figure 12-11. Comparison of Penetration vs. Standoff Curves.....	12-5
Figure 12-12. Shaped-Charge Jet Formation and Regions of Interest	12-5

Figure 12-13. Jet and Slug Masses and Velocities	12-6
Figure 12-14. Jet Element Velocity in a Conical Liner	12-6
Figure 12-15. Early Stages of Viper Warhead Jet Formation	12-7
Figure 12-16. Attached vs. Detached Shock	12-7
Figure 12-17. Comparison of Jets (Below Incoming Material Stream) from Supersonic and Subsonic Collapse	12-7
Figure 12-18. Line/Plane Wave Generator Concepts.....	12-8
Figure 12-19. Wave Shaper	12-9
Figure 12-20. Trumpet-Shaped SC Liner	12-10
Figure 12-21. Optimized Liner Design	12-11
Figure A-1. The Toll of Attrition.....	A-2
Figure A-2. The Tank as Mobile Machine-Gun Nest	A-3
Figure A-3. Early AT Tank.....	A-3
Figure A-4. Czechoslovakian Towed AT Gun.....	A-5
Figure A-5. Viper Warhead SC Jet Forming	A-6
Figure A-6. P/L Versus Velocity, Showing Various Approximations	A-7
Figure A-7. The M60, MBT 70, and M1 Tanks	A-8
Figure A-8. A Nonballistic Bonus of Obliquity.....	A-8
Figure A-9. Confined Glass as an SC-Defeating Armor.....	A-9
Figure A-10. Bradley IFV with RA Modules	A-12
Figure A-11. ERA Plates Ride First One Side Then the Other of the Rod.....	A-13
Figure A-12. Typical Tandem SC RPG.....	A-14

1. TERMINAL BALLISTICS

The study of fighting vehicle armor and antiarmor munitions is driven by the terminal ballistics of the impact of the projectile on the target. The munition designer hopes to defeat the armor and kill the vehicle and its weapon system. The armor designer seeks to thwart such intentions.

The effects of impact can range from no effect, to extreme knocking and shaking of an impacted object, to deeply penetrating and even perforating the target. The study of penetration mechanics examines penetrating impacts, which are of particular interest to the military. A subclass of penetration mechanics is the study of the penetration by nonenergetic projectiles (kinetic energy [KE] penetrators) as opposed to those projected by an energetic warhead, such as a shaped-charge (SC) jet. This monograph is focused on the details of KE penetration in general.

There are also nonperforating munitions, such as the high-explosive (HE) plastic (HEP) round, discussed in detail in Appendix A, Section A.3. It is a spin-stabilized, full-bore, bullet-shaped projectile with a thin, ductile casing filled with plasticized HE. It has a base detonating fuze with a slight delay, which allows the explosive to squash out when it contacts the face of the armor before it explodes. The shock wave reflecting off the rear surface of monolithic hull armor throws a spall off the back about the size and shape of a very large, free-form, table-top ashtray. While making no through hole, the massive chunk of metal and a lot of smaller debris bounce around the fighting compartment, seriously endangering the crew. For various reasons, the HEP round is no longer considered a significant threat against modern tanks.

Among other nonperforating defeat mechanisms is shock. While the HEP round certainly delivers the ultimate shock, the formation of the spall is the armor-defeat mechanism. Most antiarmor munitions that do not perforate do not generate a spall, but they do slam a vehicle very hard, which can break one or more critical components.

Mine-throw is another defeat mechanism, in which a large explosive charge imparts motion to portions of, or the entire vehicle, again severely damaging critical components, often the occupants. And sometimes, an HE round will break a critical exterior component such as a wheel or track, rendering the vehicle next to useless. We will concentrate on penetrating munitions in this work.

1.1 KE PENETRATION

A KE penetrator uses the energy of its motion to push into and hopefully through, a protective barrier. Figure 1-1 visualizes a number of processes operating during the penetration of an armor plate target (rolled homogeneous armor [RHA]) by a modern, large-caliber, long-rod penetrator. With the rod striking the target at sufficiently high velocity, the stress (the force per unit area) in both the rod and target exceed that necessary to cause their respective materials to flow.

The figure is a cross-section of a rod penetrating a thick target plate. The rod is eroding, with the spent material lying along the cavity wall and being ejected up range as fine debris. The target material is pushed aside laterally, as well as up and down range. Entrance lips have formed asymmetrically due to the obliquity of the target. The penetrator-target interface is close to the rear of the target, and a predictable pattern of cracking of the material (indicated by the interior lines) has formed as a result of the target deformation. If there were no more penetrator left, or if the existing penetrator were to slow

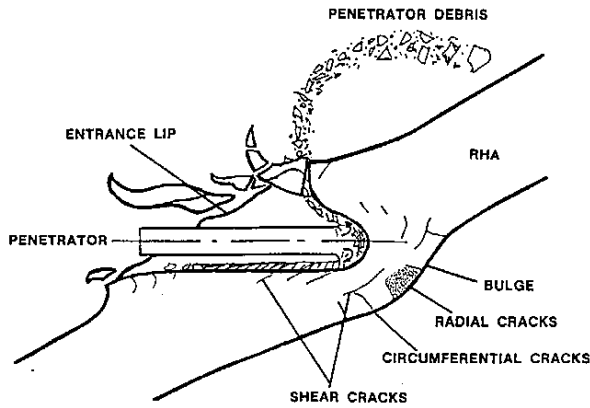


Figure 1-1. Generic KE Penetration (Source: Silsby [1]).

to a stop at this point, a partial penetration would result. In the case illustrated, a bulge has been produced. If the rod overmatches the target, the target is completely perforated. The remaining tail of the rod (called the residual penetrator), smaller rod fragments, a rear surface scab (improperly called spall), larger target fragments from the breakup of the scab, and smaller target fragments from the penetration channel are projected off of the target's rear surface. Computational results from the early hydrodynamic elastic-plastic (HELP) Code are quite close to an actual radiograph of the penetration (Figure 1-2) [4].

An actual shot is quite violent, is over in an instant, and much of the penetrator material is usually reduced to highly deformed and hence very hot chips, which may or may not burn up quickly. High-speed cameras and flash radiographic shadowgraphs typical in a terminal ballistic range cannot show what is occurring inside the target. An experimenter must pay attention to detail, exercise good housekeeping during the conduct of a test series, and be observant. When the experimenter carefully marks the test articles before the shot and cleans up after each shot to recover as much residual material as possible clearly related to that specific shot, the consistent set of signatures on the penetrator and target residue that can be related to individual shots will slowly

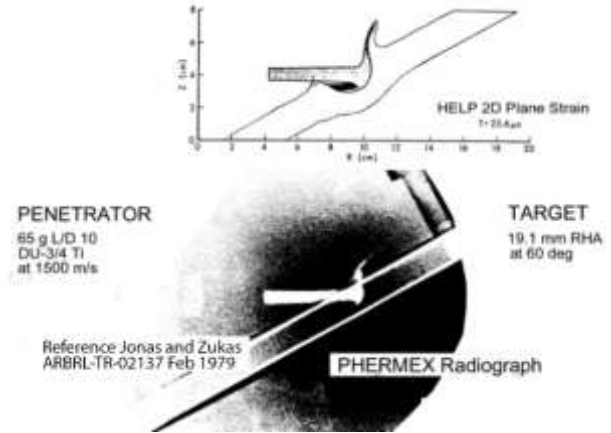


Figure 1-2. Computation from HELP Code and Radiograph (Source: Jonas and Zukas [6]).

reveal details of the processes involved. Mating surfaces from fracture, markings from flow, and other clues permit reassembling many of the major fragments to see how the target and penetrator failed (ruptured). With enough test firings, and hence observations, the entire process becomes apparent.

If sufficient funding is available, current computer modeling of penetration mechanics provides a plausible, detailed, time-resolved picture of the flow processes. In addition, you can set up a reduced-scale firing point and take a single, penetrating flash radiograph per shot through 4–6 in. of steel at the Los Alamos National Laboratory's (LANL's) Pulsed High-Energy Radiographic Machine Emitting X-rays (PHERMEX) flash radiography facility, which is primarily used to image the implosions of nuclear warhead designs. (The PHERMEX radiograph and computational run at the corresponding time in Figure 1-2 are in a slightly rearranged form from that of Jonas and Zukas 1979 [6]).

1.2 ACCURATE PENETRATION MEASUREMENT

Figure 1-3 shows various ways of measuring the depth of penetration channels. However, view c shows the true penetration depth.

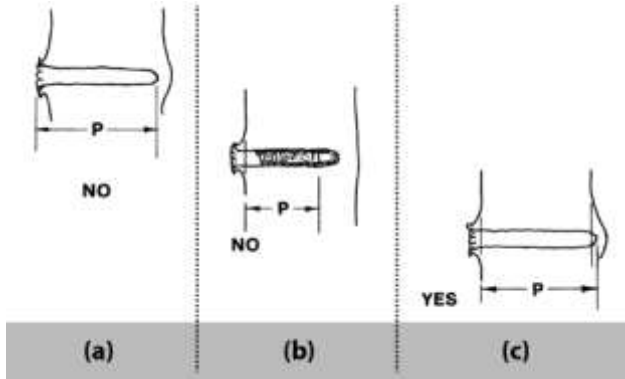


Figure 1-3. Measuring Penetration Depth (Source: Silsby [1]).

If penetration is defined as the path length of the penetrator-target interface, in view a, that length would be from the undisturbed face of the target where struck to the bottom of the channel where the penetrator-target interface was when penetration stopped. The top left measurement starts at the top of the entrance lips, material that was pushed up-range after initial touchdown, so the actual penetration depth is not shown. In view b, some legitimate penetration is ignored because it is measured to the back of the unrod. View c shows the true penetration depth as is sometimes seen in practice, because the target material is pushed down-range ahead of the penetrator, so that the penetrator must push its way through more than the initial thickness of the target plate to perforate.

Figure 1-4 shows penetration measurement in a stack of targets. Frequently it is necessary to lay up a number of plates (a laminated target) to achieve adequate thickness to stop a long-rod penetrator (LRP). The penetration measurement method shown in Figure 1-4 is correct (more or less) because the penetrator-target interface must push its way through each plate, for which bulging is suppressed by the stemming effect of the plates behind, then penetrate the final target plate as if it were the only plate in the stack. In reality, this would be true only if the stack of plates shown were backed by a lot more plates. Otherwise, at some point in the penetration process, free surface effects would result in some of the

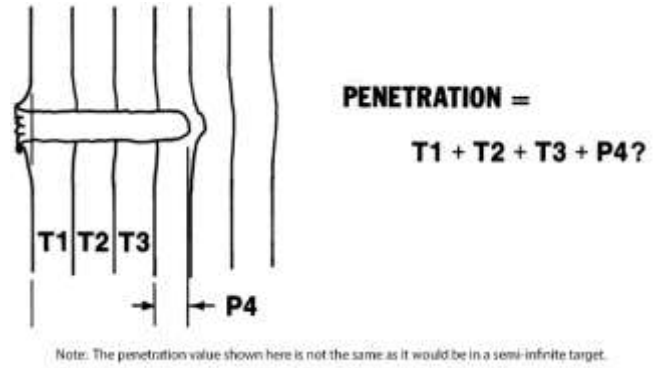


Figure 1-4. Measuring Penetration in a Laminated Target (Source: Silsby [1]).

rear plates separating, so that the penetrator would have to transit some bulged material.

1.3 ARMOR

Armor is anything used to protect something and has ranged from a sheep's fleece (aegis) to wooden shields to extremely hard metals. Circumstances sometimes severely constrain the choices available, as with armored transparencies (windows). There are many drivers to armor design, usually cost and performance. The measure of performance is usually the weight needed to stop a threat of some given penetration capability.

A good, low-alloy steel of intermediate strength and rather high elongation to rupture is almost universally used where cost is the only driver, and each nation has its own recipe. The U.S. uses RHA, a low-alloy, deep-hardening steel similar to American Iron and Steel Institute (AISI) 4340 but with lower carbon content to reduce the number of fragments generated in the event of a perforation. It through-hardens to the desired value in very thick sections and, being cross-rolled, its properties are nearly isotropic.

Where weight becomes important, as on ship superstructures, a high-hard steel alloy typical of that used to make saw blades is used, or aluminum is

substituted. In weight-critical applications such as in aircraft and body armor, more expensive materials are used such as titanium or magnesium, ceramics, composites, and/or fabrics of strong, tough fiber. Often, layers of various materials can be more effective against a given threat than can a monolithic slab of one material. Armor can be applied to an existing design, but weight is almost always reduced by incorporating the armor into the structure and supporting features as much as possible, while at the same time using necessary components such as the engine to protect the more valuable and irreplaceable crew members.

1.4 PENETRATOR MATERIALS

As with armor, the choice of penetrator materials is driven by the application. Density, strength, and toughness are important for KE penetrators. Iron (as steel) is relatively inexpensive, as are uranium and tungsten. For explosively driven applications, other properties can be more important than cost, and copper, aluminum, molybdenum, and uranium liners in explosive warheads form them into high-velocity, lethal penetrators. U.S. antiarmor KE penetrators used in combat are almost always made from a uranium alloy, because the material does not mushroom as much in penetration, and therefore, more of its KE is used to increase the depth of penetration than is the case with tungsten. In addition, uranium is essentially free because it is a by-product of producing enriched uranium for power production and nuclear weapons. However, it's mildly radioactive, but the practice ammunition is universally uranium-free.

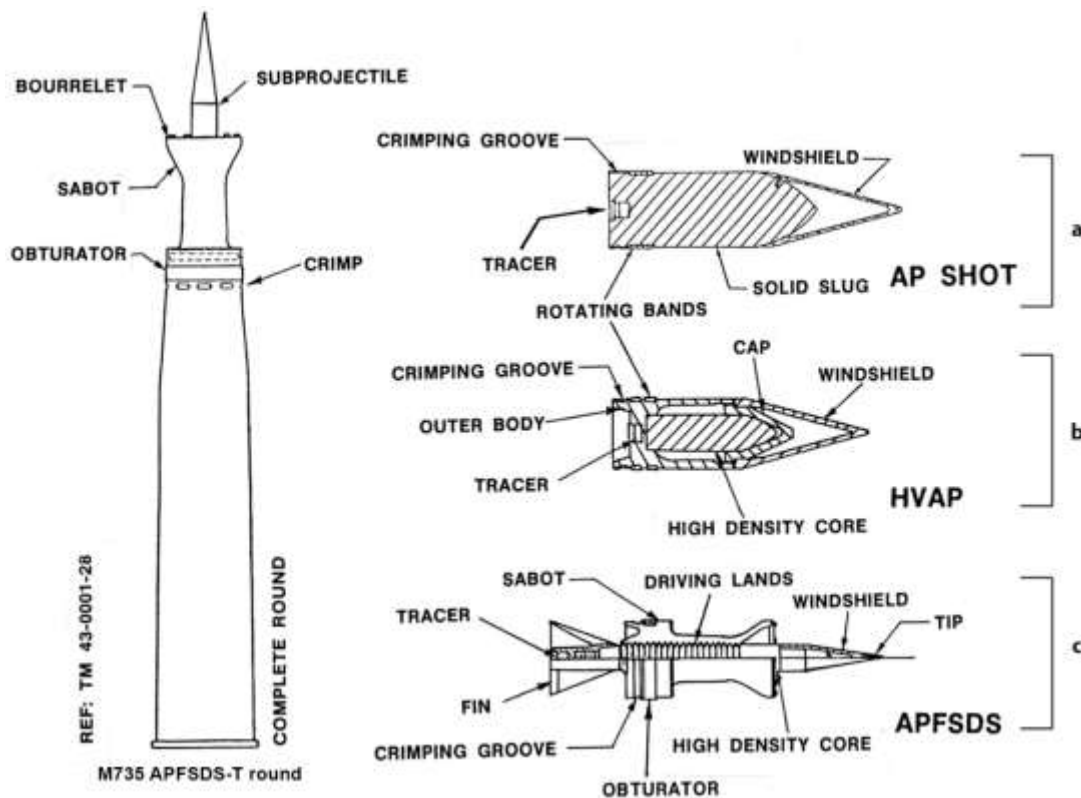
2. EVOLUTION OF CURRENT ANTIARMOR THREATS

2.1 KE PENETRATORS

With the introduction of the tank, armored with a layer of very competent, tough, and strong steel, antiarmor KE ammunition began as full-bore, hardened-steel solid shot, with some variations in the design details. Improvements in performance were gained at the expense of increasingly larger guns, which became increasingly costly and unwieldy. However, increased awareness of the basics of penetration mechanics permitted improved performance while retaining the

existing gun systems longer, resulting in a tremendous cost savings. Figure 2-1 shows the evolution of KE penetration, leading to an early LRP round that would be shot out of a large-caliber tank main gun, scaled as though all were fired from the same service weapon.

Externally, a modern LRP round would not look much different from an early one, as the extended length of the modern rod is buried in the propellant bed within the case. At some point, designers realized that with an appropriate profile of the sabot body, sufficient friction forces could be generated with smooth mating surfaces, as the friction chuck in a lathe can adequately grip cylindrical bar stock. A short section of driving lands is used to prevent axial slip at the beginning of the powder burn.



Grooves in the sabot engage driving lands on the penetrator to transfer accelerating forces from sabot to penetrator.

Figure 2-1. Evolution of Antitank KE Penetrators (Source: U.S. Department of the Army [7, 8]).

The round¹ in view a in Figure 2-1 is called armor-piercing (AP) shot. A very tough, reasonably hard, full-bore, solid tool steel projectile² is fired at what would be an extremely low velocity by modern standards. AP shot strikes at such a low velocity that it does not erode in penetrating most materials, but opens a hole, through which it advances, akin to the manufacturing process of piercing or punching. A punch can sink into a thick solid **by exceeding the solid's flow stress (which depends on the material's uniaxial yield strength and loading geometry**. For a flat-nosed cylindrical punch and a thick plate, the punch must be at least about three times as strong as the material being pierced). The force opening the armor material, working over a distance, expends projectile energy. This action slows the penetrator,³ and if the armor is thick enough, stops it.

By reducing in-bore mass from that of the AP shot, more energy from the propellant can be imparted to the projectile. This concept was exploited in the hypervelocity AP (HVAP) round, view b, for the 90mm tank cannon introduced at the end of World War II (WWII). A lightweight aluminum carrier surrounds a smaller penetrator of a dense material such as tungsten carbide. The flight body itself has the same presented area and drag coefficient, but lower overall mass, and hence will slow more with distance downrange, but by launching at a higher muzzle velocity, the round should have a higher striking velocity except at extreme range. The higher density of the penetrator results in a higher impact pressure for the same velocity, and hence deeper penetration.

An evolutionary improvement on the HVAP round was the HVAP discarding sabot (HVAPDS) round for the 105mm cannon (view b) in which the core and cap were carried in a smaller flight body, which was in turn pulled up the gun bore by grooves in the lightweight carrier

called a sabot mating with outstanding driving lands on the penetrator. The sabot (French for "boot") is shed away, or discarded, from the projectile on exiting the gun muzzle. The AP shot and the HVAP are spin-stabilized, requiring a rifled gun tube for accuracy, while the HVAPDS projectile is unstable at typical spin rates for solid shot. Rather, they are fin stabilized like an arrow and must be fired from a smooth bore tube or be despun by use of special driving band designs if shot from a rifled tube. However, they are generally rolled at about 100 revolutions per second to cancel out the effect of small disturbances in flight caused by variations from perfection in actual rounds.

In the modern AP fin-stabilized, discarding-sabot (APFSDS) round (view c), the payload mass was kept about the same as the HVAPDS by further reducing the diameter and stretching the length of the penetrator. Ballistic-quality, high-density engineering materials such as sintered tungsten alloy (WA) powder metallurgy products and depleted uranium (DU) alloys were developed concurrently with other aspects of the LRP ammunition design. Being fin-stabilized, the APFSDS round can be fired from a smoothbore gun. The smaller presented area of the flight body results in a lower loss of velocity to drag. The resultant higher striking velocities result in the rod eroding as it pushes through the target material. Thus, the longer the rod, the thicker the armor it can perforate. As rod lengths increased, so did sabot parasitic mass. Advances in sabot design and materials and in interior ballistics have actually resulted in ever-increasing muzzle velocities for longer and longer and hence more and more lethal LRPs.

¹ Round: The complete piece of ammunition, or alternately, a projectile in flight.

² Projectile: The entire entity projected by the gun, either in the gun bore, or alternately, flying through the air after the sabot has been discarded.

³ Penetrator: That part of the projectile intended to penetrate the target. Other parts, e.g., fins, are just parasitic mass as far as the penetrator is concerned.

2.2 LETHAL MECHANISM OF KE PENETRATION IN CHEMICAL ENERGY (CE) WARHEADS

Most practical CE warheads produce one or more KE penetrators intended to defeat a target by perforation. This section discusses KE penetration as a major element of the terminal effectiveness of such weapons.

Historically, the first CE warhead was the HE fragmenting munition, typically artillery rounds, bombs, and grenades. While the blast from a bare explosive charge is effective and can make a major dent in thick armor plate, it is the fragment cloud from the metal or other casing that is most lethal. A rule of thumb in warhead test facilities is that a well-designed containment facility that can reliably contain all possible fragments repeatedly will also withstand the blast. A typical fragmenting munition **would be an "iron bomb" dropped from an airplane** or an HE shell fired from a gun. According to the Federation of **American Scientists' Military Analysis Network's** Department of Defense (DoD) 101 web site [9], a U.S. Mark 82 500-lb dumb bomb has a bit over 200 lb of HE in a casing weighing roughly 300 lb.

The velocity of HE-thrown fragments is about as fast as or faster than the fastest projectile from the highest-performance, single-stage powder gun, 1,500–2,500 m/s. Fragment velocities are computed using the Gurney equations [10]. These equations are physics-based models originally developed by R. W. Gurney of the U.S. Army Ballistic Research Laboratory (BRL) in the early 1940s for plates on sheets of explosives, and they were expanded by others to encompass all conceivable geometries. They predict the throw-off velocity of an inert plate or shell contacting a layer of explosive, with or without tamper, using an experimentally derived constant for the energy of the specific explosive in question. The expansion and rupture of the casing into fragments use up some of the energy initially imparted to the metal sheet, and air drag

slows the resultant fragments rapidly as they approach the intended target.

The size of a fragment from a monolithic shell containing a simple explosive fill depends on the explosive loading conditions, the metallurgy of the case, and the case wall thickness. For example, the slivers from a particular 155mm howitzer HE round are about the size of a little finger, and many can perforate more than ¼ in. of armor steel at close range. The actual design of fragmenting warheads is usually much more sophisticated than just a shell filled with HE.

A range of technologies is available to optimize the fragment mass distribution. Modern warheads can be a simple shell of nonballistic material over an array of preformed fragments. As the detonation wave passes, these fragments are compressed radially. Metals are very stiff (nearly incompressible) and, for stresses not too far above the yield stress, are modeled as undergoing elastic expansion or contraction to the yield point and are considered incompressible in the plastic regime. (Under conditions of explosive loading, however, metals can be significantly compressed, but this is generally ignored in warhead design.) Under this assumption, compression in a direction of one of the three mutually perpendicular axes (e.g., radial [perpendicular to the axis of revolution]) is accompanied by the extension of the individual fragments in the other two axes (e.g., axial [parallel to the axis of rotation] and circumferential [tangent to the circumference]). Any conditions of confinement will affect the partitioning of the expansion, but not the total expansion. (An example of this is the continuous, welded railroad rail. Unable to extend along the direction of travel when heated or cooled, it simply expands in the directions normal to the direction of travel.) As the shock wave encounters free surfaces on the fragments to be accelerated, some of the material in each fragment may be thrown off, so final striking mass may be less than intended. There are a number of ways

to optimize fragment mass and direction and maximize velocity.

The penetration ability of individual fragments depends on their material, their striking geometry (attitude), and the vector velocity of impact relative to the intended target. The velocity of the fragments depends on their mass, and hence density, so a tradeoff is made to optimize terminal effects. For example, against aircraft targets, aluminum may be used for the fragments to gain maximum velocity and hence maximum hole size.

2.3 THE SC WARHEAD

The next CE warhead to be developed following HE fragmenting munitions was the SC or lined-cavity charge. It uses a metal-lined conical or similar cavity in the front of a cylindrical or, as shown in Figure 2-2, a truncated, conical-cylindrical explosive charge to produce a very high-velocity, thin, stretching jet on detonation (similar to a coat-hanger wire). Because it is primarily an antitank (AT) weapon, it is referred to as a high-explosive antitank (HEAT) round. An early, typical SC round, the M830, is compared to an early, typical LRP round, the M829, in Figure 2-3. A small, long, cylindrical spike on the SC warhead mounts the impact fuze well forward of the SC body to give time for the jet to form and stretch to its intended length. Both the M830 and M829 are designed for the Rheinmetall-designed 120mm smoothbore cannon on the M1 tank.

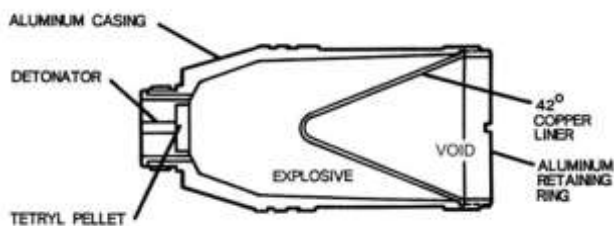


Figure 2-2. Cross-Section of an Earlier SC Warhead (Source: Dietrich [2]).

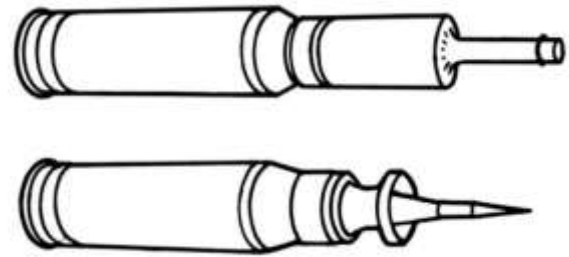


Figure 2-3. Typical SC (top) and LRP Rounds for the 120mm M256 Tank Cannon (Source: Silsby [1]).

After initiation, a detonation wave sweeps through the explosive charge forward over the liner much faster than the forward velocity of the warhead, throwing the liner progressively forward and inward onto itself on axis. The intense stagnation pressure at the center of the material sends a thin jet of high-velocity material forward and leaves a low-velocity slug, which does not contribute to lethality except that it is necessary to the formation of the highly lethal jet (Figure 2-4).

The jet stretches as a result of a velocity gradient resulting from the exact design of the warhead. The farther from the target that the warhead is detonated (the standoff), the longer is the jet striking the target and the thicker the armor it can perforate. Typically, the jet tip can be moving at over 10 km/s, while the last effective portion of the jet might be traveling at 2 km/s.

Engineers selecting metals for military applications typically consider ductility, a measure of how much a material stretches in tension before breaking. Most materials that are ductile are also malleable, that is, they can be severely deformed in compression before breaking up, although the correlation between malleability and ductility is not universal. The SC liner is typically made of a very malleable material, usually copper or a higher-density material such as tantalum. In military applications, the jet material is solid metal, well below its melting point, and where the slug goes is unimportant. In their primary civilian use, to perforate oil

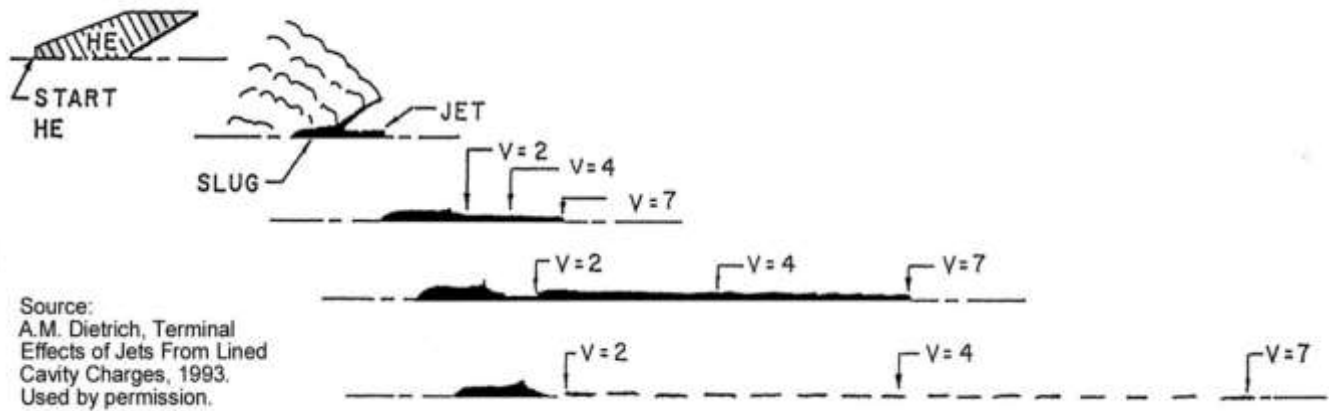


Figure 2-4. SC Jet Formation (Source: Dietrich [2]).

well casings, liners will often be powdered metal in a frangible binder. The jet they throw will perforate the well casing and penetrate the strata but not plug the hole, as would a solid slug, thus allowing the oil to flow back into the well.

For the military SC, at some elongation, the jet will break up (particulate) and will gain no further penetration capability with time (and distance down range). Rather, as the particles move off axis and tumble, performance declines. Figure 2-5 shows a typical penetration-standoff curve for a post-WWII era military SC warhead. Current SC design technology is very mature and so is not discussed in detail in this monograph.

The jet from a SC warhead penetrates hydro-dynamically, i.e., the impact pressure is so high relative to the penetrator and target material strengths that they appear to be strengthless fluids. SC penetration is essentially independent of velocity, depends on relative densities, and for a given combination, length alone is the determinant of depth of penetration under ideal conditions.

In a real warhead, the jet does not have a lot of standoff, so elongation is limited, but the jet creates a deep

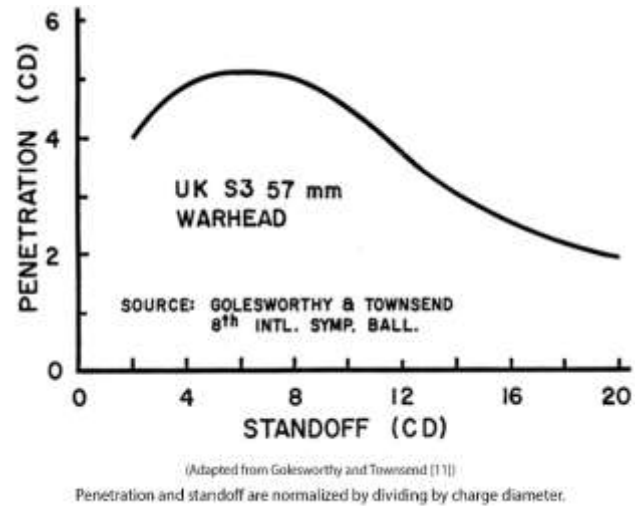
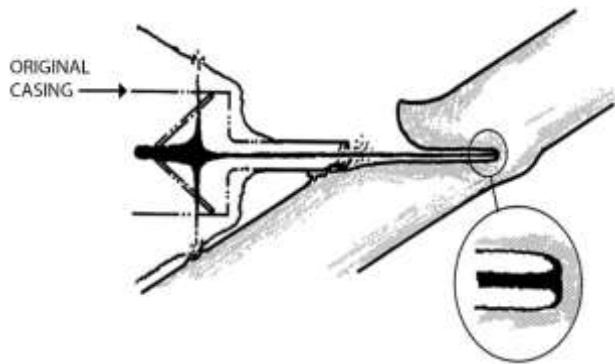


Figure 2-5. Typical Penetration-Standoff Curve (Source: Silsby [1]).

tunnel, which allows the rear portion of the jet to elongate more than expected from the standoff alone. Figure 2-6 illustrates SC penetration. Many warheads throw a nearly radial spray of very high-speed debris that leaves a characteristic splash signature around the primary penetration.

Some tank main gun systems use a round in which the casing on a SC warhead has been designed for fragmentation, so one round serves as both an AT and an antimateriel round. This design reduces the SC's



Phantom line shows original casing.

Figure 2-6. Typical SC Penetration of Armor Plate (Source: Silsby [1]).

effectiveness to some extent relative to that from a nearly full-bore liner, as performance scales with linear dimension. However, using a more sophisticated liner geometry ensures adequate jet penetration performance. There are many practical advantages of not having to choose between loading an HE or a HEAT round. From personal observation of the effects on range impact area infrastructure of one such round, about half of the fragments can perforate ¼-in. structural steel at close range.

2.4 OTHER LINED-CAVITY CHARGES

Nonjetting variants of the lined-cavity charge evolved contemporaneously with the SC. One example is the hemispherical liner warhead. The interaction of the advancing detonation front with the hollow hemispherical liner first accelerates its central element forward at high speed, while with time the material is thrown increasingly on axis on top of the earlier material until the detonation front has swept the warhead. The impact forces elongate the building penetrator, which, like the SC jet, elongates in flight and ultimately breaks up, but at much greater range than the SC jet. The result is a relatively short, LRP-like projectile that is lethal at very long standoffs (Figure 2-7). Note that while the liner material piles on itself and elongates as in the SC warhead, it does not form a jet and slug, so that all of the liner mass is effective.

Another lined-cavity charge is the explosively formed penetrator (EFP) (Figure 2-8). A carefully designed liner, usually mildly curved and often of variable thickness like a lens, lines the forward end of a puck-like explosive disc, also usually having a very carefully engineered shape. Central detonation from the rear throws either the center (rearward folder) or the periphery (forward folder) forward relative to the rest of the metal and produces a



Figure 2-7. Penetrator from SC with Hemispherical Liner (Source: Dietrich [2]).

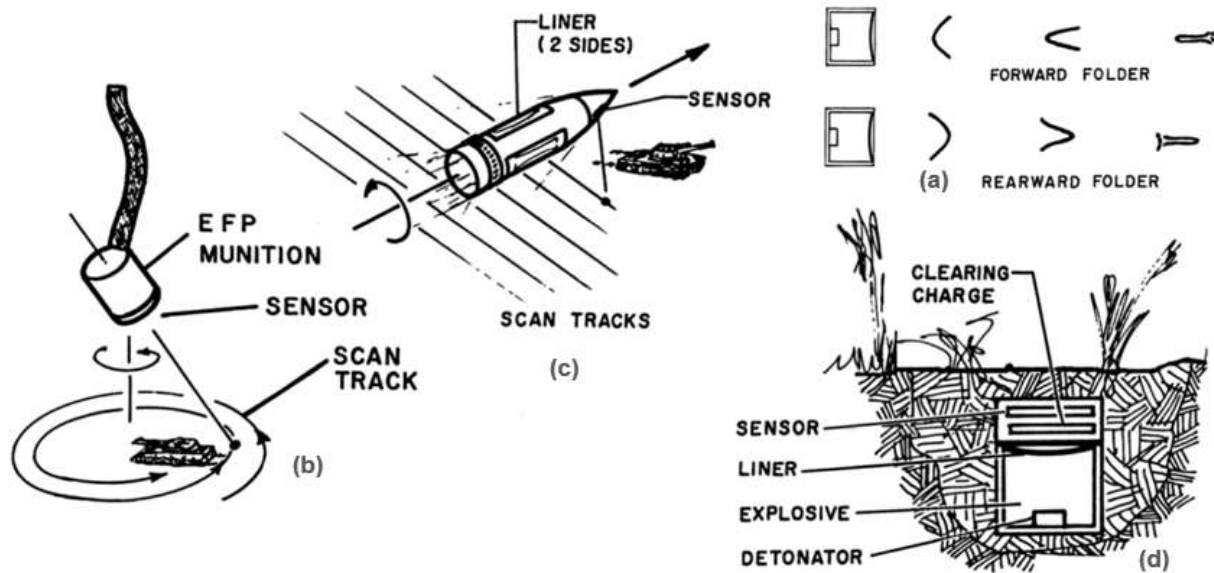


Figure 2-8. EFP Smart Munitions (Source: Silsby [1]).

shorter slug, again incorporating most of the liner mass. Unlike the SC, which forms a jet that springs off a slug, and the hemispherical liner, which forges itself into a stretching slug, the EFP merely forges a nearly cylindrical, thin metal disk into a nonstretching slug with little or no mass loss. Slugs from both the hemispherical liner and from the EFP warheads travel at about 2,500 m/s.

Figure 2-8 view a shows the two classes of EFP warhead design. The results on a target are about the same. In view b, a submunition dispensed from an artillery or rocket round falls over the target area. It is suspended from a special parachute such that its sensor scans an ever-decreasing spiral on the ground. It is initiated at the appropriate time after a target is detected, attacking the relatively thinner roof armor of the tank. In view c, an artillery round scans for a target as it flies over the battlefield. At the appropriate time after target detection, the warhead initiates. There would be more than one liner to provide adequate ground coverage.

View d illustrates an EFP AT mine. When the sensor detects a tank above it, the fuzing initiates a programmed sequence that first blows off the overburden and sensor hardware with a black powder charge, revealing the liner, then detonates the explosive to form the slug that perforates the relatively thinner armor on the bottom of the tank.

2.5 THE IMPORTANCE OF INCREASED KE PROJECTILE STRIKING VELOCITY

The history of the evolution of the KE projectile has been a series of increases in velocity and in length. Velocity increase is extremely important at ordnance velocities because impact pressure rises with the square of the striking velocity and penetration increases until the impact pressure is much higher than the strengths of the materials involved, and penetration becomes like a liquid-on-liquid process (hydrodynamic penetration).

Figure 2-9 shows typical data for penetration per unit length (P/L) of penetrator into a solid (monolithic, semi-infinite) armor target, as a function of striking velocity. The data are from Tate et al. (1978) [12], Silsby (1984) [13], and Cuadros (1987) [14]. The various regimes are labeled with bars spanning the velocity range. Note that what one person labels as a blistering 5,000 ft/s is **another person's** much slower 1,500 m/s. Also note that what one person calls hypervelocity is really hypervelocity, while the muzzle velocities for HVAP shot are on the low end of the ordnance velocity interval. SC jets strike in the 7–9 km/s velocity regime, while the speed of sound in steel is about 6 km/s. Because the interface between the penetrator and the target sinks into the target at some fraction of the striking velocity, almost all penetration is subsonic relative to the speed of sound in metallic and ceramic armor.

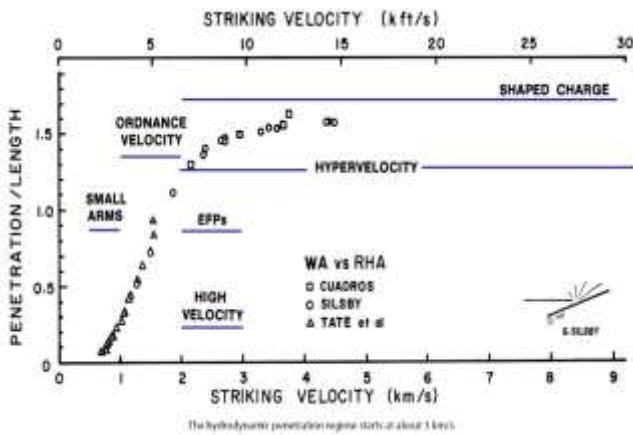


Figure 2-9. Typical P/L vs. Velocity Data for Tungsten Long-Rod Penetrators vs. RHA (Source: Silsby [1]).

Over the whole curve, the increase in penetration with velocity is the greatest at typical tank cannon LRP velocities. By adjusting the gun and projectile system to slightly increase velocity while launching the same length of penetrator (but not necessarily the same diameter), it will be able to perforate thicker armor, and hence defeat more heavily armored tanks. Again, the curve is per unit length of penetrator. By doubling length, penetration is likewise doubled, at least to a first

approximation. In the remainder of this monograph, “KE penetrator” refers to a long, fast KE penetrator and not AP shot or an HVAP round.

2.6 ADVANTAGES AND DISADVANTAGES OF KE VS. SC AMMUNITION

2.6.1 KE Ammunition Advantages

In general, explosively filled rounds can only endure limited acceleration without risking an in-bore detonation and hence have a low muzzle velocity relative to antiarmor LRP rounds. This disadvantage, coupled with their bluff bodies, makes explosively filled rounds more subject to disturbances in flight such as buffeting cross winds and gives more time for the disturbances to grow before impact; hence, they are less accurate than KE rounds.

In contrast, the flatter trajectory of a KE round reduces inaccuracy from poor range estimation, which results in a better probability of hitting a target. The KE initially imparted to a SC round does not contribute to its penetration, and its blast does not couple well to heavy structures such as tanks. However, when a KE round fails to perforate and is stopped in a target, most of its KE is absorbed by the target, producing a severe shock. In a perforation, more behind-armor debris is generated by a KE projectile as opposed to a SC jet, which increases the **KE projectile's** probability of a kill given a perforation. In addition, the inert projectile in KE ammunition helps reduce vehicle vulnerability if its ammunition stores are hit.

2.6.2 KE Ammunition Disadvantages

There are disadvantages to KE ammunition as well. Its velocity decay reduces its effectiveness with range to target. While it is never good practice to fire over

friendly territory, the SC round at least is composed of a single projectile following a predictable trajectory. In addition, the sabot petals ejected from a KE round endanger a large area ahead of the gun, and the KE ammunition has poor spotting ability. The ideal tank engagement from the friendly force's point of view is attack from a prepared ambush. Given that the ambusher can only fire two or three shots before becoming vulnerable, and there may be two more from a nearby, prepared firing position, it is imperative that the gunner be able to determine his hit point promptly so as to re-lay (re-aim) the gun for subsequent shots. The small diameter of the KE round leaves only marginal space for a tracer, which is necessary for the gunner to judge the trajectory before impact.

Also, while a KE round just disappears into the dirt or trees, if the SC round detonates, it creates an unmistakable signature. The blast, flame, and smoke from a nonlethal hit or close strike have considerable **shock and screening value, possibly slowing the enemy's counter-fire**. Finally, whereas the LRP is strictly an antiarmor munition, the multipurpose SC munitions have intentionally traded away some of their impressive penetration capability to add a fragmenting case, so some antipersonnel rounds normally carried can be replaced with them, **increasing the tank's capability in its primary role as a tank killer**. These advantages and disadvantages of KE ammunition vs. HEAT rounds are summarized in the following lists.

KE ADVANTAGES VS. HEAT

- **High velocity results in:**
 - Flatter trajectory, hence less influence of ranging errors
 - Shorter time of flight, hence less influence of target lead errors

➤ **Highly lethal behind-armor debris fan**

➤ **Maximum available energy goes into penetration**

➤ **Inert projectile reduces vulnerability**

KE DISADVANTAGES VS. HEAT

➤ **Velocity decay reduces penetration capability with range**

➤ **Discarded sabot petals endanger a large area ahead of the gun**

➤ **Poor spotting ability**

➤ **No psychological shock/screening in a nonlethal hit or near miss**

➤ **Lack auxiliary antipersonnel/anti-materiel effect of HEAT's blast, case fragments**

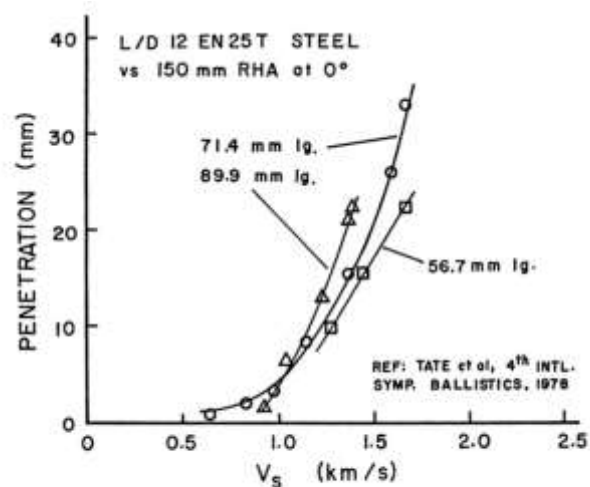
3. NORMAL INCIDENCE SEMI- INFINITE PENETRATION: DATA

Chapters 3 through 7 will address only KE penetration. A good approach to understanding the penetration process is to study the simplest interaction geometry first. After the processes at work are understood, then additional factors can be explained one at a time. The simplest interaction is for a penetrator in the form of a long right circular cylinder of uniform properties to attack a half-space of armor. The rod trajectory is at right angles to the target face. This is referred to as normal incidence penetration. The rod axis lies along its line of flight, not tipped (yawed). The process is then symmetric around the striking rod's axis and is two-dimensional. That is, the values of variables depend on two distances: along the axis and along the radius, but not along the third dimension, the angle around the axis from some arbitrary plane containing the axis of symmetry, e.g., vertical.

The effect of various penetrator and target parameters (variables) is discussed in this chapter, as opposed to the effect of striking geometry parameters, such as target obliquity and yaw. Rather than a discussion involving a fixed velocity, the information is presented as a curve that relates response to increasing velocity. Note that most of these data were generated at reduced geometric scale, i.e., with small penetrators and targets, not something shot from a tank cannon. Also, there is a fundamental difference between the behavior of the commonly used steel and tungsten penetrator materials and that of DU. The data used in this chapter are initially from attack by steel alloy penetrators, then some tungsten (powder metallurgy) alloy rod data are used.

3.1 EXPERIMENTATION AND DATA INTERPRETATION

Figure 3-1 illustrates total penetration (not penetration per unit length [P/L]) for various lengths of a British tool steel rod into a very thick armor steel target. Note that the penetration increases with rod length, as expected. However, the curves cross, and may not even have the same shape suggesting a more complex process than expected. **An experimentalist's job when exploring new concepts is to determine the underlying physics where possible, or barring that, at least generate sufficient data at appropriate points so the underlying physics can be modeled empirically with sufficient accuracy to be useful in the development process.**



(Adapted from Tate et al. [12])
 All rods are British EN25T steel of length-to-diameter (L/D) ratio of 12.

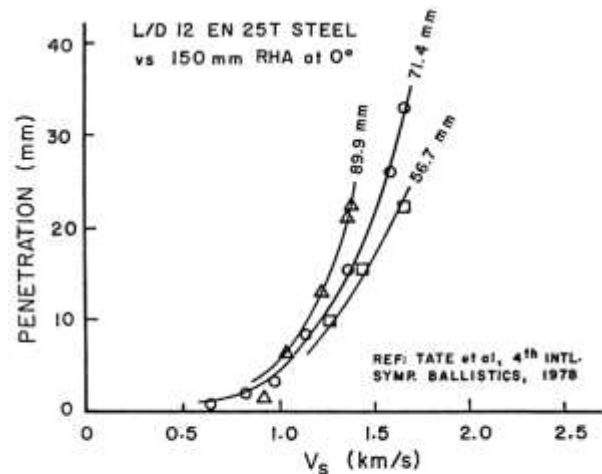
Figure 3-1. Penetration vs. Velocity for Three Rod Lengths (Source: Silsby [1]).

Data should be interpreted carefully. Each data point is a sample of reality, as representative as the experimenter can practically achieve, but undoubtedly subject to random error not necessarily normally distributed. For well-behaved data, and absent any knowledge of the physics behind the process, the best curve to fit through three points is a straight line. If the behavior is constant, the line will be more or less horizontal. The straight line

is an approximation to the behavior studied in the region where the data exist. The straight-line fit allows generation of actual numbers that predict future behavior and some estimate of the errors in the experiment by seeing how the individual points vary from the straight line fit that minimizes the error. With only three data points, there is no way of estimating the actual behavior very far away from the region of the data points. So maybe the nearly straight line for the 56.7-mm rod length is curved like the line through the extensive 71.4-mm data set. A few more data points at the extremes would help to improve the precision of the curve.

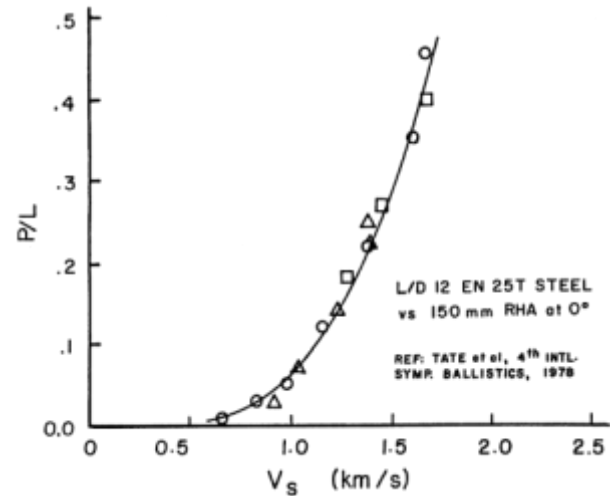
Smooth processes should result in similar curves, not ones that cross, like the 71.4-mm and 89.9-mm lines shown in Figure 3-1. The only reason the 89.9-mm line for the longest rod crosses that of the middle one is to try to approach its lowest data point. However, the error due to the fit must also be balanced among the other points. Each point is weighted equally in the fitting scheme when the error distribution is unknown. It would appear that no simple curved line would be able to fit well through the two bottom points. Maybe there is a gross error in the lowest point, and the curves look like those in Figure 3-2 and Figure 3-3.

It does not seem unreasonable for one single data point in a set of 15 to be an outlier. However, if it is, and is in the wrong place on the graph (at the extremes of the curves), it could make interpretation difficult. Again, a few more data points would clarify this uncertainty. A **statistician's rule of thumb in curve-fitting** is that at least five data points plus the number of parameters in the fit are needed before the fit will not be unduly influenced by outliers [15]. By any measure, the data set for the 56.7-mm long rod in Figure 3-1 is a bit inadequate if the performance curve is a parabola originating at some point on the horizontal axis (zero velocity would certainly result in zero penetration, while target strength would



(Adapted from Tate et al. [12])
 Without information about the shape of the curves to expect, this interpretation of the data is less plausible than that of Figure 3-1.

Figure 3-2. Another Interpretation of the Same Data Set as Shown in Figure 3-1 (Source: Silsby [1]).



(Adapted from Tate et al. [12])

Figure 3-3. Normalizing Penetration by Rod Length Simplifies the Data (Source: Silsby [1]).

suggest a positive velocity below which no penetration would be observed).

Plotting data as they become available can make it easier to resolve questions about the data. Shots should be concentrated at extremes and at velocities where the data would best influence the shape of the regression. A

certain number of shots in a firing program should be allotted in advance to clean up the data after the preliminary analysis, even if it means scheduling a second block of time in the range. The clean-up shots must be planned in addition to those allotted for repeating shots when there is something obviously wrong (bad velocity, bad yaw, target mounted upside-down and backwards in the butt, etc.). It is important to make extra penetrators and targets in the beginning, because finding identical materials later on may be difficult, and producing a small batch of any part is not economical.

Do not throw out any data point as a result of how well or poorly it fits a curve. The postulated curve may not reflect reality, or there could be a lot of real variability in the process, as opposed to error in measurement. Preset criteria should be used to decide when to disregard data, e.g., yaw in excess of 1° or velocity outside a plus or minus 20-m/s window. Then all data that falls outside the window of acceptability should be excluded from the analysis, not just the points that are inconvenient for your hypothesis. The variation in penetration data is not usually normally distributed, which is an assumption that underlies most commonly used data-fitting schemes. Small variations in measured velocity, materials properties, etc. probably are normally distributed, but the effect of pitch and yaw is probably nil up until some threshold, then it only degrades performance, never improves it, at least on normal incidence targets.

One measure of penetrator vs. armor performance is to measure the velocity at which the penetrator will just perforate a given armor. Candidate penetrator designs can then be compared quantitatively. In this so-called “limit velocity” testing, knowing the exit velocity adds significant information, so striking velocity vs. residual velocity plots largely supplanted the earlier method for determining the limit velocity that just used whether or

not the target was perforated. Lambert and Jonas [16] of BRL developed an early computer data-fitting algorithm that used information from both perforating hits and nonperforations.⁴

To collapse the datasets in Figures 3-1 and 3-2 to the same curve, divide **by the rod’s initial striking length** (normalizing the data) (Figure 3-3). A simplifying scheme such as this aids in spotting bad data points also. It has the same result as pooling data from several sets. If the rule used is good, it increases confidence in the shape of the curve while slightly broadening the region around this central trend in which the actual behavior could be expected to lie if a large number of additional shots were fired.

3.2 EFFECT OF ROD LENGTH ON DEPTH OF PENETRATION

The data presented and their interpretation in Section 3.1 reveal that increasing the length of a long-rod penetrator at a given striking velocity increases the penetration depth proportionally, while increasing the striking velocity of a given length of penetrator increases the depth of penetration. The data here suggest that this depth of penetration increases strongly with velocity, but as later data will show, the curve turns down at about 2 km/s and becomes nearly flat at about 3 km/s.

3.3 EFFECT OF PENETRATOR DENSITY ON PENETRATION

Next to length, penetrator density is the most important factor affecting penetration. Compare the two sets of long-rod (L/D 10 and above) data on the plot of P/L vs. velocity shown in Figure 3-4. Data for WA penetrator density of 17.3 gm/cm³ [13, 12] are supplemented with a single curve summarizing a large amount of P/L data for

⁴ See the Bibliography for useful resources for the analysis and interpretation of large amounts of data.

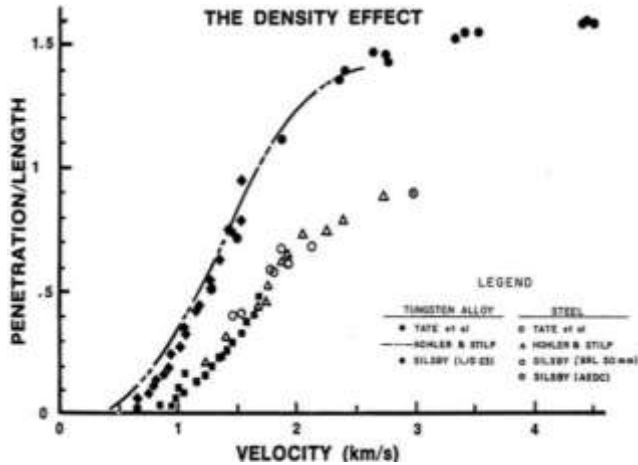


Figure 3-4. Effect of Penetrator Density on Penetration (Source: Silsby [1]).

approximately L/D 10 WA rods with densities of 17.0 and 17.6 gm/cm³ [17]. Well below this curve is a set of steel data [12, 18] (density of 7.83 gm/cm³) and is supplemented with a limited number of high-velocity, steel-penetrator, long-rod data from BRL's 50mm high-pressure powder gun in Range 309A [19]. The two sets of data are quite representative of their respective classes. Note the clear difference between their plots. It would be clarifying to collapse the data onto one curve.

This chapter presents observed data, while Chapter 4 presents the underlying physics. As will be derived in Chapter 4, if one considers the momentum balance on two strengthless jets of the same cross-sectional area of materials of different densities impinging on one another, one can solve for the relative penetration of one into the other. This number is proportional to the square root of the ratio of the two densities, totally independent of velocity. Empirically, this so-called "density law" has worked well for modeling SC jet-target interactions, where the average jet velocity is very high. While the KE penetrator data presented in Figures 3-4 and 3-5 show that penetration increases monotonically from zero to a bit above this density law number (theoretically 1.49 for typical ballistic WAs on steel and exactly 1 for like-on-like impacts), the data do appear to be flattening out near

the density law value at high velocities, and the difference between the two curves in each figure appears to be proportional to the velocity.

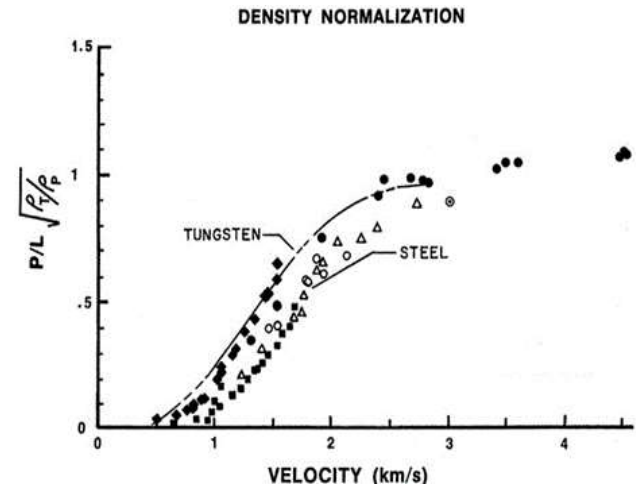


Figure 3-5. Normalized Density Curves (Source: Silsby [1]).

The raw data in Figure 3-4 are corrected by this factor and replotted in Figure 3-5. (Since the ratio of target-to-penetrator density is unity for steel on steel, only the tungsten-on-steel curve is affected.) Using this factor reduces the spread between the two curves considerably, but obviously doesn't completely remove all differences, particularly at ordnance velocities, the range of velocities from current powder guns (about 1–2 km/s).

3.4 EFFECT OF PENETRATOR AND TARGET STRENGTHS ON PENETRATION

There are two strengths involved in penetration: penetrator strength and target strength. At striking velocities where the penetrator erodes, penetrator strength has little effect on penetration. While the effect of target strength is significant, it is not as significant as target density.

3.4.1 Strain Rate Effects on Material Strength

Material strength is dependent on the rate at which strain (deformation) is applied. Under ballistic impact, both penetrator and target materials tend to act stronger than observed in a tensile or compression test conducted at normal deformation rates. This observation is confirmed by the results of special tests (Hopkinson bar impact tests) developed to measure material properties at strain rates up to about 10^6 mm/mm per second, typical rates encountered in ballistic impacts. Increases in apparent strength of up to about three-fold over quasistatic strength may be observed, with this strain rate effect more apparent in some materials than others.

3.4.2 Temperature Effects on Material Strength

Temperature also affects material strength. The hotter a material is relative to its melting point, the lower is its strength. Over the most extreme temperature range available in the environment, this effect is probably not noticeable in tungsten, sinter-alloy, LRP, but it is a minor influence in steel. The difference in temperature between an armor plate shot at 10°F during the winter and at perhaps 160°F after being in the summer sun all day will be reflected in the data when a very sensitive measure such as limit velocity is used. (It is more significant that small changes in the temperature of the propelling charge will significantly affect the muzzle velocity, and hence the outcome of a test, but the striking velocity should always be measured and recorded.) It is important to either conduct tests under reasonably constant conditions (there will be no noticeable difference over a range of typical indoor temperatures) or record the (estimated) temperature of the components in case some questions arise.

3.4.3 Penetrator Strength

No homogeneous set of data from the literature could be found to compare the effects of penetrator strength, i.e., data where all factors other than strength were held constant. Data from disparate sources with penetrator hardness, and hence strength, varying from very soft to about a hardness of 55 on the Rockwell C (HRC) scale, unfortunately were sparse and included data from shots with and without bulges and revealed no systematic trend.

3.4.4 Target Strength

The data showing the effect of target strength in Figure 3-6 come from a comprehensive work by Hohler and Stilp [18] and from Sun, Wu, Zhao, and Shi [20] in China. Hohler and Stilp were unclear about whether the strength reported was yield or ultimate. Target strengths varied from that of typical structural steels to that of armors. There is an almost linear correlation between hardness and strength [21], so strengths are shown that were inferred from hardnesses where strengths per se were not reported. Strengths and hardnesses were not

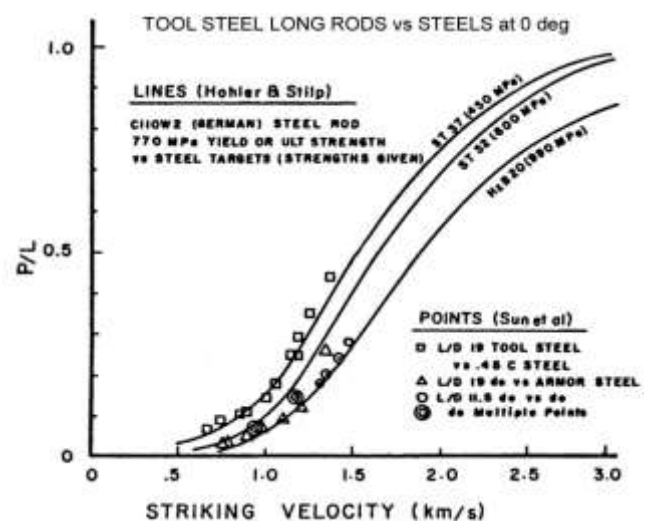


Figure 3-6. Effect of Target Strength on Penetration Depth
 (Source: Silsby [1]).

3.6 PENETRATION HOLE VOLUME

Hole volume is related to both penetration depth and hole diameter. Armor-piercing shot will produce a hole whose diameter is just that of the shot. At higher velocities, an eroding penetrator will produce a hole of a characteristic diameter depending on striking velocity, strength, and failure behavior, which vary considerably among penetrator materials. Conceptually, as the striking velocity for an LRP drops, at some point the hole diameter will just be large enough to pass the erosion debris. If the eroded penetrator debris is laid into the hole at the speed the interface advances, the hole diameter must be 1.414 times the rod diameter to just pass the debris. While it has been postulated that hole volume in typical ductile metallic targets may be proportional only to striking energy, experimental researchers such as Hohler and Stilp [17] have found that to be the case only at striking velocities well above the ordnance velocity regime (Figure 3-8).

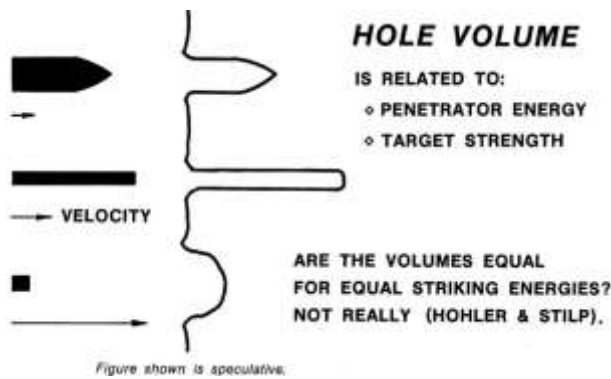


Figure 3-8. Hole Volumes are not Entirely Proportional to Striking Energy (Source: Silsby [1]).

3.7 THE L/D EFFECT

Penetration depth is not necessarily independent of rod length and diameter. Under a set of conditions where the aggregate sum of all of the various nonsteady state effects was not close to zero, an effect of L/D on penetration depth would be expected. (Of course, there

could be large differences in behavior from that occurring during steady state, but they would balance each other out, and would not be noticed unless we set out to study them in detail instead of just looking at the final penetration depth.)

These effects can be grouped into start-up and end-of-penetration effects. The penetrator could be heavily influenced by the free surface of the target face until the penetrator-target interface had sunk a number of rod-diameters into the target where the target material is heavily confined. Similarly, when the interface gets within some number of rod-diameters of the target's rear surface, target self-confinement drops. If an LRP were fired into a very thick target down a long hole, so that penetration both started and stopped deep in the interior, constraint conditions would be considerably different than striking the same target on an open face. Differing P/L values for the two different striking conditions would be evidence of such a free-surface effect.

Several other end-phase scenarios could result in an L/D effect. The target is penetrated by the penetrator-target interface. While this feature advances at some fraction of the striking velocity, its speed is not negligible. As the last of a penetrator is spent on the target, perhaps the zone under it continues to advance a bit. Likewise, under certain striking conditions, penetrator material everting into the penetration channel can have a forward velocity. Perhaps this annulus of material then slams into the bottom of the channel, increasing the depth of penetration a bit. These possibilities will be discussed in Chapter 4, which addresses mechanics rather than data uninformed by physical understanding.

An L/D effect on the P/L vs. velocity curve is expected when significant influences cause the total penetration to be different than expected from the steady state rate. In mathematical form, this can be written:

$$\frac{P}{L} = \frac{P_{uniform} + k}{L} = \frac{P_{uniform}}{L} + \frac{k}{L} \quad (1)$$

The k is probably a function of velocity, and the $\frac{P_{uniform}}{L}$ term would be approximated by very long rod data, where the presumably short-lived, unsteady state effects are swamped by the long duration of the steady-state phase. If it is assumed that the hole growth was reflected in the seemingly linear hole diameter vs. velocity data, the second term could be refined by writing it as aV/L , where a is a constant.

3.7.1 Normalizing L/D Data

The L/D effect is quite significant as shown in Figure 3-9, which illustrates copious iron-on-iron data from numerous sources cited earlier [17–20, 23]. These data can be normalized by finding a k in Equation 1 that collapses all the data onto one curve.

The normalized curve shown in Figure 3-10 shows significant reduction in spread. The value of k was computed from data at one striking velocity. Note that the L/D 5 line blends into the L/D 1 line, and that the

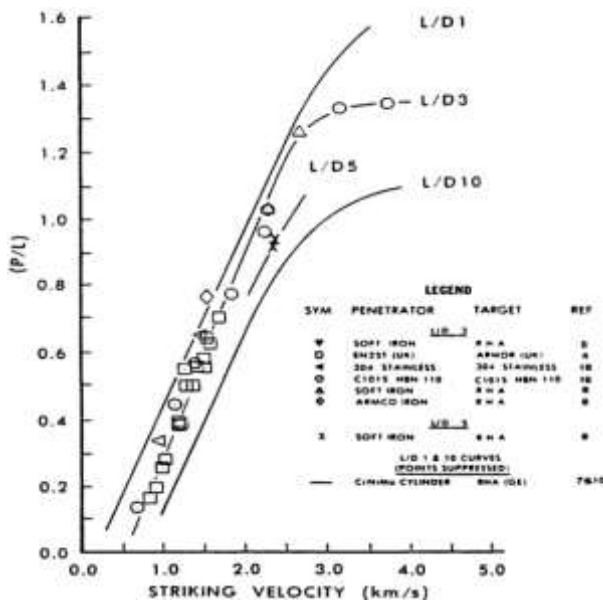


Figure 3-9. P/L vs. Velocity as a Function of L/D (Source: Silsby [1]).

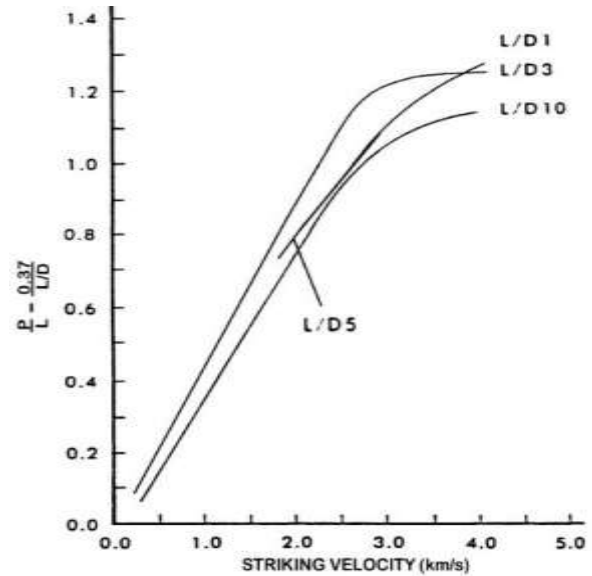


Figure 3-10. Normalization by L/D (Source: Silsby [1]).

L/D 1 and L/D 10 curves lay essentially on top of each other up to about 2.5 km/s, seeming to imply that whatever effect causes this difference in penetration is independent of velocity. This result **doesn't appear to** support the hypotheses about secondary penetration and target inertia causing additional hole growth, as these phenomena should increase dramatically with increasing striking velocity. Note that the value for semi-infinite penetration for an infinitely long rod is only a few percent below that of an L/D 10 rod, which implies that the hole growth term is small.

3.7.2 Exploiting the L/D Effect

If the P/L for an L/D 1 penetrator is significantly greater than that for an L/D 10 penetrator, it has been suggested that an existing rod be cut up and spaced out, as suggested in Figure 3-11, to improve overall penetrator performance. This possibility was once an intriguing topic for discussion, **but now the reason why it doesn't** work has been discovered. The debris from individual segments is everted and rebounds back towards the

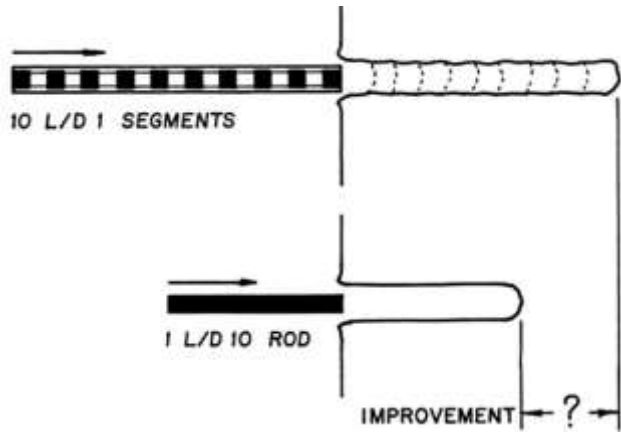


Figure 3-11. Exploiting the L/D Effect (Source: Silsby [1]).

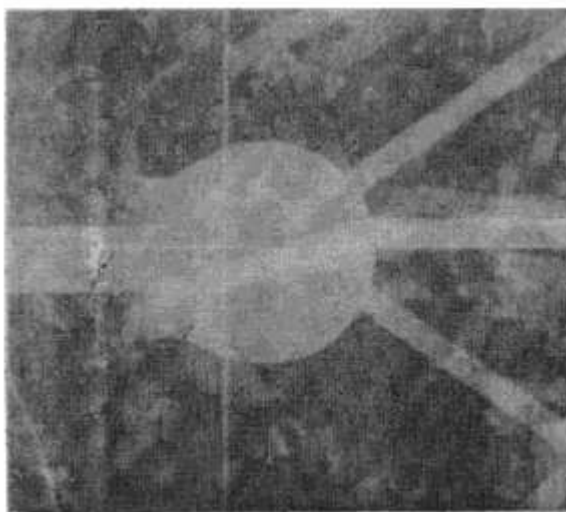
penetrator axis, interfering with the following segments, a familiar phenomenon in SC jet penetration.

3.8 MORE MATERIAL PROPERTIES IMPORTANT IN SEMI-INFINITE PENETRATION

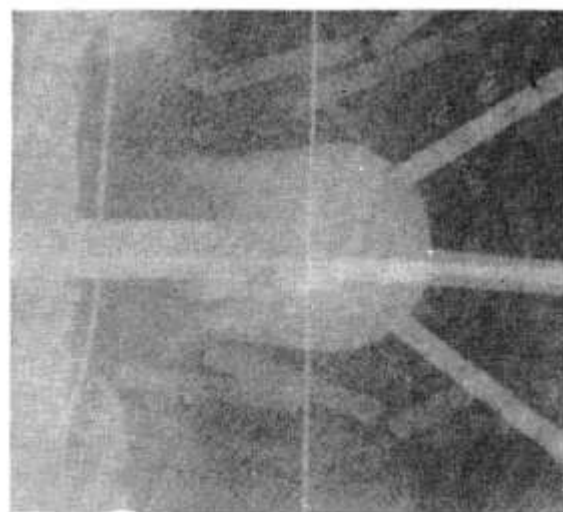
Most of the semi-infinite penetration process that counts occurs with the penetrator and target in a state of compression and shear. The compression tends to keep cracks shut and not induce them to run rapidly. Under

these circumstances, the notch sensitivity of materials is not as important as when the materials are in a tensile stress state. Many times, the materials are being employed in a relatively soft and very tough state, with very large critical stress intensity factors, as in RHA. A pair of radiographs, shown in Figure 3-12, illustrates an important point that is not well understood: A target degrades a penetrator only when and where it contacts it. At normal incidence, the degradation is in the form of erosion, while at oblique incidence, the penetrator is both eroded and given a tipping rate. If identical penetrators at identical velocities perforate a brittle and a ductile target of otherwise similar properties, it is irrelevant in terms of the effect on the rod that the brittle target was later found as dust, while the ductile target is intact with the exception of a hole in it. Ductility and strength are usually not independent properties. If structural integrity and second-round hit protection are not issues, in armor, it is advantageous to trade away ductility for strength, so as to erode more of the rod with the same thickness and weight of armor.

The 1-in. diameter ball on the left in Figure 3-12 is a steel bearing ball, while the one on the right is an aluminum



STEEL BEARING BALL TARGET



CERAMIC GRINDER BALL TARGET

Figure 3-12. Steel (left) and Ceramic (right) Ball Targets (Source: Silsby [1]).

oxide ceramic grinder ball. The two shots, BRL Scaled Armor Concepts Program shots 292 and 293, were fired in 1978 to settle the question of whether the penetration process was the same or different in these two quite different target materials. Two identical penetrators were fired at identical velocities at the identical size balls and radiographed at close to the same time delay into the target. The penetrator, a rod about one-third the ball diameter, is entering the ball from left to right. (A common convention in ballistics and in this monograph where feasible, is that figures are drawn showing flight from left to right.) Both penetrators exhibit the water-splash like entrance signature in the penetrated zone. The radiographs reveal no significant difference, though multiframe radiographs are hard to interpret because several later images are overwritten on the same film. In this case, the residual fragments and pieces of the three small wooden dowels that supported the ball from the plywood to the right and the half-tone rendition further obscure the images. The only difference noted after the shots was that small but discrete chunks of the steel ball were left, while the ceramic was shattered to dust.

3.9 EFFECT OF SIZE (GEOMETRIC SCALE)

One of the most troubling considerations in terminal ballistic testing is having to operate at reduced scale due to launcher limitations, cost considerations, etc. It is well known that many materials are grainy as a result of their composition or processing. For example, concrete is an engineered composite in which the coarser part of the aggregate is gravel or crushed stone, and the finer part is sand. The distribution of sizes is carefully controlled to minimize void volume that must be filled with the cement-water paste that cures to a rock-like matrix. Most structural concrete includes steel reinforcing bar. If you have to test a munition such as a bomb designed to penetrate concrete, it is best to conduct many carefully controlled tests economically. Gun launching a reduced-scale simulant seems like the best approach. It would seem logical to make every part of the penetrator and

target a reduced-scale geometric model of the real thing. Modeling the concrete, including a reduced-scale reinforcing bar and the aggregate, would be challenging.

There are other considerations of this reduced-scale modeling. What about reduced-scale vs. full-scale penetrators of sintered and/or cemented alloys such as tungsten-nickel-iron? Should you start with finer powders and use scaled-down processing equipment to make the rods? What about precipitation hardening alloys such as DU alloyed with $\frac{3}{4}$ weight-percent titanium (DU-3/4Ti), or the maraging steels? How would the grain size of the base metal be scaled down, and what would be the metallurgical effects of scaling down the size of the precipitate, if possible? How would harden and temper alloys, of which RHA and 4340 are typical, be scaled down? Notch sensitivity definitely **doesn't scale geometrically**. Different fracture behaviors between model and prototype are possible.

Although it is challenging, scaling is not a serious impediment to developmental testing. No experimental evidence has been found that suggests that the result of a geometrically scaled test was far from that of the prototype. In the data for tungsten rods on RHA targets, presented earlier in Section 3.3 and shown again in Figure 3-13, the penetrator masses fired at ordnance velocity were less than 100 gm [12]. Three of the four Silsby hypervelocity data [13] are clusters of three shots at well separated requested velocities, with one or two 125-gm and one or two 250-gm geometrically scaled long rods. Only the three darkened symbols in Figure 3-13 (of the four Cuadros data [14]) are points in which the penetrators weighed in excess of 700 grams. Only the highest-velocity shots appear to be significantly above the trend.

The most important factor favoring reduced-scale testing is that many reduced-scale tests can be fired for the price of a single, full-scale test. The thorough understanding of the underlying mechanisms gained by extensive,

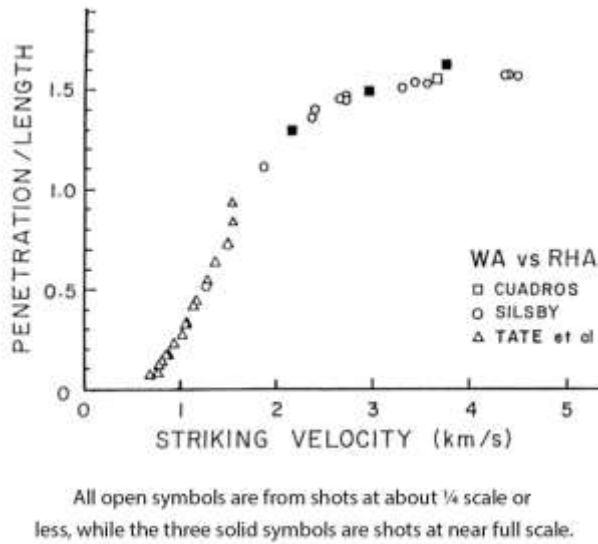


Figure 3-13. The Effect of the Geometric Scale of the Experiment (Source: Silsby [1]).

reduced-scale, exploratory testing can be applied to optimizing performance. In addition, a limited number of full-scale shots in the region around the optimum will prove (or disprove) the concept and at the same time provide a test of the scaling.

The size of the model should be as close to that of the prototype as practical or economical. Also, the model **materials' engineering properties (strength, elongation to rupture, etc.)** should be as close to those in the prototype as possible. For example, a model penetrator whose diameter is, say, **20 times the material's** characteristic grain size will probably behave the same as a full-scale penetrator that is 50 times the grain size in diameter.

Mass drops as the third power of the decrease in size, or scale factor. Thus, a small reduction in scale can frequently relieve a constraint imposed by excessive in-bore mass for gun-launched work. If a small velocity increase were needed from an existing gun, it would not be unreasonable to fire a model-scale ordnance velocity

shot at, say 80% scale, where the mass would be about 50% that of the prototype.

Within reason, every geometric dimension is reduced by the same scale factor. The aggregate in the concrete is scaled down. Thicknesses, lengths, hole dimensions, etc. are made smaller by the same amount in both penetrator and target. All material properties are kept the same as those of the prototype. Ideally, the model would be **made from the prototype's material or of its raw materials**. If practical, available materials are used. For example, the hardness of RHA varies with thickness (but not in the through direction in any plate): the thinner the plate the harder (and hence stronger) it is. Rather than slice thin plates from the corresponding thick ones, we have the temper drawn on thin plate to bring the hardness down to the value of the prototype. This method is a simple operation involving heating the plate to relatively low temperatures and holding it long enough to let the metallurgical transformations complete (typically a few-hour operation at most).

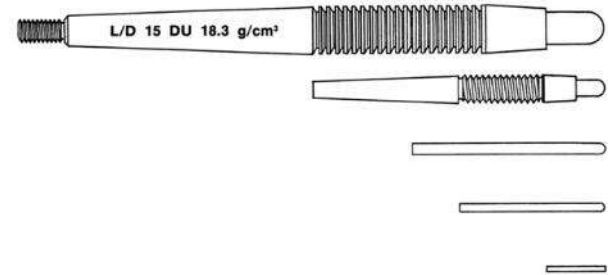
Geometric scaling cannot be applied to root radii on highly stressed areas of the penetrator or target because the stress intensity factor governs whether or not the material flows or cracks locally, not the average stress in the region around the radius or discontinuity. The stress intensity factor depends in turn on the size of a radius or other discontinuity (such as a typical flaw, crack, or inclusion) in the material. Typically, the size of driving lands and other features on a real projectile is limited by the minimum root radius that a single point tool can consistently generate during the entire finishing cut over the part. If the radii are below about 0.5 mm (0.020 in.), tools may be worn during cutting and may need to be replaced.

Thus, two factors militate against reducing the size of critical features on a scaled-down rod or target. One is that the prototype features are already so small that you will not be able to consistently reproduce them at a

smaller size anyway. The other factor is that high-strength materials such as penetrators typically have relatively low fracture toughness values, so that large part-sections are brittle rather than ductile. Thus, root radii and part geometry, and possibly metallurgy, should be adjusted to produce the desired stress concentration factor on impact, while considering changes in material property with strain rate, and so on. These adjustments are challenging to even the best stress analyst. It is recommended that parts be designed to be as simple as possible so that internal flaws rather than made-made features are the likely limiting factors. In this way, the model and prototype will likely perform the same. However, any brittle behavior should be noted.

To scale a penetrator down significantly, make the length that of the prototype times the scale factor. If the prototype is not close to a simple cylinder in geometry, make the model rod as close to the overall geometry as practical, e.g., long tapers are modeled as long tapers, long cylinders of different diameters are modeled as long cylinders of scaled diameters, etc. However, small details are not included. For example, a threaded fin hub will be modeled as part of the basic rod, adjusting model rod diameter slightly to maintain correct overall scaled length and mass. Features necessary for firing at reduced scale are freely included, e.g., using 60° V-form threads for traction launch. When there is no pressing need for all of the full-scale detail to be included on the reduced-scale rod, make it a hemispherically nosed right circular cylinder of such a diameter that the factor by which the mass is reduced is the cube root of the scale factor. This diameter is called the effective diameter.

Figure 3-14 shows how decreasing the scale factor affects the design, mass, length, and diameter of a penetrator. Drawn for the purposes of illustration only, the large penetrator on the top typifies an LRP. Made from an unusual uranium alloy having a density of



SCALE	MASS	LENGTH	DIAMETER
FULL	1000 grams	250 mm	16.67 mm
HALF	125 grams	125 mm	8.33 mm
THIRD	37 grams	83 mm	5.56 mm
QUARTER	16 grams	62.5 mm	4.17 mm
TENTH	1 gram	25 mm	1.67 mm

Figure 3-14. Geometric Modeling of a Penetrator as Scale Factor Decreases (Source: Silsby [1]).

18.3 gm/cm³, a 250-mm-long L/D 15 rod would weigh exactly 1 kg. The effective diameter of this speculative rod would be 16.67 mm.

As can be seen in Figure 3-14, a 50% decrease in scale radically drops the mass from 1 kg to 125 gm. The cylindrical forward part, which would mount a wind screen, has been scaled exactly, while the root radius at the intersection with the taper is identical to that of the prototype. The driving lands have been replaced with nonfunctional helical threads with the same root radius as the prototype, but with a minor diameter scaled down by 50%. The fin hub has been eliminated to provide a larger bearing area for push-launching. The rear taper would be the same, and minor irregularities in mass would be ignored. If necessary to provide enough bearing area, the taper on the rod would be altered to increase base diameter but maintain the correct scaled mass. At smaller scale, the rod becomes a hemispherically nosed right circular cylinder and finally loses the hemispherical nose.

4. NORMAL INCIDENCE SEMI- INFINITE PENETRATION: MECHANICS

Understanding penetration mechanics contributes to the understanding of the penetration data. Remember that the semi-infinite targets are being struck by long rods at normal incidence at ordnance (tank cannon) velocity.

4.1 THE REACTION OF PENETRATOR MATERIAL UPON PENETRATION

Upon penetration, the rod erodes while forming a cavity in the target. The main concept is that the rod everts, or turns back on itself, as though forming a tube. However, the material in the tube is not necessarily continuous. For the usual materials used in antiarmor LRP, the large shear deformations almost always result in particulation of the everted material. At the right striking velocity, this material lines the penetration channel and can be picked loose from a sectioned target. More-ductile penetrator materials will actually yield a continuous tube. Figure 4-1 illustrates the physics more clearly.

In Figure 4-1, view a, the important features of the penetrator are shown in the line art above the centerline. Below the centerline, a photo-composite evokes what the event must have looked like while in progress. An appropriate length of a photograph of an unfired rod (1) forms the tail. The sectioned tubular recovered penetrator material (2) from one shot, and the recovered cap (3) from another are pasted onto a drawing of the average penetration channel from two semi-infinite shots. The photo-composite is shown sectioned behind the cap, while the line art above the centerline is shown in full cross-section. The original undeformed teeth on

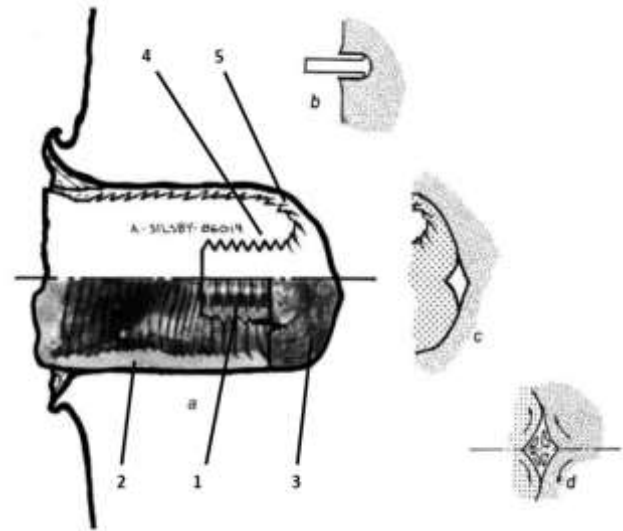


Figure 4-1. Penetrator Eversion During Penetration (Source: Silsby [1]).

the incoming rod (4) are badly sheared with additional sheared surfaces extending from the sharp root radii (5).

While the threads serve as tracers, improving the ability to determine the process from the recovered target and penetrator residue, it is not clear which way the teeth should point. The orientation appears to be correct from continuity considerations.

Rod erosion is a shearing process and is confined to a zone near the penetrator-target interface. Viewed standing still relative to this interface, penetrator material feeds into this zone from left to right as a rod and exits from right to left as a tube. Target material advances on the interface from the right and is pierced and opened by the action of the impact inertial forces of the penetrator stream. The penetrator-target interface can be considered to be a rigid punch sinking into the target at the interface velocity. The conservation laws, continuity considerations, an empirical relationship between relative erosion of rod and target vs. velocity, and various assumptions can be invoked to compute the rod material exit velocity with good agreement with reality. At ordnance striking velocities, the exiting tube

moves up-range at a very low velocity relative to the target, and, in fact, penetrator material is sometimes found adhering to the channel wall.

In the shot illustrated in Figure 4-1, the teeth on the surface of the rod restrict material flow at their base, while the root radii create high stress concentrations. These factors constrain the creation of new surface to the zone between teeth. These lines of shearing are suggested by the finer lines in the drawing, while the original tooth profile is suggested by the heavier lines. The newly created sheared surface is particularly evident in the first few teeth behind the mushroomed head in the composite photograph. Creation of the everted tube can follow one of two widely different paths. Depending **on a balance between the penetrator material's strain hardening and thermal softening properties**, the tube can either be smooth and continuous, or comprise a number of highly sheared zones forming chips, exactly as seen in machining metal.

Figures in the literature typically show the rod material flowing into the target interface and coming out as detailed in Figure 4-1, view b. This is probably an oversimplification.

Compression forces predominate over shearing forces in the zone of material near the center of the rod at the interface. Under this loading, it is quite likely that a dead zone forms as shown in the larger scale detail of Figure 4-1, view c. Such a rod (and target) flow field is much more understandable than that depicted in view b. The doubly cusped dead zone, comprising either penetrator or target material or both, and only casually active in the flow process, acts as a more or less rigid feature facilitating the opening of the rod and target materials as in the metal-forming operation of piercing. The friction with the flowing penetrator and target materials would create a tendency for the material in the dead zone to circulate as indicated by the arrows in the additional detail in Figure 4-1, view d.

Experimental terminal ballistics work shows that, at tank cannon velocities, the rear of a long rod decelerates only slightly until it is nearly consumed. In fact, you can set your imaging trigger delays by this assumption. Only when the rod erodes down to a few diameters in length does the speed drop seriously. See, for example, the extensive literature referenced in an excellent BRL survey paper by T. Wright [23].

4.2 THE REACTION OF TARGET MATERIAL UPON PENETRATION

In semi-infinite penetration, the target material **doesn't** go very far. This fact is also true in deep penetration of finite targets. Little or no target material is actually evacuated from the target in creating the penetration channel. At impact speeds even in the hypervelocity regime, the target material is essentially incompressible. Even under stresses causing general yielding, the bulk modulus of metals is too high to accommodate the creation of a void volume without gross target material flow, observed predominantly at the nearest free surface, which is usually the struck surface. Figure 4-2 illustrates the movement of the target material. The gridded surface through the target in the plane of impact on the left would deform something like that shown on the right. Think of the zones as annuli around the axis that have the same volume before and after penetration.

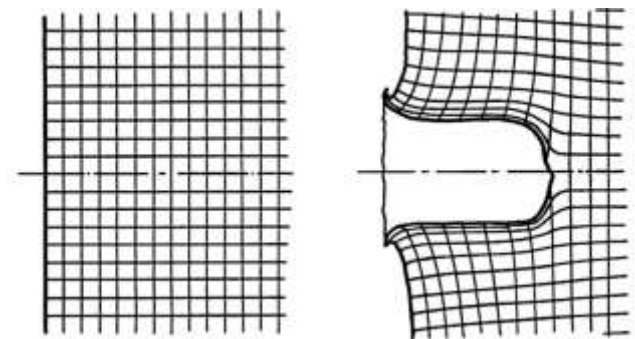


Figure 4-2. Target Material Displacement After Penetration
(Source: Silsby [1]).

(This figure is only illustrative and not from any experimental data. For discussion of experimental data from confined split targets, see the BRL report by Bruchey and Glass [24].)

4.3 SIMPLE PHYSICAL RELATIONSHIPS

Remember that we are discussing LRPs impacts on semi-infinite RHA targets at normal incidence. We are used to thinking of the target as being fixed and the penetrator as attacking the target with a striking velocity V . Instead, imagine that you are moving down range at such a speed that you are standing still relative to the penetrator-target interface. Mathematically, this is accomplished by subtracting the interface or penetration velocity, U , from the instantaneous velocity, V , of the rod, and the zero velocity of the target (Figure 4-3). Now the rod velocity relative to the interface is $(V - U)$, and the target velocity is $-U$ (i.e., to the left in Figure 4-3). What is the velocity of the exiting tube of material? The only way it can lose energy going around the corner in the interface is through friction degradation of KE into heat through plastic work.

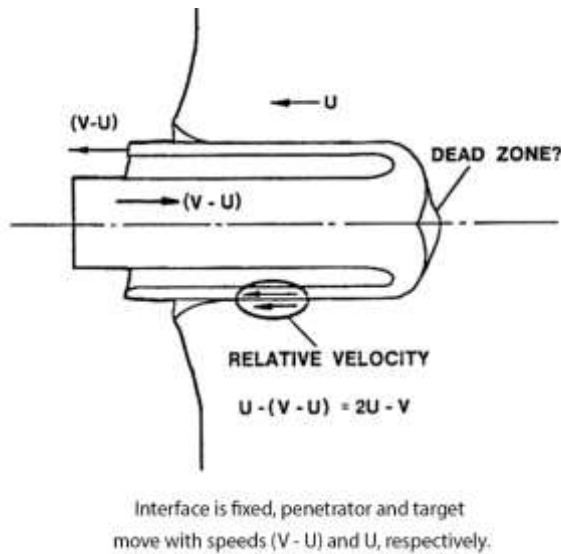


Figure 4-3. Everting Penetrator (Source: Silsby [1]).

How much energy is lost to plastic work was deduced indirectly by observing the results of shooting small WA long rods into two 6-in. cubes of armor back-to-back at increasing velocities. The testing was conducted to generate penetration vs. velocity data to compare with an earlier lot so as to qualify (or not) a new lot of tungsten rods for a customer. Only the first block was penetrated; the second block served to restrain the first block inertially for a time so it would act more nearly like a semi-infinite target. Up to some velocity, the bottom of the hole had a residual penetrator stuck in the bottom of the penetration channel, but no tungsten debris. At about 1700 m/s, the penetration channel was lined with a tightly adherent layer of tungsten chips and the residual rod at the bottom. Above that velocity, the bottom of the channel was choked with debris on top of the last of the penetrator. Apparently, at lower velocities, the debris headed up-range and did not wedge into the target channel. At about 1700 m/s, the debris came out radially and lodged against the wall of the channel. It had no velocity relative to the wall of the penetration channel that would dislodge it. Beyond this velocity, the debris headed down range, and it was dislodged again coming to rest on the base of the residual rod. If it is assumed that the everted material turns the corner without losing any velocity, this threshold velocity would be about 1600 m/s, a good correlation: some energy is lost, as it must be, but not much. Under that assumption, the thickness of the stream of everted penetrator material can be calculated as well.

Thus, with a small error, every little packet of material is assumed to maintain constant speed while being severely redirected, as in a train going around a sharp curve, exiting with a speed $(V - U)$ relative to the observer fixed at the interface. By subtracting exiting material speed from target speed, the relative velocity can be determined between penetrator and target, which is $2U - V$. Section 4.4 discusses how to determine the value of U .

4.4 DERIVATION OF INTERFACE VELOCITY, U

The interface velocity, U , can be related to the P/L value observed from experiment. In Figure 4-4, three snapshots of the penetration are presented. At the top, the rod, traveling at its striking velocity, V , is just touching the face of the target. At some intermediate time, the rod has partially eroded and sunk some depth into the target. Assuming there is no deceleration of the rod, it is then completely eroded, and the penetration is finished (bottom). The average velocities of the tail of the rod and of the interface are calculated as shown in the figure. Then, one velocity is divided by the other, and the common increment of time is cleared out. The minor mathematical manipulation of dividing all terms by penetrator (only) overall length, L is then performed to obtain the amazingly simple relationship for U/V . In reality, the rod does decelerate, and usually some uneroded rod remains, but the principle is the same.

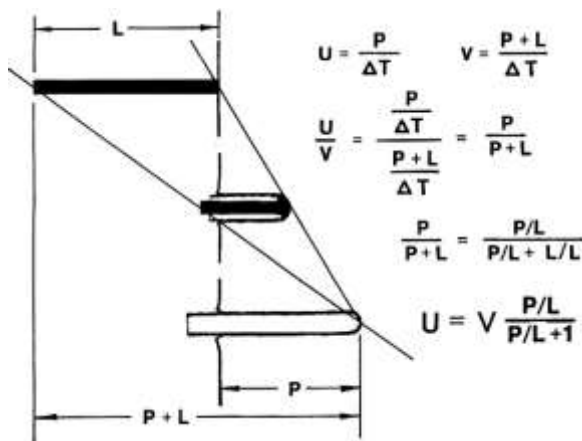


Figure 4-4. Simple Mathematical Relationships Yield Value for U (Source: Silsby [1]).

4.5 DERIVATION OF THE DENSITY LAW

Two coaxial streams of strengthless liquids of equal areas and different densities impacting each other can be used to explain the derivation of the density law. When viewed from a frame of reference fixed in relation to the

lower-density stream (for convenience called the target stream), the material from the higher-density stream (called the penetrator stream) is burst open at the centerline and exits in a sort of conical spray in which the thickness of the diverging exiting spray decreases with radius to satisfy conservation of mass. The material of the lower-density stream exits similarly, in contact with the inner surface of the higher-density stream, with the two streams in general sliding radially relative to each other. The interface moves relative to the frame of reference.

A familiar, albeit sort of two-dimensional (2-D), analog of this is a tire rolling on a flooded pavement that throws a spray of water out ahead of the line of contact moving with the vehicle, the tire being one stream and the water being the other. However, a special frame of reference can be selected along the common axis of the two streams such that it is fixed at the interface between the two streams, and the exit streams are at 90° to the axis (Figure 4-5).

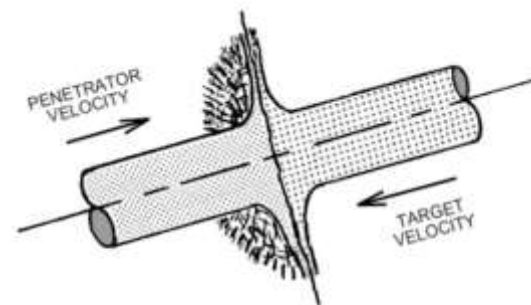


Figure 4-5. Streams of Equal Area but Different Densities Impinging on Each Other Coaxially (Source: Silsby [1]).

Imagine a control volume comprising a right circular cylinder with a larger diameter than the liquid streams centered on this origin and coaxial with them. Because the streams are strengthless, there is no force applied at the surface of the control volume, and the vector time

rate of change of momentum within the control volume must be zero.

Call the cross-sectional area of the streams A and a unit interval of time Δt . Arbitrarily, call the lower-density stream the target stream and the higher-density stream the penetrator stream. Call the velocity of the penetrator stream V_p and that of the target stream V_t . Using this nomenclature and equating momenta,

$$\rho_t AV_t \Delta t V_t = \rho_p AV_p \Delta t V_p, \text{ or}$$

$$\rho_t V_t^2 = \rho_p V_p^2 \quad (1)$$

Then call the distance traveled by the target stream P , the penetration of that stream, and call the distance traveled by the penetrator stream L , the length of penetrator consumed in penetrating the target stream in a unit time. Then:

$$\frac{P}{L} = \frac{V_T \Delta t}{V_P \Delta t} = \frac{V_T}{V_P} \quad (2)$$

Rearranging Equation 1 and taking the square root gives:

$$\frac{V_T}{V_P} = \sqrt{\frac{\rho_P}{\rho_T}}$$

And substituting in Equation 2 gives the density law for hydrodynamic impact, also known as the hydrodynamic limit:

$$\frac{P}{L} = \sqrt{\frac{\rho_P}{\rho_T}} \quad (3)$$

To put this in perspective, for steel-on-steel (or any like-on-like) impacts, the hydrodynamic limit is 1, while for typical ballistic WAs, it is about 1.49 (Figure 4-6).

Applying the assumptions of hydrodynamic (no strength) behavior to ordnance velocity penetrator-target interactions is not as accurate. There are at least two problems. First, as the velocity drops into the ordnance velocity regime, the impact pressures drop,

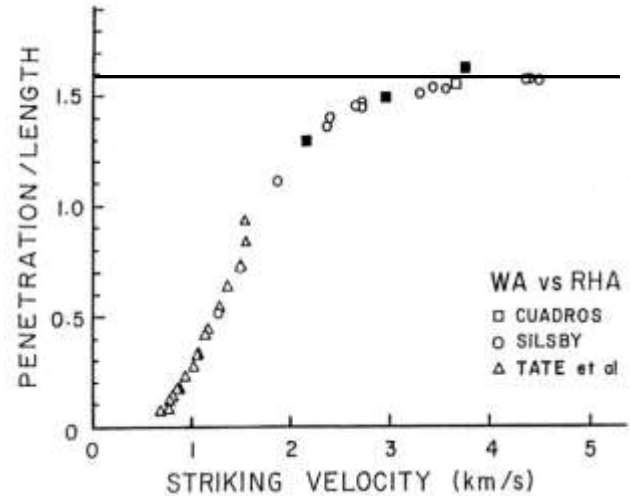
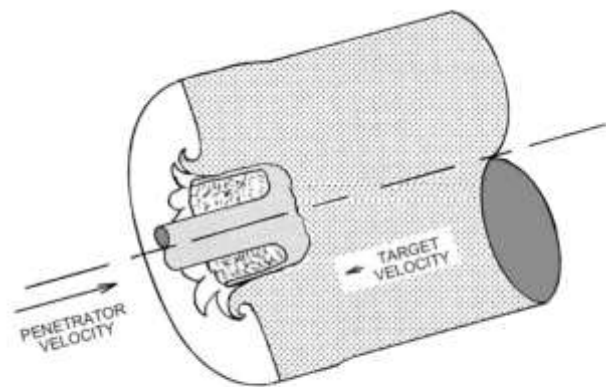


Figure 4-6. Tungsten on Steel Long-Rod Penetration Data with the Hydrodynamic Limit Superimposed (Horizontal Line) (Source: Silsby [1]).

and the hydrodynamic assumption gets less and less plausible. The other problem involves the geometric boundary conditions on the real situation. The small cylinder of target material to be swept by the penetrator material is surrounded by a large additional amount of target material disposed in such a fashion that it is very effective at constraining radial flow of target material in question both by inertia and strength (Figure 4-7).



Shown with origin at the center of mass.

Figure 4-7. Small Penetrator Diameter, Large Target but Different Densities on Each Other Coaxially (Source: Silsby [1]).

4.6 THE INFLUENCE OF PENETRATOR STRENGTH AT HIGHER VELOCITIES

The data on the effect of penetrator and target strength on penetration shown in Chapter 3 seem to indicate that target strength is important and penetrator strength is not, but this is only true at higher velocities. Remember that, against the same target, a hardened-steel core in AP shot is more effective than a soft core in conventional full metal jacket ball ammunition. Loading conditions and geometry dictate the stresses generated, while material properties determine the response. For a strong penetrator, as velocities increase, first it penetrates rigidly, and then at a threshold of velocity, begins to erode while penetrating. Figure 4-8 shows the semi-infinite penetration of a long rod, which has a long, quasi-steady-state phase.

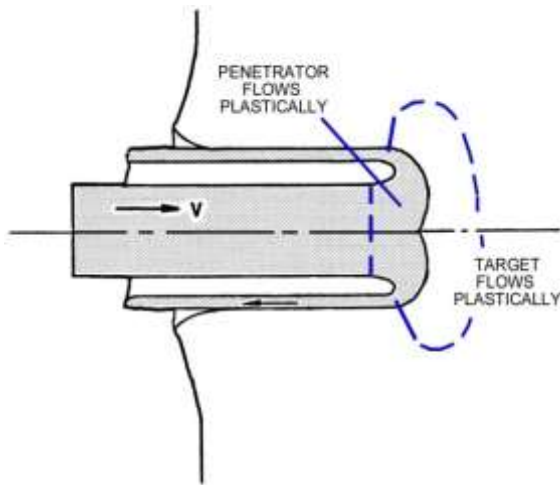


Figure 4-8. Deep Penetration (Source: Silsby [1]).

The penetrator is impacting at such a velocity that the impact pressure is higher than the rod strength, and it flows. The rod material feeding into the plastic zone is loaded in compression but cannot support more stress than the yield stress value of its material under the loading conditions that occur. The target material ahead of the deforming rod has a characteristic pressure above which it cannot resist, higher than the uniaxial

compression strength of its material due to the heavy confinement radially and axially.

The vector time rate of change of momentum of the plastically deforming penetrator material being turned from its forward direction due to being trapped between penetrator and target adds a hydrodynamic pressure component to the maximum stress that the penetrator material can exert on the target by its strength.

The strength component is the penetrator material's plastic flow stress, the equivalent in a triaxial state of loading to the yield stress in uniaxial loading. It is a function of both uniaxial compressive yield stress and the loading geometry. Increasing the impact velocity will not change the penetrator strength or decrease the target strength. Rather, the time rate of change of **momentum in the penetrator's plastically flowing zone** increases with increasing velocity and is responsible for the increase in penetration with velocity. It is the pressure at the penetrator-target interface generated by the velocity, density, and curvature of the outward-flowing penetrator material stream that advances the interface. The hydrostatic pressure in the turning stream of the penetrator metal increases with depth from atmospheric pressure at the surface to a maximum at the target interface.

As velocity increases, the interface pressure increases with the square of the velocity, until soon only inertial forces are important. There is also a change in momentum of the target material as well, as it is being violently displaced outward from the centerline. Penetration then increases only slightly with velocity once the hydrodynamic forces greatly exceed the strengths involved, although the diameter of the hole continues to increase. (See Section 4.7.) This hydrodynamic limit is reached at about 3 km/s for tungsten or uranium on steel.

4.7 UNBALANCED UNSTEADY STATE EFFECTS

Two separate effects that would both tend to increase the depth of penetration are frequently postulated and seem plausible. One is target inertia. The penetrator-target interface is plowing through the target at the interface velocity. While the interface speed is some fraction of the striking velocity, it is not negligible. It could well be that even when the penetrator has been spent on the target that the target material ahead of it would continue to recede for a bit as a result of its own inertia. Figure 4-9 illustrates the process. This effect should be most apparent in high-density, low-strength targets struck at high velocities, e.g., a lead 0.22-caliber rifle bullet fired into a lead block.

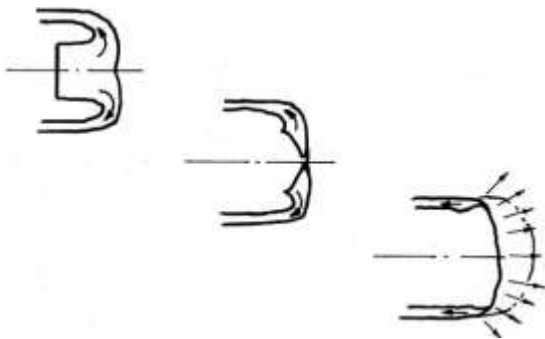


Figure 4-9. Target Hole Growth due to Target Material Inertia (Source: Silsby [1]).

A second process possibly contributing to additional hole depth is secondary penetration. If the residual penetrator material has significant forward velocity relative to the target, it could cause additional penetration beyond that caused by the penetrator itself. Figure 4-10 illustrates this process.

To determine whether target inertia and secondary penetration are likely to occur, insert real numbers into the simple relationships for the interface velocity U (as discussed in Section 4.4), and plot the secondary striking velocity for the steel and tungsten long-rod data from Figure 3-4. Remember to use P/L and not P/L normalized

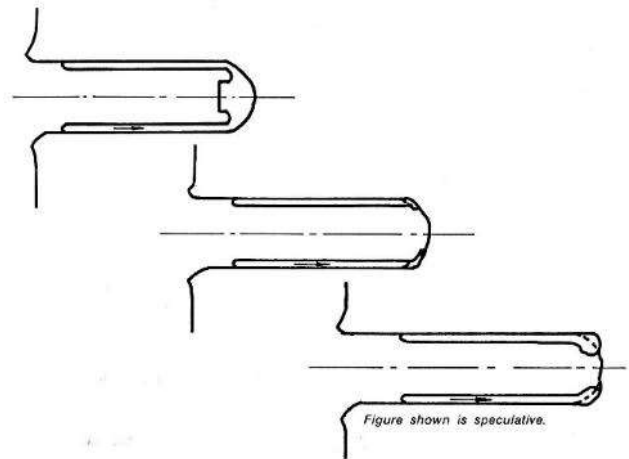
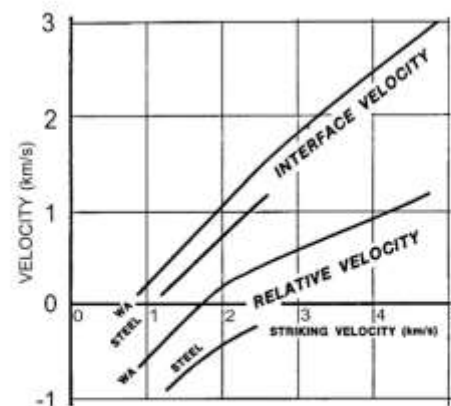


Figure 4-10. Secondary Target Penetration Caused by Forward-Moving Penetrator Residue (Source: Silsby [1]).

by the square root of target-to-penetrator density. The results are presented in Figure 4-11.

Figure 4-11 indicates that the interface velocity is just positive for striking velocity, V_s , above 1 km/s, and approximates the function $U = (V_s - 1 \text{ km/s})/V_s$, which rises from nothing at $V_s = 1 \text{ km/s}$ to about $1/2 V_s$ at $V_s = 2 \text{ km/s}$, and approaches the value of V_s at infinite V_s . That is, the interface velocities range from about $1/2 V_s$ to



For steel-on-steel and tungsten-on-steel data from Figure 3-4. Note that the horizontal axis is within the graph, not at the bottom.

Figure 4-11. Interface Velocity and Relative Velocity Between Penetrator and Target vs. Striking Velocity (Source: Silsby [1]).

about $2/3 V_s$ in the high end of the ordnance velocity regime. Everted penetrator material from a steel penetrator will always go up-range regardless of V_s , while tungsten debris only begins to head down range at $V_s > 1.7$ km/s, and only breaks the 1-km/s velocity threshold for penetration of armor steel at a V_s of 4 km/s. Secondary penetration is unlikely to occur at ordnance velocities.

4.8 SUMMARY

The empirical data in Chapter 3 and an understanding of the physical processes discussed in Chapter 4 can enable engineers/analysts to make realistic judgements or initial calculations about situations of interest. For example, using 1) the discussion of the L/D effect (Section 3.7); 2) the segmented penetrator design discussed in Section 3.7.2 and shown in Figure 3-11 and again in Figure 4-12; and 3) assuming a striking velocity of 1500 m/s into RHA and a 20-mm diameter, an engineer/analyst could answer the following questions.

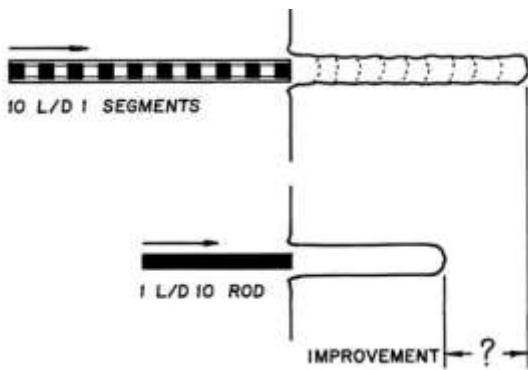


Figure 4-12. Segmented Penetrator (Source: Silsby [1]).

1. Assuming the segments are 20 mm in diameter, what would be the expected penetration of the L/D 10 rod and the 10 L/D 1 segmented design?

The tungsten-on-RHA data in Figure 3-13 indicates the P/L at 1500 m/s is about 0.75, so an L/D 10 20-mm rod would be expected to penetrate to about 150

mm. Assuming that the P/L vs. L/D data for steel-on-steel (Figure 3-10) were similar to that of tungsten, then an L/D 1 segment would penetrate about twice that of an L/D 10 rod at 1500 m/s. So the segmented penetrator might be expected to penetrate 300 mm.

2. What would the velocity of the everted material be relative to the penetration channel wall?

Using the equations in Figures 4-3 and 4-4 would indicate that the eroded penetrator material would be moving up-range relative to the target at about 214 m/s.

3. If the 94% tungsten hole diameter data are representative, how much clearance or interference would there be between the incoming segment's outer diameter and the inside diameter of the everted spent penetrator material?

Figure 3-8 would indicate that the hole diameter would be about 1.9 times the rod diameter or 38 mm. When viewed relative to a fixed coordinate system attached to the interface, the penetrator material comes in and goes out at the same speed s . By continuity, the outgoing material volume of $\pi(r_o^2 - r_i^2)s$ equals the incoming volume of $\pi r_p^2 s$. Eliminating π and the common speed, $r_p^2 = r_o^2 - r_i^2$, or $r_i^2 = r_o^2 - r_p^2$. Inserting the numbers, $r_i^2 = ((19 \text{ mm})^2 - (10 \text{ mm})^2)$ or $r_i^2 = 361 \text{ mm}^2 - 100 \text{ mm}^2 = 261 \text{ mm}^2$, hence $r_i = 16.16 \text{ mm}$, well clear of the penetrator outer diameter. However, the concept did not actually work due to the everted material rebounding off the channel walls and converging on the incoming penetrator.

5. NORMAL INCIDENCE PERFORATION

5.1 PERFORATION VS. PENETRATION

What happens if there is a rear surface to the armor, and **it isn't too far from the front surface**? Many people know that a bulge forms on the rear of a thick, ductile target element, breaking out as the rod emerges. Earlier discussions concentrated on either a cause-and-effect look at things, or the process of gross plastic deformation, as might be seen in forging or other metal forming operations.

At a time-scale of microseconds, disturbances travel millimeters, a good size scale for looking at the details of the process. The localized reactions of materials to the localized applications of force or displacement propagate as waves, spreading throughout the entire penetrator and target in time, reflecting and re-reflecting, combining on a broader scale to dictate the gross behavior observed. To provide a different perspective from which to understand penetration mechanics in general, and the perforation process in particular, without going into great detail, consider the wave mechanics of the interaction.

5.2 WAVE MECHANICS

As the rod strikes the front of the target, elastic compression waves spread throughout the target and **penetrator at their respective material's bulk sound** speed. This speed depends on the elastic modulus and density of the material and is about 6 km/s or 6 mm/microsecond (μ s) in steel. Ahead of the wave front, the material is undisturbed. Behind the wave front, the particles of material are accelerated to some

characteristic speed, which is well below the penetration velocity. The wave spreads out, and its strength drops due to geometry, the inverse square law. For every free surface the wave encounters, material is free to move without bumping into other materials and slowing down, and so inertia carries the material into a state of tension. This reflected tensile wave propagates back inward at the bulk sound speed. The result of a wave reflecting off a free surface in a direction normal to the **surface is essentially a doubling of the material's particle** speed in the zone behind the reflected wave.

Additional penetrator material is constantly feeding into the interface zone, causing continuous acceleration of the materials to try to escape the advancing interface. Over a long time compared with the time it takes the elastic disturbance to cross the zone of interest, and due to multiple reflections of the stress waves, the material gains sufficient speed for gross plastic deformation to be recognized wherever there is a velocity gradient (which is just about everywhere). The speed at which a plastic, as opposed to an elastic disturbance, propagates is low to nil, so that plastic flow is confined to the immediate vicinity of the advancing interface. The relatively small rod mushrooms and flows radially. The struck face of the target around the penetration hole is accelerated up-range as the interface sinks into the target, forming a petalled impact splash surrounded by a broad, low mound.

In the meantime, the disturbance reflecting off the **target's rear surface is at first weak but gets stronger and** more localized as the penetrator-target interface approaches. The material in the zone directly in the line of the penetration picks up speed fastest, while the particle motion in surrounding zones is slower and has both a radial and normal component. A growing bulge forms. The material ahead of the penetrator is moving faster and faster but is being restrained to some degree by the strength of the target material and always

maintains contact with the (slowly decelerating) penetrator.

Penetration can be considered imposed deformation, rather than as an imposed force resulting in acceleration resulting in deformation. The strengths of the materials limit the amount of force that can escape the immediate area where they are applied. Rather, a rigid conceptual entity, the penetrator-target interface, forces its way into an essentially incompressible, plastically deforming target, pushing target material aside and into a shape dictated primarily by the presence of free surfaces at which gross deformation can occur. In the process, the level of compressive forces necessary to get the material out of the way is generated but affects the material only through the flow process. The strain state in the material determines when and where flow and fracture occur.

As the interface gets close to the rear surface, gross bulging begins. Microscopic fractures appear in the target interior, growing in response to continued increases in strain, and coalescing into gross failure planes. If conditions are right, the residual rod breaks out of the rear of the target. Figure 5-1 shows a moment in time before and a moment in time after breakout. Note the different spatial and temporal distributions of the

various classes of behind-armor debris. In Chapter 6, a similar figure will show how obliquity influences the spatial distributions.

Figure 5-2 is a series of photographs showing the progression in deformation of the target rear surface as the penetrator nears it and then achieves perforation.

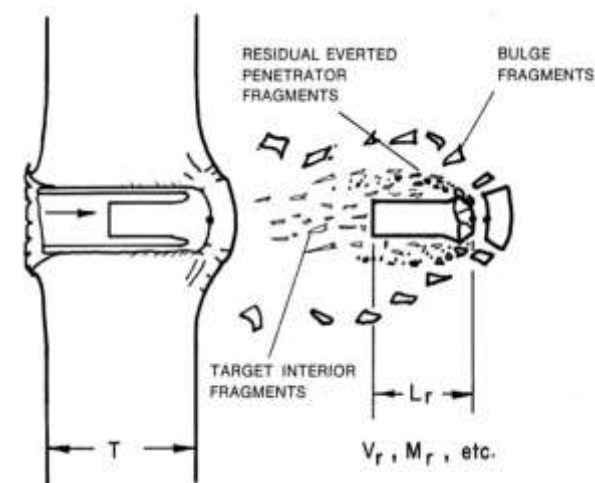
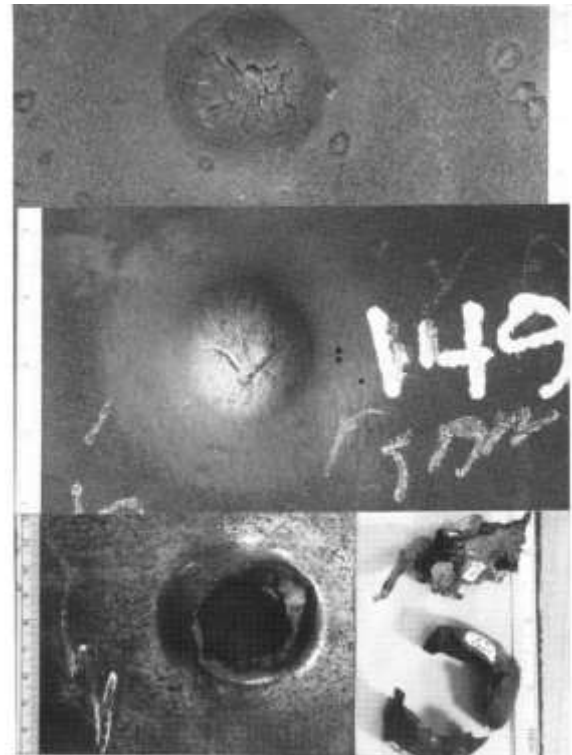


Figure 5-1. Normal Incidence Perforation (Source: Silsby [1]).



The right panel in the lowest view has sheared-out inner exit lips (below) and a badly mangled residual penetrator (above).

Figure 5-2. Target Deformation from Bulge to Perforation (Source: Silsby [1]).

Figure 5-3 is a photograph of a sectioned target perforated by a large-diameter, short L/D ratio penetrator simulating an EFP. Rebounding elastically off the residual penetrator's mushroomed tip, the plug or scab is the fastest thing behind the target (by tens of meters a second). Next is the residual rod with a characteristic mass, M_r , length, L_r , and velocity, V_r , respectively. The material sheared loose from the periphery of the target scab forms a bubble-shaped



Figure 5-3. Sectioned Perforated Target (Source: Silsby [1]).

cloud of debris corresponding to the velocity gradient in the target rear region that formed it. A more collimated, higher-velocity cloud of smaller debris forms from the residual penetrator material that was not fully everted at breakout.

Figure 5-4 shows the residual piece of the perforating EFP simulant and the plug of target material recovered from the range. The dark blue color is from the extreme heat from the plastic deformation of the parts.



Figure 5-4. Residual Penetrator (left) and Target Plug (right) (Source: Silsby [1]).

5.3 LIMIT MEASURES: V_L , V_{50} , Θ_{50} , AND $V_S - V_R^5$

How does penetration vs. velocity relate to the real measures of performance, that is, to ballistic limit measures such as limit velocity? A ballistic limit is a threshold of some parameter above or below which the penetrator gets through the target, and below or above which it does not. Ballistic limits can be used to compare the performance of various penetrators against standardized target designs, or the performance of various armor or armor components against a standardized threat projectile. In all cases, only data from fair hits are used. That is, data should not be used from a high-yaw hit where some part of the side of the penetrator struck the penetration channel wall, or data from a shot in which the projectile bent, broke, or was foreshortened from excessive launch acceleration, or data from other circumstances not representative of the desired interaction. While such data should not be used to find a desired value, it should be reported, as data are very expensive to generate and perhaps others could glean something useful from results. Also, measure and record as many factors as possible such as target plate actual thickness, hardness, ambient temperature, etc., because many things will influence the outcome of a test significantly.

The introduction of flash radiography allowed researchers to accurately measure the length and velocity of the uneroded portion of a penetrator behind the target (if one was present). Several empirical formulae were proposed, and techniques were developed to use this additional data to increase the accuracy of the limit velocity estimate or to reduce the number of shots needed to get a value with a particular confidence level. Several of the seminal papers on these $V_S - V_T$ techniques are not accessible on the web for various reasons, but a BRL report presenting test and

⁵ For more information on the various measures of limit velocity, see Misy 1978 [25]. Grubinskas 1993 [26] provides an overview of how the V_{50} ballistic limit velocity requirements specified for testing high-hard armor (HHA) (MIL-A-46100) evolved over successive revisions of that standard.

analysis guidelines for the Penetration Mechanics Branch, Terminal Ballistics Division by Zook, Frank, and Silsby [27] is available on the web. In addition, it provides a concise and detailed discussion of these guidelines, as well as presenting a good snapshot of the state of the art in gun range techniques of the time (1992).

5.3.1 V_L – Ballistic Limit

Before flash radiography, the easiest way to determine a limit velocity was to fire at a set of targets at a series of increasing velocities and to observe if a perforation occurred. Since different services had different ideas about what was unacceptable, different criteria were used to determine if a particular shot was to be considered a perforation in marginal cases. The Navy considered any crack through which light could be seen to be a defeat of the target. The Army was worried about wounding, so they put a thin aluminum witness panel behind the armor. If there were any perforations of the witness plate, the shot was counted as defeating the target. To distinguish this criterion from that of the Navy's, it is referred to as the **Protection Ballistic Limit**.

5.3.2 V_{50} – Ballistic Limit Velocity

A refinement on V_L is to plot points on a graph of probability of perforation vs. striking velocity. In the case where one can only observe if the target was perforated or not, the individual points are plotted on either the zero or 100% probability lines. There is usually a zone of mixed results in which some perforations occur at a velocity below which other shots fail to perforate. Once enough data with an acceptable distribution are generated, a cumulative probability of perforation curve is fit to the points (Figure 5-5). The point on the curve where there is a 50% probability of perforation is called the V_{50} limit velocity. In this approach, the velocity corresponding with other probabilities can also be

obtained, e.g., V_{10} is the velocity at which it is estimated that only one shot in 10 would get through.

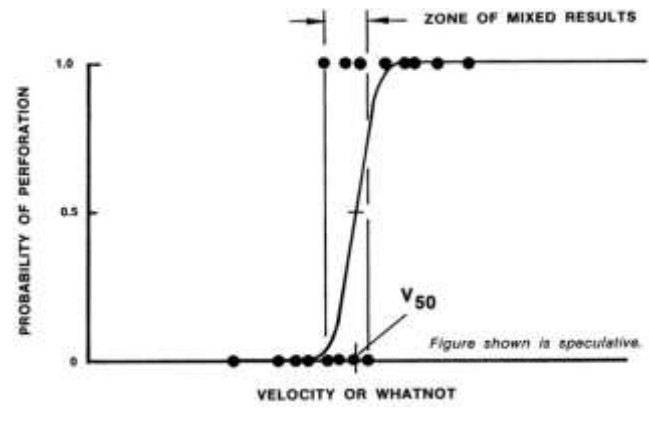


Figure 5-5. V_{50} Curve (Source: Silsby [1]).

5.3.3 θ_{50} – Ballistic Limit Obliquity

A variation on V_{50} has the advantage of not requiring that ammunition be taken apart to remove or add propellant. This θ_{50} procedure consists of firing ammunition at a fixed velocity and varying the obliquity at which the target plate is mounted. As the obliquity increases, for a first-order approximation, the difficulty of perforating the target increases with the line-of-sight thickness. Other, more subtle factors are also involved, but target thickness should be chosen so that the round is stopped at lower obliquities, typically 45–60°, where the second-order effects are negligible. **One concern is that the θ_{50} cannot be directly correlated with the V_{50} .**

5.3.4 V_s-V_r – Striking Velocity vs. Residual Velocity

Once flash radiographic velocity measuring schemes had been developed, data from individual shots provided more than a one-bit performance value. So-called V_s-V_r procedures to take advantage of this extra information were developed, most notably, a method developed in the early 1970s by Grabarek [28] of BRL for LRP data. The

four-parameter empirical function that he chose fit the data well in the velocity range of interest, but not at values beyond some large multiple of the limit velocity. Grabarek only used data from perforations to fit to his formula.

Lambert and Jonas [16] of BRL developed a three-parameter, nonlinear, least-squares fitting routine (Figure 5-6). In Lambert and Jonas's scheme, both perforations and nonperforations factor in the fit, which minimizes the root-mean-square error between *all* data points and the form of the curve, not just data from perforations.

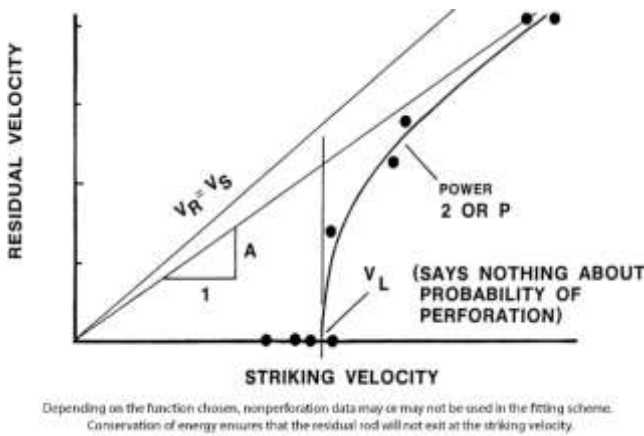


Figure 5-6. V_S - V_R Curve (Source: Silsby [1]).

The continuous function is defined as zero below the limit velocity, and at and above the limit velocity as a hyperbolic-like function whose curvature is defined by a variable power term, P , and which is tangent to a vertical line through the limit velocity and an asymptote through the origin of slope, A :

$$V_R = A(V_S^P - V_L^P)^{\frac{1}{P}} \quad (1)$$

The parameter P is restricted to the range of 1 (which would yield a straight line) to 8, at which the curve hugs the intersection of the asymptotes tightly. If the penetrator lost no velocity going through the target, the slope of the asymptote would be 1, and in realistic long-

rod penetrator scenarios, the slope of the asymptote is a bit under 1. Lambert was unable to develop a closed-form fitting scheme. Rather, he wrote a computer program that fits the function starting with $P = 1$ and computes the root-mean-square error. The program then increments P by 0.1, computes the root-mean-square error and compares it with the previous value, continuing this loop until the root-mean-square error begins to increase, at which point it reports the parameters from the previous iteration as the best fit. While this program is not perfect, Lambert found no instances with real data where the errors so generated did not have a single minimum. His examination of a lot of LRP data (not fragment-like data) suggests that if A is not a bit under 1 and P is not a bit under 2, something about the testing is not representative of the conditions under which the fitting procedure was developed.

5.3.5 Advantages and Disadvantages of Limit Velocities

Limit velocities are very sensitive, so a design should not be selected just based on a number, but rather on the principle that to have the best chance for a catastrophic kill, it is essential to get the maximum amount of residual rod behind the target. A rod whose length is based on armor effective thickness and the P/L for the lowest striking velocity expected is marginal anyway. But V_L s are useful for comparing one rod design against another just *because* they are very sensitive measures of performance.

5.3.6 Reliability of Limit Velocities

The goal of the curve-fitting here is to produce estimates of the sought-after parameters. Associated with every regression scheme is a measure of the reliability of the result. If one more shot were to be fired, typical in every way including variability, how would the result of the fit change? If the curve varies considerably as additional

points are added, more shots are required. In general, data should be plotted as they are generated. Also, both the goodness of the fit overall and trends in where the fit is better or worse (a residual plot) should be examined. There are many useful discussions of how to determine if there is a good fit, but be aware that errors in residual velocity may not be normally distributed. The observed outcomes are a balance between factors in which a disturbance significantly reduces performance versus ones that tend to boost performance. Such factors do exist, in particular a slight favorable yaw when striking an oblique target, but they are usually far outweighed by unfavorable factors.

Not only are sufficient data needed, but they are needed in the right regions of the domain to adequately determine the parameters, and hence give reliable results. In the Lambert and Jonas procedure, data near the limit velocity determines the estimate of the limit velocity, data near the knee of the curve determines the value of P , which determines the curvature there, and data at high velocities determine the value of A , the slope of the asymptote. If there are three parameters to be fit, three shots are used up just to satisfy these three degrees of freedom, so that five or six data points give only a crude fit. When economics limits the program, just concentrate shots around the most important point: limit velocity. The hyperbolic-like fits are, in reality, not quite right, as the strain to failure in the target may well have occurred well before the penetrator velocity drops to zero. A shot in which the plug is subsequently perforated by the uneroded penetrator is rare, but it does occur.

It is also not generally appreciated that the fits were developed specifically for residual rod data and should not be based on the other types of residual velocities. If the rod is consumed in the target, and only target debris is thrown off, the variability of the process is much greater. While it is possible to obtain a reasonable estimate of the limit velocity in this instance, a lot more

shots need to be fired. When the number of shots is limited, residual “cloud velocities” can be used carefully when penetrator debris is present.

5.3.7 The Other Performance Measure: The Witness Plate

With so much knowledge about the performance of RHA at normal incidence, it is a natural choice for its use to measure the effectiveness of whatever remains of the penetrator behind a target. A piece of thick RHA is installed at some reasonable distance behind the target, usually at normal incidence. Remember that distance equates to time for disturbances in the residual rod to grow, almost always to the detriment of performance. Any deep penetration reflects what could be done to a heavy component such as the breech ring of a tank main gun. The depth of penetration certainly represents the minimum thickness of a component that could be perforated, such as an oil pan. The witness plate need not be RHA, and indeed a material should be selected so as to provide the appropriate response over the range of attack conditions selected. In most work involving perforations, however, much more information can be gathered by behind-armor flash radiographs. Armor is inexpensive and information is valuable, so a witness pack should be placed as close to the rear of the target as possible while still allowing for a pair of radiograph stations. Figure 5-7 shows the results of attack by the



Note that the conditions for shots 1, 6, 7, and 8 destroyed most of the slug.

Figure 5-7. Aluminum Witness Plate for Aluminum Slug Residuals, 10 Shots (Source: Silsby [1]).

residue of a scaled, high-velocity aluminum slug perforating a scaled, reinforced-concrete panel representing typical urban structures. This 2½-in.-thick witness plate was used on 10 shots.

In some diagnostic work, for example to characterize specific elements of a complex armor design, much of the residual rod is left and several (many) witness plates must be stacked up to accommodate the expected depth of penetration. Typically for tank main gun threats, the stack would consist of a number of 2-ft. × 2-ft. pieces of 6-in. RHA held together with heavy straps and heavy welds (Figure 5-8).

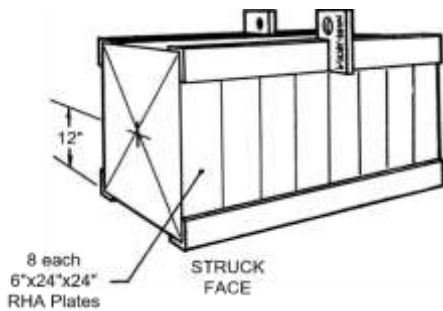


Figure 5-8. Witness Plate Stack for Diagnostics Involving Deep Penetration (Half Geometric Scale) (Source: Silsby [1]).

The witness plate concept is expanded on if vulnerability information is sought. Simple plates of the appropriate material (e.g., aluminum) and thickness (e.g., 3/16-in.) can represent a component of interest (e.g., the chassis of a radio) to measure the lethality of the behind-armor debris spray. This concept is expanded upon by the use of a witness pack. A typical witness pack would be an assembly consisting of 0.020-in. aluminum, 1-in. of cane fiberboard, another sheet of 0.020-in. aluminum and another 1-in. of cane fiberboard followed by a piece of ¼-in. aluminum and 1-in. of cane fiberboard, then something thicker and tougher, such as low-carbon steel or RHA. This scheme permits recovering, identifying, and weighing many of the fragments and establishing a spatial pattern of lethality of the behind-armor debris field that can be compared among penetrator designs or

armor designs. Given that behind-armor radiographs provide little that can be directly tied to lethality, witness packs are actually far more valuable than their low-tech nature suggests. **Further, since they don't need** electricity, running water, or air-conditioning, they can be used by any ordnance developer anywhere in the world. However, occasionally they burn up. The fragments fall into the ashes and cannot be related to the track of holes they produced in the metallic sheets and plates, so fire-resistant materials should be used for witness packs.

5.3.8 Relationship of Perforation to Penetration

Conceptually, it's easy to relate semi-infinite penetration vs. velocity curves to the limit velocity. Select a target thickness or a striking velocity so that the end of the penetration channel gets close enough to the rear surface for breakout to occur. Think of this plug thickness as being free additional penetration. People have tried this approach, using some empirically generated factor of one to two rod or channel diameters, and produced reasonable results, particularly when working with high-hardness armor. However, this approach provides considerable license in interpreting results, particularly in determining breakout allowance. Figure 5-9 illustrates this concept.

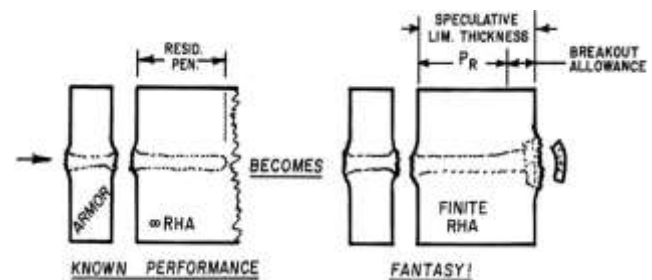


Figure 5-9. Speculation Leads to Inaccurate Breakout Allowance Measurement (Source: Silsby [1]).

In Figure 5-10 the data points are plotted as if original target thickness were the total penetration. The limit

velocities fall right on the penetration vs. velocity curve for semi-infinite armor, implying no gain in penetration from plugging. This result is probably due to the ductility of RHA. By coincidence, the target stretches into a bulge which fails just about as the interface passes the rear target surface. While the plug is attached to the armor, it is resisting penetration of the rod, so that target ductility tends to increase the apparent thickness of a target plate when compared with plate of less ductility. This ductility effect just cancels out the additional penetration due to plugging. Figures 5-10 and 5-11 provided a baseline in a study of the effect of yaw on long-rod penetration.

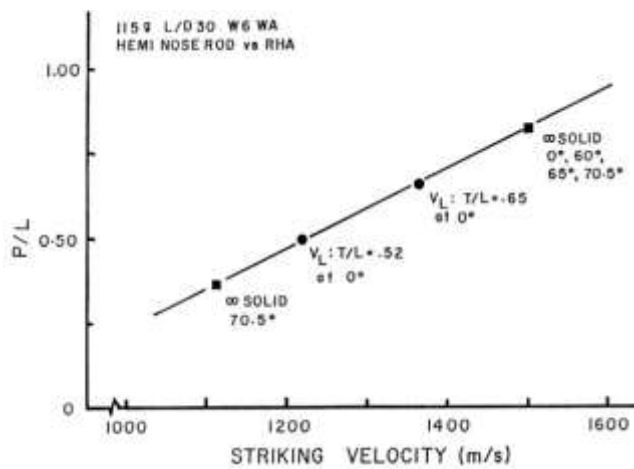


Figure 5-10. One Case in Which Limit Velocities Fall on the P/L Curve (Source: Silsby [1]).

5.4 VEHICLE ARMOR OBLIQUITY AND LINE-OF-SIGHT THICKNESS

An understanding of penetration mechanics enables understanding of real targets, i.e., vehicle armors. They are complex and their design is driven by real constraints. They are finite, with armor thickness limited by allowed weight for the armor. To provide some extra protection, armor is intentionally arranged at obliquity, inclined in both the vertical and horizontal planes. Attack can be affected from any direction relative to the tank. Line-of-sight thickness goes up rapidly when obliquity exceeds about 60°. (This benchmark is where the line of sight is twice the plate thickness.) For several reasons, the penetrator designer quits trying to get the rod through the armor at attack obliquities exceeding about 70°, where the line of sight through the armor is about three times its normal thickness. The line-of-sight thickness gets too large, ricochet becomes possible, and **there isn't much of interest behind the armor there** anyway. Spaced armor is used where possible, such as applying skirting plates outside the road wheels, and other armor schemes are limited only by the designer's imagination. Ultimately, each armor element influences how the penetrator is affected.

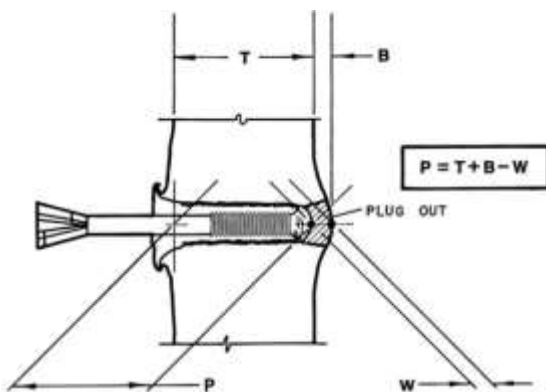


Figure 5-11. Ductility Could Just Offset Plugging to Explain Figure 5-10 (Source: Silsby [1]).

6. EFFECTS OF OBLIQUITY, SPACING, AND LAMINATION

Previous chapters have examined the much-idealized penetration process of an unyawed penetrator striking a target of a very large lateral extent at normal incidence. In this chapter, the effects of obliquity, spacing, and lamination are discussed.

6.1 OBLIQUITY

Obliquity is a measure of the inclination of the plate relative to the shot line at the strike point. In the U.S., it is reported as the angle between the outwardly directed target normal and the negative of the striking velocity vector. Inclining a plate increases its line-of-sight (LOS) thickness, an important factor in penetration mechanics. The armor designer, however, is given a threat, a presented area to protect, and a weight budget usually in terms of areal density (the mass of armor allowable in a unit of presented area), which would translate into a given LOS. Obliquity is just one of the factors that can be used to improve armor performance on a weight-for-weight basis.

Earlier lower-velocity, armor-piercing rounds had ogival noses, which were necessary to keep the shot together as it pushed through the armor. The inclination of the struck armor face resulted in a lateral blow to the penetrator, perhaps breaking off the nose. If the obliquity were high enough, a ricochet could result. A typical example of these applications is the turret of the WWII generation of main battle tanks using cast armor (Figure 6-1).

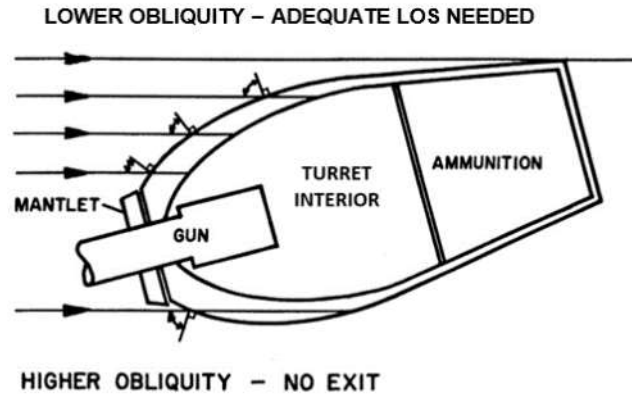


Figure shown is speculative.
 Typical WWII-style cast turret. The thicknesses vary to provide uniform resistance to penetration at the most extreme off-axis attack azimuth expected.

Figure 6-1. Obliquity in Armor Design (Source: Silsby [1]).

6.2 NATURAL COORDINATE SYSTEM FOR OBLIQUE IMPACT

Although it is natural to think in terms of horizontal and vertical, there is the problem of describing obliquity in terms of “the plate top is inclined towards the gun” or giving an angle from the horizontal. The U.S. definition of obliquity applies equally well to curved surfaces, as suggested by the dashed lines in Figure 6-2, and is a natural coordinate system for describing obliquity, that is, it is independent of any external reference scheme.

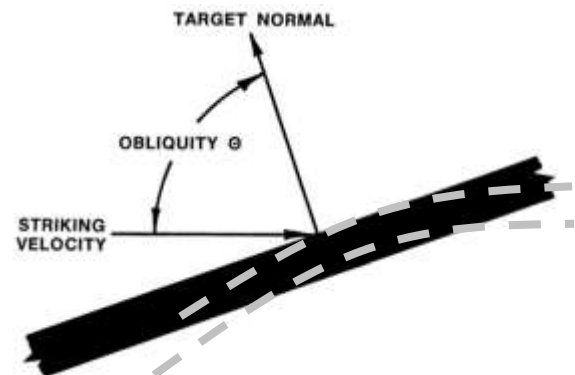


Figure 6-2. Natural Coordinate System for Describing Striking Obliquity (Source: Silsby [1]).

When obliquity is defined as the angle between the striking velocity vector and the outwardly directed target normal at the strike point, it is independent of the orientation of the striking velocity vector and the target relative to a gravity datum, as well as of the curvature of the target element face at the strike point.

Semi-infinite penetration is the most primitive, and hence the most consistent, performance datum you can have for a penetrator. With an empirically generated P/L vs. velocity curve and the correction factor for target finite thickness, obliquity, and spacing for material properties, etc., you can then make a rough estimate of the minimum length of penetrator necessary to defeat almost any modern target at a given striking velocity.

6.3 OBLIQUE ARMOR

6.3.1 Armor Will Usually not be Struck at Normal Incidence

Geometric effects are very important in armor design and defeat. If frontal armor were just a big plate of steel mounted vertically on the face of the vehicle, the length of the shot line through the armor would increase with the azimuth of attack from off of head on (zero degrees), making it harder to get through. The same concept applies to attacks from above and below the horizontal plane. For all but extreme values, obliquity is not a useful defeat mechanism per se for either LRP or SC jets. Figure 6-3 shows the relationship between armor element geometry and attack geometry that determines the striking obliquity. Although a horizontal line is shown in the figure, orientation of the element relative to the horizontal is immaterial.

In general, the shot line will have a non-zero azimuth and altitude relative to the target normal. The LOS thickness can be computed using principles of descriptive geometry. First, view the geometry from a line in the

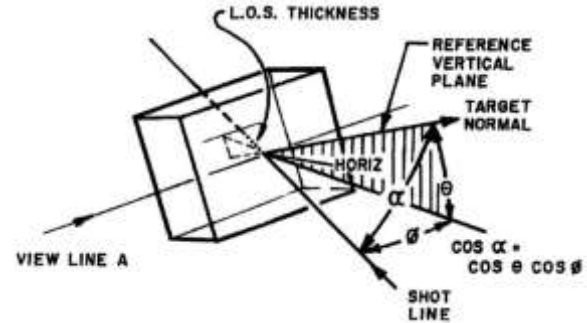
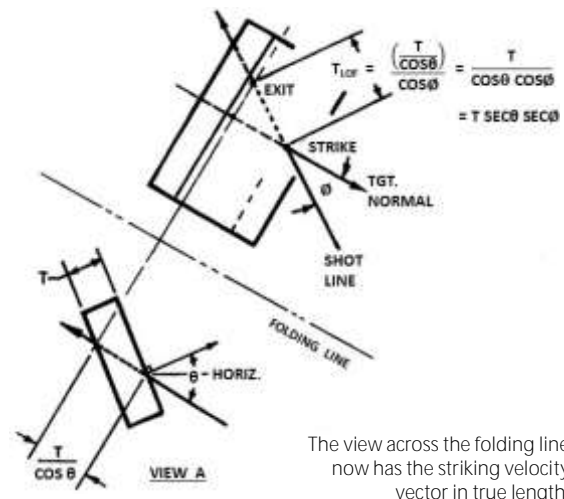


Figure 6-3. Relationship Between Vehicle Armor Geometry, Attack Geometry, and True Striking Obliquity (Source: Silsby [1]).

plate plane containing the strike point and normal to the vertical plane containing the target normal.

The vertical cross section of the armor plate along the line labeled “View Line A” in Figure 6-3 is also shown in Figure 6-4 (labeled “View A”). In Figure 6-4, a folding line parallel to the shot line projects a view from this view showing the strike and the horizontal in the back of the plate in true length. The length of the line through the armor along the section containing the target normal is $T/\cos \theta$, and the length along the shot line is $(T/\cos \theta)/\cos \phi$ or $T/\cos \theta \cdot \cos \phi$ or $T \sec \theta \cdot \sec \phi$.



The view across the folding line now has the striking velocity vector in true length.

Figure 6-4. Detail of Figure 6-3 Relationships (Source: Silsby [1]).

6.3.2 Features in Oblique Perforation of a Thick Target

Figure 6-5 presents the features seen in a thick oblique perforation. Many of the features such as lips on an impact splash and the formation of cracks in a bulge are the same as those seen in the normal incidence **perforation. Those features that aren't** the same can be understood in terms of the wave mechanics and the interaction geometry. As the target is struck on the face, the rod nose is subjected to asymmetric forces trying to rotate it (up in this case). These forces are resisted by the inertia of the rod material and its strength. Ultimately the rod tip is flattened somewhat where it first rode on the target and snaps off just behind this first zone of contact, followed by a characteristic chip of material that shears out of the compressed zone in the localized bend behind the rod tip. A highly polished, semi-elliptical, debossed feature called a nose print or nose engraving is seen on the target face where the rod touches down. At **the feature's down-range end**, target material begins to be evacuated in the typical roughened surface of a penetration channel in armor steel. The rod maintains a slight rotation rate upwards as it begins to penetrate the target.

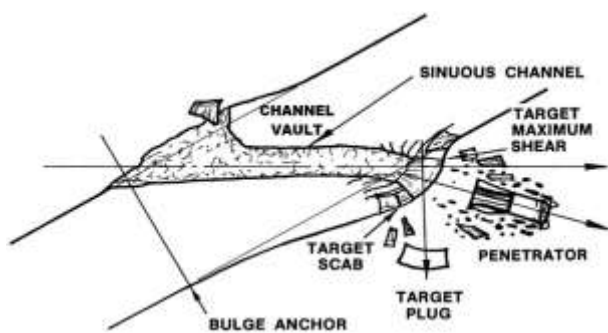


Figure 6-5. Oblique Perforation of a Thick Target (Source: Silsby [1]).

Target (and penetrator) deformation is the result of compression waves propagating into the target (and penetrator) and interacting with the free surfaces encountered. On the wave front encountering a free

surface, the forward velocity of the particles behind the wave front no longer have to push on target material in front of them and the disturbance reflects back into the material as a tension wave. Material inertia dominates the process, and while wave speeds are considerably faster than the penetration velocity, it takes a relatively long time for noticeable deformation to develop away from the interaction zone. The elastic wave speed is proportional to the slope of the stress-strain curve so that as the yield point is reached, wave speed drops to zero and deformation is localized.

Target material below the centerline is heavily constrained by its geometry and by inertia, while that above it is free to accelerate out, resulting in the observed gross asymmetry of the penetration channel until the rod fully enters the target. Two long, curled chips (not shown) are plowed out at the side of the entrance gouge and are usually sheared off. A final heavy chip or fragment is usually sheared out above the entrance to the full penetration channel at what is called the channel vault. Something resembling steady state penetration then continues until the interface gets near the exit face of the target. None of the up-range debris is shown in Figure 6-5 except for a final large chip that is typically seen as the penetration channel narrows to a more or less steady-state diameter. The everted penetrator material may be directed up-range, have zero velocity relative to the target, or be directed downrange. Some flakes of target material may be broken off the channel wall and be given some velocity by the everting penetrator material. As the penetration channel deepens, the influence of the free front surface decreases and that of the back free surface increases. A growing bulge forms along the target rear surface, and if some of the penetrator remains uneroded and with significant speed, as it approaches the target rear face, the bulge localizes and finally a target plug is ejected and pushed out of the way by the residual rod.

Depending on the amount of the overmatch, the target plug can exit well beyond the target normal (near the limit condition) to just a bit below the shot line for a large overmatch. The annular zone of target material just beyond the exit is stretched and broken into larger and faster chips, while the material being everted off the penetrator encounters no down-range resistance and leaves the exit hole at velocities up to that of the exiting residual rod. The inclined rear free surface causes the penetration channel to turn toward it, more so for near-limit conditions and less so for a large overmatch.

The stress wave radiating into the target (and penetrator) spreads on a spherical front so that the target face material picks up an increasing velocity component parallel to the plate face when observed farther and farther off the shot line, all the while of lower and lower value. The shape of the rear surface bulge is the result of the movement of the projection of the interface along the target rear surface. The strongest reflection off the back face of the target occurs directly under the location of the interface at the time the portion of the compression wave in question was radiated into the medium. The distance from interface to free surface grows shorter as the path gets deeper into the plate and closer to the rear surface, resulting in larger and larger deformation normal to the plate plane, being the largest at the point directly under the penetrator. The bulge curves back to undisturbed plate abruptly beyond that point. The first place that plastic deformation is significant is a feature called the bulge anchor. This point always occurs more or less directly under the strike point regardless of plate thickness.

In oblique perforation, as in normal incidence perforation, the plate material from the bulge, the plate material from the channel path, and the penetrator material develop distinctly different debris distributions behind the armor and the obliquity adds a third dimension to this. In this instance, the asymmetry of

loading results in the bulge first fracturing loose from the target at the end away from the bulge anchor.

A circumferential through-crack proceeds around the nascent plug, and the down-range (upper, here) end begins rotating away from the plate, hinged about the up-range (lower, here) end. If penetration stops before the plug is free, a hanging bulge occurs. If the penetrator overmatches the target considerably, the plug is projected nearly along the line of the striking velocity vector. As striking velocity decreases towards the limit velocity, the angle of departure of the plug moves toward the target normal. (It is not limited by the normal, however.)

The channel is slightly sinuous, turning towards the free surface first at the front and then at the back. The most pronounced curvature occurs on the exit face side, and particularly when attacked near the limit velocity, as the rod is slowed to nearly zero velocity. On sectioning a nearly perforated target, or looking at a just barely perforated one, it is not unusual to see that the exit path has dropped to rod diameter and turned nearly normal to the surface. Figure 6-6 shows the distributions of the fragments from the various zones of origin. Note that if each individual debris fragment were tracked back, the trajectories would seem to originate from an extended zone at the end of the channel, a zone in which the fragment last interacted with the channel wall or other debris.

As LRPs evolved along with modern armors, it was noticed that obliquity increased the weight efficiency of the armor designs. Initially, the effects of obliquity were modeled as $T_e = T \sec \beta^{\theta}$, where T_e was the effective LOS thickness and β was an empirically determined number that varied with penetrator and target geometry. It took quite a while to realize that the model was wrong and that the effect of rod diameter had to be factored in.

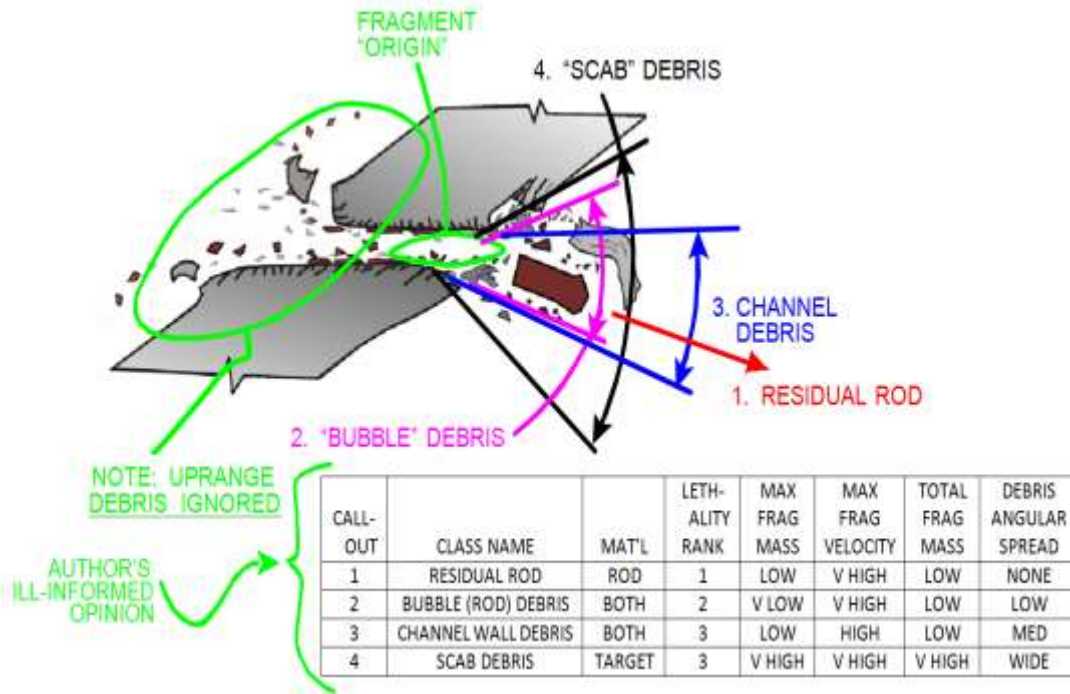


Figure 6-6. Behind-Armor Debris Classes (Source: Silsby [1]).

6.3.3 Measuring Penetration in an Oblique Impact

The illustration in Figure 6-7 does not indicate the true depth of penetration.

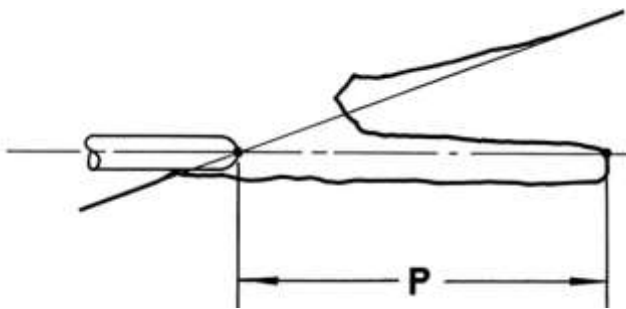


Figure 6-7. Incorrect Measure of Depth of Penetration (Source: Silsby [1]).

Figure 6-8 shows the correct measure of penetration. For a plate of thickness T , the bottom of the penetrator nose (in this example) must first run up on the surface of the armor while advancing an amount $D \tan \theta$ before the

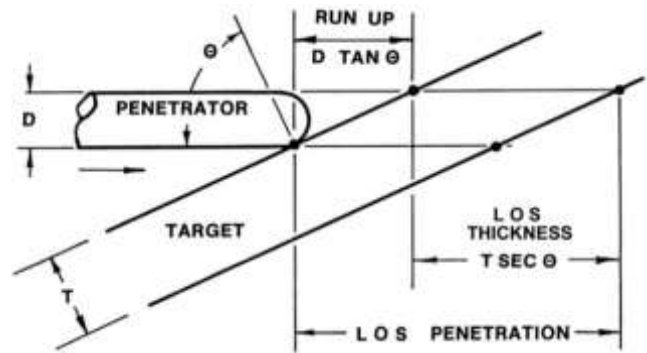


Figure 6-8. Effective Interface Path Length Depends on T and D (Source: Silsby [1]).

first point on its top first breaks the plane of the initially undisturbed surface of the target face. During this time, an initial gouge is being created in the target, while the rod material is being bent up and disrupted. The rod must then advance an additional $T \sec \theta$ before clearing the original back plane of the target. The entire time the rod is in contact with the plate, it is being eroded. It is the interface path length approximated by $T \sec \theta + D$

$\tan \theta$ rather than the target LOS thickness that determines how much rod is eroded, explaining the increased weight effectiveness of oblique armor. Note that the run-up correction is independent of the plate thickness.

6.3.4 Oblique Perforation of a Thin Target

Figure 6-9 shows two thin-plate orientations and a resulting oblique perforation. Which orientation resulted in the deformed residual penetrator shown? Thin plate orientation "A" resulted in the illustrated residual rod.

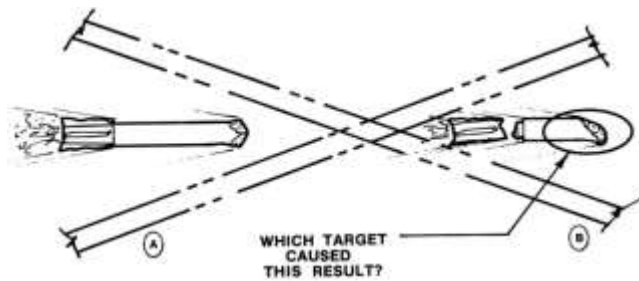
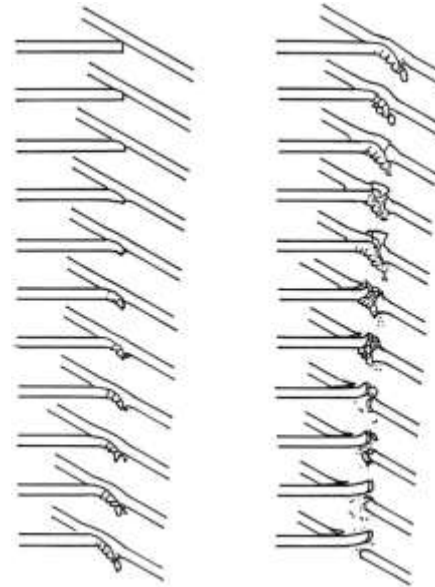


Figure 6-9. Examples of Thin Target Plate Orientations and a Resulting Perforation (Source: Silsby [1]).

Figure 6-10 shows the perforation of a one rod diameter-thick plate, drawn as if the rod were still (fixed) and the plate were enveloping it from right to left. While the start-up and breakout phases are based on radiographs, the middle of the process is speculative.

6.3.5 Penetrator Design Considerations for Attacking Oblique Armor

Notice that the blunt nose of this laboratory rod illustrated in Figure 6-10 promptly bit in, but even then, there was a series of short periods of bending of the rod before the effected zones snapped off. The application of these transverse forces contributes to an overall bending of the rod. If a rod is less ductile than the rod shown, this may contribute to snapping off of a leading



The rod erodes for a long period of time before it begins to break out of the plate. The plate material below the shot line then provides considerable constraint, forcing the tip of the residual rod up.

Figure 6-10. Perforation of a T/D 1 Plate at 60° Obliquity (Source: Silsby [1]).

portion of the rod during penetration. The impulsive loading leads to rod vibration in the bending mode, causes tipping (downward in this case) of the rod, inducing a rotation or pitching rate in the rod, and adds a **lateral component to the rod's velocity**, deflecting the trajectory of its centerline. In long, high-density rods, the rotation rate is small and vibration inconsequential. For example, if the rod were drawn here rotating at the real rate that it had picked up, it would not be discernible at this scale. Nonetheless, the effects are significant. Anything that prolongs the time during which lateral forces are applied or increases the magnitude of force the rod can sustain, will enhance the effect on the rod, to the detriment of its performance. These enhancements can include long, tapered noses on the rod proper, or long, strong, wind screens or thick layers of soft windscreen material between rod tip and target. In general, it is easier to tip strong rods than soft ones, and easier to tip rods made of a material with a higher elongation to rupture than ones of equal strength material that is more brittle.

Several other factors are involved in attacking an oblique target. Figure 6-10 shows the bending behind the nose of the rod as it exits the target, caused by its overriding debris in the last part of the event. After the nose was bent down repeatedly at the beginning of the penetration, it gets bent up just at the end. Again, this effect can result in bending of the rod, and/or in significant amounts of rod being broken off and can induce pitch and shot line deflection. In addition, the target plate has little or no clearance above the rod, so that any disturbance in the plate or in the rod trajectory could result in subsequent interference with the rod. Figures 6-11 and 6-12 illustrate the effects of oblique targets on penetrators.

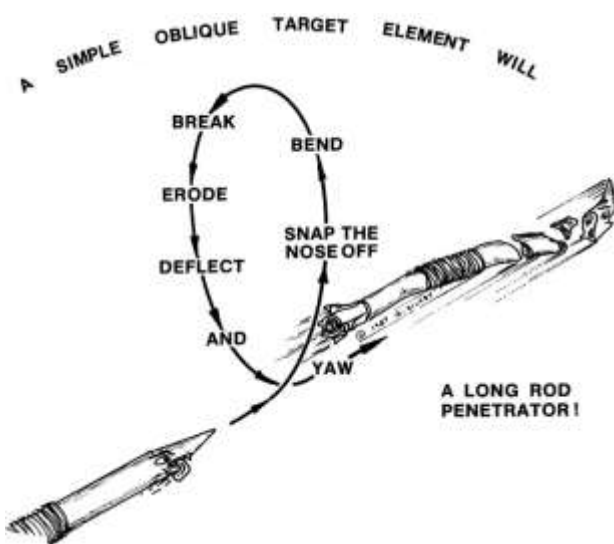


Figure 6-11. Effects of an Oblique Target on the Penetrator. Imagine the effect of several spaced elements (Source: Silsby [1]).

6.4 SPACED ARMORS

Providing spacing behind an armor element maximizes the time for yaw to increase before the rod strikes the next element. Figure 6-13 shows one type of spacing, a skirting plate, which is a lightweight curtain of armor placed outside tank road wheels.

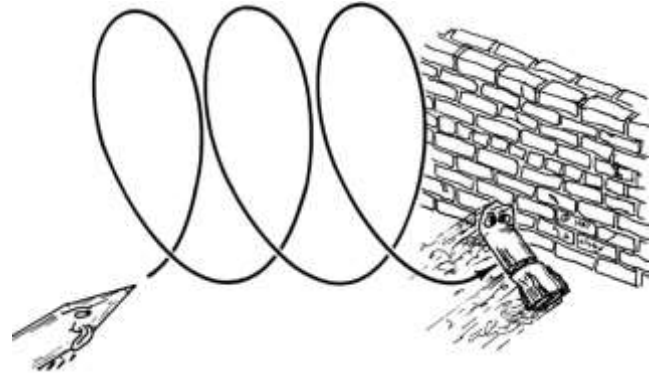


Figure 6-12. The Effect of Several Spaced Elements on the Penetrator (Source: Silsby [1]).



Skirting plates provide effective protection for a small increase in weight. Notice that the skirting plate is relieved where the road wheels can serve the same purpose.

Figure 6-13. Spaced Armor: Skirting Plates on Israeli Merkava Mk I Tank (Source: Wikimedia [29]).

Spacing many target elements apart is effective because after each penetrator-target interaction, time and space allow disturbances to the penetrator to grow. However, mass spread over a volume has a moment of inertia. The farther the mass is from the center, the higher the moment of inertia, and the more slowly the applied torques (forces tending to cause the object to rotate) cause the object to accelerate in rotation. This higher rotational moment of inertia is detrimental to weapon effectiveness because more power is needed to achieve the desired slew rate of the gun turret. High rotational moments of inertia also require additional weight in

suspension systems to keep the vehicle from pitching violently when running on rough terrain.

If the plates in a spaced armor array are parallel, their spacing can be described by the minimum distance between them (along a normal to the plates). This description reflects airspace as an effective element in the armor. Small changes in the airspace distance can make quite a difference in armor performance. Airspace and striking obliquity are the most important parts of the target geometry. See the lower set of dimension lines in Figure 6-14. The armor array described is really a five-element array: The first element is the first plate, the second element is the first airspace, the third element is the second plate, and so on.

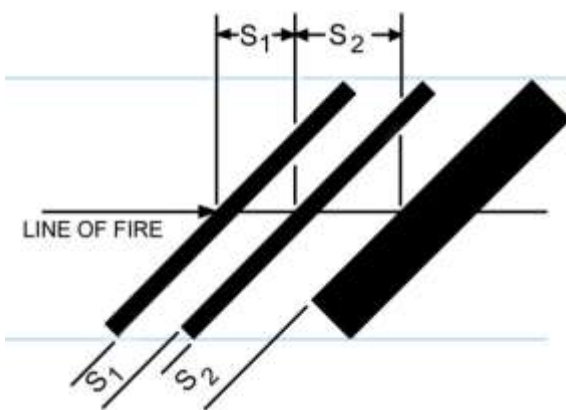


Figure 6-14. Spaced Armor Array (Source: Silsby [1]).

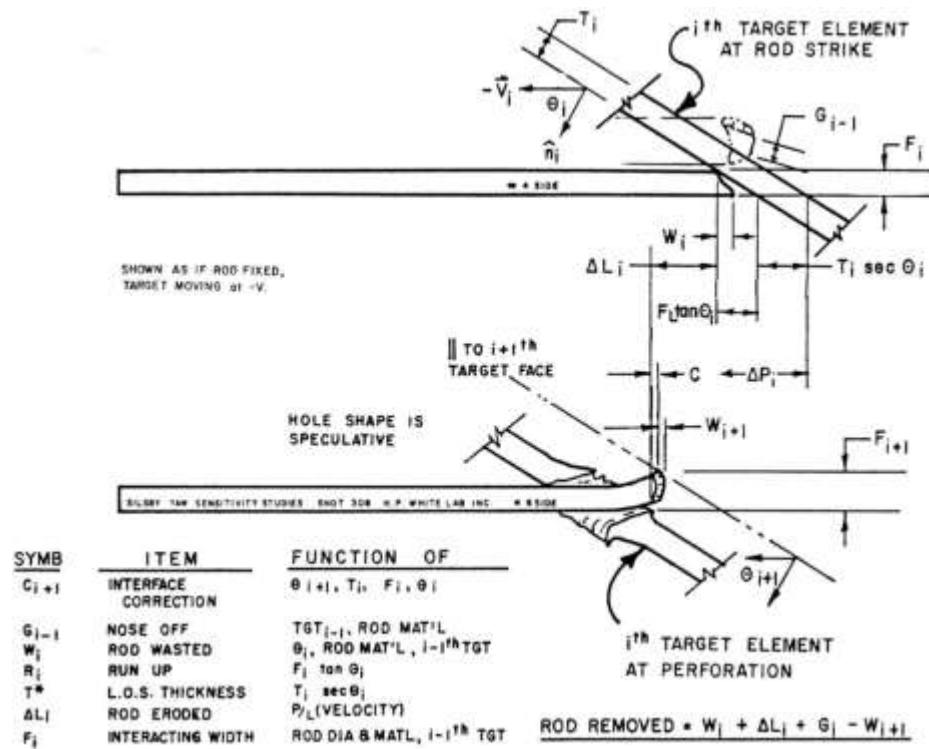
For various reasons, elements in an armor array may not be parallel. See the corrugated appliqué on the USMC Amphibious Assault Vehicle (AAV) shown in Figure 6-15. In this circumstance, the results of a shot depend on both the exact armor geometry and the exact shot line through the armor array. The distance from struck face to struck face along the line of fire could be described as in the upper set of dimensions shown in Figure 6-14 and include the thickness and obliquity of the individual plates where pierced by the shot line.



Armor performance will vary depending on hit location.

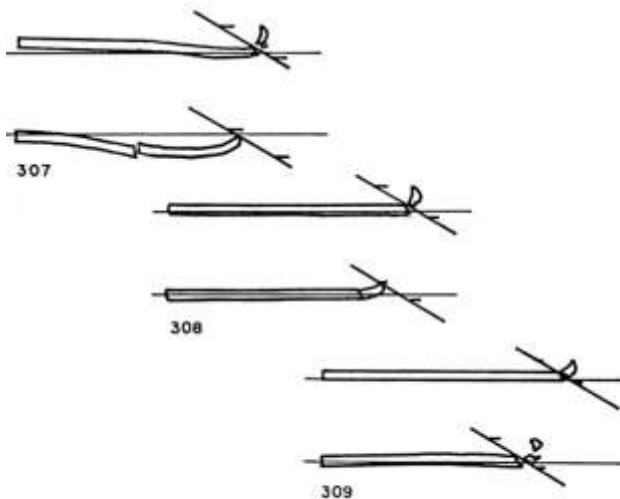
Figure 6-15. Corrugated Appliqué Over Plate Armor on the USMC AAV7A1 (Source: USMC [30]).

Spacing degrades penetrator performance before it reaches the final hull-side armor of a tank. Tracking the amount of rod an individual oblique target element degrades is complex. Figure 6-16 shows a rod erosion budget using actual, typical deformed rod shapes from yaw sensitivity studies. The figure shows the target flying right to left at the stationary rod. The tip of the rod in phantom view in the upper part of the figure is high enough to not contribute to the perforation and hence is wasted material, which nonetheless has to be included on the rod to ensure target defeat (charged to the earlier target element in this case). Depending on the actual shape of the leading edge of the rod, some material is off the shot line and is likewise wasted. The length of rod **actually eroded is shown as ΔL_i and is probably** obtainable from the P/L curve. The effect of a second thin plate on a rod after exiting a first thin plate is shown in Figure 6-17. The tracings are from three x-rays from yaw sensitivity studies, range work by Silsby, reported by Roecker and Grabarek in 1986 [22]. As in Figure 6-16, Figure 6-17 is arranged as if the rod is standing still and the plates are traveling from right to left at the striking velocity. The long horizontal line is parallel to the striking velocity vector. The lines drawn obliquely are at the plate obliquity, while the short horizontal lines show the extent of the actual hole in the



Although every bit of rod removed is important, engineers/analysts would never actually try to account for the various effects seen here.

Figure 6-16. Erosion Budget for a Long Rod Perforating a Thin, Oblique Plate (Source: Silsby [1]).



This W6 tungsten sinter alloy (discussed in Section 6.5) is a bit too brittle.

Figure 6-17. Typical Rod Breakup on Spaced Oblique Targets (Source: Silsby [1]).

plate, which matches the envelope that the rod sweeps out almost perfectly. No one would actually perform this sort of analysis in a real development program. It is just presented here to illustrate all the physical processes involved.

6.5 LAMINATED TARGET ELEMENTS

Laminated target arrays are a subset of spaced arrays in which the spacing is zero. However, as in optics, the materials on both sides of the interface between elements dictate the results significantly. Irresistible forces at the interfaces usually open up the stacks at some point after which some spaced effects are seen.

Particularly for large-caliber work, it is necessary to assemble thick targets out of a number of target plates. While every effort is usually expended to keep the target elements together, it is usually in vain. For generating semi-infinite penetration data, the typical target is a laminated stack of 2-ft square plates, set at normal incidence. The general practice is to hold the stack together by welding two 1/2-in.-thick by 4-in.-wide straps of hot rolled steel plate on each side, or 5-in. x 5-in. x 1/2-in. angle along the edges, using full-penetration, 1/2-in. fillet welds.

After the shot, most of the welds or the straps themselves are broken, due to the bulging of the target plates along the shot line, both up-range and down. What appears to happen is that during penetration of the first plate, the stack is being driven together, and bulge formation on the rear of the first plate is suppressed. The relief wave off the front of the first plate accelerates the plate material near the impact point locally up-range. (The force is sufficient to bend a thin plate even though it is secured at its edges.) This force ultimately opens a gap between the first and second plate. This gap appears to occur either about the time the penetration interface enters the second plate, or sometime after that. Once the first plate is out of contact **with the second plate, the second plate's face is free to** accelerate up-range, and so on. In the meantime, the compression wave reflects off the rear element, accelerating it down range, well ahead of the penetration. The process of unloading from the rear proceeds, with each plate in turn separating from the next one. The result is a small but significant decrease in resistance to penetration.

The resistance to penetration of a laminated stack of plate drops dramatically as it is inclined at increasing obliquity. The disturbance tending to separate the plates operates across their normal thickness, while the time the rod is in an individual plate depends on the LOS thickness and hence the obliquity. The plates have time

to open up before the penetration interface gets there. This effect can be seen in the yaw data [22] plotted in Figure 6-18. W6 WA is a sintered tungsten with 6% nontungsten alloying ingredients. Limit velocities for 4-in. and 5-in. RHA generated earlier are interplotted in this graph forming the baseline for comparison of rod penetration vs. velocity for the yaw sensitivity studies.

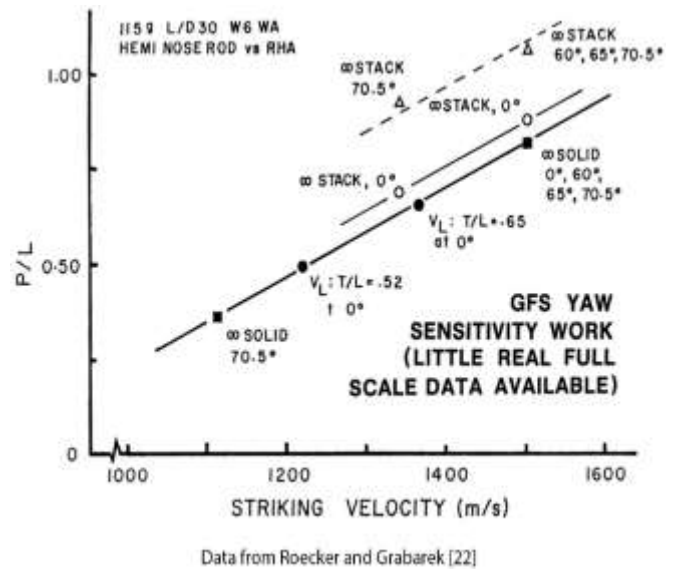


Figure 6-18. Effect of Lamination on Target Performance
 (Source: Silsby [1]).

Semi-infinite penetration data should be generated using as few and as thick plates as possible, so that interpretation of results are confounded the least by this additional, unavoidable variable. For penetrators of sufficiently small diameter, long bars can be cut from 6-in. or 12-in. (proof test) RHA to provide a nearly semi-infinite length along the shot line, though the proximity of the lateral free surface will slightly reduce the ballistic resistance.

7. UNFAIR HITS

The rod does not always strike the target in an ideal interaction, particularly in terminal ballistic testing. The results of shots that might be suspect must be disregarded and not included in the analysis. It is good practice to determine in advance just what is unacceptable and disregard all such data without regard to whether they fit some preconceived notion about where they should go on the graph.

7.1 FREE SURFACE EFFECTS

As discussed in Chapter 6, the effect of free surfaces on oblique penetration is significant. Thus, a shot close to the edge of a plate or other free surface might not generate data that are representative of that from more centered hits. Specifications for ballistic testing usually require that the results of a shot be disregarded if the penetrator strike is less than some seemingly arbitrary distance from the edge, such as three tank gun calibers. Likewise, shots falling too close to holes from earlier shots might be affected either by changes in material properties or by the free surface and are generally disregarded (Figure 7-1).

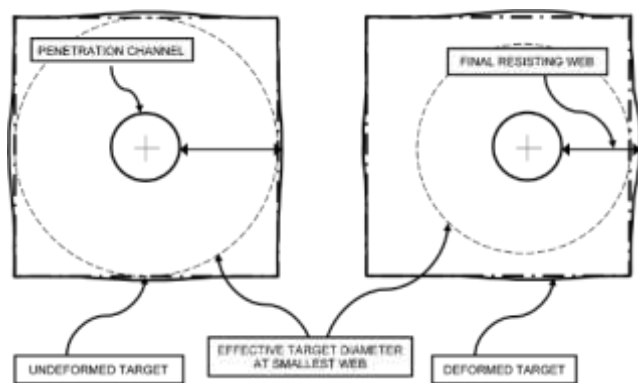


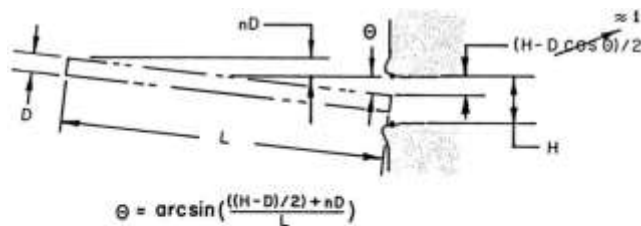
Figure 7-1. Centered vs. Uncentered Normal Incidence Penetration on Thick Square Target (Source: Silsby [1]).

When a normally incident penetrator is generating a channel well-centered in a relatively small square target as shown in the left side of Figure 7-1, there are four planar zones where the web of material between penetration channel wall and free lateral surface is at a minimum. It is at these locations where bulges on the sides occur. The smaller the target extent relative to the hole diameter, the larger the bulge. A cylindrical target of the same diameter as the width of the square target would have a uniform zone of material that would all be pushed out radially to admit the penetrator. The corners on the square target act as bolsters helping the material in that area to resist stretching. Presumably, the depth of penetration in the square target would be deeper than that in the circular target of the same width so that the same amount of plastic work was done on both targets. If the same target were struck under the same conditions, but offset from its center significantly, then there would be one planar zone that would offer significantly less material to resist bulging, and the bulk of the plastic deformation would be noticed on that face. Presumably again, the depth of penetration would be deeper than that of the larger square or cylindrical targets struck well-centered.

If the penetration is deep enough and the channel close enough to the sidewall, the actual penetration path would turn toward the free surface, and the projectile could exit the side face, albeit with most of its momentum down range. Therefore, small target elements would probably need to be thickened near the edges to provide more or less the same ballistic resistance over the struck face. Alternately, armor consisting of many small elements on a size scale similar to or smaller than that of the penetrator would tend to scatter the path of a penetrator and absorb its energy in a series of interactions, as in the break of a pool game.

7.2 YAW

Yaw has a notoriously adverse influence on penetrators, but it is not characterized well. Rules of thumb no longer apply as rods have gotten longer. The effect of yaw can be understood in terms of the side or body of the rod interfering with the penetration channel as the penetrator sinks into the target. Figure 7-2 shows the yaw impact geometry. A penetrator of diameter, D , and length, L , is flying such that its axis is inclined by an angle, θ , to its velocity vector. Its nose strikes a target and creates a hole of diameter, H , through which the rest of the rod must pass. If the yaw exceeds some critical value, the rod body at the rear will interfere with the sidewall of the hole. The higher the yaw, the farther forward contact occurs, and the shorter the penetration channel will be before the influence of the interference will occur.



Shortly after touchdown, the rod is eroding and is only slightly influenced by eccentric loading at the plane where the rod yields and begins to flow plastically. The eventual impact of the channel sidewall on the side of the rod leads to rod bending, rod breakup, the ricocheting of rod material across the channel, and the subsequent deviation of the penetrator-target interface from the line of the initial striking velocity.

Figure 7-2. Yawed Rod Impact Geometry (Source: Silsby [1]).

The rod dimensions and empirical penetration data from yaw sensitivity study firings conducted for Roecker and Grabarek [22] illustrate how rapidly the amount of unaffected rod diminishes with increasing yaw. The 115-gm, L/D 30 W6 WA LRP has a length of 195 mm and a diameter of 6.50 mm. Attacking RHA at 1400 m/s, the hole diameter is 11.9 mm. Table 7-1 shows the fraction of rod clearing the hole and the associated yaw angle as a function of the interference.

Table 7-1. Fraction of Rod Length Clearing Hole*

Interference (Rod Diameters)	0	1/4	1/2	3/4	1
Fraction of Rod Length Clearing Hole	1.00	0.59	0.42	0.36	0.29
Yaw Angle (Degrees)	0.8	1.3	1.8	2.2	2.7

* 115 gm, L/D 30 W6 tungsten LRP (195 mm long, 6.50 mm diameter) attacking RHA at 1,400 m/s. (Source: Silsby [1])

When only a very small length of the rod only slightly interferes with the channel entrance, penetration depth is unaffected. But as the interference increases, serious problems arise. At grazing incidence, the rod tail tends to ricochet across the penetration channel, where it could subsequently strike the other side and tend to ricochet again. Thrashing of the rear of the rod while the front end is penetrating and eroding can cause the shot path to deflect and the rod to break. At larger interferences, the rod is broken up behind the impact point, destroying its ability to penetrate much further. Figure 7-3 shows a sectioned target showing typical

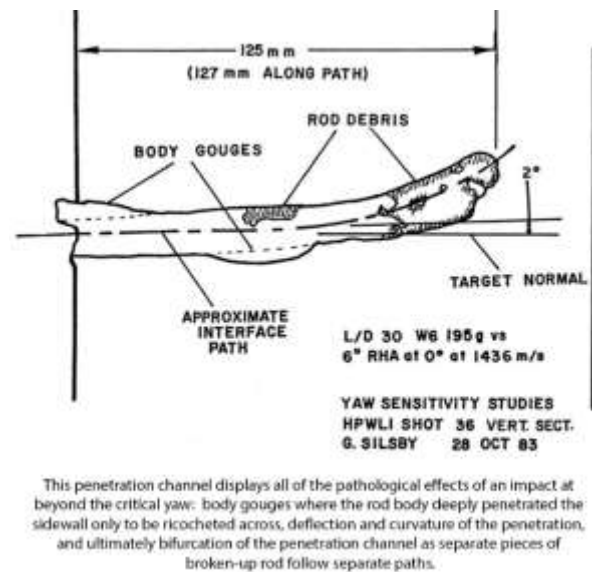


Figure 7-3. Yawed Rod Penetration at Normal Incidence (Source: Silsby [1]).

features seen in a deeply penetrated target attacked by a rod yawed slightly over the critical yaw. Note that the rod apparently broke up near the end of the penetration, as evidenced by the bifurcation of the penetration channel.

With the introduction of obliquity, it becomes apparent that yaw is a misnomer. For the normal incidence target, the direction of the rod yaw is not important, because it had no naturally preferred direction. However, an oblique impact involves a plane of symmetry, usually arranged as the vertical plane in a terminal ballistic test. Under these circumstances, it is natural to refer to the **rod's orientation in terms of the aeroballistic definitions**. Yaw then is the left or right component of the total yaw, while pitch is the up and down component (Figure 7-4).

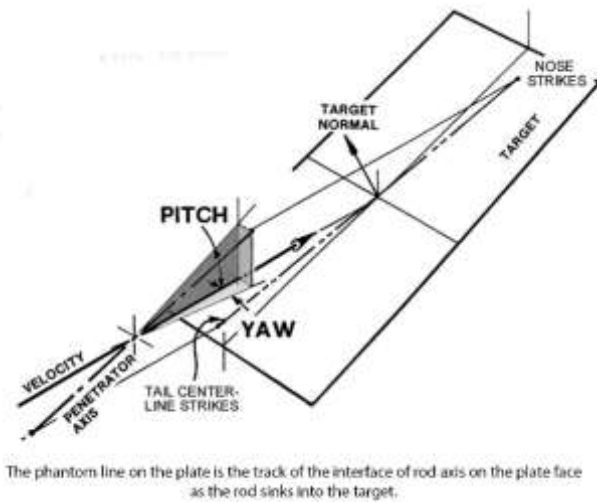


Figure 7-4. Yawed and Pitched Impact on an Oblique Plate Target (Source: Silsby [1]).

Oblique targets are much more sensitive to pitch than yaw. The more unfavorable the rod's initial attitude is, the higher the rotation rate that can be induced in the rod in the unfavorable direction. If the rod pitch is high, the rod path can actually be redirected out the front surface of a thick target. Figure 7-5 shows the sectioned target from such an impact. However, a slight initial favorable pitch (up in this case) is beneficial; it reduces

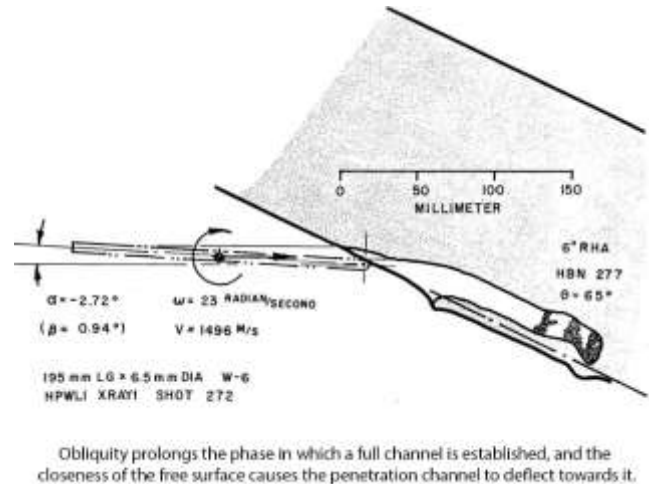


Figure 7-5. Yawed Rod Penetration in an Oblique Target (Source: Silsby [1]).

the pitching rate induced and requires a bit more rotation before achieving a particular unfavorable attitude. This is one of the few factors that definitely are at odds with the assumptions under which the Kinematic Empirical model of penetration can be used (discussed in Chapter 8). However, when interface path length effects are accounted for (which cannot be determined accurately in advance), the results are consistent.

The asymmetry of the hole seen in Figure 6-10 results in asymmetric limits on pitch in the favorable versus unfavorable directions. ("Favorable" is a deceptive term in that **it doesn't take much pitch in either direction to affect penetration accuracy**. "Less unfavorable" is a more accurate term.) See Roecker and Grabarek (1986) [22] for more details on the effect of yaw on penetration.

Note the increased total penetration in the laminated target as indicated in Figure 7-6. No curve was fit to the monolithic data because lack of repetition of the data at the extremes prevents forming a plausible estimate of the variability there, leading to extreme uncertainty in the most critical regions of the curve.

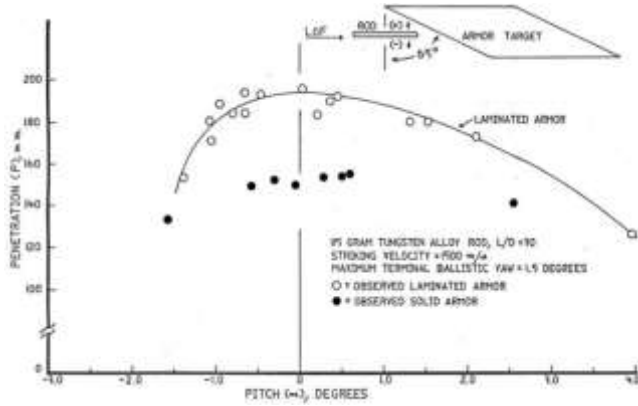


Figure 7-6. Example Curves Comparing the Effect of Pitch on Penetration for a Monolithic and a Laminated Oblique Target (Source: Silsby [1]).

One additional effect of yawed impact is not obvious but is particularly significant in oblique impact. Implicit in the study of penetration mechanics is the idea that only events at the interface affect the process of penetration. Consider the case of yawed rod impact at such small yaw angles that the body of the rod does not interfere with the sidewall of the penetration channel. There is no lateral force on the rod (other than due to uneven application of force over the interface due to material irregularities). For strictly geometric reasons, the interface path, and hence the penetration channel, inclines in the opposite direction to the striking yaw. The angle depends on the P/L ratio and the striking yaw (Figure 7-7). Essentially, the penetration channel is a mirror image of the rod at strike, with the hole diameter enlarged by the appropriate hole-to-diameter ratio, which is a function of

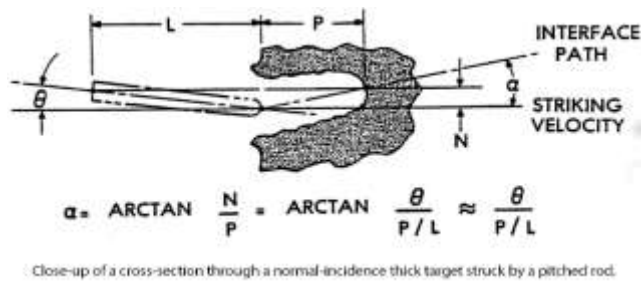


Figure 7-7. Inclined Interface Path in Yawed Normal Incidence Impact (Source: Silsby [1]).

the instantaneous velocity, and the P/L ratio, again a function of the instantaneous velocity. If the path inclines towards the rear surface of an oblique target, the path length through the target is shortened, making it easier to defeat. If the interface path through the target is inclined in the opposite direction, the target will be harder to defeat. Figure 7-8 illustrates this point. Be alert to this effect in experiments involving oblique thick targets, particularly if you observe a large scatter of data around a limit velocity. In the example of the 60° plate obliquity shown in Figure 7-8, note a total of 6% variation in the amount of armor along the two interface paths (independent of thickness) from a plus and a minus 1° striking pitch.

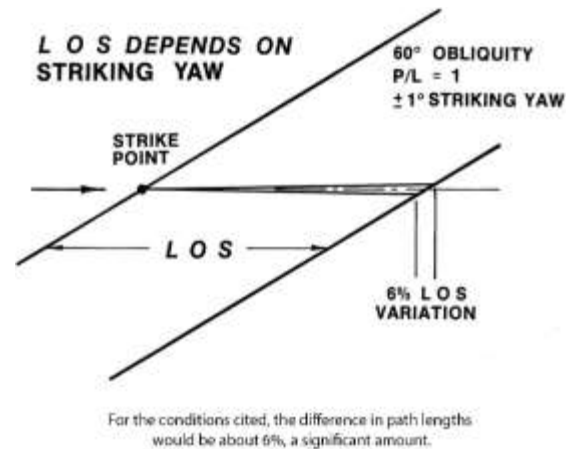


Figure 7-8. Inclined Path Changes the Effective Target Line of Sight Traversed in Oblique Impacts (Source: Silsby [1]).

8. ARMOR AND PENETRATOR DESIGN AND MATERIALS

8.1 ARMOR VS. ARMOR PLATE

Armor should not be confused with armor plate or an armor forging. Armor is the complete protective package design interposed between the potentially lethal attacking threat and the vulnerable components behind it. Sometimes armor is just a piece of armor plate, but even then, the material, heat treatment, thickness, and obliquity all determine a threshold of performance needed by the threat to defeat the armor. The way in which the armor package is mounted (its set of boundary conditions) can be as important as the design of the armor itself.

8.2 ARMOR IS A COMBINATION OF GEOMETRIES AND MATERIALS

Real armor is described in terms of *geometries* and *materials*, each with its range of properties (Figure 8-1). The *geometry* can range from solid to spaced, to laminated, and so on. *Material* properties can range from strong to weak and ductile to brittle; they can be energetic in the case of reactive armor (RA), and so on (Figure 8-1).

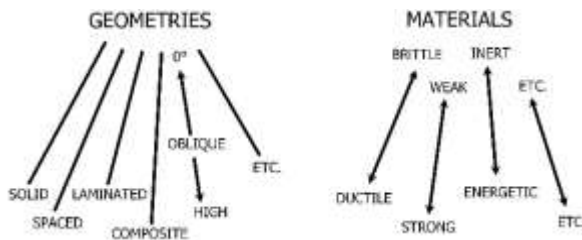


Figure 8-1. Real Armors are Combinations of Geometry and Materials (Source: Silsby [1]).

Each line in the figure represents a characteristic. Some characteristics are continuous variables such as thickness and obliquity, suggested by the arrows on the lines. Some are discrete, e.g., the design is made up of one, two, or three elements. Some are descriptive, such as being a spaced array or a composite. Some characteristics are independent of others, such as oblique and laminated, while some are interdependent, such as ductility and strength. In armor made up of a number of individual elements, each element can have its own set of characteristics.

An interesting geometry for slowing bullets is a bin loosely filled with relatively indestructible balls having about the same mass as the bullet to be stopped. If the bullet strikes a ball nearly head-on, the ball absorbs most of the momentum of the bullet and in turn strikes additional balls, and so on. If the bullet strikes the ball at a grazing incidence, the bullet is deflected a bit but not slowed much and hits another ball. If the bullet strikes the ball at a middling obliquity, the bullet is significantly deflected, and the ball recoils at an angle to the striking direction and they both strike additional balls. After a number of impacts, the bullet and balls have lost their momentum to random commotion, just like the break in a pool game, while any plastic deformation or fracture also absorbs energy. This process of multiple elastic collisions is the basis for moderating (slowing) the speed of a neutron using water, whose hydrogen nuclei are about the same mass as a neutron.

Another example of geometry for slowing bullets is the snail-shaped bullet trap. The bullet enters an aperture and strikes the more or less circularly curved wall of the trap at a grazing incidence, being redirected in multiple ricochets around the periphery of the trap, to fall to the bottom and out a collection chute when spent.

8.3 AREAL DENSITY IS THE MOST IMPORTANT CHARACTERISTIC IN FIGHTING VEHICLE ARMOR

An armor's areal density is the most important characteristic to consider when comparing armor designs. Areal density is the total mass in a unit presented area of armor along a shot line of interest. Typically, the areal density of armored fighting vehicle (AFV) frontal armor from the forward attack azimuth and of the side armor from the 90° attack azimuth is most significant. Areal density is usually given in kilograms per square meter or pounds per square foot. A 1-in. thickness of RHA and other steels at normal incidence has an approximate areal density of 200 kg/m² (40 lb/ft²).

For example, assuming that ¼-in. steel would adequately **protect against most battlefield threats, which it won't**, and that you wanted to add this thickness to four doors of a Humvee at about 1 m² (10 ft²) per door. This **addition would represent 200 kg of a Humvee's** approximately 1,000-kg (2,200-lb) payload capacity, and this design would not protect the vehicle from attack from the front nor protect other critical areas.

8.4 COMPARING REAL ARMOR DESIGNS TO MONOLITHIC RHA

For real armor arrays, versus monolithic RHA, the mass efficiency, E_m , of the armor design in question would be the ratio for a given presented area of the armor to the mass of RHA having the same performance. A variant of this for appliqué is to determine the amount of extra RHA needed that would produce the same residual penetration in a semi-infinite RHA witness pack replacing the primary vehicle armor in question. Figure 8-2 illustrates this concept.

Space is not limitless, either. The armor designer must fit the appropriate protection between the interior envelope in which the systems function, e.g., the fighting

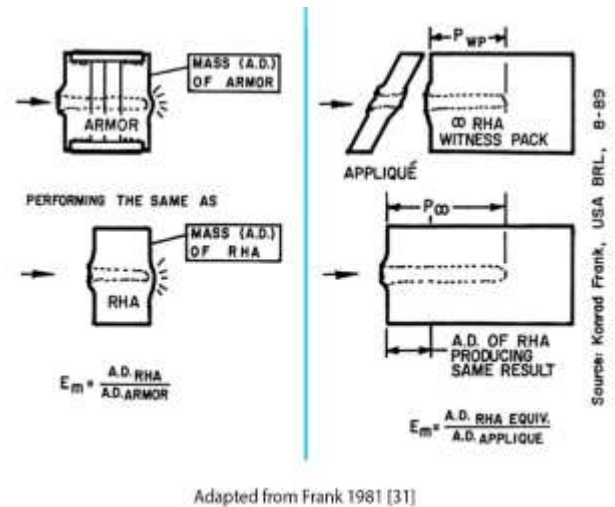


Figure 8-2. Determining Mass Efficiency of an Armor (left) or Appliqué (right) Design (Source: Silsby [1]).

compartment, and the outer envelope, which has its own upper size limit, e.g., the tank must pass through a railway tunnel on a flatcar. E_s is the efficiency measure related to space required and is the ratio of target thickness to RHA thickness at the same limit velocity (or other metric). Figure 8-3 illustrates this concept.

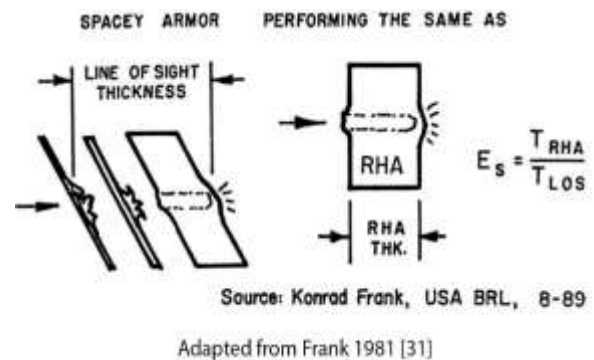


Figure 8-3. Determining the Space Efficiency of an Armor Design (Source: Silsby [1]).

Experience will give good starting estimates for E_s and E_m for similar classes of targets. Data on materials closer to those of the target should yield better results. For example, if it is proposed to up-armor a vehicle that has thick aluminum armor by adding either a thick aluminum

or thick high-hard steel skirting plate, consider generating the E_s s and E_m s in terms of the aluminum or high-hard steel.

Knowing the areal density of an armor design, one can use perhaps readily available RHA performance data to estimate a minimum level of protection. This estimate is performed by calculating the thickness of RHA at normal incidence that would have the same weight as the same presented area along the line of fire as the armor design. **This value is called the target's RHA-equivalent thickness.** The P/L curve for RHA at the striking velocity in question can indicate how much of the threat rod or other threat the (semi-infinite) RHA would remove. If the threat **projectile isn't at least this long (or sufficiently effective if in the low striking velocity regime)**, the striking velocity rod length must be increased to be effective against the target.

Different constraints will usually result in different armor designs. Where space is not a constraint, spacing will be used to advantage to provide a lighter armor. Where space is constrained, as on a tank, weight will increase, and if weight is an issue, more expensive materials will be used.

Semi-infinite penetration is the most primitive, and hence the most consistent, datum you can have. With an empirically generated P/L vs. velocity curve and correction factors for target finite thickness and obliquity and for material properties, etc., a rough estimate can be made of the minimum length of rod necessary to defeat most any modern target at a given striking velocity. *However, having just enough penetrator length to erode to a depth in a semi-infinite armor equal to the target line-of-sight thickness is not enough length to defeat targets at significant obliquity.*

8.5 DEFEAT MECHANISMS

There are a number of defeat mechanisms, both of the rod and the target. Table 8-1 summarizes these. Each is defeated when it no longer performs its intended function. The armor must serve as a protective barrier. **The penetrator's function is to perforate that protective barrier.** The rod can be decelerated to a stop in the armor or can be eroded completely without the last bit of rod actually being stopped. (It turns the corner in the hole and tries to continue up- or down-range.)

Table 8-1. Rod and Target Defeat Mechanisms

ROD	TARGET
➤ Decelerate to a Stop	➤ Perforation
➤ Erode Completely	• Residual Rod Present
➤ Deflect Shot Path	• Residual Rod Absent (Not Worth a Toot!)
➤ Ricochet	➤ Non-Perforation
	• Destroy Structural Integrity

Source: Silsby [1]

Another defeat mechanism is for the path of the eroding interface to be deflected into a more benign direction. At high obliquities under unfavorable striking conditions, a shot can enter the face of the target, only to turn and come out the entrance face. The most extreme case of this behavior is ricochet. It occurs at extreme obliquity with very strong rods or targets. Ricochet is distinguished from deflection in that no target material is evacuated. The target signature is a long, slightly debossed polish mark on the armor.

Armor is obviously defeated when it is perforated. However, it is necessary for the residual rod to have significant length to significantly damage hard components behind the armor and yield a catastrophic kill. ("Significant length" is typically one to two rod diameters.) However, although there may be no residual

rod behind the armor, vehicle crew can still be severely injured or killed.

It is possible to defeat an armored system by sheer shocking power. The defeat mechanisms from shock range from damaging unprotected delicate components to breaking welds and tearing loose and even tossing away big chunks of material. If a critical system or the structural integrity of the vehicle itself is compromised, such as from jamming of the turret or gun, it is out of action even if it is not obviously destroyed. There are a number of simple shock-isolating devices and techniques, which are beyond the scope of this monograph. Two common isolation means are rubber in shear and the simple and inexpensive (coiled) cable isolator as shown in Figure 8-4. Friction between stands of the cable also provides needed damping.



Four assemblies of coiled cables are captured between pairs of bars on the outside, two per side. This box mounted a hard disk drive.

Figure 8-4. (Coiled) Cable Shock Isolators (Source: Silsby [1]).

8.6 MATERIALS IN BALLISTICS

The subject of terminal ballistics is inextricably linked to the following:

- Materials science and metallurgy.
- Understanding stress and strain and both elastic and gross plastic deformation.
- Understanding how dislocations weaken materials relative to the expected strength of a

material when computed as the sum of the atomic bonding forces.

- Understanding how hardness is measured and how it relates to material strength.
- Fatigue and fracture mechanics.
- Manufacturing processes, to include metrology and both destructive and nondestructive examination techniques.

Engineers/analysts involved in the design or evaluation of penetrators, armor, and other targets should be knowledgeable about the terminal ballistics components in the preceding list. Another requirement is to be able to judge whether computational results are plausible according to natural law and to be able to design simple and efficient experiments that will confirm or deny any performance claims made.

A proficient and knowledgeable terminal ballistics engineer/analyst can predict the outcome of most shots. Puzzling results may require additional shots and experimentation, so it is important to have the hardware and expendables for several more shots than the program would seem to require, to be able to quickly explore promising leads. (The number of shots needed in a program includes extra shots to get the experimental setup right, the instrumentation checked out, and an allowance for bad shots that normally occur.) It is much less expensive to have additional hardware prepared in advance to be able to continue a program for a short time than to go through the process of **planning out a separate program if needed. Even if it's not needed to confirm some questionable or promising result, the hardware can be used to fire a few critical shots quickly to investigate any issues or questions that may develop after the testing has been completed and documented to see if further work is warranted.**

8.6.1 Armor Materials

Armor materials can be metallic, ceramic, or composite; there are also armors made of specialty materials. Metals are not only plate but can be forgings or castings or sinter alloys as well. (The properties of the latter are improved by hot isostatic pressing to close defects and give a sounder product.) There are a number of ferrous and nonferrous metallic armors. The most important from the tonnage perspective is RHA.⁶

8.6.1.1 Armor Steel Alloys

Any metallic element, in this case iron, can have other metallic and nonmetallic materials intentionally or unintentionally incorporated to form an alloy. Those atoms whose radii are close to that of iron can be substituted for iron in the crystalline structure, while compatible elements with sufficiently smaller radii can fit within the matrix. In both instances, the lattice is strained making it harder for dislocations to run, hence strengthening the material. Typical interstitials are hydrogen, so small that it readily moves through the iron lattice at room temperature. In the case of steel, the typical interstitial is carbon, which has just the right radius to create the unusually complex microscopic structure that can be developed on demand in steel. At room temperature, only very small amounts of carbon can be found dissolved in iron because it is too big for the lattice. By heating iron and letting the lattice expand, the carbon can fit within the interstices and a lot can be dissolved (liquid iron can dissolve more than 6% by weight). When iron cools, the carbon emerges and forms iron carbide, which is very strong. The iron carbide aggregates into very small laminae separated by thin layers of nearly pure iron, which is very weak. The hardening process in steel begins by heating the steel

sufficiently to dissolve the carbon and then quenching it rapidly to room temperature to retain the carbon in a nonequilibrium solid solution that is extremely hard and brittle. The steel is then reheated (tempered). The amount of carbon that emerges from solid solution to form lamella of iron carbide depends on the temperature, and because of the soft iron matrix, the bulk strength drops with increased tempering temperature. More importantly, the toughness (resistance to breakage) increases. Limiting the carbon content will limit the strength that can be achieved. A wide range of properties can be obtained from any suitable alloy composition using the quench and temper process.

As with carbon, various elements will form compounds in a metal alloy instead of substituting into the matrix or being interstitials. These compounds tend to segregate at grain boundaries, usually weakening the bulk metal (sulfides and the like), but if the compound is dispersed finely enough throughout the matrix (at the nano-scale of about 50 atoms in an aggregate), it can strain the matrix and block the flow of dislocations, strengthening the material.

RHA. RHA is a high-strength, low-alloy, through-hardening steel similar in composition to AISI 4330 steel (nominally 0.30% C). The compositions vary among manufacturers. Armor steel has many of the same requirements as gun tube steel and as the armor on naval surface combatants and in submarine pressure hulls.

The concentration of alloying ingredients is low, and the goal of the alloy design is to yield a relatively high-strength steel that can be heat treated to achieve very high toughness and very low frangibility, with the properties uniform through the thickness of the plate.

⁶ One of the most recent major improvements to the M1 tank's armor was to replace some of the material in the armor in the turret front with uranium [32]. It is interesting to consider that while the basic metal is inexpensive, the Army is willing to pay a premium for the Department of Energy (DoE) to process a relatively small quantity of whatever product geometry was needed for this undoubtedly custom production.

(Unlike processes such as case hardening, where the surface is hard to some depth, then soft.) Frangibility in steel is exacerbated relative to that of many other alloys because part of the hardening process involves forming microscopic laminae of iron carbide (separated by nearly pure iron), which are stress intensifiers. The lower the concentration of carbon, the lower the number of fragments produced when the plate is perforated. (For example, chromium is added to premium iron welding rod because it preferentially forms nodular as opposed to laminar carbides, which reduces the brittleness of the weld.)

RHA is bought to a performance rather than a property specification, although there are a number of property restrictions in the specifications. The specifications for RHA (MIL-DTL-12560K [33]) describe several classes with thicknesses from 2.5 mm (0.098 in.) to 152.4 mm (6.000 in.) unless otherwise stated. Class 1 is heat treated to develop maximum resistance to penetration. Class 2 is 2.00 in. maximum thickness and has maximum resistance to shock. Class 3 ranges from 0.250–12 in. thick and is intended for ammunition testing. It is not intended for use in combat vehicles and has tighter specifications on thickness. Class 4 armor is intended for fighting vehicle armor. It has the same maximum carbon content as Class 1, but a lower tempering temperature is used to give it higher resistance to penetration than Class 1 armor. Its thickness ranges from 2.5–69.9 mm (0.098–2.75 in.). Class 4a is produced by the usual quench and temper process, while Class 4b is air hardened or auto tempered to achieve the same goal for properties in the same thickness ranges.

The RHA specifications do not include guidance about the concentration of any alloying elements, except for carbon, which is restricted to a maximum of 0.27–0.31% depending on the desired plate thickness. Specifications are also included for the known deleterious elements phosphorus, sulfur, copper, nitrogen, titanium, aluminum, lead, and tin. RHA manufacturers declare a

chemistry, and the specification then limits the variation from this in future production lots.

The specified hardness range varies with the thickness, the thinner plate being harder. If designing a reduced-scale test, draw the temper on the plate to that of the full-scale value. Hardnesses range from about 210 Brinell for 12-in. plate for ammunition testing to 470 Brinell for the thinnest plate specified. Also restricted are the total phosphorous, total sulfur, and combined phosphorus plus sulfur. These two elements form soft compounds at grain boundaries and embrittle steel. Hardness varies with the desired nominal thickness of the plate. The Charpy V-notch energy absorbed in breaking a specimen is specified as a function of Brinell hardness of the plate. Tests with one of a set of specific (now obsolete) service rounds are specified to determine if the ballistic limit meets or exceeds a given value, and tests with one of a set of custom shocking rounds on a weld seam are specified to determine if the plate meets minimum weldability standards.

The manufacturer submits qualifying samples to the government for testing, and if they pass, draws a limited number of representative samples from subsequent lots for quality-assurance testing. If the manufacturer changes the composition, the new product must be resubmitted for qualification testing. Armor plate has traditionally been cross-rolled to ensure as nearly uniform properties as possible, but there is no military specification that addresses this topic. As the billet reaches some thickness in the reduction from the bloom, the ribbon of hot steel is cut to some length that will yield a final length of 144 in. of sound steel. These pieces are alternately roll reduced in the longitudinal and transverse direction until the final desired thickness is achieved. Figure 8-5 condenses Army armor steel specifications from several sources ([21], [34], and various standards ca. 2018) into a single graphic. Nonmilitary ballistic researchers are forced to use the widely available

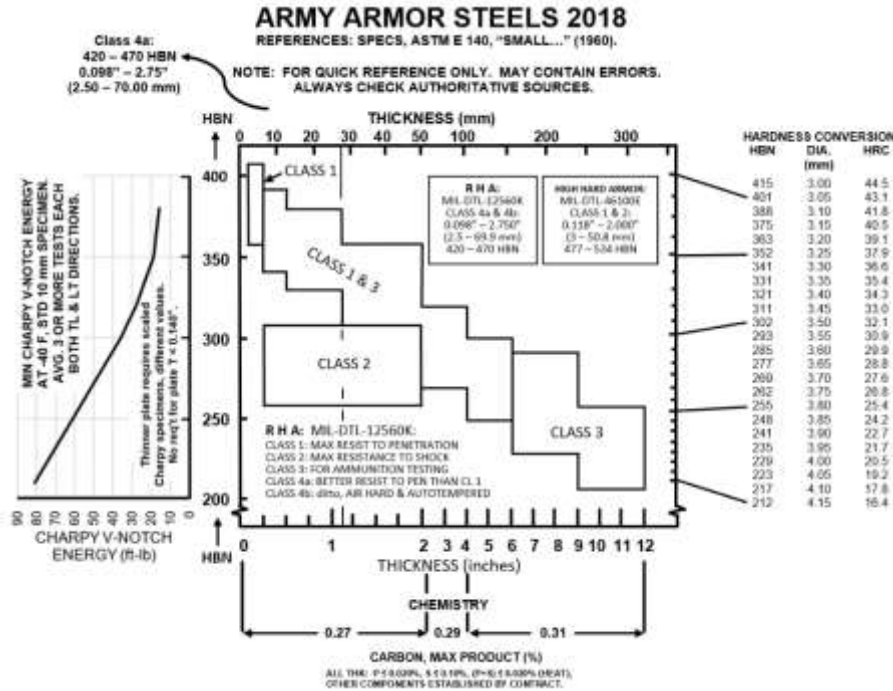


Figure 8-5. Army Armor Steel Specifications (Source: Silsby [1]).

commercial 4340 alloy as a surrogate for RHA, but by virtue of its lower carbon content, RHA is more readily welded, important in fighting vehicle construction. Many nations have their own RHA recipes, which vary greatly based on national prejudices. Metallurgy has progressed significantly since the initial specifications for armor plate were written, and a number of nations have improved their armor over time. For example, based on a recent paper by Lothar Meyer [35], a long-time German ballistics researcher, Germany has increased the strength of its armor while maintaining its toughness, thereby achieving increased resistance to penetration for the same weight. A recent paper by Mehran Maalekian [36], also a German researcher, discusses the effects of alloying ingredients on steels.

High-Hard Armor (HHA). HHA (MIL-DTL-46100E with Amendment 1 Notice 1 [37]) is a variant of saw steel. As with RHA, it is designed to be as tough as practical and with minimal frangibility. HHA specifications are similar to those of RHA, with the exception of the increased

hardness, typically 500 Brinell. HHA can be drilled with commercial, high-speed, tool-steel drill bits, but a large amount of lubricant is needed, along with low surface speed and a heavy feed to keep the cutting lip below the work-hardened zone created as the drill advances. Another hard armor plate is ultra-HHA (MIL-DTL-32332 [38]), typically 600 Brinell, covering thicknesses of 3 mm (0.118 in.) to 16 mm (0.630 in.). It is a quench and temper alloy primarily intended for use as an appliqué on ground vehicles but can be welded by special techniques. There are two classes of ultra-HHA. Class 1 is designed for better resistance to penetration than MIL-DTL-46100, while Class 2 is designed for better resistance to penetration than Class 1.

There are many requirements for steel (and other materials) that are not independent of other requirements, for example, wear resistance versus strength and hardness, and so on. Observe the welded beads of material on the working surfaces of loader and

backhoe buckets designed to resist abrasion, while the base material is designed to a specific strength.

Dual-Hard Armor. Another armor plate is dual-hard armor. Although the original military specification, MIL-S-46099C, appears to have been cancelled, there is continued interest, as discussed in Gooch et al. 2005 [39]. Dual-hard armor presents a hard face to break up bullets and a softer back to deform without cracking. Two plates of different armor steels are roll-bonded together and roll reduced to be a bit thicker than required. The compositions of the two materials must be adjusted such that the materials bond properly **and don't distort very much** on heat treating, so the properties of the individual layers are less than ideal compared with the properties if the individual layers were not metallurgically bonded. It is also possible to locally vary the properties of a single material by a heat-treating process such as induction hardening specific sites or by differential quenching or tempering.

Dual-hard armor has been used for gun shields for pintle-mounted 0.50 cal machine guns on boats and smaller ships. The parts are cut to shape from as-rolled (soft) plate. Typically, the rolled product is not flat enough for the specifications. After hand straightening the plate by bashing it on an anvil with cross-peen hammers in specific places at a specific orientation, the somewhat less irregular plate is put on the magnetic chuck of a Blanchard grinder, with the high spots on the underside **shimmed up so the plate won't deform under the** clamping force. The high spots on the upper surface are then ground off, and the plate is flipped and shimmed as required, and the high spots are ground off the other side. This process is repeated until the correct thickness is obtained. Equal amounts of steel must be removed from both surfaces so that the ratio of the two layers stays within specifications. Once the sides are bent, the part is heat treated and cleaned, and it is ready to be

painted and installed. Another variant is tri-hard armor, where a softer core holds hard outer surfaces together when struck. Kleponis, Mihalcin, and Filbey [40] demonstrate that shooting a functionally gradient armor such as dual-hard armor soft-side first improves armor performance.

Incompatible materials can be bonded by explosive welding. In this process, the sheet to be bonded is stood off a small distance from the backer plate, and the appropriate thickness of an appropriate explosive is applied. The detonator is located at a corner to eliminate the need for a line-wave generator, which launches the sheet progressively. The intent is to have the flyer plate impact at such an angle that the surface material of both sheets is jetted outwards creating a clean interface and a series of curled, interlocking surfaces, which are then mashed down further by inertia. Figure 8-6 is a schematic of the process, while Figure 8-7 shows a cross-section through an explosively bonded sandwich.⁷

There are many current iron alloys such as the maraging steels that can be made stronger and tougher than RHA, but their cost exceeds their benefits, both because of the cost of the ingredients and the cleanliness required in their production. Typical of these is the 17-4PH steel (17% cobalt, 4% nickel, and 4% copper). This is a precipitation-hardening alloy in which the copper is dissolved to form a solid solution at high temperature. The bar or plate is typically sold in the solution annealed state. The desired part is machined to dimensions that will yield the desired finished dimensions, then placed in a heat-treating furnace in air at approximately 900°F for 4 hours. In this precipitation-hardening treatment, the copper forms a fine, well-dispersed precipitate of a size that can resist the movement of dislocations. The part does not distort significantly (less than 0.001 in./in.) particularly when compared with the distortion seen in thin plates when quenched and tempered. The

⁷ The NobelClad website (<https://www.nobelclad.com>) provides a video of the explosive welding process.

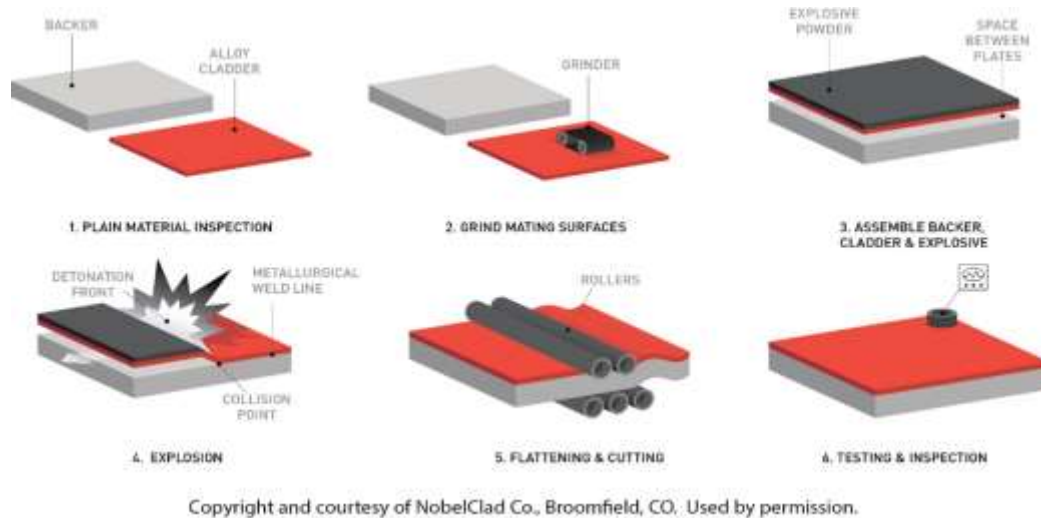


Figure 8-6. Process Schematic of Explosively Welded Metallic Sandwich (Source: NobelClad Co. [41]).



Three plates, explosively bonded. The cut is perpendicular to the collision line. The interlocking "breaking wave" patterns, similar to the familiar Greek stepped-fret motif, are caused by vortices forming and then being crushed together. Explosion welding can bond otherwise incompatible materials. Photo copyright and courtesy of NobelClad Co., Broomfield, CO. Used by permission.

Figure 8-7. Surface Cut Through Explosively Welded Metallic Sandwich (Source: NobelClad Co. [41]).

processing produces an attractive gold finish on the maraging steel that does not need to be removed. In this H900 condition, yield is about 285 kilo-pounds-per-square-inch (kpsi), and ultimate tensile strength is about 200 kpsi [42].

8.6.1.2. Other Metallic Armors

Steel has a particularly complex and useful hardening mechanism when heat treated when compared with those other metals that can be strengthened by precipitation hardening, such as many aluminum, titanium, and magnesium alloys. Many metals cannot be strengthened by heat treatment at all. For these metals, where a harder part is needed, whatever work hardening occurred during primary reduction (rolling, forging, etc.) can be left, the part can be intentionally strained in tension, or the part can be partially annealed from the as-rolled state to a desired softer state.

Aluminum is used as armor, e.g., on the Bradley Fighting Vehicle. The 5083 aluminum alloy initially used in the M113 armored personnel carrier (APC) was incorporated in the first general-purpose specification for wrought aluminum alloy armor plate, MIL-DTL-46027 in 1959 [43]. Problems with the 5083 composition were corrected, and the 5456 alloy was added in Revision C in 1964 [44].

The Army developed its own variant of the high-strength 7075 aircraft aluminum alloy (7039) that had better ballistic resistance than 5083 and seemed to promise a fair certainty that welds would endure indefinitely under

Table 8-2. Aluminum Alloys Used as Armor and Their Military Specifications

Alloy Desig.	Specification	Spec. Status	Comments
5083	MIL-DTL-46027K	Active	Weldable; used on original M113 APC; properties have evolved with time.
5456	MIL-DTL-46027K	Active	Weldable; developed to improve on 5083.
5059	MIL-DTL-46027K	Active	Weldable; recently added.
7039	MIL-A-46063H	Inactive	Better than first two; used on M551 AFV. SCC issues.
2519	MIL-DTL-46192C	Active	Better than 7039; SCC same as 5083.
6061, 6055	MIL-DTL-32262A	Active	Commercial PH alloy can replace 5083; not tested for weldability; used as appliqué.
2139, 2195, 2060	MIL-DTL-32341A	Active	High-strength aerospace alloy; not tested for weldability; used as appliqué.
7085, 7056	MIL-DTL-32375B	Active	Two tempers: Better ballistics and better resistance to shock.
5083	MIL-A-45225F	Active	Also 5456; forged armor.
5456	MIL-A-45225F	Active	Forged armor.
2219	MIL-A-46083D	Active	Also 5083, 5456, 7039; 2219; extruded armor.
2219	MIL-A-46118E	Active	2219 rolled armor plate and forgings.

Source: Doherty et al. [43].

field conditions. This alloy was ensconced in MIL-A-46063 (1963) [45]. Thickness ranged from ½ to 4 in. inclusive. The basic specification imposed limits on values of chemistry, mechanical properties, stress corrosion resistance, and ballistic limit. However, stress corrosion cracking (SCC) continued to be a problem, and research to find a better alloy proceeded [43]. At present **that military specification (Revision H) is “inactive for new designs and is no longer used except for replacement purposes” according to an archived 1989 DoD Index of Specifications and Standards (ISS) [46].** The ISS itself is now inactive and has been replaced by an electronic repository. (Register for an Acquisition Streamlining and Standardization Information System [ASSIST] user account at <https://assist.dla.mil>.)

A third-generation aluminum alloy, 2519, was developed with its specification, MIL-A-46192, which was promulgated in 1986. This alloy was considered for the Mobile Protected Gun program, cancelled in 1997, and for the Crusader program, cancelled in 2002, and was

used in prototype hulls for the Expeditionary Fighting Vehicle program, which was cancelled in 2011 [43].

About 2007, Doherty et al. [43] began ballistically characterizing a number of promising aluminum alloys as candidate armors with the 0.30-cal AP round and the 20-mm fragment-simulator projectile and ultimately qualified five more alloys and wrote three more specifications for them. Table 8-2 lists the currently used aluminum armors and their military specifications. The current military specification used for aluminum armor, MIL-DTL-46027J [44], imposes further detailed specifications on the commercial 5083, 5456, and 5059 alloys (which are its three classes). These are all strain-hardened alloys. Thickness ranges from 0.250 through 3.000 in. inclusively. The specification imposes limits on chemistry, ballistic limit, mechanical properties, and may include stress corrosion resistance. Other metallic armors, such as titanium [47] and magnesium alloys [48], are used primarily in personal armor.

8.6.1.3 Composite and Ceramic Armors

Based on their high strength-to-weight ratios, composites such as epoxy-reinforced fiberglass have been proposed as armors, but due to their low densities, any primary hull of an AFV would have to be unrealistically thick to resist even the smallest hand-held HEAT threat. Although vehicles with composite armor may be seen on the battlefield, they require additional armor. The failure mechanism that occurs in softer matrix materials reinforced with long, stiff fibers is that as the reinforcing fiber is pulled in tension, it tends to elongate along its axis and contract normal to the axis. If an adhesion failure begins, it will then propagate into the matrix as a progressive failure.

Ceramics are really composites of the desired very hard ceramic grains cemented together with a lower-melting point matrix. There are 90%, 95%, and 98% aluminum oxide ceramics. The rest of the composites consist of glass that acts as a binder. Ceramics are naturally very hard but very brittle. Their toughness can be significantly increased by including ingredients that create defects that resist the advance of crack tips, such as zirconia-toughened alumina. Unless the failure in the material is self-limiting, the design will have to be tiled to maintain a reasonable low probability of defeat by a second-round hit. However, as tiles get smaller, their ballistic resistance drops by weight. With smaller size comes a higher probability of a hit on a joint, a weak spot. The adjacent tiles need to be buffered from the blow delivered by the rapid radial expansion of the tile that is penetrated. As with all other design challenges, cost is always a driver. The three important ceramics used for personal armor are aluminum oxide, silicon carbide, and boron carbide [47]. Table 8-3 lists their density, cost, and performance.

Table 8-3. Three Common Armor Ceramics as of 2007

Material	Approx. Density	Approx. Cost	Performance
Aluminum Oxide	3.9 g/cc	Inexpensive	Least
Silicon Carbide	3.2 g/cc	\$40/lb seeking \$35/lb	Intermediate
Boron Carbide	2.54 g/cc	\$90/lb	Best

Source: Jones [47]

8.6.1.4 Special Circumstances

A number of special circumstances require special approaches. Necessary hull penetrations have to be armored, such as to accommodate a telescope or vision block. Typically, a pair of prisms whose diagonals act as mirrors are used to offset the line of sight, and extra armor is included in back of the outer one and in front of the inner one. Cameras can replace telescopes and vision blocks but are more likely to be damaged.

Armored transparencies also present a number of design challenges. The outer surface needs to be very hard to resist scratching. Sapphire (single-crystal aluminum oxide) is the second hardest naturally occurring material, after diamond, and is transparent over a wide range of wavelengths. At present, sapphire is inexpensive enough for it to be considered for use in armored windows. (It is widely used on scanner windows.) The back-face material of a transparency should be able to deform without shattering and projecting a lot of fragments into the fighting compartment if perforated. In addition, the transparency should not distort the image significantly. The complete assembly should be able to take several hits and still have enough clear, transparent area to be useful.

The amount of personal armor needed currently to protect against rifle fire accounts for most of an **individual's load-bearing** capacity. Many considerations

for personal armor can be transferred to fighting vehicle armor. For example, in a lightly armored vehicle, somewhat flexible interior blankets of Kevlar or a similar material can be used to catch secondary debris from a SC jet perforation, reducing the vulnerability of the occupants in the line of fire. Some standoff is useful as it allows the debris to separate, rather than all attacking at a very small zone.

Radical design changes can reduce the weight of armor required, as in the newly introduced Russian T-14 Armata MBT. An auto-loader on the main gun eliminates the requirement for a human loader. The remaining crew is concentrated in a smaller and hence lighter armored compartment [48].

8.6.2 Other Penetration-Resistant Materials

While tanks are designed to hunt tanks, they are often called on to attack other targets. They are especially useful for taking out bunkers and other reinforced-concrete structures, log and earth bunkers, sandbags, earth berms, etc. Be aware that there is extensive military guidance on how to build these structures, the resulting protection levels achieved, etc. In addition, in concrete construction, heavy steel reinforcement is used to resist ballistic attack, to include through-lacing to keep as much concrete in place as possible even when thoroughly fractured. The ends of the reinforcing rods should be bent back (hair-pinned) to prevent pull-out. The resistance to penetration depends on the care used in designing the mix and in curing the concrete, as anyone using a powder-actuated stud gun will learn. Modern concretes include fiber-reinforced concrete, high-strength concretes, as well as air-entraining concrete. The latter has myriad small bubbles, into which ice can expand, protecting the concrete against freeze-thaw cycles. However, these bubbles make the concrete easier to penetrate.

Softer materials might present fusing problems to SC munitions, which typically must be able to penetrate brush without detonating. LRP's can penetrate a surprising distance in things such as dry sand and still be lethal, as was demonstrated in Operation Desert Storm.

8.6.3 Penetrator Materials

After considering the basics of terminal ballistics as briefly discussed in Chapter 1, penetrator designers must focus on the details. Most importantly, they must design penetrators to have optimum ductility. If the ductility is too high, the penetrator comes out of an oblique element with too much of the bent nose intact and strikes the next plate like a banana hitting a brick wall. If the ductility is too low, the rod breaks up excessively and the pieces are not likely to stay in train, in which case they are wasted on the next element.

Spaced armor, more than anything else, has been the **driving force behind the metallurgist's continued** development of very tough, high-density penetrator materials. At present, typical materials that have been successfully used have been uranium alloys and tungsten-nickel-iron cemented/sintered-powder metallurgy alloys.

After examining uranium alloys originally developed for use in (the nonfissile parts of) nuclear weapons and experimenting with other compositions, the U.S. has settled on the original U-3/4 (weight-percent) titanium alloy. The metal is available almost for free as a by-product of the nuclear power industry. It is a precipitation-hardened alloy, so exotic processing is unnecessary. A tremendous amount of metallurgy and engineering had already been devoted to its production and to optimize its properties to include long-term storage considerations such as deterioration and corrosion resistance.

Although not as good on a weight-for-weight basis as uranium, the tungsten sinter alloys were developed over a long period of time and at considerable expense in the hopes of replacing the radioactive uranium as the primary penetrator material, without success. After careful sintering of the powder preform, the resultant billet is turned to a standard diameter and is cold rotary swaged to reduce the cross-sectional area so as to work-harden the material, then is usually strain-aged, a process similar to stress relief. Hot isostatic pressing was seen to improve the properties of sinter alloys. Hot means a high enough temperature that diffusion is rapid, and isostatic pressing means applying sufficient pressure on the surface so that porosity is eliminated.

When the ammunition family for the M256 gun on the M1 tank was being developed, custom-made penetrators in ballistic-quality 90% to 96% WA could be acquired commercially in reasonably small lot sizes in a number of countries worldwide. However, once the demand for ammunition production was satisfied, a tremendous shake-out occurred in the industry, so that now there are only a few sources for both WA and uranium penetrators.

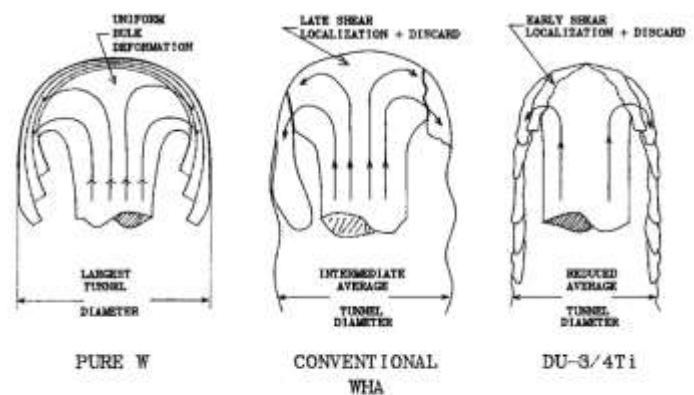
For steel-on-steel work, AISI S7 and other shock-resisting tool steels have been so strong and tough that Charpy machines have been unable to break standard 10-mm² specimens for a long time now.

The uranium alloys perform better than WAs because of the way they fail (plastically deform and fracture) in the ordnance velocity regime (which is more or less arbitrarily defined as between 1- and 2-km/s striking velocity). Lee Magness, Jr. of the Lethal Mechanisms Branch of the Weapons and Materials Research Directorate of the U.S. Army Research Laboratory (ARL) discovered the explanation of this phenomenon [49].

In the commonly used tungsten sinter alloys, in the zone of deformation at the leading end of the eroding rod, work-hardening predominates over thermal softening.

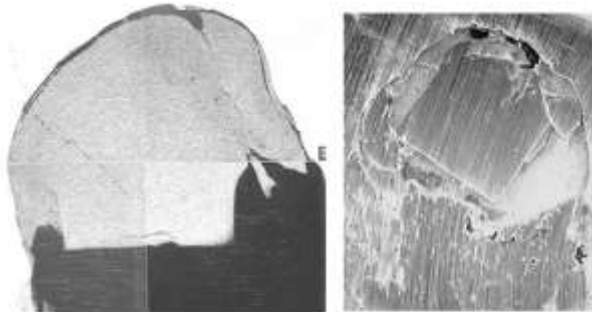
As a zone of WA is deformed along a surface of maximum shear, it work-hardens and stops flowing, and the less deformed material around it takes up the flow. This process proceeds until the entire leading zone of material is thoroughly work-hardened and chips break off. At this point, the head of the tungsten rod has been significantly mushroomed. With the commonly used uranium alloys, thermal softening predominates over work-hardening, and as a zone deforms in shear, it loses strength. Shear deformation then localizes further in that zone and in a runaway process, chips are shed off at this adiabatic shear surface. The head of the penetrator is only slightly mushroomed. Some people refer to this process that results in a chisel-shaped penetrator tip as “self-sharpening,” but since the material is eroding, not penetrating rigidly, this term is a misnomer.

In both the tungsten sinter alloys and uranium alloys, as the remaining rod advances, it pushes open a channel and the process repeats. Given that the KE of the penetrator must first enlarge the cavity ahead of it to advance, the penetrator that can push open the smaller hole will have more energy left to advance the penetration. Figures 8-8 through 8-12 show the failure modes for pure tungsten, a tungsten nickel-iron (W-Ni-Fe) sinter alloy (tungsten heavy alloy [WHA]), and the U-3/4Ti uranium alloy. Figure 8-8 illustrates a common



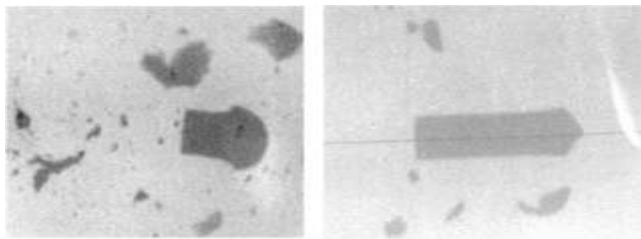
Target is RHA struck at ordnance velocity. Striking velocity is upward.

Figure 8-8. Comparison of Penetrator Failure Modes (Source: Magness [49]).



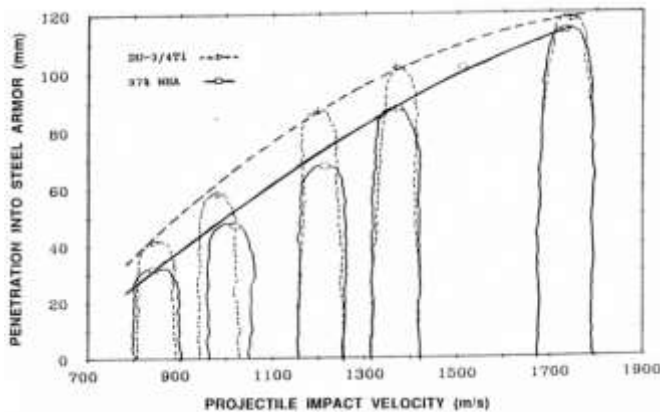
W-Ni-Fe (left), U-3/4 Ti (right). Semi-infinite penetration of RHA at ordnance velocity. Residual rod has yawed nose-right in right image.

Figure 8-9. Comparison of Residual Penetrators (Source: Magness [49]).



W-Ni-Fe (left), U-8Mo (right).

Figure 8-10. Comparison of Residual Rods After RHA Perforation (Source: Magness [49]).



As velocity increases, inertial effects dominate the determination of hole diameter and the advantage of DU decreases.

Figure 8-11. Comparison of Penetration Channels as a Function of Velocity (Source: Magness [49]).

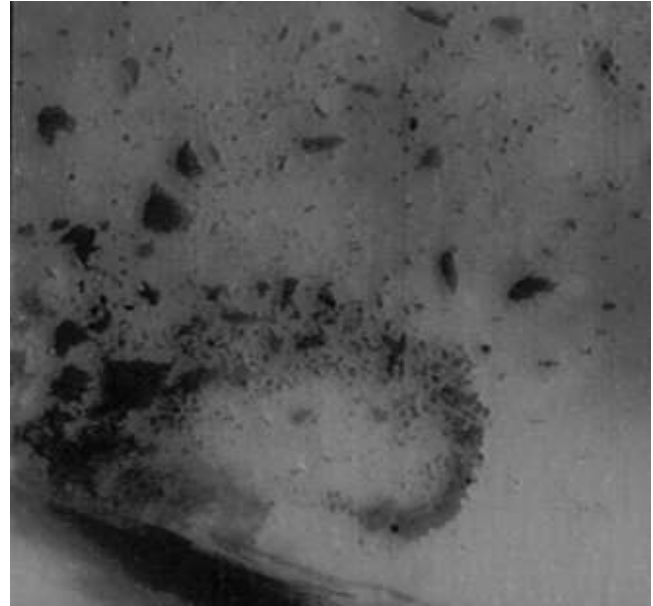


Figure 8-12. DU Long Rod Eroded into Shear Chips as it Perforates a 70.5° Steel Plate Target (Source: Magness [49]).

misconception that pure tungsten is brittle. Most pure metals will be brittle if they have picked up very small quantities of hydrogen, oxygen, nitrogen, carbon, or other deleterious elements, but are usually quite ductile if very pure, as the tungsten on the left in Figure 8-8 shows.

8.7 THE PENETRATOR MUST BE DESIGNED WITH THE SABOT AND PROPELLING CHARGE FOR MAXIMUM LAUNCH VELOCITY

Penetrator failures are usually a consequence of a (usually perceived as minor) failure of one or more small design details. The mastery of the art of penetrator design depends upon the practitioner's skills, knowledge, training, and experience in the rapidly evolving discipline of penetrator design.

Successfully launching an antiarmor projectile at the maximum velocity possible from a gun of a particular bore diameter, travel, and chamber volume (rifled or smoothbore) could be the subject for another entire monograph, but a penetrator designer needs to

understand the constraints entailed in developing a successful penetrator design. Everything launched from a gun has a peak acceleration beyond which it fails in bore. Because the tank is just the life support system for its gun, if the gun bore is destroyed, the tank is useless.

Launching an antiarmor projectile at maximum velocity is vital because 1) the lower the time of flight, the less time a moving target has to travel, and 2) a smaller drop decreases the effect of unfavorable aiming factors.

However, today's LRP travels in excess of Mach 5, so aerodynamic heating is a problem that has to be addressed. If a bit of fin or nose is burned away, the round doesn't fly as straight.

8.7.1 LRP Round Design

In its simplest form, the LRP, as conceived by the Russians (e.g., the Bm15 [Figure 8-13]), is an effective penetrator thrown from the gun like a javelin, gripped using driving lands at its middle by a sabot that transmits the force of the base pressure on the sabot bulkhead to the penetrator flight body itself. Ancillary functions are imparted to the design such as spinning-up the round to



U.S. Navy EOD graphic. Nose has been damaged. Not clear are canted holes in the three sabot petals that impart spin as gun gases are vented up the bore, copper buttons on the substantial steel fins that act as bore riders, and machined leading edges on the fins that create lift to lock the round into a desired roll rate in flight.

Figure 8-13. The Russian Bm15 LRP and Sabot (Source: Wikimedia Commons [50]).

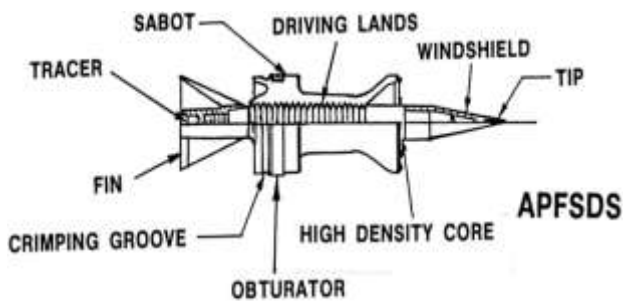
some small roll rate, typically about 100 revolutions a second, as well as ensuring a clean sabot discard.

The propelling charge design needs to be optimized to stretch the base pressure-time curve and lower its peak acceleration to optimize the conversion of the CE to KE. This optimization is achieved through the selection of the correct propellant, particularly its composition and geometry. Propellant composition is constrained by concerns that high temperature will shorten the erosion life of the barrel, while its geometry is used to tailor the burn rate with time. An LRP extends deeply into the propellant bed, creating a long and narrow propelling charge geometry, which is concerning, so the ignition train needs to ensure that the propellant is ignited reliably and repeatedly over the operating temperature range in which the weapon system operates.

In U.S. designs, where parasitic weight is minimized, the aluminum fins are particularly susceptible to being damaged on pulling out of the propellant bed, as are the propellant grains themselves, which would cause irregularities in the propellant burn and undesirable shot-to-shot variability in the ballistics. In addition, the parts immersed in the burning propellant have to be protected to keep from being ignited.

At some acceleration, the tail end of the rod extending from the sabot will be pulled off by an excessive tensile load. At another value for acceleration, the unsupported length of the rod forward of the sabot will buckle.

Early in the development of LRP ammunition, a reasonable length of rod could be launched with a zone of driving lands extending along about one-third of the rod length. The sabot was a bit longer than the engagement length using a bell forward to increase the wheelbase. The sabot material was relieved as much as possible in its middle to reduce weight, with a short, full-bore section aft with an obturating band to seal in gun gasses. Figure 8-14 shows the M735 APFSDS round.



The central region of the sabot is relieved to a saddle-shaped cross-section to relieve weight. A small metal ring screwed to the front of the sabot petals and notched at the joints in the sabot, called a bourrelet, controls the discard of the sabot. A plastic obturating band on the heavy rear bulkhead of the sabot seals gun gasses from leaking forward up the bore while decoupling the sabot body from the rifled tube. Machining the fins creates a lifting force to lock in projectile spin at a desired value in flight. Adapted from TM 43-0001-28 [7] and TM 43-001-28-3 [8].

Figure 8-14. M735 Flight Body and Sabot (Source: Silsby [1]).

As the effectiveness of fielded armor increased, it was necessary to lengthen the rods. Lengthening the sabot increases in-bore mass and reduces the muzzle velocity, so again, every effort is made to reduce mass. A tapering forward sabot section provides lateral support to the added projectile length forward with minimal added mass. Likewise, from the rear, a tapered rearward sabot section with driving lands carries the inertial load of the rear of the rod. This double-ramp-saddle configuration can be seen in various forms in Figure 8-15, which shows the evolution of the M829 family of LRP ammunition.

The friction sabot provides tractive forces on the rear portion of the rod. The rear profile of the sabot is tailored in a long, thin taper so that, like a collet in a lathe, the pressure of the gun gases clamps the sabot to the rod with a uniform friction force that increases as the gas pressure and hence acceleration increases. A short length of rod and the tail fins can be left projecting to the rear, with the length depending on the maximum acceleration, the unsupported mass involved, and the strength and cross-sectional area of the rod material.

The solution for the shape of the profile is a long trumpet-shape that ultimately comes close to bore



(All LRP ammunition is the same overall length.) Note that as the rod is lengthened, the fins intrude deeper into the propellant bed until the M829A3 is forced to use base ignition. Stick (vs. granular) propellant geometry promotes rapid propagation of the flame front in the propelling charge. The rod now extends essentially the full length of the stowage compartment.

Figure 8-15. M829 Family of LRP Ammunition (Source: Bharat-Rakshak [51]).

diameter, where the sabot forms a bulkhead. Back when manufacturers used a mechanical taper attachment on lathes, the shape was approximated by a uniform taper, but with computer numerically controlled lathes, the profile can be exact. The surface of the sabot assembly and the zone where the rod emerges rearward is coated with a continuous elastomer to form a gas-tight seal, and small driving lands are usually provided to ensure that the rod does not start to slip rearward as the shot starts to travel up the barrel.

The ramp-saddle configuration is retained in the body and forward. The forward portion of the rod is supported against buckling by a reverse taper sabot feature, with some short length of the rod unsupported, again determined by acceleration, mass distribution, the beam-buckling formula, and the material properties. The evolution of the U.S. M829 APFSDS round illustrates

these trends. The M829A2 round broke from tradition and uses a graphite-composite sabot (Figure 8-15).

8.8 TOXICITY OF TUNGSTEN

One other very significant property of tungsten has come to light recently that will surely affect the DU vs. WA debate. Until a series of studies was conducted, uranium was presumed to be the more troubling material because of its radioactivity. It emits alpha particles (helium nuclei) and electrons, neither of which has much range in air. However, efforts were devoted to reducing troop exposure to uranium and to remediating the range areas in which it had been tested in the open air. Although some of the troubling toxicity issues with tungsten were known, in particular nickel compounds, the danger from tungsten sinter alloy rod corrosion was unknown. As a result, the WAs were incorrectly assumed to be fairly inert.

When samples of WA intended for penetrators were implanted in rats, the rats died, as did those implanted with pure nickel. Those animals implanted with tantalum as a control survived. One such animal study was conducted by J. F. Kalinich et al. [52], and its references can be used to track the increasing concerns about WA. In at least one of a number of similar studies conducted earlier on DU in response to Gulf War veterans with retained DU shrapnel, larger pieces of DU caused a significant increase in soft tissue sarcomas [53].

8.9 USING THE KINEMATIC EMPIRICAL MODEL

There are no simple models of long-rod penetration based on first principles that can predict the performance of any rod on any target. The current, complex, penetration-mechanics computer codes are producing quite realistic results but are still too expensive in terms of coding and code-tending personnel time to render testing obsolete.

When a simple penetration model is found, it will use realistic values for material properties that can be measured by some means separate from firing the ballistic test in question. This nearly ideal model will have a minimum of parameters, which will relate to penetration mechanics, and it will not be necessary to consult an expert for the currently accepted values for the parameters. Until this type of long-rod penetration model is available, practitioners will relate everything to effective rod length and target thickness (actually, interface path length) and use a crude but effective model, the Kinematic Empirical model, coupled with **extensive testing for results**. “Crude” means that the expected results are within 20% of the real results. “Effective” means that the predictions are close enough that a lot of experimental effort is not wasted before you can home in on the final result. Time delays can be set from trigger screens for the radiographs, and a usable image is produced on the film 95% of the time. The model has been in common use since it was appropriated from the study of shaped-charges.

It is necessary to empirically determine the P/L value for the particular rod-and-target combination at the striking velocity in question, or absent that, the P/L value for the rod material vs. RHA, or, less desirably, for a rod material of similar density vs. RHA. Therefore, it is helpful to accumulate as much P/L data as possible.

In the Kinematic Empirical model, the penetrator-target interface is followed through the target, element by element, and rod erosion is measured at each spot, and alternatively, the penetration depth in the individual target elements is measured. The penetration interface is assumed to follow a straight path through the target, which can be wrong. If the interface path is known (empirically), use that interface path length instead. The rod is assumed not to decelerate, which definitely is wrong, but is usually not too far from right when overmatching a target. No allowance is made for the forces acting on rod and target. (The study of dynamic

events without regard to forces is the discipline of kinematics.) Figure 8-16 illustrates the estimating process for a short piece of penetrator and a single target element. Remember that some allowance might have to be made to adjust the penetrator-target interface path length for obliquity or other effects.

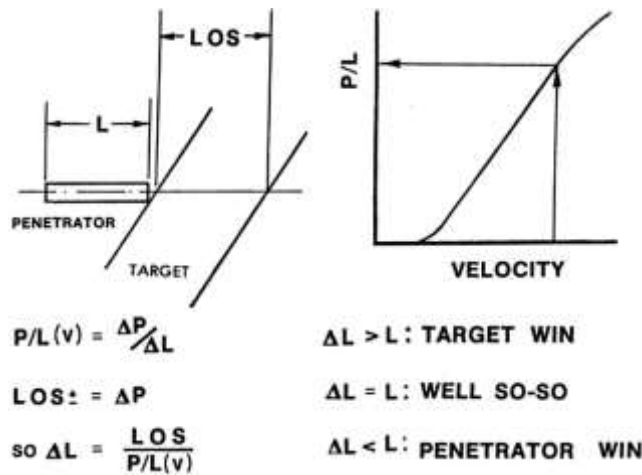


Figure 8-16. Estimating Relative Penetrator and Target Erosion
 (Source: Silsby [1]).

A series-parallel approach is used in the Kinematic Empirical model if there is more than one penetrator element attacking the target. Every piece of penetrator is assumed to sweep out target material within the presented area of that penetrator piece normal to its velocity vector. The length of each penetrator piece is assumed to be the longest continuous dimension parallel to the velocity vector for that penetrator piece. The penetration of this effective length is then determined from the P/L value at the actual striking velocity of that piece on that target element, if known, or from the striking velocity on the first element of the target otherwise. If the trajectories of two individual elements are judged to be closely aligned, the penetrations are summed. One piece begins penetrating where the previous piece stopped. If the shot lines of two pieces are not closely aligned, each piece makes its own penetration in the target.

At low obliquity, each element of the target, no matter what it is, is conceptually converted into a monolithic plate of RHA or other ballistically characterized material at normal incidence having the same mass per unit area normal to the shot line as the real target element. When the obliquity exceeds some significant value, such as 45°, the line of sight must be corrected for rod diameter as well as target thickness. The thickness of the RHA (the RHA equivalent thickness) for that element is divided by the P/L value for the striking velocity in question to determine the amount of rod eroded by that element. If there is rod left, the process continues. If a particular target element erodes the rod completely, the rod is defeated.

The Kinematic Empirical model will not account for a rod being snapped off, for rod foreshortening (for very soft rods), for ricochet, or for any other perturbations to the projectile. It also does not account for the effect of breakout, which influences perforation significantly in high-hard (low-ductility) target elements at high obliquity. Therefore, no allowance is made for breakout, and the hope is that some other effect such as target ductility will offset it sufficiently so that the results will be close to reality.

9. MOVING METAL WITH EXPLOSIVES

9.1 INTRODUCTION

Earlier chapters have discussed a number of penetration principles. For example, penetration increases with velocity until at around 3 km/s, when it is nearly constant with increasing velocity. For long penetrators such as LRPs and SC jets, penetration can be predicted reasonably well by the density law. For an SC jet, the effective length is the difference between jet tip and tail velocities times the break-up time, but effective length can be degraded by jet misalignment, target compressibility, and target strength.

This chapter approaches **penetration from the designer's** perspective of defeating a target. If a penetrator designer considers a jet-forming, lined-cavity charge (SC), then he or she must examine a number of design variables to optimize performance of the proposed warhead design. If faced with a fixed maximum jet velocity and jet energy (i.e., jet mass), then increasing the density of the jet material increases penetration, while the accompanying decrease in jet volume results in a decrease in jet diameter and a decrease in the diameter of the hole in the target. But *can* materials be substituted arbitrarily, say, uranium for copper, in a liner design? Suppose the design constraints are a fixed jet energy and jet material density; then increasing jet velocity increases penetration and decreases hole diameter by decreasing jet diameter. But are there limitations on jet velocity? And how is it controlled? The penetrator's **energy source, the explosive charge, and** how it interacts with the shell or cavity liner to launch a lethal penetrator are examined in this chapter.

9.2 FUNDAMENTALS OF EXPLOSIVES

Explosives are useful because they contain a lot of energy in a small volume and can release it essentially instantaneously on command. Explosives are used extensively in ordnance. Some of the most sophisticated uses are in the family of lined-cavity charges, where the metal liner is forcibly deformed into a highly lethal antiarmor projectile launched at very high velocities. In various formats, a weapon that can be easily carried can destroy a modern Main Battle Tank (MBT). Explosives are divided into those that detonate, for example, trinitrotoluene (TNT) and those that can only burn (deflagrate) such as black powder. With the exception of improvised explosive devices, only the detonating explosives can move metal.

An explosive material is a subcategory of energetic materials. Energetic materials can be stimulated to decompose in a disturbance that progressively and orderly sweeps through the material and releases energy. At the interface between unreacted and reacted material, the parent explosive is chemically being decomposed, and the by-products then recombine into more stable by-products. Typical examples of energetic materials are the material on a match head, gun propellant, and glyceryl trinitrate (nitroglycerine [NG]). Many substances burn in air, such as gasoline, but are not energetic materials. Energetic materials contain all of the necessary materials to react, either as a mixture (black powder) or as part of the molecule itself (NG) and do not need air or other additional chemicals to support the reaction.

Typical nonexplosive energetic materials are pyrotechnic compositions used to generate light, heat, or gas, while explosives are intended to generate large volumes of gas extremely rapidly, often at high temperatures and extreme pressures, for the purpose of breaking up masses of material, for use in military ordnance, and in civilian applications such as demolition explosives,

aerospace hardware such as explosive bolts, and oil-well perforating guns. Energetic materials are not usually categorized; rather, their intended use distinguishes them. For example, nitromethane can detonate and contains enough oxygen to release significant energy on decomposition. It is not used as an explosive for practical reasons, but is often used as a racing car fuel where it is intended to burn with supplied air. It is usually burned with a fuel-rich mixture to reduce the flame temperature to reasonable levels.

In many energetic compositions, the reaction is oxidation. However, any set of chemical species can exhibit oxidation by the increase of the oxidation state of one or more of the reactants (with a corresponding decrease [reduction] of the others). Chlorine can substitute for oxygen. In thermite, a mixture of iron oxide or other suitable metal oxide and aluminum metal or other suitable reducing agent, a straightforward reaction reduces the oxide to pure metal with the generation of sufficient heat to melt it. Thermite is primarily used in a welding process. A mixture of powdered zinc and sulfur makes a good fuel for amateur rocketry. Some energetic materials are just highly unstable compounds that react to some slight stimulus, for example, sodium azide or xenon tetroxide.

The exact composition of the reaction products depends upon the resultant temperature and pressure and whether there has been adequate time to establish equilibrium. They can subsequently further react as the products expand down to room temperature and pressure, and mix with the surrounding medium, usually air. For example, the relative concentration of carbon monoxide to carbon dioxide produced is higher at higher temperatures and lower at lower temperatures. Often the products of the reaction are flammable; for example, carbon monoxide can burn to carbon dioxide at lower pressures. Flammable by-products can be seen in the second muzzle flash in some artillery fire when the

hot gun gases mix with air as the gun tube empties following shot ejection.

Note that chemical reaction rates depend strongly on temperature. The underlying explanation is that molecules can only react when they get close enough. Temperature is a measure of the distribution of the speed at which the molecules move and impact other molecules; and as energy is added, the temperature rises. A chemist's rule of thumb is that reaction rates double for each 10°C rise in temperature, more or less. Thus, it would be expected that the sensitivity of the explosive would increase with temperature, until some temperature is reached that initiates the reaction without need for further outside stimulus.

Safety is a particular concern with energetic materials, particularly explosives, because of their destructive nature and their sensitivity. There are many items that are too dangerous to be allowed to be shipped, rendering them useless for all practical purposes. Items must be designed with their shipping containers to present the lowest transportation hazard class possible both for economy and for safety in transportation and use. Furthermore, the designer must consider ways to keep the initiation of one or more rounds from propagating to adjacent rounds in storage, whether in an ammunition dump or in an AFV. Many safety issues depend very specifically on design details. Explosives safety is discussed further in Chapter 13.

9.3 DETONATION VS. DEFLAGRATION

Burning releases heat, which in turn can melt, vaporize, and decompose the adjacent material, with the exact processes depending on specifics. The fuel and oxidizer then mix, ignite and burn, closing the cycle. The mixture does not need to be stoichiometric, that is, there may be an excess of fuel or oxidizer and may contain chemical species that do not contribute to the reaction. The final

composition and state of the by-products depend upon local conditions of initial temperature, pressure, concentration of species, confinement, and heat-transfer considerations (quenching). The burning rate of energetic material is temperature dependent. For substances such as propellants, where they may need to be used over a wide range of initial temperatures, the composition will often include additives to reduce the temperature effect as much as possible. If the initial composition and the compositions and amounts of the by-products are known, the energy released and the temperature of the gases at any given pressure can be computed from the handbook values of energy of formations and the specific heats of the by-products at the temperatures involved.

Burning usually progresses smoothly and linearly, but if the material is relatively transparent to infrared radiation, ignition can occur at a distance from the burning front. In granular beds, burning grains tend to jump around, igniting material at some distance, and can lead to serious problems, e.g., when trying to burn-off excess granular propellant. In confined channels, the reaction products can propagate ahead of the burning front. The effect is the basis of the pyrotechnician's quick-match. Quick-match is a loosely spun and plied cotton cord soaked in potassium nitrate with a coating of fine black powder adhered with dextrin solution and dried, serving as a fuze. It is contained in a tube only a bit larger than itself, and when it is lit on one end, the fire flashes to the other end very rapidly. It has been replaced by the much more reliable and safe shock-cord.

Shock-cord is a thin-walled plastic tube with a dusting of finely ground explosive on the inside, typically pentaerythritol tetranitrate. UTC Aerospace Systems offers a thin-layer explosive (TLX™) and an initiating TLX (ITLX™) with a higher explosive loading. When a flame is applied to one end of the shock-cord, a flame very quickly comes out the other end, just enough to initiate a compatible blasting cap, which is a big safety

improvement over detonating cord. This accelerating effect of channels on confined gases is also the cause of the rapid spread of fire when initiating a granular bed of gun propellant.

In detonation, a strong shock wave disrupts certain chemical bonds, and the products subsequently recombine in a fashion that uses less energy in the bonding, with the rest of the excess energy increasing the temperature and pressure of the final reaction products. A shock wave results when something tries to move faster than the speed of sound in a medium. The reaction causes a compression wave to propagate into the by-products (and unreacted material), increasing density and sound speed. So as the detonation takes hold, the zone of compression of the material at the interface is continuously overtaken by the disturbing event. Eventually, an equilibrium state is established where an extremely thin layer of highly compressed material, a shock wave, is advancing into the undisturbed media. The width of a shock front is approximately that of the mean free path of the molecules in the undisturbed media. On the undisturbed side ahead of the shock, the material is at its initial state of temperature, pressure, density, and velocity. Behind the shock, the media are hotter, denser, and moving forward at some velocity depending on the strength of the shock. "Chapman and Jouguet originally (c. 1900) stated the condition for an infinitesimally thin detonation. A physical interpretation of the condition is usually based on the later modeling (c. 1943) by Zel'dovich, von Neumann and W. Döring (the so-called ZND detonation model)" [54].

Shock strength is measured by how much faster the shock wave moves relative to the elastic sound speed of very small amplitude in the undisturbed medium. Because the propagation of a detonation wave is supersonic, the detonation velocity is probably only slightly sensitive to initial temperature. While only explosives detonate, most explosives will burn as well.

9.4 FOREST-FIRE MODEL OF DETONATION PROPAGATION

Burning is a relatively slow process, while detonation in large volumes of explosive proceeds faster than the local speed of sound. The detonation velocity in many military explosives is about 7,000 m/s. The bulk compressive sound speed in solids is highly variable, computed as the square root of the ratio of the material's bulk modulus (compressibility) to its density. In steel, it is approximately 5,500 m/s, while in polyvinyl chloride, the common plastic with the closest density to that of TNT, the sound speed is a bit less than 2,500 m/s. In addition to a compressive wave, solids will support a shear wave, but it travels slower than the compressive wave. The sound speed in liquids is generally less than that of solids of the same material; for water, the sound speed is about 1,500 m/s; and in gases, it is lower still (about 350 m/s in air). As a first-order approximation in bulk explosives, detonation occurs instantaneously, converting a solid or gas mixture into reaction products at the same volume but at much higher temperature and pressure.

However, moving metal (or other material) with explosives requires knowing the exact route the detonation front takes and how motion is imparted to the material over time. The fastest propagation of a disturbance in an explosive is the detonation front, so the detonation front expands out in three dimensions from the point of initiation in all directions at its characteristic speed in a so-called forest-fire model (Figure 9-1) until the entire explosive charge has been initiated. The forest-fire analogy was adapted when computer modeling was young and performed in two dimensions at the most.

In this model, a sophisticated, two-dimensional SC warhead is populated by little trees forming a forest. The detonator and booster have initiated a "burn" on the centerline at the rear of the warhead. The fire has burned along the trees between the rear case wall and

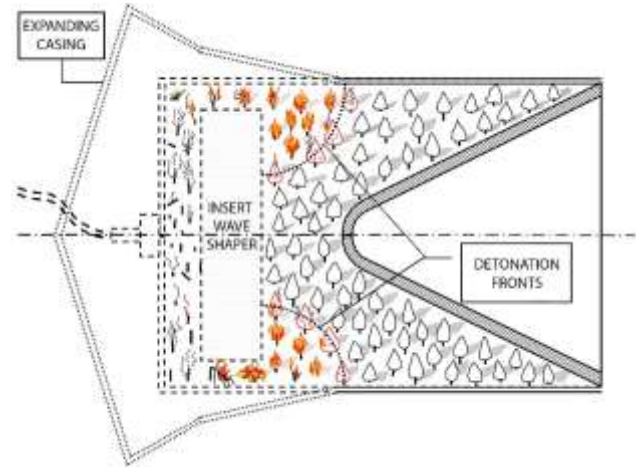


Figure 9-1. Forest-Fire Model of Detonation (Source: Silsby [1]).

the inert wave-shaper, turned the corner and proceeded forward between wave-shaper and casing, and broken out into a pair of circular detonation fronts converging on the liner. The dashed lines to the left indicate where the components were prior to detonation, and the dotted lines indicate approximately where the casing material would be at the moment shown.

There are circumstances where the detonation can get ahead of itself, for example by crossing sufficiently narrow gaps, whether by a sufficiently strong air shock or by propagating sufficient disturbance in an adjacent inert solid material, or by material jetting from the surface of a cavity, whether an unintentional void or some intentional feature. There are also circumstances where a detonation wave propagating in a strand of explosive such as detonating cord can disrupt a strand of explosive it is contacting without detonating it. Puzzling behavior resulting from developmental designs involving complicated explosive trains can often be attributed to unplanned events such as these, while such behavior can also be exploited in some highly sophisticated applications, for example, explosive logic, but that topic is beyond the scope of this work.

9.5 SENSITIVITY AND POWER

Sensitivity refers to both sensitivity to accidental ignition, as from impact, friction, or static electricity, and the power of a detonator needed to reliably initiate the explosive. These terms are related. Each explosive composition has a characteristic threshold of input energy needed to initiate a detonation. Explosives that are very sensitive and can be detonated with a small stimulus are called primary explosives, while less sensitive ones that require a detonator are called secondary explosives. A third class of explosives is so insensitive that it needs a booster of secondary explosives to initiate it. These are called extremely insensitive explosives and are typically used as blasting agents both because some are inherently inexpensive and because they do not require the same degree of special handling in shipping, handling, and storage as do more sensitive explosives.

Explosives are seen to initiate when sufficient heat to start a reaction builds up microscopically due to rapid deformation, and the decomposition releases additional heat and builds rapidly to detonation. Impact, heating, and pinching or shearing explosives are likely to cause initiation. Finely comminuted explosives are typically more sensitive to ignition by friction and static electricity than when they are in the form of a compact solid. Explosives technologists have long recognized the influence of compression of a granular explosive on its sensitivity to ignition. As a charge is increasingly compressed from its bulk density as a loose powder, it first loses sensitivity due to the reduction of the opportunity for intergranular friction as voids are reduced. Then when individual grains are broken in the pressing process, sensitivity goes up. "It is possible to compress an explosive beyond a point of sensitivity, known also as *dead-pressing*, in which the material is no longer capable of being reliably initiated, if at all" [55].

Sonoluminescence perhaps explains the sensitivity of some explosive charges. It was discovered in 1934 by H. Frenzel and H. Schultes. They put an ultrasonic transducer in the developing solution tank for processing photographic film in an attempt to speed up the process and noticed spots of light on the developed film. They realized the light came from the collapse of bubbles. Then, Felipe Gaitan and Lawrence Crum produced single-bubble sonoluminescence in 1989, permitting the systematic study of the subject. The light is seen to originate from the ionization of the gas in the bubble as it is compressed radically on bubble collapse [56]. The compression of many tiny voids in pressed explosives may be the source of initiation when they are simply compressed suddenly with no gross shearing of the material, as would occur during in-bore acceleration of a gun-launched warhead. The absence of small gas pockets would explain dead pressing. Training material for explosives technologists mentions the incorporation of (glass) microballoons in the oil phase of emulsion blasting explosive/blasting agent as a sensitizer [57].

Major drivers in warhead design are the amount of acceleration to which the charge will be subjected before engaging the target and the rigors of its storage and handling. Air-delivered bombs and rockets must survive accidental release and impact on a hard surface without detonating the explosive. Gun-launching potentially subjects the warhead to the highest accelerations and hence deleterious forces, with the indirect-fire mortar, artillery piece, and howitzer potentially posing less of a challenge than the direct-fire tank cannon. Damage in handling or launch typically would result in cracks in the explosive fill or detachment from the casing, which in turn can increase sensitivity. In addition, ammunition is subject to unfriendly fire, so the least sensitive explosive to be effective should be used.

Again, the least sensitive initiating device that is practical should be used. Blasting caps come in a variety of loadings to match the charge they are intended to

initiate. Some blasting caps have a cup molded in their tip that collapses and jets like an SC to intensify the shock and improve their initiating capability. Many military explosive trains such as artillery fuzes are staged, that is, they start with a very small, easy-to-initiate detonator, followed by a medium-sensitivity, medium-power (and usually rather sensitive) booster, followed by the main charge. Military fuzes are designed to keep the munition safe during assembly, storage, shipping, and handling, and yet render it live after appropriate launch conditions have been sensed. Fuzes may also incorporate target-sensing elements and self-destruct features.

The fuze designer faces increasing challenges with decreasing diameter of the round, as there is decreasing volume in which to store the initiating energy (capacitor or battery) and decreasing volume for the proximity sensor and for the mechanical, electrical, and explosive elements. The topic of fuze design is beyond the scope of this work, but Fowler [58] provides further discussion.

Using a fuzed munition in a manner different from that for which it was intended is extremely dangerous. An example would be in firing an anti-aircraft round with a proximity fuze in a horizontal trajectory near the ground, as in gun range work. As soon as the fuze arms, its proximity sensor is activated, and when it senses the ground, the round explodes. A very knowledgeable person needs to alter the fuze to disable the proximity function but have it still initiate on impact. In addition, working with foreign fuzes can be dangerous because they often have only primitive safe-and-arm functions.

For practical reasons, a very safe initiating device is needed. It should require a serious effort to initiate it, always initiate when commanded, and deliver sufficient energy to reliably detonate the charge for which it is intended. Blasting caps have evolved from requiring burning fuzes, which were problematic in wet environments and gassy mines, to requiring small

electrical impulses, which were sometimes initiated accidentally by radio transmissions or stray current (ground loops) to the present models, which use large electrical impulses. They won't initiate if the leads are plugged into a 110 volts alternating current outlet.

Each explosive composition has an inherent energy content, which is its main measure of performance and is reflected in its ability to do work. Higher power means less explosive is needed to do the job, or material can be thrown faster for a given mass of explosive. High power is especially important in the military and particularly where total weight of a munition is critical, such as air-launched missiles. One measure of explosive power that can be experimentally determined quite simply is the Chapman-Jouguet pressure [59]. The lower end of a vertical cylindrical column of the explosive of interest in a standardized size is immersed in pure water, a substance whose equation of state is extremely well characterized. The explosive and the water are imaged through slits by streak cameras to determine the detonation velocity of the explosive and the shock in the water, from which the power of the detonation can be computed.

Unless there is some important constraint, economics dictates that the designer restricts choices to the least expensive compositions that will be effective. TNT has a number of beneficial traits, one of which is insensitivity to initiation by small-arms fire. The higher-energy explosive cyclotrimethylenetrinitramine (RDX) and a somewhat more powerful relative, HMX, were developed in the run-up to WWII [60]. Because of its complicated synthesis process, HMX is expensive, and its use is limited to designs where performance is critical: anti-aircraft missile warheads and SCs. Physically identical warheads may be loaded with different explosive compositions depending on the branch of service using them. The Navy loads all of its ordnance on board the ship, where it stays for the entire cruise unless used up, while the Air Force keeps its ordnance safely away from its aircraft except while on sorties. The imperative for insensitive

munitions drives the Navy much more so than the Air Force.

In addition to the all-important drivers of stability and cost, each explosive composition has a number of other practical properties such as density, strength, melting point, toxicity, corrosivity, and so on. As in all other industries, demand drives production. There is not a lot of demand for military explosives, so there are only a few plants in the United States producing them, and a relatively small number of products produced in each. Some chemicals such as lead styphnate, widely used in noncorrosive primers for small-arms ammunition, are not produced in the United States at all due to economic reasons. Many are toxic or physiologically active (e.g., NG) or cause contact dermatitis (e.g., TNT [61]). Each of these other characteristics factor into the overall cost of the finished munition design and hence constrain the final choices.

9.6 FAILURE THICKNESS AND CONFINEMENT

If a long, cylindrical charge of HE detonates with nothing surrounding it, some of the energy of the reaction is lost in lateral expansion of the products. When the diameter is large, the detonation velocity does not vary much with diameter, but as the diameter decreases, an increasing fraction of energy is lost in expansion of by-products off the sides relative to the energy in the forward-moving shock. This result is accompanied by a decrease in the detonation velocity in the direction of the axis of the cylinder. At some characteristic diameter, called the failure thickness, the detonation will no longer propagate, and the remaining strand of explosive merely burns. This threshold is referred to as the detonation-to-deflagration transformation. Adding a nonenergetic, confining outer layer, as in the lead sheath of detonating cord, will increase the ratio of energy directed along the axis to the energy lost radially, reducing the diameter of

the explosive column at which the transformation occurs.

For example, gun propellant is usually a mixture of HES, e.g., nitrocellulose (NC) plasticized with NG, extruded or otherwise formed into granules with dimensions small enough to prevent detonation. This fact does not mean that gun propellant cannot be detonated. A large enough initiating stimulus or sufficient confinement, or circumstances that physically pack the propellant while it burns can result in the opposite effect, a deflagration-to-detonation transformation.

This is a very important issue in the vulnerability of military systems involving ammunition and propellants. If a tank cannon round is stood on its base and a SC jet is fired through the top few inches of the propellant, a pressure gage nearby will measure a slight increase in the air shock pressure over that which would have resulted by the passage of the SC jet alone. A small amount of the propellant was detonated by the penetrating jet. If the path of the jet is lowered a few inches, the pressure goes up. If the path of the jet is lowered further, at some depth the entire propelling charge detonates due to the confining nature of the propellant column in a vertical orientation. The shock energy is compacting some of the adjacent propellant against outlying material. If there is very little between the disturbance and a free surface, most of the material involved is just scattered away. With enough surrounding material, a sufficient quantity can be involved to collectively liberate enough energy to continue the process unrestrained.

Likewise, if an explosive warhead on a round of ammunition is detonated with a donor charge, the propelling charge will detonate. This reaction also explains the “bonus effect” when the warhead of a missile detonates before the rocket grain has burned out. The rocket propellant can be detonated by the warhead causing considerably more damage than if the warhead

alone had functioned. Some warhead casings are designed specifically to initiate any remaining propellant.

9.7 HIGH DETONATION VELOCITIES MEAN TIMING IS CRITICAL

Depending on the application, the time between sending the initiating signal and the actual functioning of the detonator can often need to be small, and, more importantly, the *variation* of the interval to functioning of a number of detonators initiated simultaneously may need to be very small. The most demanding application in moving metal with explosives was in certain implosion nuclear fission weapon designs, which required complicated electronic triggering circuitry and expensive initiating devices, but there are some conventional warhead designs now where this is also an issue.

In cases where initiation of the explosive load at multiple points is required, until recently the use of complicated and expensive devices was needed since the response of standard detonators is not accurate enough to fulfill the requirements. With the new initiator technology available (e.g., exploding foil initiator) designs needing precise, multipoint initiation such as focused fragment warheads are practical [62].

9.8 FABRICATION: CAST, PRESSED, OR MOLDED; SHEET, PLASTIC, AND POLYMER BONDED

The fabrication of explosive charges begins with chemical engineering and ends with the load, assembly, and pack operations in manufacturing. Explosives are almost always mixtures of ingredients, e.g., Composition (Comp) B is a castable mixture of 60% RDX and 40% TNT, with 1% of paraffin wax added as a phlegmatizer, a material intended to reduce the sensitivity of the

explosive [63]. Comp B is insensitive to small-arms fire. The ingredients must be produced in the physical and chemical state needed, followed by mixing of ingredients and forming the charge. Throughout the process, the need for safety is paramount, as is close control of all process variables to ensure the quality of the final product. Much of the equipment seen and processes used have been adapted from the food-processing and pharmaceutical industries. The final form of the product determines how it is produced, and the form is determined by the munition in which it is used. The explosive can be either incorporated in a casing or other assembly or be a stand-alone product.

A stand-alone product will typically be produced by solvent or solventless extrusion, pressing, molding, or casting. The latter three require demolding, which requires a mold release sprayed on the mold or incorporated in the product, such as stearates. Stearates or a similar product may also help reduce sensitivity. Gun propellants are typical stand-alone products. While most NC-based gun propellants are produced by extrusion, spherical propellants are produced by an agglomeration process from a water emulsion. Typical gun propellants can be granular (e.g., cut to short lengths typically with an L/D ratio of less than 2.5) or stick, in which the extruded propellant is cut to desired long lengths, typically tied around the part of the body of a sabot LRP that intrudes into a cartridge case. Propellants are typically graphite-coated (glazed) after drying to reduce their susceptibility to ignition by static electricity and, in the case of granular propellants, to make cartridge case filling by pouring easier. Typical processes often include intermediate steps. Extruded propellant typically starts as a (usually perforated) strand that is then chopped to length while still wet with solvent, while spherical propellant is separated by size (classification). Each size class of spherical propellant can then be run through a specific gap between a pair of rollers to yield a fixed “web” size (the minimum thickness in the through direction).

Another class of stand-alone product includes sheet explosive, demolition charges, blasting cartridges, and similar products. Sheet explosive can be molded with a flexible polymer binder, allowing it to conform to simple curved surfaces. Demolition charges would typically be molded directly into their casing as part of the manufacturing process, and the design would include wells for blasting caps for ease of use. Plastic explosives such as C4 are intended to be molded by hand into the required shape. Typical uses would be conforming demolition charges to an object to be destroyed or to fabricate field-expedient munitions such as large EFPs. The plastic explosives incorporate wax-like ingredients and motor oil to yield a moldable, clay-like consistency [64].

Most explosive charges for warheads are formed in place. Bulk explosive charges are often melt-cast, which requires stringent measures to exclude voids and shrinkage cracks, which can contribute to sensitivity or failure to function properly. Individual charges can be pressed from powders, which usually contain admixtures to make them press easily. Separation of the charge from the case is undesirable, so the designs may include a bonding agent between the casing and the charge. Coatings might also be used to prevent corrosion of the liner or casing, or when the materials are otherwise chemically incompatible.

There are a number of high-end, polymer-bonded explosives, also referred to as plastic-bonded explosives. The DoD ISS [65] lists a number of compositions of powders for extruding and molding and compositions for casting and pressing. One particular ingredient seen in a lot of warhead explosives is aluminum powder. Its inclusion results in a more powerful blast overpressure effect, particularly useful in stoving-in relatively flimsy structures, e.g., in depth charges and anti-aircraft missile warheads.

9.9 PROJECTING METAL WITH EXPLOSIVES

Typical examples of coupling HE energy to metal include the shell casing of an HE round, the casing or jacket of preformed fragments of a fragmenting warhead, or the liner of a lined-cavity charge. Two simple physical models, the Gurney model for velocity (speed) and the Taylor model for angle, are used to predict the velocity and the trajectory of a piece of thin metal in contact with an explosive charge.

9.9.1 Predicting Speed: The Gurney Equations

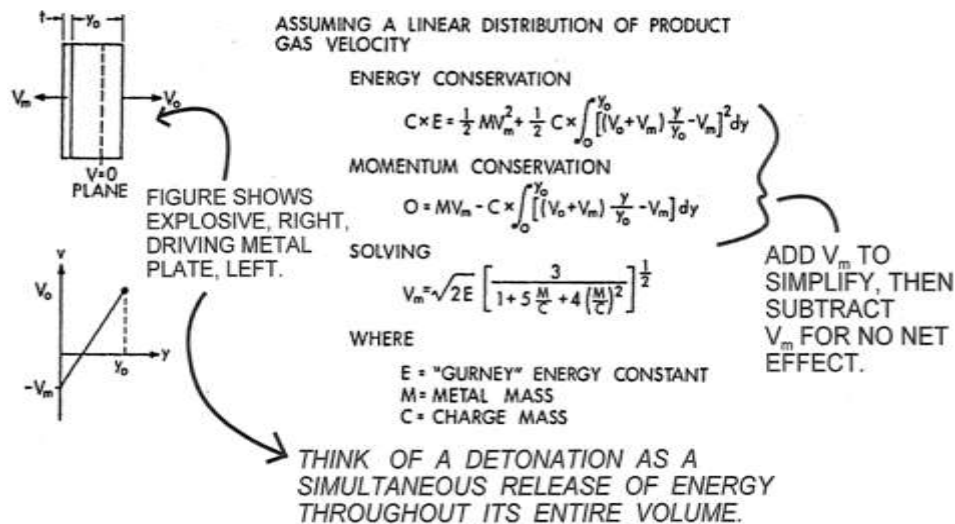
The Gurney model predicts plate speed in terms of a simple algebraic function of the ratio of charge mass to metal mass and a constant characterizing the explosive's energy density. The predictions are reasonably accurate where the charge geometry matches the assumptions, but seriously overpredict velocity where some of the explosive energy does not go to accelerate the adjacent case material, e.g., at the ends of warheads. Note that "scaled" charges (having the same relative masses) produce the same value for speed regardless of geometric size.

Consider a sandwich of a flat plate of inert coherent material, usually metal, on a flat layer of explosive, at rest relative to a frame of reference. If the explosive were detonated instantaneously throughout, it would throw the plate off normal to the plane of the assembly. Because of the geometry, the plate would maintain its integrity and initial thickness (with the exception of throwing off metal from the edges more or less in the plane of the plate). The explosive by-products, being gases, would expand in both directions: following the plate in one direction and out into the void in the opposite direction. Somewhere in the thickness direction, there is a plane parallel to the plate at which explosive by-products are standing still relative to the initial frame of reference.

It is assumed that the gases have a linear velocity distribution, which can be used to compute a total amount of KE due to their motion. The gas that is first off of the bare explosive moves away from the frame of reference at an unknown velocity, V_o , while the gas against the flyer plate is moving at the flyer plate velocity, V_m , in the opposite direction, two unknowns. Likewise, the flyer plate has a KE due to its velocity, also V_m . Each explosive composition liberates a characteristic amount of CE from the rearrangement of the atomic bonds, easily computed from experimentally determined values of bond energies. Some of this energy goes into thermal and pressure times specific volume energy in the by-products and the rest contributes to increasing the KE of the by-products and flyer plate (from zero originally). Gurney assumed that each explosive had an empirically determined specific energy, the Gurney energy, E , which he equated to the KE of the moving metal and gases. Writing the equation for the conservation of momentum gives a second equation and permits solving for the velocities, of which the velocity of the metal plate is sought (Figure 9-2). The models are one-dimensional, and the values charge mass (C) and metal mass (M) are masses per unit length.

The Gurney equation is traditionally written as $V_m = \sqrt{2E} \times f\left(\frac{M}{C}\right)$ where $f\left(\frac{M}{C}\right)$ is a function of the geometry. The various functions are generally available as curves for particular geometries, as shown in Figure 9-3. The approximation is typically good over the range of $\frac{M}{C}$ values shown. Kennedy [66] provides an extensive summary of values for the Gurney constant, $\sqrt{2E}$, which has units of velocity (in Figure 9-3 km/s [mm/ μ sec]). Note that the shape of the curves implies an optimum coupling efficiency around the point of steepest ascent.

Using the open-face sandwich equation to form an expression for the ratio of plate KE to explosive reveals an optimum. Applied to SC design, the plate models a very small element of the conical liner in turn modeled as a 2-D V of infinite length. Additional velocity can be gained after passing the maximum, but with diminishing returns (Figure 9-4). Note that the location and value of this optimum are sensitive to geometry; the flat plate is illustrative and can be thought of as a limiting case for an imploding cylinder (infinite radius). For imploding cylinders, the optimum point shifts down and to the right.



Adapted from Kennedy [66]

Figure 9-2. Derivation of the Gurney Equation (Source: Dietrich [2]).

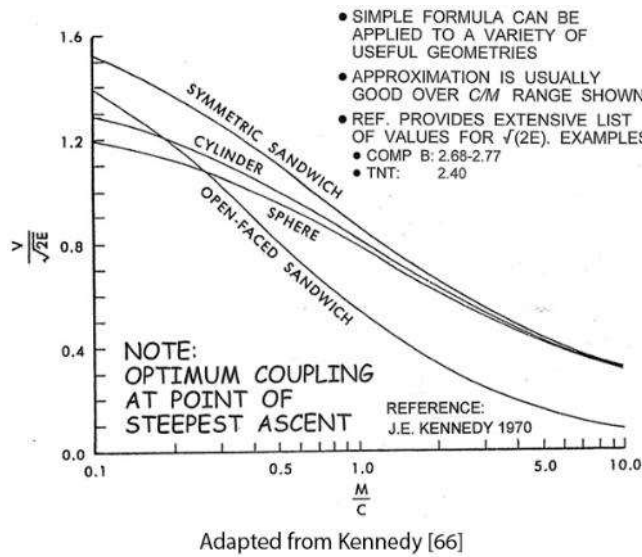


Figure 9-3. Other Flyer Plate Curves (Source: Dietrich [2]).

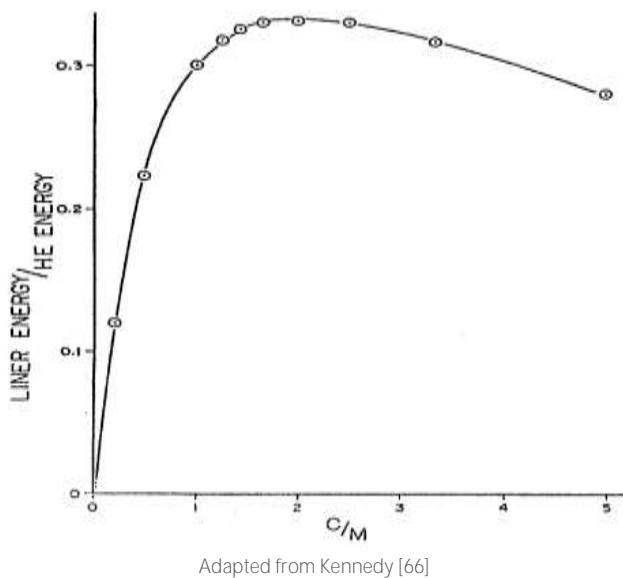


Figure 9-4. Gurney Flat Plate Curve (Source: Dietrich [2]).

Tamping or confinement of the explosive can be used to improve the coupling of energy. Generally, this tamping is not weight-efficient, especially with diameter constraints (as in tube-launched warheads). However, the tamping may be provided by a heavy casing necessary for structural support for gun-launched projectiles or for fragmentation effects. Tamping in effect shifts the “neutral plane” in the Gurney model (Figure 9-5).

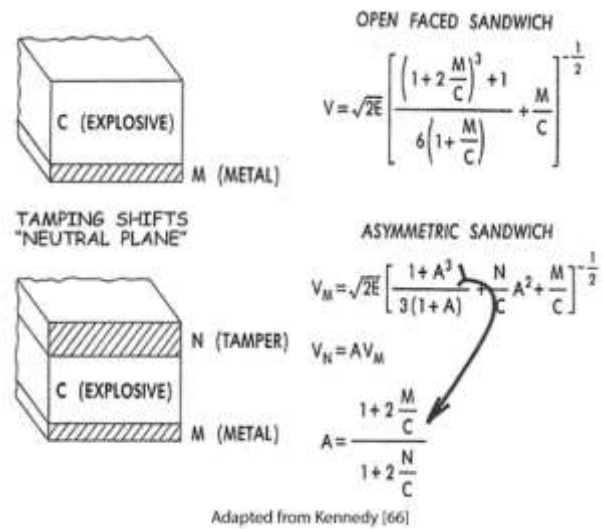


Figure 9-5. Tamping (Source: Dietrich [2]).

9.9.2 Predicting Trajectory: The Taylor Angle

While the Gurney model supposes that the detonation impinges on the metal at normal incidence, another condition to consider is a detonation wave sweeping along the charge at grazing incidence (normal to detonation front parallel to plate plane) and throwing the metal off at a characteristic angle, θ , as shown in Figure 9-6, in which the detonation is moving from right

ASSUMING THE MOTION TO BE ROTATION WITHOUT STRETCHING (i. e. SHEAR):

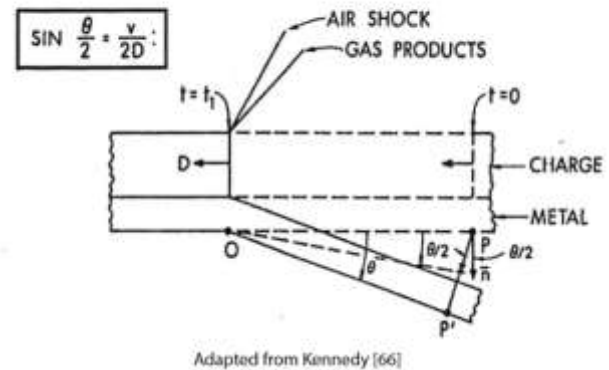


Figure 9-6. Taylor Model for Throw-off Angle (Source: Dietrich [2]).

to left. For “ideal” explosives, i.e., those of practical interest, the metal velocity (speed), V , and the detonation velocity, D , are related such that the projection angle is about constant for a fixed plate thickness. This angle will never be higher than that given by the free expansion of the gas products. This limitation places practical constraints on warhead design as will be discussed in Chapter 10.

9.9.3 Improvements to the Gurney and Taylor Models

In reality, the expanding casing may fragment, opening gaps through which the expanding gas cloud can leak. Predebon, Smothers, and Anderson [67] improved the computational capabilities of the Gurney and Taylor models and analyzed the fragmenting casing phenomenon as it applied to fragmenting warheads. Using the HEMP code [68] and modeling the fragments as a fluid layer (Fluid Model, shown in Figure 9-7) having the same mass as the initial set of fragments, i.e., as a layer of metal that stretches indefinitely and does not allow the expanding gas to pass through, gives a more realistic approximation than do the Gurney and Taylor models. Taking into account the leaking gas yields an even more realistic model (Elastic-Plastic with Gas Leakage Model) (Figure 9-7).

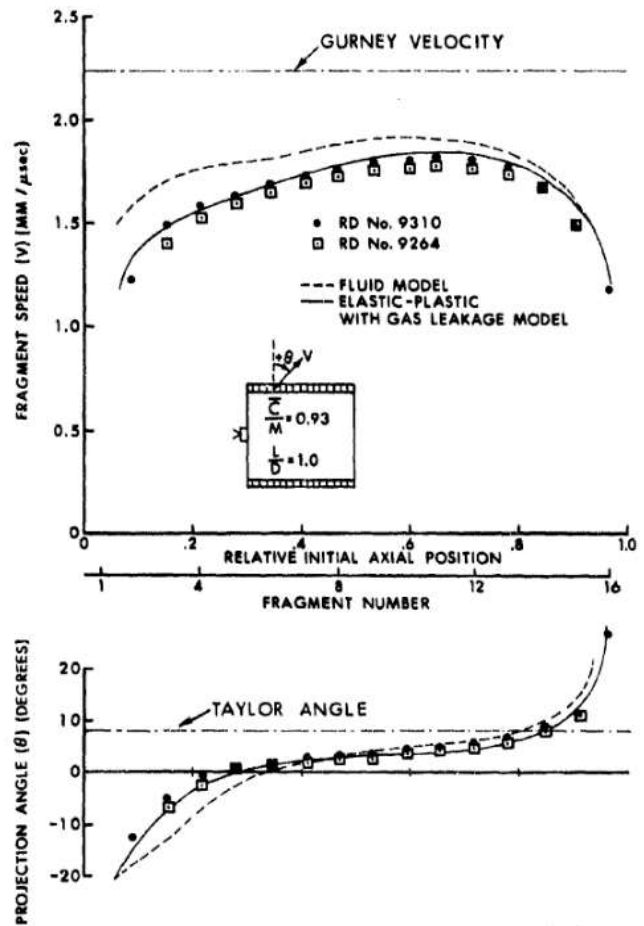
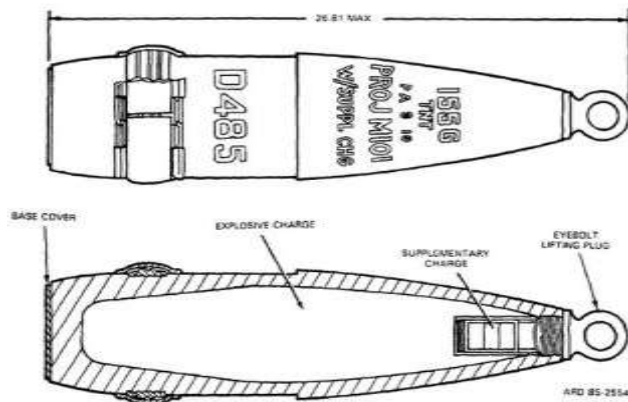


Figure 9-7. Comparison of the Fluid Model and the Elastic-Plastic with Gas Leakage Model to the Gurney and Taylor Models (Source: Predebon, Smothers, and Anderson [67]).

10. FRAGMENTING WARHEAD DESIGN

10.1 THE FRAGMENT THREAT IS UBIQUITOUS ON THE BATTLEFIELD

The threat of fragmenting warheads is the first constraint that the designer of AFVs must consider. Small-arms fire is a close second. The entire vehicle, perhaps with the exception of the bottom, has to be able to protect the occupants in the fighting compartment against the effects of the warhead. The simplest HE warhead is the HE shell (Figure 10-1). When the fuze initiates, either on contact, or more often at some height above the ground, the body of the shell is fragmented, moving out in all directions at high velocity, in an ordered fashion. The nose and base typically stay together as individual pieces.



The lifting eye is used to handle the round. It is removed and a fuze is screwed in prior to firing. Note the supplementary (booster) charge and the smoothly rounded transitions between internal features to minimize the concentration of strain (deformation) in any area as the explosive fill is compressed due to setback forces on firing.

Figure 10-1. The Ubiquitous HE Round (Source: U.S. Department of the Army [69]).

Land military forces rely extensively on ordinary, heavy-duty vehicles to provide the everyday flux of essential

people and supplies, vehicles that were not designed for combat situations. The effort to armor the High-Mobility Multipurpose Wheeled Vehicle (HMMWV) to withstand roadside bombs, often just repurposed HE shells, demonstrated how much weight was needed just to stop artillery fragments, weight that reduced the payload to essentially zero, accompanied by all kinds of unintended consequences. As is always the case, up-arming the HMMWV led to escalation of the threat. It is apparent that something on the order of an APC is still not adequately protected against the kinds of threats that modern insurgents use. The use of these threats led to the development of the very massive Mine-Resistant Ambush-Protected vehicle, which, due to its size, is restricted to rather flat and solid terrain and has many other practical issues.

10.2 ESTIMATING ARMOR REQUIREMENTS REQUIRES KNOWING FRAGMENT CHARACTERISTICS

Determining how much armor is needed begins with estimating the mass and velocity of the threat projectiles, in this case, fragments. Knowing the material and the spatial distribution of the fragment cloud and the individual geometry and speeds of the fragments allows the designer to select a worst case. For example, most of the case-body fragments from an HE round are more or less finger-sized and -shaped. They are generally much more of a threat than a rifle bullet. The worst case would be for the fastest one to strike well-aligned and end-on. Usually, it is assumed that the fragments arrive in one flight (simultaneously) and well spread out, so that each target at the extreme of the effective range of the warhead gets one and only one lethal hit. However, it is possible that a target must withstand a sequence of repeated hits at the same spot, similar to an attack by an automatic weapon.

Given the attitude of the fragment with the greatest penetration capability that could be expected to strike

the vehicle, typically the one with the longest length along its trajectory, a vehicle armor designer uses the P/L vs. velocity relationship, L/D effects, and clipping of material by the sides of the penetration channel due to yaw to estimate the depth of penetration. Then by using rules of thumb, computational modeling, or experimentation, the designer estimates how much more thickness is needed to stop the worst threats for the fragment material expected. Since the entire fighting compartment of the vehicle must be protected, undoubtedly the choice will be either RHA or aluminum for cost reasons. Usually, the armor box also forms the body of the vehicle, but it is also possible to design a space-frame vehicle chassis upon which armor panels are mounted. In this case, the space frame must withstand the high stresses from fragment impact and blast.

Conversely, for the warhead designer, the mass and velocity of the fragments needed to be thrown from the warhead under development depends on the results sought. Sailors understand that, sometimes, the right mass and velocity of fragments is zero, as in the concussion hand grenade used by naval forces. While concussion alone is not a very effective kill mechanism, at least a concussion grenade is less likely to punch holes in the thin steel hull of a ship when tossed alongside to deter ill-intentioned swimmers, divers, or boaters.

10.3 FRAGMENTING WARHEAD TECHNOLOGY IS MATURE

The topic of fragmenting warheads is well covered in the literature and indicates that a number of organizations are active in research and development. A recent paper by Breech [70] extends the Gurney equations to two dimensions for a 2-D (cylindrical) charge with end-plates. He improves on the recent method of Li et al. [71]. Both methods depend on simplifications of the methods typically used to derive the Gurney and Taylor models. It would only be coincidental that the detonation wave

would impinge on the walls of the warhead at normal or grazing incidence. In reality, the designer is going to use such simplifying assumptions to develop a few promising geometries and then optimize the performance using location and number of points of initiation, body geometry, wave shapers, and other available metrics to tailor the detonation front as desired. Designers now rely on computational methods verified by the occasional critical experiment for the final designs.

10.4 WARHEAD DESIGN PROCESS

Design is a creative process, and there are probably a number of different designs that would meet the needs of the user. In military designs, the final choice is determined by exhaustive testing and evaluation, and many people contribute to the final design. The designers must consider the total environment in which the device will be used—from manufacture, to transportation, to storage, to use, and to ultimate disposal—and should design-in extra margins to meet anticipated problems and to allow for future improvements easily.

Because reliability is vital, the designer aims for simplicity by minimizing the part count and using proven technology as much as possible. Minimizing costs is also important. Particularly in military applications, where the outcomes of battles can be determined by logistics, the systems engineer seeks to minimize the number of fielded munition designs, often trading away a bit of performance to permit one warhead to be used on multiple targets, and hopefully deployed from more than one launch platform, as well as across services and among allies. The before and after pictures in Figure 10-2 show how adding a fragmenting sleeve to the Hellfire missile provided capability against personnel and light vehicle targets and other targets of opportunity that its SC warhead alone could not reliably deliver. Some



Adding fragmentation capability to the Hellfire missile allows catastrophic destruction of targets of opportunity.

Figure 10-2. Results of Adding a Fragmentation Sleeve to a Hellfire Missile (Source: Gilliam [72]).

nations design-in fragmentation casings as a matter of doctrine.

In general, the designer and user must decide whether to use separate designs for separate users. For example, the Marines would normally use the same MBT as the land forces, but all of their ammunition would need to pass Navy insensitivity standards, which the Army may not require, as one of their primary missions is to assault across a beachhead from naval vessels. Similarly, the vehicle itself may need a number of upgrades to permit it to be driven into a ship and anchored against the forces of heavy seas.

Based on systems engineering and survivability and lethality analysis, usually by others, the (team of) designers is given a delivery system, suite of targets, description of engagement terrains, employment doctrines of the user and defender, logistical

considerations, etc. The designers then use their skills and knowledge to determine vulnerabilities in the targets that can be exploited and then develop possible kill mechanisms. It is unusual that a designer will be involved with the development of a new system, so parameters such as existing gun bore and ammunition storage compartment dimensions will usually impose very stringent constraints on physical dimensions. For example, when the A-10 tank killer was being developed, it was determined that a 30mm round would be needed to perforate the tops of opposing tanks, and then the entire system was designed around an airworthy 30mm automatic cannon.

The designer first starts with the intended target. If the goal is the incapacitation of personnel, a one-size-fits-all generally recognized standard is for the fragment to perforate a 0.5-mm (0.020-in.) thick sheet of aluminum. This testing can be performed with a piece of projectile residue about the size of the tip of the lead in a graphite pencil moving at perhaps half the muzzle velocity of an effective tank cannon, approximately 700 m/sec. Air targets are almost as vulnerable as people, and a kill or mission-abort can often be achieved without significant structural damage. Reliably taking out materiel such as trucks requires fragments that can perforate about 6 mm (1/4 in.) of structural steel. Perforating 20 mm (3/4 in.) of armor requires sizable fragments. A conventional HE round may not be able to perforate that armor thickness. Another specific kill mechanism by fragment attack that might be desired would be to initiate or disrupt explosives, e.g., in the warhead of an attacking Antitank Guided Missile (ATGM) by an active protection system. The kill mechanism here would be much more complicated to model than a simple perforation. In theater missile defense, though the targeted missile body itself would be very lightly built, the payload may present a rather hard target, and a fragmenting warhead design that ensures some specified probability of a kill given a clean engagement

would require general knowledge of the designs that would be faced.

Fragmenting warhead design involves a number of classic engineering trade-offs to ensure enough lethal fragments per area at maximum range. Velocity vs. range depends on fragment initial velocity, mass, and morphology (drag). Fragment initial velocity is a function of the type of explosive, the mass ratio of explosive charge to fragment mass and to some extent, the time available for the fragments to be accelerated before gaps appear between them and the explosive by-products start to escape. Once this happens, the fragments are further accelerated by gas drag, which is harder to model. The more energy that can be extracted from the gas, the better. Providing a means to contain the expanding gas, such as with a thin, ductile, metal liner or overlapping two or more layers of projectiles (bricking) [67], will have some beneficial effect.

In the case where the fragments are formed by the case rupturing, the strain to rupture depends on the ductility of the casing material, the nature of the (bi- or possibly tri-axial) loading, and any physical or metallurgical process used to predispose the casing to fragmentation. One other consideration is how much of the initial fragment is lost and hence wasted during the fragment formation and acceleration process. Initially, the casing is compressed in the through direction as the detonation wave and subsequent high-pressure mass of gas work to push it away. This process increases the amount of radial and axial strain the material can sustain before rupturing. Once the expanding shell is unloaded in the third (through) direction, the material responds to 2-D stretching in its own local plane. How much of each **nascent fragment's mass stays with the parent and how much is shed as small and ineffective fragments** are complex issues.

During the compression and expansion from the explosion, the shell material will be heated and

weakened, while the strain of expansion may work-harden it, further complicating efforts to predict behavior. Previous experience with the materials in question is very useful, but small changes in metallurgy, heat treatment, and other processing variables can result in large changes in rupture behavior. One way to characterize a material is through a series of tests in which cylinders of the material with increasing internal explosive loads are shot to find the strain to rupture under realistic loading conditions. There are a number of ways to control fragment size and minimize wasted mass. In Figure 10-3, the lower panels show the warhead construction, and the upper panels show the fragment patterns. But even with preformed fragments, the shock loading from the detonation may cause some of the fragment material to spall off.

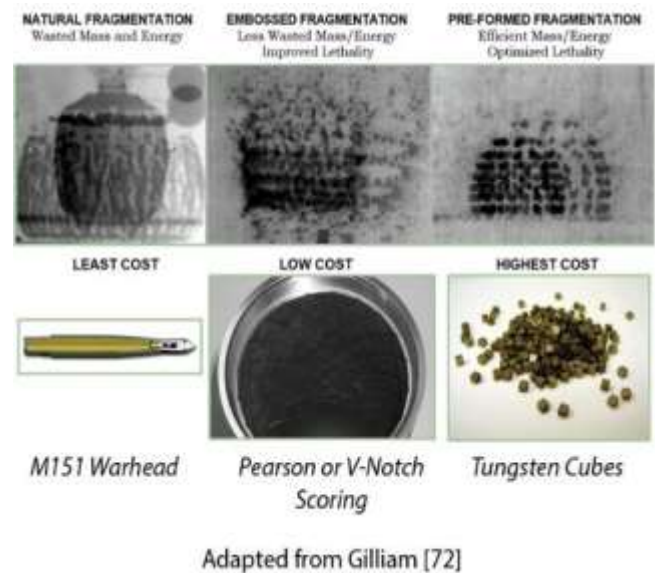


Figure 10-3. Fragment Production Techniques (Source: Silsby [1]).

Waffle liners (not shown in Figure 10-3) also provide some control over fragmentation. They are formed by a very inexpensive process in which a thin, plastic shell that will just fit into the empty warhead body is vacuum-formed with a pattern of V-shaped ridges projecting into the cavity. It is inserted into the warhead body, and then the explosive fill is added. When the explosive

detonates, the Vs produce jets that cut the casing into fragments at the desired locations [73].

When an HE shell or any other warhead detonates, the initial velocity of the shell must be added to the velocities of the fragments determined by static detonation (Figure 10-4). Any relative motion between projectile and target that is not parallel to the outwardly directed target normal creates an effective yaw, a particular problem with SC jets moving laterally relative to a target.

Once the designer has developed the means of projecting the right mass of fragment at the right speed, an efficient pattern must be developed. Note in Figure 9-7, shown earlier, that base-detonating a cylindrical warhead results in a forward bias in the projection of the fragments and in higher velocities of the forward fragments. Various initiation schemes are used to create various patterns [67]. The warhead itself does not have to be cylindrical. Barrel shapes initiated at two points some distance in from the ends tend to provide a more uniform pattern fore and aft, while the opposite shape, thinner at the mid-plane rather than thicker, tends to concentrate more fragments towards the midplane. Fragmentation research is ongoing, and there are many highly sophisticated warheads that can be programmed to concentrate additional fragments in a preferred direction. For example, see **Manfred Held's patent for a focused fragment warhead** [74].

HE rounds present a specific safety hazard that may not be obvious in a risk assessment until the conditions are examined. If two, closely stacked parallel rounds (or other more or less cylindrical munitions, such as bombs) detonate at nearly the same time (in the order of milliseconds), when the two expanding munition bodies impinge, the impact may meet the conditions necessary for a jet, two in fact, that will emerge as sheets of very high-speed metal in the directions normal to the plane containing the axes of the munitions. This metal is

capable of traveling long distances, penetrating deeply, and detonating any explosive in its path. Walker [75] examines a means to mitigate this threat in the context of ammunition stored in a tank.

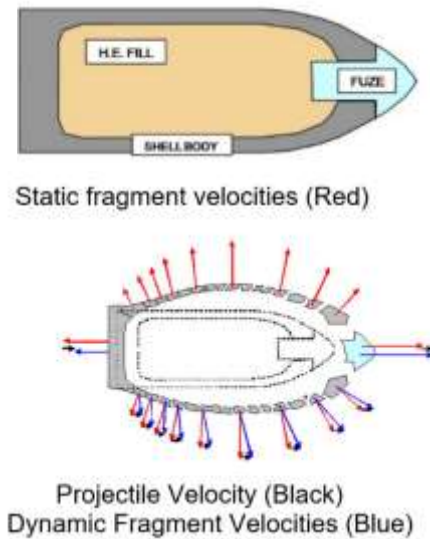


Figure 10-4. Add Projectile Velocity to Calculate Correct Fragment Velocities (Source: Silsby [1]).

11. NONJETTING LINED-CAVITY CHARGE DESIGN

11.1 INTRODUCTION

More than a hundred years ago, seemingly anomalous behavior was observed when blocks of explosive with cavities were detonated on thick, ductile metal plates. This observation led to the evolution of lined cavity charges, which produce a collimated, high-velocity, jetting penetrator capable of deep penetration, a fundamentally different kill mechanism than that of the fragmenting warhead. Relatively lightweight warheads were capable of defeating the heaviest monolithic armor plate of the time, driving innovation which gave rise to various modern armor technologies. In the course of studying jetting lined-cavity charges, researchers began to seriously investigate nonjetting lined-cavity charges.⁸

The nonjetting lined-cavity charge was the next step up in sophistication from the fragmenting warhead. These devices are rather arbitrarily categorized into EFP warheads and the hemispherically lined charge. This technology is well-developed and easy to understand, so it will not be explained in depth. Actual warheads would be designed using computational modeling.

11.2 EFPs

EFPs, also called Misznay-Schardin charges, originated at about the same time as the SC. They consist of a layer of thin, ductile metal in contact with an explosive charge, with either or both having a thickness that changes with location. There are a number of variables that interact to determine the success of the design. Success is relatively insensitive to the explosive chosen. The path by which

the detonation front reaches the liner is a function of the initiation point and charge design, including any wave shaper or explosive lens that might be used. Finally, the liner material and geometry are critical. The shape of the liner or its thickness can be varied to get it to collapse as it flies off. The goal is often to form aerodynamically stable shapes so that the warhead can be detonated at a significant stand-off from the target.

Because of the stand-off, adding a fragmentation capability to the case is probably ineffective. The length of the slug formed is about that of the radius of the liner. Very ductile (actually, malleable) liner materials are typically chosen, and higher density is preferred, so copper and tantalum are often used. Typical striking velocities might be about 2 km/s, so penetration can be (over-) estimated using the density law. Some mass may be lost as the ends slap up against each other, as suggested in Figure 11-1 (a) showing forward vs. rear folding.

Typical applications of EFPs are as artillery-delivered munitions for top-attack on tanks as an assault-breaker. One design, implemented in the U.S. as the M898 Sense and Destroy Armor is dispensed as a cargo submunition, hung from a special parachute that causes the warhead, with seeker, to scan a decreasing spiral on the ground, detonating at the appropriate time and driving a slug into the top of the vehicle (Figure 11-1 [b]). A second concept, not implemented, has the liners formed in the side of an artillery shell. It scans in a helix, essentially successive lines on the ground, and detonates similarly (Figure 11-1 [c]). In another application, the EFP is used as a land mine for bottom attack on AFVs (Figure 11-1 [d]). When the sensor detects the passage of the target vehicle, a clearing charge blows away the overburden and then the main charge functions, forming a slug that attacks the bottom of the hull. EFP mines can also be set horizontally and used as off-route mines.

⁸ See Kennedy [76], Sandstrom [77], and Mah [78] for additional information on the development of lined-cavity charges.

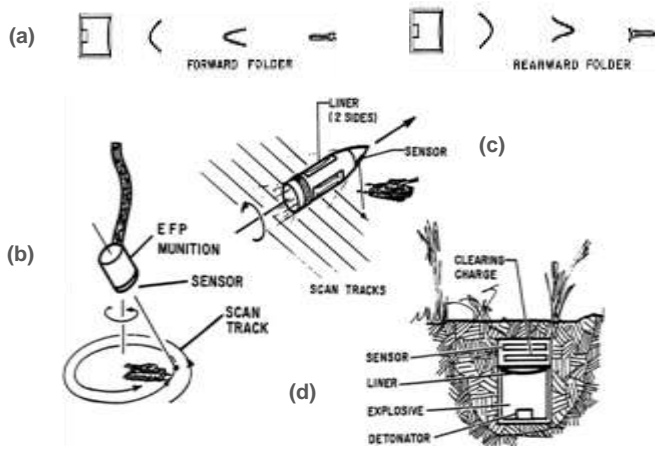


Figure 11-1. EFP Munition Concepts (Source: Silsby [1]).

The characteristic performance features of the EFP are that it forms a more or less nonstretching, rod-like projectile traveling at higher than tank-cannon muzzle velocity that incorporates most of the mass of the liner in an aerodynamically stable shape that does not break up into individual particles. Fields of AT mines are intended to break up, slow down, and channelize assaults to give the defender time to respond in force. The EFP's ability to attack from a long and variable standoff makes it an effective choice as an off-route mine, neutralizing the effect of mine ploughs or mine rollers. A shortcoming is that its slug length is limited to about the radius of the charge, although this can be improved upon somewhat with sophisticated designs.

Typical of the AT EFP mine is the U.S. M75 AT mine (Figure 11-2). It is "emplaced" by being thrown from a dispenser and lands on the surface of the ground. Arming information is transmitted electronically while being thrown from the dispenser. It is equipped with a self-destruct function. Because it is not known which side will land facing up, it is made symmetric about its horizontal mid-plane. The effect of a heavier version of such a mine on the hull of an APC is shown in Figures 11-3 and 11-4.

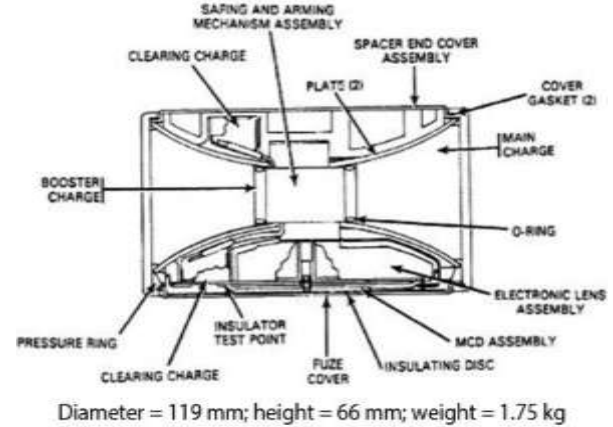


Figure 11-2. U.S. Antitank HE M75 Mine (Source: U.S. Department of the Army [79]).



Figure 11-3. Casspir APC Hull Attacked by the TMRP-6 Antitank Mine (Source: Smit [80], Used by permission).



The appliqué has eroded the slug to practically nothing, as evidenced by the splash in the primary hull.

Figure 11-4. Mechem Appliqué on Casspir Hull – Details
 (Source: Smit [80], Used by permission).

11.3 HEMISPHERICAL LINER WARHEAD

The hemispherical liner warhead design bridges the regimes of the EFP and the SC. Studying the processes involved in forming the penetrator in detail provides insight into many of the nuances of the design process of any lined-cavity charge.

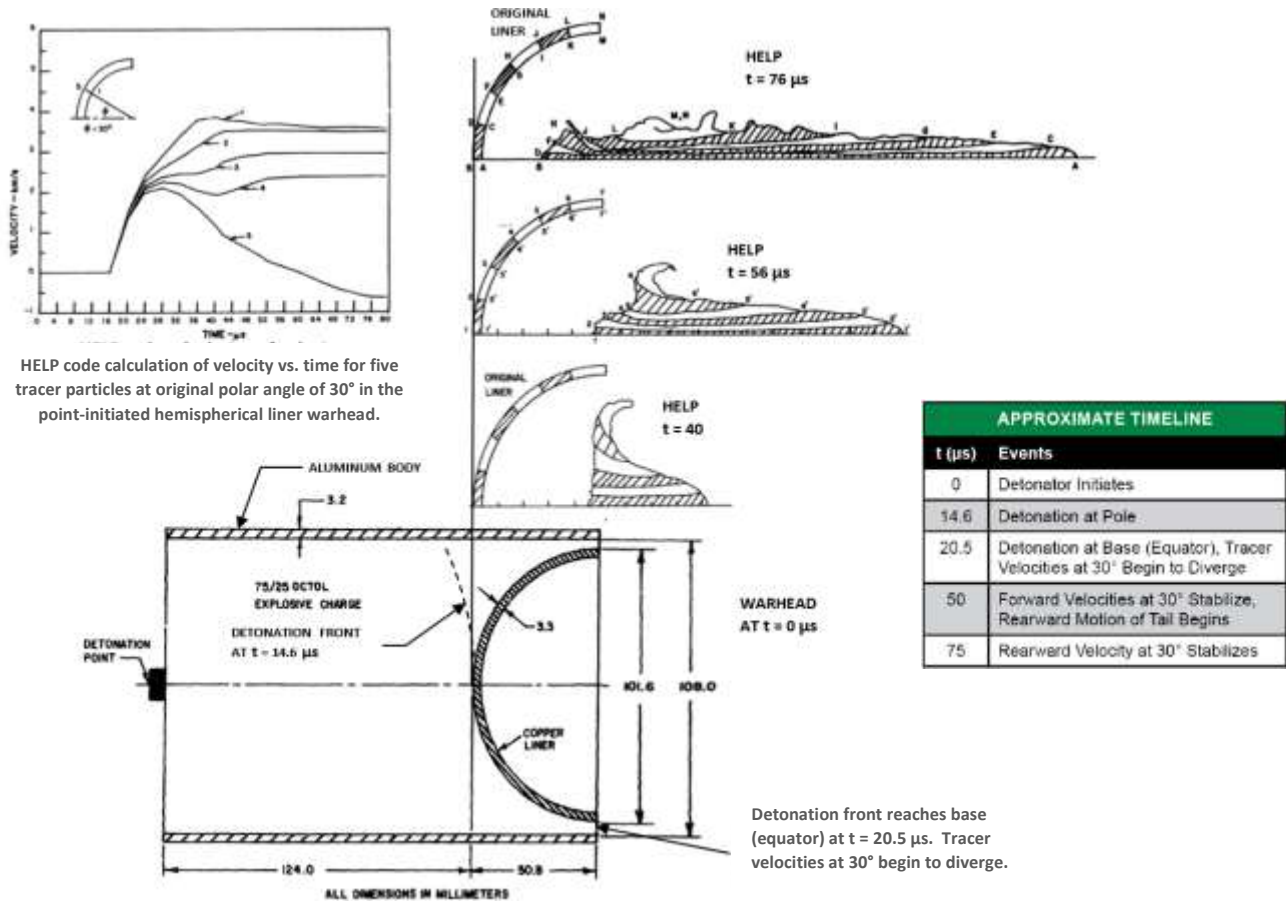
The hemispherical liner is set into a cylindrical charge initiated at its end. As the detonation wave reaches the center element of the liner, the pole, it throws it forward at high velocity. The detonation wave sweeps over the liner from pole to base (equator), progressively throwing metal inwards into a rather compact convergence zone. The detonation velocity is much higher than the velocity of the thrown metal, so the time to sweep over the liner is a fraction of the time it takes the liner material to pile

up. Because the liner is a hemisphere, the distance to the convergence point is about the same for all elements, while the outer elements are driven by less explosive, so the interval over which the material arrives is longer than it took the detonation to sweep the liner. Successive material piles on with an increasing component of radial velocity, although the lower relative mass between explosive and liner mitigates this to some extent. The effect of the radial velocity of the later-arriving liner metal is much like running the earlier elements to arrive through a rotary forge. Unlike the EFP, the core is not hollow.

Summarizing hydrocode simulation work by Chou et al. [81] and Walters and Golaski [82], Summers, Walters, and Dick [83] report that the material near the pole “forms a rod along the axis of symmetry. As subsequent liner material reaches the axis of symmetry, it forms concentric tubes of increasing average radius which stretch from the tip of the jet to the tail.” Unlike the EFP, the penetrator stretches, and like the SC, may ultimately break up into discrete particles.

The best way to visualize the process would be an $x-t$ plot, which for SC analyses has the downrange direction (x) to the right and time (t) progressing upward. Figure 11-5 approximates this process by showing snapshots of the vertical sections of the penetrator at successive times above a cross-section of an unexploded warhead.

The upper left plot in Figure 11-5 shows that the velocity of the tracer particles at a 30° angle first begin to move at about 16 μ s after initiation when the detonation front passes. (The particles are distributed from the free surface [1] to the surface adjacent to the explosive [5] along the radial ray.) The velocities begin to show divergence about 25 μ s after initiation, indicating that the outermost particle has piled onto the core near the tip and subsequent particles are arriving in turn along the core towards the rear, and significant pressure from



HELP hydrocode simulation (Adapted from Walters and Golaski [82]).

Figure 11-5. Collapse of a Hemispherical Liner.

the convergence of the radial flows has built up. All except the rearmost tracer element have constant velocities at about $50 \mu\text{s}$, which indicates that the pressure has been converted into velocity, with the penetrator stretching. Note that the inner element velocity has dropped to zero at about $60 \mu\text{s}$ and ends up at about 500 m/s rearward by about $75 \mu\text{s}$, as the last of the material from the equator finally is smeared nearly radially onto the core in a short region near the rear of the penetrator, hammering it radially and forcing material behind that zone rearward.

While Pugh, Eichelberger, and Rostoker developed a closed-form solution for the mass and velocity in a conically lined SC (the PER model [84]), Summers, Walters, and Dick report that this has not been done for

the hemispherical liner, at least up to the time of their 1990 paper examining the velocity of the pole regions of hemispherical liners [83]. They performed experiments to verify Japanese and German research findings in the 1940s, supported by later hydrocode work by a number of U.S. researchers, that for a hemispherical liner, material arriving on axis behind the tip of the penetrator results in faster motion than the tip, so that by removing some of the material at the pole, a longer penetrator could be formed. The simple explanation by Summers, Walters, and Dick is that the material from the pole forms a long cylinder upon which subsequent material arrives, while removing the pole material removes this central plug and allows the subsequent material, thrown at an increasing angle to the axis, to jet, as in an SC.

The exact distribution of liner mass and its velocity can be seen to be due to the particular interaction of the detonation wave with the liner. For a centrally initiated cylindrical charge, the shorter the charge along the x axis, the more curved the detonation front is when it reaches the liner and the lower the ratio of explosive to liner mass in general. If the charge is lengthened, the detonation front gets flatter. The liner thickness and/or charge geometry can be varied radially, and the initiation scheme can also be altered. Details such as the exact amount of explosive between the case wall and the liner also need to be examined.

Computational mechanics allows examination of arrangements that would be hard to analyze experimentally. Walters and Golaski [82] report on a hemispherical liner whose thickness decreased by half from pole to base, which resulted in a penetrator similar to the one from a uniform liner, but more compact as it approached the rear. They also reported hydrocode work in which the hemispherical liner was surrounded by a hemispherical layer of explosive whose outer surface was initiated simultaneously. The result was as expected, a compact mass of material consolidated in its original order, from which the inner layer formed an elongated conical spike whose tip originated at the pole of the charge and whose base was formed from material from the inner layer of the base of the hemisphere.

12. JETTING WARHEADS: THE SHAPED-CHARGE

12.1 INTRODUCTION

The basic mechanics of the SC were discussed in Chapter 2, which described the evolution of threats to armor. The behavior that characterizes the SC is the production of a coherent stretching jet of fast-moving metal capable of deeply penetrating armor and other materials at a reasonable standoff. As shown in Figure 12-1, the fuze initiates the warhead's charge, a blast ensues, and if the warhead was designed correctly, a residual length of jet and some target and jet debris exit the armor into the fighting compartment with lethal effect.

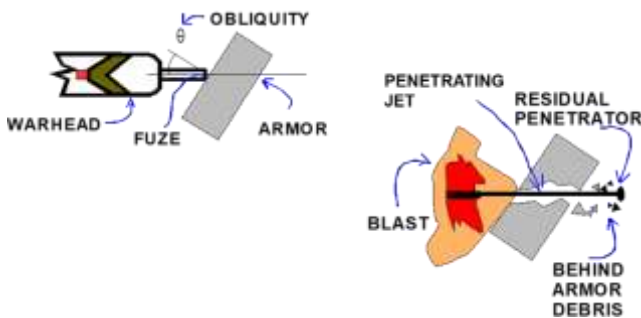


Figure 12-1. The SC Warhead Initiation and Penetration (Source: Silsby [1]).

12.2 JET FORMATION, STRETCHING, AND PARTICULATION

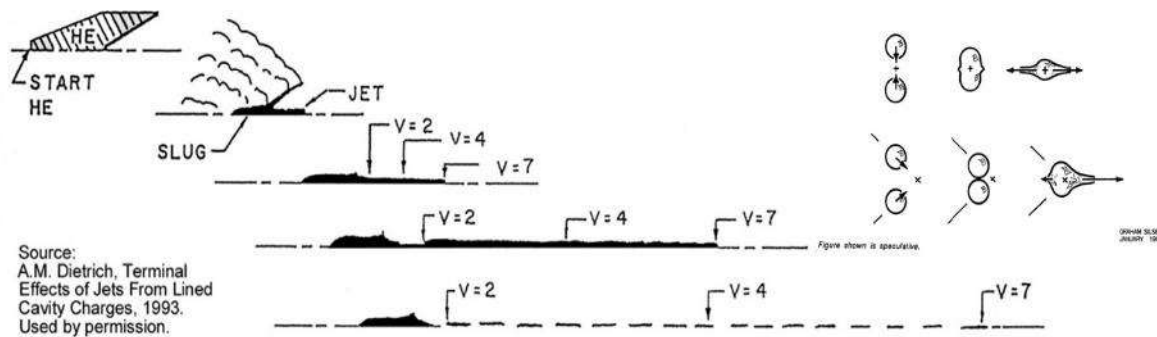
The jet is formed as a result of the convergence of the metal liner thrown inward by the explosive charge. A variation on the conical liner, where the material converges on an axis of symmetry, a jet can be formed by its 2-D analog, a linear SC. The liner of its cavity is a folded sheet of material elongated perpendicular to the plane of the V. The liner material converges on its plane

of symmetry. In both geometries, when the conditions are right, the incoming stream of material divides into a fast forward-directed stream, the jet, and a slow, more massive portion, the slug. Depending on the exact design, the slug can go up-range or down-range. In the simpler designs with a more or less cylindrical charge along the length of the conical liner, the continuous decrease in the ratio of explosive mass to liner mass from apex to base of the liner causes a velocity gradient in the jet which in turn causes it to stretch and ultimately to particulate. Flash radiography is used extensively to characterize jets. Figure 12-2 illustrates the linear collapse process and the stretching and particulation of the jet. It shows the upper half of a vertical cross-section through the device at successive times. Jet formation is similar to what happens when two droplets of water are impacted at various angles, as in the inset in Figure 12-2.

With fiducials in the view (objects with accurately known locations, typically piano wire on the face of the film cassette) and range geometry and flash tube locations and flash times known, velocity and mass distribution can be estimated accurately.

The highly ductile copper jet ultimately particulates, as seen in Figure 12-3, a radiograph of the same jet at three times from three stacked flash tubes. Summers, Walters, and Dick [83] state that the stretching jet does not actually fragment simultaneously, but rather over some time interval, usually beginning at the tip and working rearwards. Practically, however, for evaluation and analysis, the breakup can be considered as occurring at a particular time, the jet breakup time, the average of the beginning and end of breakup. After breakup, the particles no longer stretch. Rather, the space between the particles increases. This is a special case of a segmented penetrator.

Contrary to popular opinion and consistent with the jet behaving like a stretching, ductile solid in radiographs, most jets from malleable liners are below their melting



The law of conservation of momentum requires that the sum of the momentum in the jet and slug equal the sum of the momentum in the collapsing liner (less slight energy losses from metal deformation). A small mass of jet springs forward at high velocity off the massive, slow-moving slug.

Figure 12-2. Collapse of the Liner, and Jet Formation, Stretching, and Particulation (Source: Dietrich [2]).



Figure 12-3. Radiograph of a Particulated Jet (Source: Dietrich [2]).

temperature and are polycrystalline. Before the advent of accurate computer modeling, a number of techniques were used to investigate the state of the jet. Flash radiography was used to perform Laue crystallography of the jet on the fly. A number of researchers have performed two- (or more) color (wavelength) pyrometry (radiometry), which relies on assumptions of the emissivity of the surface, e.g., Von Holle and Trimble of BRL [85]. Recently Uhlig and Hummer of ARL [86] used magnetic diffusion analysis and five-color radiometry to determine that a copper jet tip particle had a bulk temperature of about 1,200 K and compared that result with that of several hydrocodes. While all of the results have varied considerably, and examination of some soft-recovered jet particles in the past has shown some signs of melting along the core, the preponderance of the evidence indicates that the measured temperatures are well below the melting point of pure copper (1,357 K).

12.3 PORTRAYING THE JET: THE X-T PLOT

The jet on a plot of distance vs. time can be portrayed as in Figures 12-4 through 12-6. It is a convention in the study of ballistics to plot down-range distance to the right and time increasing upwards. Figure 12-4 is a typical plot. Callout **1** indicates the jet at three times: **a** indicates a continuous jet, **b** indicates a jet at breakup, and **c** indicates a particulated jet. Line **2** is the trajectory of the tip, and line **3** is the trajectory of the tail. To a good approximation, the jet appears to originate from a point in space and time, called the virtual origin. Extending the tip and tail trajectories back in time to where they intersect and calling that the origin of the *x-t* plot produces the plot in Figure 12-5.

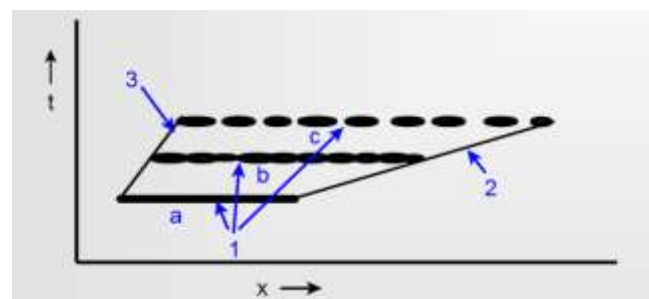


Figure 12-4. Typical *x-t* Plot (Source: Dietrich [2]).

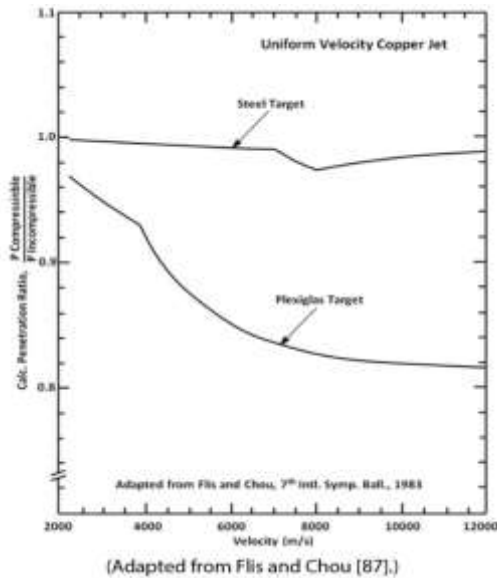


Figure 12-8. The Effect of Target Compressibility.

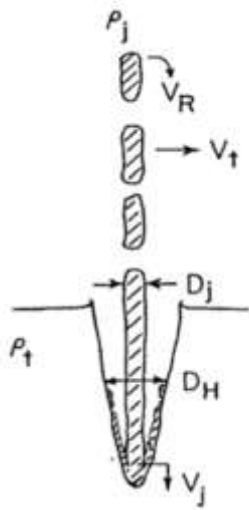


Figure 12-9. Particulated Jet Misalignment (Source: Dietrich [2]).

As with an LRP, the penetration channel from the jet is a mirror image of the jet, scaled up in diameter based on the hole diameter to local jet velocity relationship and shortened by the penetration vs. velocity relationship. Only the jet material that reaches the jet-target interface will advance the penetration. When a particle drifts too far off line, it can graze the penetration channel wall, reducing or eliminating its penetration capabilities. When a particle tumbles, it may also impinge on the

channel sidewall, as well as presenting a shorter effective length. The farther back in the jet the particle is, the longer the time a perturbation has to grow.

Other effects reduce the capability of the particulated jet. As a result of the velocity gradient in the jet, the penetration channel reduces in diameter with depth. Back-streaming eroded jet material in the channel further chokes the channel, and may be directed inwards, with both effects potentially interfering with the jet and, particularly with poorly aligned or rotated jet particles, reducing penetration further. Finally, as the jet velocity drops toward the tail, at some point the target strength begins to reduce the relative erosion of target to jet compared with that predicted by the zero-strength density law model.

12.5 REGIMES OF JET PENETRATION, STANDOFF CURVES, AND EFFECTIVE JET LENGTH

Currently, practicalities greatly limit the standoff at which warheads can be initiated. Penetration entirely by a continuous jet requires very short standoff and is generally impractical. In most instances, penetration is by a continuous jet initially followed by a particulated jet. Penetration by an entirely particulated jet occurs only with a long standoff, is generally less effective than the mixed case, and quite hard to achieve with practical (i.e., inexpensive) hardware.

The penetration vs. standoff curve for the warhead design is determined by a statistically significant number of firings approximating service conditions and compared with the constraints on the warhead's overall envelope. Almost certainly, more standoff would be desirable than can be accommodated by the hardware constraints, so engineering judgment determines the final warhead and fusing design. Comparing the penetration-standoff curve with that of other hardware allows the designer to see whether the design seems to

be performing as expected. Figure 12-10 illustrates jet penetration vs. various standoff distances. Figure 12-11 shows a comparison of penetration vs. standoff curves.

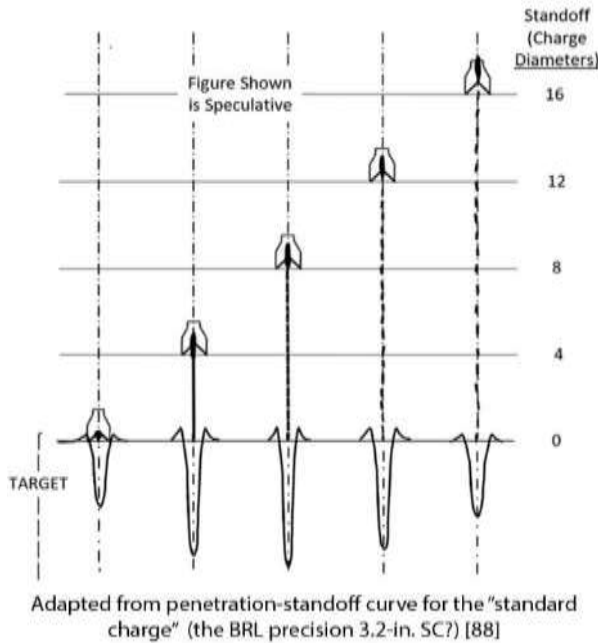


Figure 12-10. Penetration vs. Various Standoff Distances
 (Source: Silsby [1]).

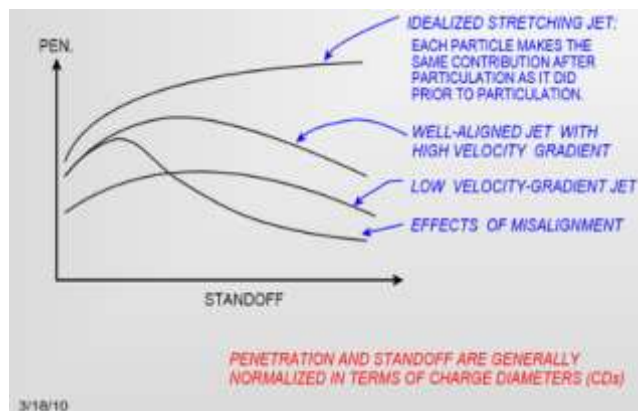


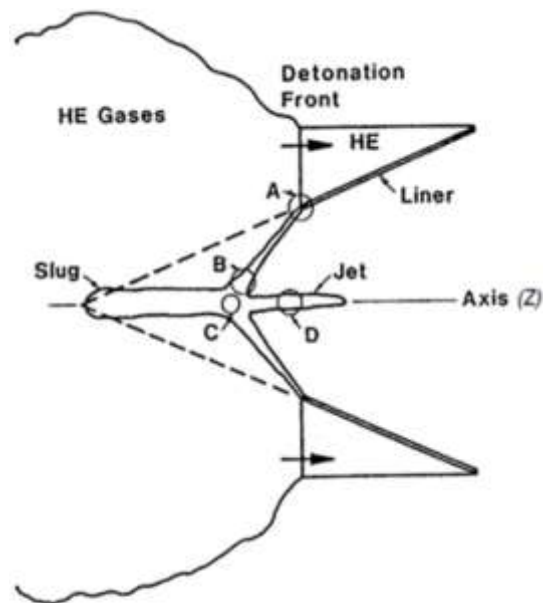
Figure 12-11. Comparison of Penetration vs. Standoff Curves
 (Source: Dietrich [2]).

The concept of a minimum penetration velocity is a useful way to express the effective jet length. The density law is used to compute the length of jet required to produce an observed penetration. It is assumed that

all material in the jet behind that length was going too slowly to penetrate. As a rule of thumb, this cut-off velocity is commonly assumed to be 2 km/s. For gun-launched LRP, this assumption is entirely unrealistic, as striking at 1.5 km/s with a high-density LRP produces extremely satisfactory results. However, the 2 km/s cutoff velocity assumption is adequate to yield a simple but reasonably accurate penetration model that produces the penetration predicted by the density law.

12.6 FORMATION OF THE JET

Because of the utility of the SC jet, the effects of the range of parameters on its formation have been widely studied. Figure 12-12 shows a cross section of SC jet formation in detail. The dotted line is the original liner position. The passing detonation front bends and accelerates the liner toward the axis, where it converges



- A-Explosive Shock Loading**
 - B-Convergent Flow**
 - C-Stagnation Compression**
 - D-Final Jet**
- Note: Ignore z-axis label.

Figure 12-12. Shaped-Charge Jet Formation and Regions of Interest
 (Source: Dietrich [2]).

on a *moving* stagnation point. There, conservation of momentum results in the liner separating into a high-velocity, low-mass jet and a low-velocity, high-mass slug. The *local* liner velocity is estimated from the appropriate Gurney relationship, while the *local* bend angle is from the Taylor model for throw-off angle; both relationships were discussed in Chapter 9. “Local” is emphasized because the charge-to-mass ratio varies along the (here) *z* axis.

Figure 12-13 shows the relationships between liner angle and throw-off angle and the jet characteristics. These equations come from a simple model assuming an incompressible fluid and using Bernoulli’s equation. While these equations begin to introduce some quantitative factors into the process, the model is too simple to be used for design, but it is presented here to show trends. Remember that the charge-to-mass ratio and hence theta varies with *x* (or *z*). From the

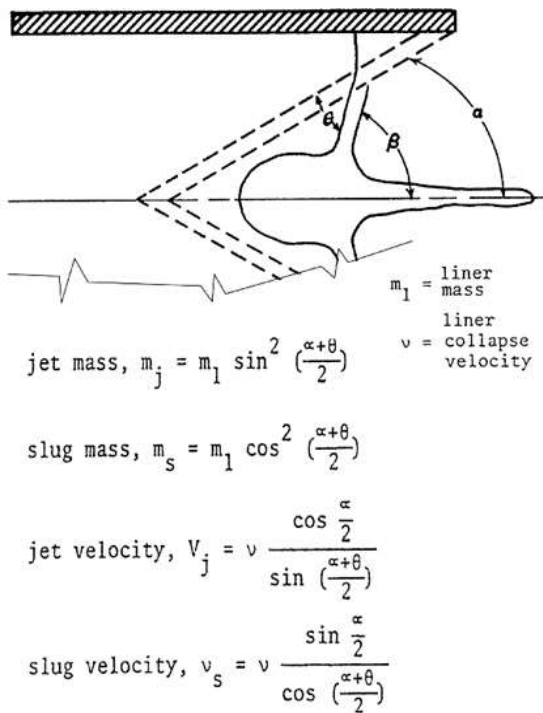


Figure 12-13. Jet and Slug Masses and Velocities (Source: Walters [89]).

relationships, it can be seen that the smaller the cone angle, the higher the jet velocity and the lower the jet mass. The decrease in charge-to-mass ratio with increasing *x* is accompanied by a local decrease in liner velocity and a local increase in collapse angle. Thus, the jet tip is faster than the tail, which is why jets from cylindrical charges with conical liners stretch. The jet typically carries over 90% of the liner KE.

If the collapse process of the conical liner and its many small elements are examined in detail, it becomes apparent that the process produces a jet with an initial inverse velocity gradient. Starting from the apex up to some point, the collapse distance to the axis is too short to achieve maximum jet velocity. Some of the following jet must push its way through this slower material, wasting jet length and reducing penetration capability. Figure 12-14 shows calculated jet element velocities, and Figure 12-15 shows a high-speed camera photo of the conical liner in a Viper warhead (for a 70-mm rocket) in the early stages of jet formation [90]. Note how the marker lines on the liner continue on the jet. To overcome this wasteful process, biconic or trumpet-shaped liners are sometimes used.

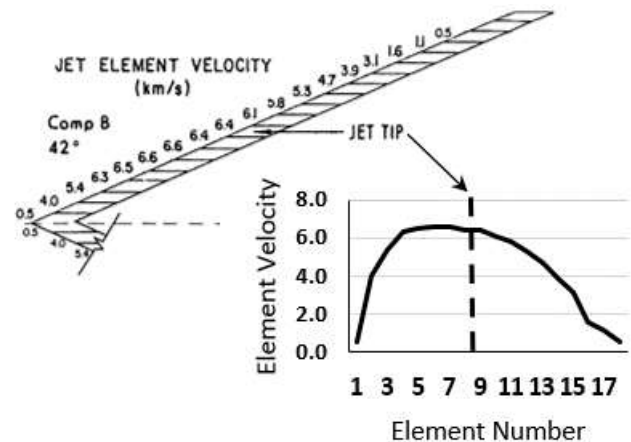


Figure 12-14. Jet Element Velocity in a Conical Liner (Source: Simmons [91]).

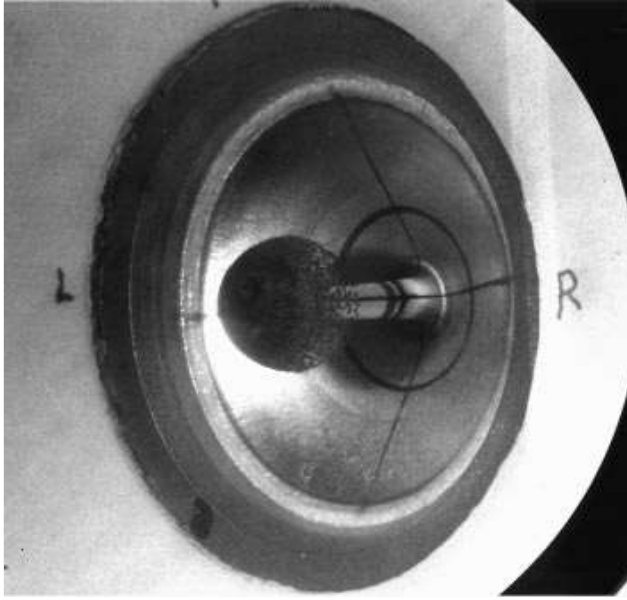


Figure 12-15. Early Stages of Viper Warhead Jet Formation (Source: Walter [90]).

12.7 ATTACHED VS. DETACHED SHOCK

Subsonic collapse velocity is necessary to form a coherent jet. See Figures 12-16 and 12-17. In the supersonic case, the region of high negative pressure causes the jet to blow apart. Wedge-shaped cavities will jet simply depending on whether the liner velocity is subsonic or not.

Cones may still form a jet for supersonic inflow if the collapse angle is large enough, but the jet will not be well collimated. Hydrocode computations show this trend towards expansion rather than clean, streamlined hydrodynamic flow. Therefore, liner materials with high shock speeds are needed in order to design narrow-angle cones to get high jet speeds. But usually, high shock speeds are due to low liner density, so tradeoffs may be necessary between jet length and jet density to maximize penetration.

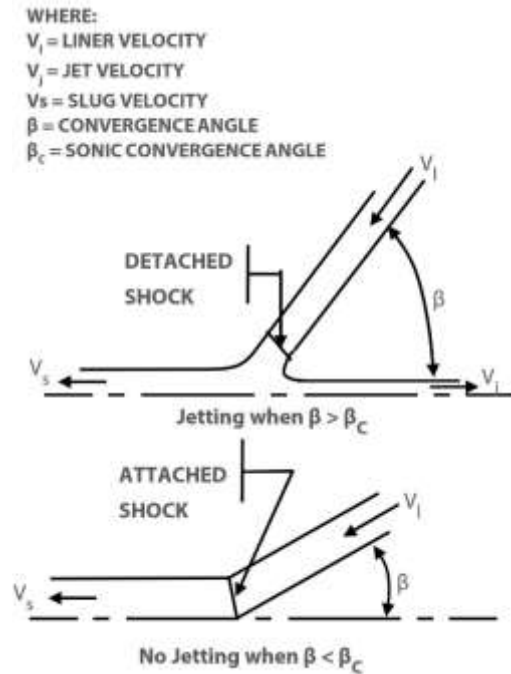


Figure 12-16. Attached vs. Detached Shock (Source: Dietrich [2]).

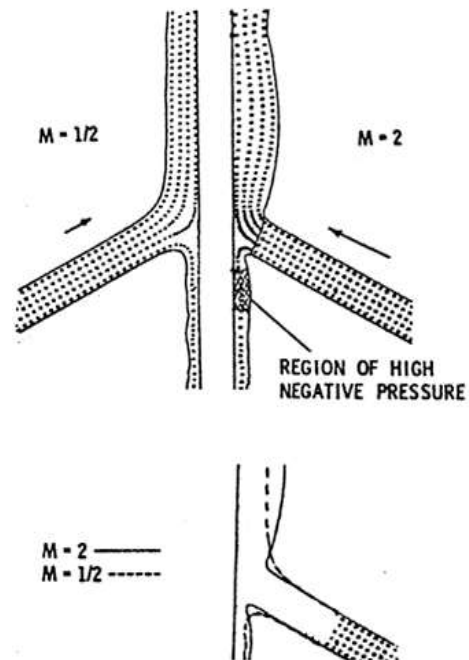


Figure 12-17. Comparison of Jets (Below Incoming Material Stream) from Supersonic and Subsonic Collapse (Source: Walters [88]).

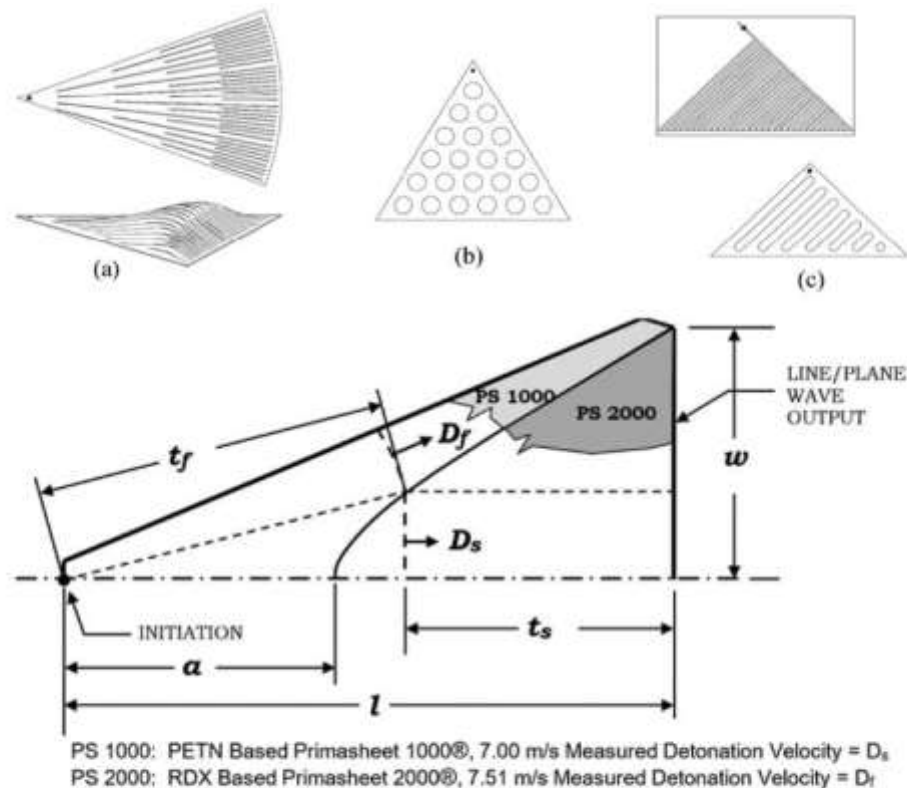
12.8 TAILORING THE LINER COLLAPSE

Many technologies to explosively tailor local metal geometries were secretly developed in the process of nuclear weapon development. Once the technologies were publicized, however, they were quickly incorporated in improved warhead designs worldwide.

For atomic weapon designers faced with the task of collapsing a hollow sphere precisely into a smaller sphere, the most straightforward method was to use multiple points of initiation and complicated explosive charge geometries to tailor the detonation front to the desired shape. The need for very precise triggering and for detonators with a very small command jitter drove the development of these technologies. However, a

solution for practical battlefield warheads can usually be achieved with a single point of initiation and an inexpensive detonator.

One example of technology used to tailor the shape of a detonation wave front is the line- or plane-wave generator. In a solid piece of explosive, the detonation front expands spherically (or on a circular front in the case of sheet explosive) from the initiation point, so for a linear or plane detonation wave, a very long distance would be required before the detonation front was arbitrarily flat. One goal in warhead design is to reduce the overall size of the device, so several ways to shorten the distance needed to generate a flat (or most any other shape) detonation front have evolved over the years (Figure 12-18). The goal is for the time to traverse each



Adapted from Morris, Jackson, and Hill [92]
 (Primasheet is a registered trademark of the Ensign-Bickford Aerospace and Defense Company.)

Figure 12-18. Line/Plane Wave Generator Concepts (Source: Silsby [1]).

detonation path from origin to destination to be the same. This is the criterion for designing a focusing lens in optics, so these techniques are frequently referred to as explosive lensing.

Using sheet explosive as an example, Figure 12-18 shows three existing techniques: Cut a sheet of explosive so that the output end is an arc of a circle and deform it into the third dimension so that the output end conforms to a straight line (or other desired shape) as shown in Figure 12-18 (a). In that illustration, radial slots were generated in the explosive to allow the deformation without possibly stretching the sheet explosive and to confine the detonation to known paths. A simple approach to achieving this design is to perforate an equilateral triangle of sheet explosive with a hexagonal pattern of holes aligned with the edges as shown in Figure 12-18 (b). When initiated at an apex, the detonation front will arrive at the entire length of the opposite edge more or less simultaneously, although with some ripple to it, depending on the size of the holes. In Figure 12-18 (c), the upper figure illustrates slots machined into a heavy plastic backer sheet into which explosive is packed. The lower figure shows a piece of sheet explosive with slots cut into it. Any technique that uses multiple traces will have some ripple associated with them that scales with the size and spacing of the explosive traces. This ripple cannot be eliminated by reducing the size of the traces, whose minimum size is constrained by the failure thickness of the explosive. However, perhaps one could take advantage of the reduction of propagation velocity as trace dimensions approach that of the failure thickness.

In the improved approach shown at the bottom of Figure 12-18, two pieces are cut and assembled from sheet explosives with different detonation velocities, D_f and D_s . For a given half-width w and a desired length from detonation point to the pole of the first piece a , and for the particular detonation velocities, the equation for an overall length l is derived such that the sum of the

time to traverse the faster explosive t_f and the slower explosive t_s is constant along every point on the interface. The interface shape is a hyperbola. This geometry also works for figures of revolution.

An effective technique to tailor the collapse velocity as a function of distance from the apex takes advantage of the different melting points of RDX and TNT in a cast Comp B charge. With the device axis vertical and the apex of the liner up, by tailoring the cooling temperature versus time, the RDX crystals settle, yielding an increasing proportion of RDX to TNT towards the base, increasing the throw-off velocity towards the base relative to what it would have been if the charge composition were uniform. Another technique, used more often in EFPs than SCs, is to vary the thickness of the liner to achieve a desired collapse velocity profile.

A radical approach to reducing the headspace in a SC is the wave shaper (Figure 12-19). A subcaliber zone of inert material is placed between a layer of explosive initiated by the detonator and the charge around the conical liner. The detonation first runs outward radially, then forward in the explosive between the wave shaper and the casing, then expands out in a circular wave front when viewed in any radial section of the charge, approaching the liner much more nearly square on.

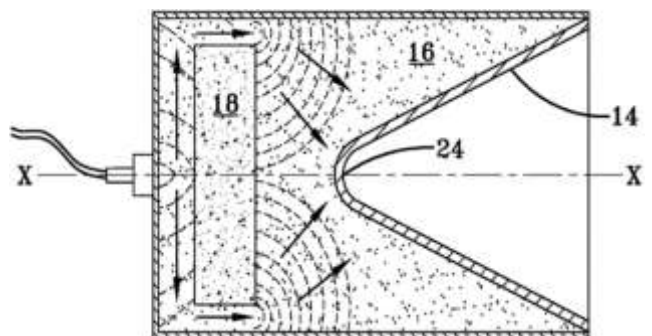


Figure 12-19. Wave Shaper (Source: Baker, Pham, and Daniels [93]).

The wave shaper, callout **18** in Figure 12-19, restricts the propagation of the detonation in the explosive (**16** in Figure 12-19) and directs it inwardly onto the liner (**14**) as shown, with favorable results. A full- or nearly full-caliber charge at the rear is necessary to get the desired convergence of the detonation front. A similar result would occur with a tapered rear region by having a layer of explosive with a higher detonation velocity on the surface of the charge.

As an example of how a designer should think creatively, note also that the apex (24 in Figure 12-19) of the charge shown here is generously rounded. The original observation leading to the SC is that lined conical cavities jet, and that a velocity gradient was necessary for the jet to stretch, leading to classical conical liners in cylindrical charges. This design seemed to satisfy inventors for a time until they began to understand the process in detail and began exploring all of the variables available to them to optimize performance. The rounded apex boosts tip velocity, reducing the amount of tip material wasted, as in the mushroom seen in the Viper warhead (Figure 12-15), which seems to have a much smaller radius. Likewise, the inventors recognized that the wave shaper does not have to be inert. By substituting energetic material for the parasitic mass of an inert wave shaper, additional blast effects can be produced for the same warhead weight. Another parameter available to a designer is the use of multiple materials in the liner, either in layers, for example, to protect a highly reactive jet core from the atmosphere in its brief travel through a target, or varying the material along the axis to tailor collapse velocity [94].

Particularly in gun-launched ammunition, the gun caliber limits warhead diameter. For a conical liner, the jet length is more or less proportional to the diameter of the warhead, limiting penetration depth, suggesting that, in parallel with examining means to tailor the shape of the detonation wave front, investigators look at nonuniform and nonconical liner geometries. Examples from Walters

2007 [88] are the tapered conical liner (conical liner thickness varies along axis) and the tulip-shaped liner (with a uniform liner thickness). The trumpet-shaped liner evolved to generate a longer jet in spite of the caliber limitation (Figure 12-20). The concept was very closely held at first. The closed form mathematical equations used in the analysis are attributed to Dr. Robert J. Eichelberger of the U.S. Army BRL [95].



French 105mm cannon-launched SC round (Photo by David Monniaux. Used by permission under the terms of the GNU Free Documentation License, Version 1.2 or any later version.)

Figure 12-20. Trumpet-Shaped SC Liner (Source: Wikipedia [96]).

A conventional, point-detonating fuze on the nose generates an electrical signal on impact carried by wires to the detonator at the rear of the charge. Serving as a backup in case of a grazing impact where the point-detonating fuze does not function, the conical, copper-colored shell in the forward portion of the projectile, ahead of the SC liner, is the inner element of the graze function of the fuzing. In a grazing impact, if the forward ogive of the projectile is crushed in and touches the inner shell, it closes a circuit to initiate the explosive as well. Note that the cavity for the explosive charge in the projectile is rounded fore and aft. This design eliminates any stress-concentration zones that may cause problems due to the extreme acceleration imposed by gun launch.

As increasing computational power became available, investigators finally aimed to truly optimize the warhead geometry, including that of the liner, which in this case would require more complex fabrication techniques (Figure 12-21). Figure 12-21 also illustrates that in a mass-efficient design, the explosive charge would almost certainly not be a right circular cylinder.

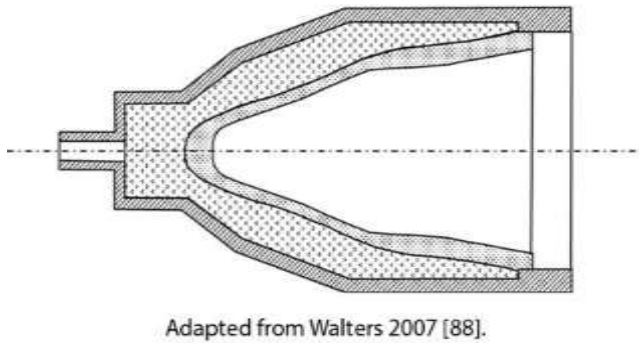


Figure 12-21. Optimized Liner Design (Source: Silsby [1]).

12.9 COLLAPSE SYMMETRY CRITICAL TO PERFORMANCE

In the early 1960s, gross variations in production-warhead performance led researchers to become aware of the sensitivity of the performance of the SC to variations in manufacturing. Very tight specifications that pressed the state of the art at the time were developed, and production warhead components were given an additional machining operation to yield the BRL 3.2-in. (81mm) precision SC warhead used nearly universally in research. The greater the concentricity and uniformity of all components, the less perturbations there are during jet formation, which will cause early particulation and particle misalignment and tumbling.

Individual grains (crystals) of explosive are usually anisotropic, and detonation velocity varies with direction relative to the crystal axes, leading to uneven acceleration of adjoining material on the microscopic scale. This situation can be complicated by a similar behavior of sound velocity in the grains of the metal. The grain size of both the explosive and the metal used should be as small a fraction of the thickness of the metal to be accelerated as possible. Researchers at the Physics International Company developed a hypervelocity launcher concept in which explosives were used to collapse a thin metal reservoir of gas to quickly generate

extreme pressures in the reservoir so as to tube-launch projectiles at extreme velocities [97]. They later found that by isolating the explosive from the metal wall with a slight air gap to reduce variations in metal velocity, the walls stayed intact for a longer duration, providing higher and more repeatable reservoir pressure-time traces and hence higher and more repeatable launch velocities.

SC jets are often surrounded by a halo of fine debris that has failed to cohere to the jet proper. This jet frazzle was not visible in flash x-ray images, but armor designers quickly realized that they could redirect its momentum inward asymmetrically early in the jet-armor interaction to perturb and degrade the jet.

Some of the seemingly most trivial details have been found to result in degradation of jet performance, for example leading the fuze wire through the cavity or in contact with the outside of the charge. The most surprising detail involved supporting a charge with the axis horizontal by laying it in a Styrofoam™ cradle. Even though the periphery of the charge was distanced far enough from the substantial support below such that the jet would have been formed before a reflected blast would reach the charge, it was found that a similar block of Styrofoam had to be placed above the charge, and the entire foam assembly needed to be fairly symmetric.

12.10 SC DEFEATING ARMORS AND THEIR INFLUENCE ON WARHEAD DESIGN

Antiarmor weapons are usually a lot cheaper than their intended targets. The long-term effect of advances in warhead design is to force potential adversaries to have to replace entire classes of materiel, which is expensive and time-consuming, reducing their assets available to wage war. In particular, the SC rapidly drove the weights of AFVs to beyond where they could rapidly advance on the battlefield. Armor designers countered as best they

could with weight-efficient armors, but they are always at a disadvantage.

Little about modern armor design can be discussed in an open forum, with the exception of the highly effective but a bit problematic active and RA designs, which need special design considerations to enable them to remain functional after attack by other than the primary threats. In these designs, the impact of an SC jet or LRP rapidly sets in motion a pair of relatively thin plates of armor material such that the trailing penetrator material must interact with more armor material than was originally disposed along the shot line. The interaction of the moving penetrator with each moving plate is the same as the interaction of a yawed penetrator at a slightly different velocity with a fixed plate at a different obliquity. With both plates in motion, the result is a pair of elongated slots being produced in the plates whose active ends are pushing on the opposite sides of the penetrator material, trying to break it up and disperse it.

The SC warhead designer quickly countered this armor design with the tandem warhead concept, in which a small leading charge activates the armor and the main charge then perforates the plates after their motion has stopped.

12.11 FUZING AND OTHER CONSIDERATIONS FOR MAXIMUM PERFORMANCE

While the fuzing should initiate the charge at a standoff sufficient to give the jet the maximum time to stretch, achievable standoffs are almost certain to be closer than the optimum.

The designer also needs to keep the material along the axis forward of the liner to a minimum, as a portion of the jet must be consumed in perforating the fuzing, aerodynamic fairing, etc. Thus, if, in a tandem warhead, for instance, a heavy disk is needed to protect the main

charge from the blast and fragments of the tip charge, the disk should be as low a density material relieved from the rear as much as possible and as small a radius as possible to reduce the length of jet it consumes. Nose fuzing should be designed to have as little material along the centerline as possible. One approach to this is the “spit-back fuze” in which a small explosive charge in the nose fuze fires a high-velocity metal slug (or jet) rearward through the hollow apex of the SC to initiate the main charge at the point of interest, usually with the use of a booster charge. See, for example, Mark F. Massey, U.S. Patent 2,764,092 [98]. **The patent states,** “... Another objective is to provide a point detonating or point initiating fuze for hollow or SC artillery projectiles which will offer a minimum obstruction to the forward explosive or jet action of the explosive charge.”

The warhead designer needs a complete understanding of how the soldier will use the weapon system available to him or her. In a gun-launched system, it is desirable to have a second round on the way as soon as possible to increase the chances of a kill. This method usually requires adjusting the aim. Thus, an adequate tracer is absolutely essential for the gunner to quickly acquire the trajectory of the outgoing round and judge how to re-lay the gun. It is likewise necessary to ensure that the round goes off if it grazes or misses the target—in the former case to provide a shock and screening effect at the target and to produce casualties among dismounts, and in both cases to indicate where it hit. However, the fuzing should not be so sensitive that it is initiated by small branches, or even rain.

The means of delivery also influences the design. Low-acceleration platforms such as rocket-propelled AT missiles put much less stress on the components, particularly the explosive charge. However, low speed implies that a maneuvering target presents a lot more uncertainty as to where it will be when the round reaches the range to target. A guidance system can greatly improve results, but at a considerable price. The

trade-off becomes the cost per kill of an expensive but accurate launch system such as a gun that uses inexpensive ammunition, versus a less expensive launcher that uses expensive ammunition such as guided missiles. Long time-of-flight provides more time for the round to be influenced by such factors as buffeting by wind gusts. A simple design feature to somewhat correct for this is to tailor the tail fin area and the round center of mass such that cross winds push the nose into the wind at a desired amount. Poor manufacturing practices and a loose fit in the launcher contribute to the rather bizarre trajectories sometimes seen in RPG attacks, and sophisticated users have been known to tape the lands on the rockets to get them to fit better in the launchers. Compared with the (design-limited) high accelerations of gun-launched rounds, lower-pressure gun systems such as the gun-mortar and recoilless rifle would seem to exert less damaging accelerations, but it is a good design practice to try to minimize the number of different delivery systems.

Although SCs were originally intended to be fired from existing rifled gun barrels, the high spin rate needed to stabilize a bullet-shaped artillery round severely degraded SC performance. This effect is caused by the conservation of angular momentum. As the spinning liner is driven inwards, its angular rotation rate must increase. The effect of any slight asymmetries is amplified by the high rotation rates, and the jet material may not be strong enough to sustain the high centripetal force needed to hold the jet together. Two approaches were adopted to compensate for the spin. The U.S. Patent 3,726,224 by Pugh and Eichelberger [99] reveals a fluted liner design. Any cross section of the cone comprises a number of identical flutes whose major face is canted a bit so that the element picks up some velocity in a direction to counter the rotation of the round.

A second method for dealing with a rifled tube is to despin the round: Rifling bands engage the rifling for obturation but are allowed to slip in their grooves so that

the round does not get spun up to high speed. Typically, the round would have a rear boom with tail fins for stability and roll at about 100 revolutions per second to compensate for any irregularities in manufacture. This type of design is constrained by the overall length of the ammunition and the need for some length of intrusion of the bayonet primer in the ammunition's propellant bed for reliable and repeatable ignition. Some nations prefer rifled tubes to ensure maximum accuracy, but most of them have switched over to smooth-bore tank cannon tubes that accommodate both LRP and SC rounds, as well as other ancillary rounds as the expected threat may dictate.

One other effect of the motion of an SC round is that of firing a warhead along an axis off the line-of-flight of the round. Most AFVs are designed like battleships: a heavy armor belt protects them from attack in the near-horizontal direction, but their roofs are relatively thin. To take advantage of this shortcoming, it was proposed to overfly the tank and fire down into the roof.

Unfortunately for the munition designer (one of few situations where the attacking munition is at a natural disadvantage), the jet's motion relative to the target is the equivalent of a yawed impact (or think of it as jet misalignment). The initial strike creates a hole into which the rest of the jet follows, that is, until its path reaches the periphery of the hole and it must start over again. The result is a trench that cannot exceed some maximum depth. One counter to this result is to generate a very high-speed jet with a lot of mass forward to create a larger crater, admitting more of the following jet length. Another method would be to impart a compensating lateral motion to the jet, a solution that is probably now achievable with the computation power available.

12.12 COMPUTATIONAL DESIGN TOOLS

Computational modeling has provided insight into details of the interactions that were not accessible to

experimentalists with even the most sophisticated and powerful flash radiography. It has also provided insights into what might be expected if material properties could be changed to values beyond those available. And, unlike experimentation, computational modeling results do not change when the model is rerun.

Computational models divide the space into elements that interact based on physical law. They start with some initial values, apply the physics to the geometry, apply the results to the adjacent cells and see how they move after a time step. Files are then managed and some “sanity checks” **are run**. This process is repeated until done or some result drifts beyond the boundaries imposed by the sanity checks. The time step should be shorter than the time it takes for an elastic deformation (dilatational wave speed) to cross the shortest dimension in the totality of the elements, typically a small fraction of that number.

When shock is involved, the shock speed will be higher than the elastic sound speed of an undistorted element, and the time steps should be proportionately shorter. Usually the code itself determines the value of the next time step. In ballistic interactions, materials are routinely dispersed, so the necessary time steps will decrease rapidly with time, severely increasing the run time. If the modeling begins with a relatively coarse but acceptable time step and then runs are generated with increasingly small steps in time, the outputs should converge to a stable result.

Correct modeling of the distortion and flow of condensed matter (solids and liquids) under extreme pressures and shock loading requires accurate equations of state, i.e., the functions that interrelate pressure, density, temperature, etc. Materials tend to go through a number of phase changes in which the molecules suddenly are rearranged in response to being compressed as the pressure rises and just as suddenly change phase as the pressure is relaxed. Each material of

interest has to be experimentally measured over the range of conditions to which it will be subjected. Fortunately, those who develop nuclear weapons have done most of this work for us.

Initially, machine constraints limited models to two dimensions, and the modelers would take advantage of any symmetry to further reduce problem size. This method created another issue: the coordinate system used. Ideally, a different code should not have to be used for different coordinate systems. A quick way of surfacing problems with a code is to subject it to conditions that the developer did not anticipate, for example, simulating a problem with spherical symmetry with a Cartesian code. The shape of the elements also influences the speed and accuracy of a run. Trying to mesh something with small radii and large changes in shape with quadrilaterals in 2-D or bricks (hexahedral elements) in 3-D proved problematic, so triangular or tetrahedral elements were introduced. Preprocessors that automatically mesh an object quickly evolved, as did postprocessing routines that plot the results intuitively.

To provide practical answers in developing better weapons systems, computational modelers have always required significantly more speed and memory than were available. Significant money was spent by the military both on computers and on computer hardware and software development to advance the state of the art. Limited computational power required efficient algorithms and required thoughtful framing of the problems to exclude as much nonessential detail as possible. To be useful in many instances, codes had to be able to handle shock waves. Particularly in the velocity regimes of explosively driven metal and SC jet penetration, results from modeling the interactions as hydrodynamic processes matched experimental results to acceptable accuracy. In a short time, elastic and plastic behavior was added. The grid could be attached to the penetrator and target (Lagrangian) and watched as the grid cells deformed, or the space could be gridded

and the material flow through (Eulerian) could be observed. For a given amount of memory available, setting up problems where the penetrator and target converged on the center of the total mass allowed the modeler to increase resolution (decrease grid size) in the zone of interaction by using fewer cells (making the grid size bigger) in the areas that would not be directly involved in the zone of interest.

Many other problems developed while trying to satisfy all of the necessary physical laws at once, and tiny, or not so tiny, inaccuracies accumulated due to such things as round-off errors. As with the time step, changes in mesh size (resolution) may result in changes in results. It is to be hoped that the results converge to some value at some reasonable resolution. Conserving momentum in mixed cells, where some penetrator material enters at one velocity and some target material enters at another, results in that cell exerting a drag on adjacent pure cells much like viscosity, while in reality there seems to be little friction between the two material streams. When a target perforation is modeled, the result is that observed penetrator residual velocities are higher than that predicted by the computational model. This discrepancy and a number of other problems can be solved by remeshing mixed cells to emulate the intermaterial boundary observed, across which material does not diffuse. At first this remeshing was done by stopping the run and remeshing by hand, which was time consuming. With increasingly more powerful computers, soon known as supercomputers, and parallel processing, it has become practical to remesh frequently, or even after each step, which is done with the Arbitrary Lagrangian Eulerian codes.

During the development of the hugely complex codes of today, the results obtained could be easily tweaked by small changes in materials properties used and adjustments in meshing. After being supplied with benchmark experimental results, all codes soon produced the desired answers. Experimentalists quickly

responded by asking that the results of a benchmark run be published before firing the benchmark shots.

Computational simulation is now the strongest of the three legs of the ballistic development stool. (Analytical and experimental methods are the other two.) However, all material properties need to reflect those of the real article, not something blindly pulled out of a library, as materials properties tend to improve as processing knowledge improves over time. Finally, the output needs to compare well with benchmark cases before the results can be relied on.

12.13 SPECIFIC SAFETY ISSUES

In addition to the usual safety issues related to energetic materials, the deep penetration capability of SCs presents a serious safety issue. SCs should be stored apex up, so that if initiated, the jet is directed into the earth. A second safety measure is the jet spoiler. A piece of material is introduced into the cavity to spoil the symmetry so in the event of accidental initiation a jet will not form. It is removed just before use. This is not seen in ordnance because in combat the soldier may be forced to use the item immediately and may forget to remove the safety device. There are several references to jet spoilers in the patent literature (e.g., Chawla et al. 1998 [100] and Barker 2002 [101]).

13. ENERGETIC MATERIALS: SOME SAFETY ISSUES

13.1 EXPLOSIVES ARE DANGEROUS GOODS

Working around energetic materials, and particularly explosives, requires the utmost attention to safety, as any single incident can result in many fatalities. In the event that the detonation of one item propagates to others, a catastrophe can ensue. It is interesting to note that explosives are the number-one Dangerous Goods category in shipping. Although complete safety is not possible, considering some safety issues can decrease the chances of a bad outcome.

Items of explosive ordnance must be as effective as possible on the battlefield, of course, while protecting the user to the maximum extent against their lethal effects. Therefore, safety functionality should be designed-in to the extent possible. Good examples are the U.S. standards developed for ordnance fuzing and the development and adoption of insensitive munitions. The designer must be experienced enough to be familiar with all aspects of use and misuse of ordnance items, materials, and methods of manufacture, etc. The novice ordnance designer must serve in the capacity of an apprentice under knowledgeable practitioners for a suitable length of time.

The physical and chemical properties of the components must be understood to ensure that parts and assemblies stay within tolerances over the full range of temperatures and other conditions to which they can be expected to be exposed over their expected lifetimes and beyond. These conditions include abusive conditions such as exposure to mechanical shock, fire, corrosive chemicals, or the like in a transportation accident. Vibration in shipping and handling can result in changes from the

original physical state, e.g., vibration of bulk propellant will mill off fine powder that usually winds up in the bottom of the drum, and presents a much higher risk of ignition when exposed to static discharge. Each composition has its own set of unique hazards. For example, though black powder will not detonate, it is treated as a Class 1.1 (mass-detonation hazard) material for shipping because it is so sensitive to friction and static discharge.

The safe manufacture and assembly of components must also be considered. Manufactured items need to be held to applicable standards by adequate internal and external quality assurance procedures. All manufacturing procedures must be protected against fire, static discharge, lightning strike, and accidental energization from the electrical system. All procedures should be practiced with inert simulants prior to the commencement of manufacturing or assembly as part of the training and certification process for personnel and to surface possible problems. Each proposed change in the manufacturing process must involve a full safety review.

End items must not only be able to function correctly over a specified range of values of the environmental variables to which they are to be exposed for the lifetime anticipated, but typically must also be safe (though not necessarily effective) when subjected to a wider window of exposures and for a longer lifetime. Environmental variables not only include the range of temperature, humidity, and atmospheric pressure (or their absence), but also the range of abuse to which they can be expected to be subjected in storage, shipping, and handling. There have been so many disasters resulting from exposure of ordnance items to fire in an accident that some modern munitions are thermally insulated. The goal is to have it take longer to heat the item to ignition temperature than the expected time it would take for the fire to burn out. However, the reliability of this insulation is not ensured. A second, well-known

thermal cause of explosions is when a round stays in a hot gun for too long, whether chambered or stuck in bore.

Some energetic materials such as NC have an active, autocatalytic mechanism working to self-ignite the product at some time, which is shortened considerably as storage temperatures elevate. If one cannot find a suitable substitute for NC, then a stringent program of surveillance of the materiel must be followed.

In addition to considerations of *stability* of individual energetic materials, the *compatibility* of any energetic materials with anything that they may contact must be addressed early in the design process. Examples are mixtures of different explosives compounds, mixtures of explosives with binder materials, and contact between an explosive and a casing material or its coating. A short paper by De Klerck, Schrader, and der Steen [102] discusses relatively current compatibility test techniques used. Samples of the pair of materials are mixed (starting with a tiny amount, of course) and are observed for such indicators of deterioration as evolution of heat (calorimetry) or gases, loss of mass, generation of by-products, etc. All but one of the techniques discussed in De Klerck, Schrader, and der Steen's paper are given in North Atlantic Treaty Organization Standardization Agreement 4147 Ed. 2 [103]. For each new material proposed for use, tests will need to be run for each possible component or contacting material. Related to chemical compatibility is storage compatibility. Detonators should not be stored with explosives, etc. The literature is extensive, and the practitioner must be thoroughly familiar with the acceptable procedures in storage, shipping, and handling of all hazardous goods.

13.2 INSULTS AND INCIDENTS

A short and certainly not complete list of insults is given in Table 13-1. This list can be used as a reference and a

checklist to help assess each design. Although most energetic items are usually in storage, one of the greatest sources of potential problems is during handling and transportation, so the packaging of these items requires special attention. All hazardous items should be engineered in conjunction with their packaging so as to meet applicable shipping and storage regulations while keeping as high a functionality as possible. A good example of this effective and safe engineering is the Bradley Fighting Vehicle, which serves as an approved shipping container for its ammunition load, so that it can be uploaded with its full complement of ammunition and placed aboard a transport vehicle and be ready to fight when it is delivered.

If possible, the design itself, or at the least the packaging, should provide antifraticide or nonpropagation measures. This design can be as simple as forcing adequate separation between adjacent items, or where space is at a premium, a buffer arrangement between warheads in an ammunition rack, e.g., the design patented by Walker, Gibbons, and Bowers of BRL [104].

SC jets pose a very lethal hazard. As mentioned in Section 12.13, a jet spoiler can eliminate the jet per se but not the explosive hazard. Storing items with SC warheads such that they are pointing into the earth will at least ensure that a jet does not leave the storage facility in the event of accidental initiation. Jetting is not confined to SC munitions. Note that adjacent explosive items, if detonated nearly simultaneously, can jet, as in a stack of artillery rounds. Walker [75] discusses this issue and how to mitigate the hazard.

It is essential to design-in the means to render ordnance items safe during their disposal and to enable the easy and complete recovery of their components to avoid a burden on the environment.

Personnel safety is a particular issue for those who have to manufacture, load, assemble, and pack ordnance

Table 13-1. Exposure Threats to Energetic Materials

IGNITION MECHANISM	TYPICAL CAUSE	TYPICAL MEANS OF PREVENTION
Friction	Black powder in threads of igniter tube while screwing on the stock.	Use a paper sleeve to cover female threads while filling; wet the screws threads with lacquer at assembly.
Crushing	Clamping an impact incendiary round in a vise to hack-saw off the jacket.	Don't do it.
Shearing	Cutting sheet explosive with scissors.	Use a knife on (an appropriately conductive) a soft surface: the wedge shape of the edge creates a state of tensile stress ahead of it pulling the explosive apart.
Impact	Smashing an exploding rivet with a hammer on an anvil to see what happens.	Don't do it.
Shock	Shock from the passage of an SC jet through the propellant bed in a cartridge.	Not much can be done. Ammunition stowage should be compartmentalized.
Heat		
Solar Heating Accelerates Deterioration of Stabilized Propellant	Storing ammunition in a transportation container.	Put a roof over the container with adequate clearance under the roof for air flow for cooling.
Fire	Lighting a piece of cannon propellant to see what would happen.	Don't do it.
Friction	Air wrenching in a cannon primer into a filled case. (Deadly explosion.)	Don't do it.
Smoldering Embers	Smoldering residue in bore ignites subsequent combustible-case cannon round.	Visually check the bore, swab the bore, or ensure that the active bore evacuator blows out the bore, but check the bore anyway.
Radiant Heat	Accidentally igniting a decoy flare while other flares are exposed.	Work with one flare at a time.
Static Discharge	Improperly grounded working surfaces.	Ground must have a high resistance to limit current.
Electromagnetic Radiation	Typically affects electric igniters.	Use less sensitive igniters, avoid creating an antenna (as happens when stretching out leads on an electric blasting cap, even with the lead ends shorted.)
Instability	Stabilized gun propellant auto-ignites. (Lifetime is shortened by high-temperature storage.)	Follow a strict program of analyzing a representative sample periodically and destroying the entire lot when the stabilizer content nears depletion.
Incompatibility	Picric acid reacts with metal parts of the fuze.	Shift to noncorrosive composition, such as TNT.
Site Contamination	NC lint infiltrates cracks between boards on walls over the years, ignites on demolition, flash fire severely burns workers.	Demolition of explosives processing facilities is very dangerous. Be sure everything in the facility is cleaned up first and be extremely careful.

items and those involved in research, development, testing, and evaluation involving energetic materials. Human error is often found to be the cause when accidents are investigated, which has led to the development of a number of common-sense safety rules.

Table 13-2 lists a number of typical incidents, their cause, and the actions that could have reduced the chance of the accident happening or could have reduced the severity of the consequences.

Table 13-2. The Human Element: Typical Accidents and Lessons Learned

INCIDENT	CONSEQUENCES	LESSON(S) (TO BE) LEARNED
SC warhead mounted with axis horizontal, shifts after setup for test.	Jet misses heavy armor target, perforates test enclosure, clips chain link perimeter fence, final point of impact unknown.	<ol style="list-style-type: none"> 1. No public access to range area, roads within area are barricaded for tests, so no one was in the area. 2. Have video surveillance to verify test setup before firing. 3. Perform SC tests on a vertical axis with the shot line into the earth.
Relying on memory, employee loads wrong propelling charge mass.	Wrong shot velocity; shot has to be repeated with expensive custom launch package and target assembly; could have damaged the gun.	Take nothing for granted, leave nothing to chance. Have prepared blank data sheet forms as a check list. Their layout should follow the work flow with a place for desired and actual values for every variable and for comments that inevitably need to be made. Write everything down as you go.
Commonly used propellants stored in loading room. Employee loads the right propelling charge mass of the wrong propellant.	Estimated peak pressure 140 kpsi, drop-block breech jammed shut. Gun to the machine shop, breech block pressed out, dressed up to correct dimensions. Heavy wall smoothbore lab gun barrel unintentionally autofrettaged, still serviceable. Back in service by mid-afternoon.	<ol style="list-style-type: none"> 1. The loading room should be empty at the start of each task. Don't leave anything in the loading room from earlier work. 2. Pay attention, check propellant container lot number against the loading requested on the data sheet when drawing from service storage cubicle and again when loading for the shot.
Foreign anti-aircraft round detonates, probably during fuze installation.	Three die instantly, only survivor bleeds out driving for help.	<ol style="list-style-type: none"> 1. Expose the minimum number of people to the minimum amount of explosive for the minimum amount of time. 2. "Foreign" equals "Be extra cautious." 3. Have a working radio range communication system. 4. Have a redundant land-line backup telephone system.
Cannon fires on hooking up firing line.	Recoil crushes the hip of the operator.	Never stand in the path of the recoil.
Round fired with obstruction in the barrel.	Expensive barrel destroyed.	<ol style="list-style-type: none"> 1. Always visually inspect the bore before loading the round. 2. Never look directly down the barrel of a gun. If you must look from the muzzle, use a mirror.

13.3 PERSONNEL QUALIFICATIONS

Most nations have a number of organizations and extensive laws and regulations devoted to promoting energetic materials safety. Persons and organizations involved must study the subject extensively until they understand the reason behind every rule or regulation. Individuals involved must be trained and enrolled in a formal, on-going process of certification and recertification to be allowed to work with energetic materials.

Many individuals display allergic reactions or contact dermatitis to some explosive compositions and may not be suited to be explosives workers. Many explosive

compositions can be toxic, so personal protective equipment and procedures need to be carefully selected.

More experienced individuals need to be certified at the level of range safety officer (RSO), the person solely responsible for the safe conduct of operations at a particular site. While any individual on the site should be authorized to shut down operations for a safety concern, only the RSO should be authorized to proceed. Each site needs to have several people available to fill this requirement, to cover absences. While anyone so certified *could* be the RSO on any day or any test, *only one person should be the RSO* on any day or any test. The personnel assigned to the operation and their particular assignments should be one of the first pieces of data written on any shot sheet (form) record. Management

should check conformance to this critical formality regularly.

Training should involve a certain amount of both formal classroom training and on-the-job training under experienced operators. Certification should involve demonstrating proficiency to a disinterested party (e.g., a member of the organization's Safety Office). The certifications need to be divided into narrow subject areas. For example, there should be separate certifications for persons working with small arms, large-caliber guns, and automatic weapons. Other examples are the certification of laboratory workers to work with experimental compositions and small quantities of energetic material in a laboratory setting versus an explosives worker who sets up tests of ordnance items. SCs present different hazards than HE fragmenting warheads.

Individuals can be certified in as many areas as applicable, and cross-training and certification are almost mandatory to ensure continuity of operations when faced with fluctuating customer demand. The organization needs to be aware of and proactively establish programs for certification in emerging technologies, for example, directed-energy weapons or electromagnetic launchers. Certifications should expire, so that if a person has not worked in a particular field for some time, they would need to undergo entry-level retraining and examination before being recertified to resume such work.

Not all persons are suitable for this work, as should be inferred from Tables 13-1 and 13-2. (The same individual was responsible for two of the entries in Table 13-1 and two of the entries in Table 13-2.) Workers should have not only the right aptitude, but also the right attitude. Management should be careful to write job descriptions so that serving as a certified energetic materials worker is not a condition of employment, so that they are free to certify and decertify individuals as needed without

giving cause for a grievance. Management also should be aware of the time it takes to properly train new employees and how this requirement impacts the work of the experienced personnel needed for the training, particularly when planning to expand the mission to include hazardous operations, to expand hazardous operations, or when the retirement or reassignment of key personnel is anticipated. Regardless of whether or not management emphasizes safety, individuals should emphasize and institutionalize safe practices.

14. CONCLUSION

Penetration mechanics is a difficult subject, particularly in the regime where both the penetrator and target materials are grossly deforming but it cannot be assumed that they act as fluids. At velocities above which the penetrator starts to erode, typically at a bit under 1 km/s striking velocity for competent, high-density engineering materials striking armor steel, penetration per unit of rod length increases monotonically with velocity to about 2 km/s and then the rate of increase drops off monotonically until the P/L is nearly that predicted by the density law at about 3 km/s, continuing to rise a bit beyond that, probably due to additional penetration by the increasing forward motion of the everted penetrator material in the channel. Penetrator and target do not intermix locally so that there is a clear interface between material streams, and one is only affected by the other where they contact.

The laws of physics always apply. As the penetrator interacts with elements of the armor, mass, momentum, and energy are conserved. The designer, whether of armor or antiarmor munitions, must keep track of how the mass is partitioned throughout the interaction until it has either all stopped or no trajectory intersects the target or other possibly significant article. During the interaction, the designer needs to know what (vector) momentum is carried by the mass as it is being redirected by the armor elements, as the time rate of change of momentum reflects the forces involved. Little energy is lost to internal heat in deforming metals. In a demonstration shot (unpublished work), Silsby and a coworker were able to measure an approximately 10% reduction in velocity of the initial WA penetrator debris splattered off the target face radially as an ordnance velocity LRP was entering a high-hard target—a 20% loss of KE.

Considerations of continuity prohibit sudden changes in direction and speed of a stream of material in motion,

dictating a dead zone (kernel) of material having a cusped profile on both its up- and down-range ends at the center zone of the interface. This kernel serves to pierce both the penetrator and target. Action and reaction are equal and opposite, so whatever the plastic flow stress is of the target in the zone of interaction, the target material there will assume a curvature that reflects the appropriate pressure on the target to generate the target flow stress, which explains the increase in hole diameter with increasing velocity in deep penetration. Estimating the time rate of change of momentum ultimately yields estimates on what forces are exerted on the armor as a whole, though the dynamic nature of the event makes analytical modeling inexact.

In deep penetration of targets with a large lateral extent relative to the penetrator diameter, thick-walled pressure vessel equations can be used to explain how a hole can be opened in a solid, elastic-plastic object: the outer boundary has been displaced enough to accommodate the hole volume, but the change is hardly noticeable because of the large radius. Equations for the deformation of a cylinder are complicated by the effect of nearby boundaries and asymmetries. Most of the plastic deformation in perforating a square target occurs in the four zones at the middle of the edges where the web of target material being stretched by the formation of the channel is the thinnest. There is a lot more material to be stretched at the diagonals. If a rod strikes a heavy target near an edge or the penetration channel is nearing the back of the target, most of the deformation of the target will be in the lightly confined zone, resulting in the penetration channel turning towards the free boundary. Material volume changes a bit in the elastic deformation regime but rebounds when the stress is removed, while material is essentially incompressible in the plastic flow regime. In plastic deformation, the dilatational component of the stress tensor (pressure) has no effect on flow and should be subtracted from the total state of stress to give the deviatoric (pure shear)

stress state, which determines the strain and the ultimate deformation.

In penetration mechanics, the overwhelming energy applied imposes a deformation that is usually dominated by inertial considerations. The properties of the materials (at the appropriate strain rates) and their deformation determines at what point fracture occurs, almost always in shear. The balance between the amount of strain hardening and the amount of thermal softening at the zones of high deformation determines whether the shear localizes (adiabatic shear) or is shifted to nearby areas (work hardening). Very malleable materials such as annealed tantalum, copper, and iron can be completely everted in a deep penetration and exit the target with nearly the same speed up-range as they struck going down-range, when observed from a center of mass coordinate system, and literally strike the gun muzzle nearly centered on the bore with the gun several meters from the target. When heavy steel-ceramic-steel targets are shot, ceramic debris routinely is found down the gun bore. Most penetrator materials are sheared into flakes during the penetration process and may exit up-range, clog the penetration channel, or pile up at the bottom of the hole depending on relative penetrator and target densities and striking velocity. With most armor materials, which need significant toughness, the rear face failure is a central plug surrounded with flakes sheared out of a ring of material from a zone of high deformation.

The totality of material projected behind the target element perforated and its state, i.e., its mass and velocity distribution, and the exact field of particles projected behind the target element determine the lethality of the interaction. Results are to a great degree stochastic, so that a statistically significant number of identical shots need to be fired to generate a distribution of the variables describing the lethality at that particular point at those striking conditions along that particular shot line. Repeating these shots over the entire vehicle from the entire space from which attack could occur is so

expensive that simplistic models are developed and calibrated to provide a means to make rational choices during the design stage or if estimating the vulnerability of opposing systems.

Everything is expensive in ballistics: the compensation of researchers and designers and the corresponding overhead; the cost of experimental hardware, facilities, instrumentation, skilled labor, and overhead; and the cost of computational assets. While it would seem prudent to rely heavily on computational modeling, the models can only predict that which has been programmed in, so that basic and applied research is needed to surface undiscovered physical processes and develop and improve useful materials. Experimental work is needed to search out new phenomena, determine the properties of new or improved materials, and verify model performance.

One of the two major goals of all of this research, development, test, and evaluation is the fielding of the next generation of tank: a fighting vehicle with a highly lethal main gun, which should weigh under 50 tons and travel over a wide range of terrain at nearly highway speeds. At the time that this monograph was being finalized, the most recent developments in Russian tank design, the T-14 Armata, were being revealed to the public [48]. It is very instructive to note the features where their current MBT diverges significantly from those on the Western hardware. As expected, the main gun caliber has increased. More significantly, they have reduced the crew to three by use of an autoloader, putting the crew in a single compartment, decreasing the volume under armor and hence the total weight, and are relying heavily on active protection.

15. REFERENCES

- [1] Silsby, G. F. "Penetration Mechanics of Anti-Armor Kinetic Energy Penetrators," self-published lecture hand-outs primarily for Baldini Resource Associates, 1987, 2004, and 2010.
- [2] Dietrich, A. M. "Terminal Effects by Jets from Lined Cavity Charges," self-published lecture graphics used as hand-outs primarily for Baldini Resource Associates, 1993.
- [3] Marean, C. W. "The Most Invasive Species of All." *Scientific American*, vol. 313, no. 2, pp. 32–39, New York, NY, August 2015.
- [4] Bower, B. "Human Ancestors Threw Spears at Prey." *Science News*, vol. 184, no. 12, p. 14, published by Society for Science and the Public, Washington, DC, 14 December 2013.
- [5] Walters, W. P. "Shock Waves in the Study of Shaped Charges." BRL-TR-3258, U.S. Army Ballistic Research Laboratory, Aberdeen Proving Ground, MD, August 1991, ADA240999.
- [6] Jonas, H. and Zukas, J. "Mechanics of Penetration: Analysis and Experiment." ARBRL-TR-02137, U.S. Army Ballistic Research Laboratory, Aberdeen Proving Ground, MD, 21005, February 1979, ADA068463.
- [7] U.S. Department of the Army. *Artillery Ammunition -- Guns, Howitzers, Mortars, Recoilless Rifles, Grenade Launchers, and Artillery Fuzes, (Federal Supply Class 1310, 1315, 1320, 1390)*. TM 43-0001-28, Washington, DC, April 1977.
- [8] U.S. Department of the Army. *Interoperable Ammunition Data Sheets for Artillery Ammunition: Guns, Howitzers, Mortars, and Artillery Fuzes*. TM 43-0001-28-3, Washington, DC, April 1981.
- [9] Federation of American Scientists' Military Analysis Network "DoD 101." <http://www.fas.org/man/dod-101/sys/dumb/mk82.htm>, accessed 8 December 2013.
- [10] Wikipedia. https://en.wikipedia.org/wiki/Gurney_equations, accessed November 2013.
- [11] Golesworthy, R. C. and I. Townsend, "Analytical Model of Shaped Charge Penetration in the Direct and Overflying Top Attack Modes." *Proceedings of the Eighth International Symposium on Ballistics*, Orlando, FL, 23–25 October 1984.
- [12] Tate, A., K. E. B. Green, P. G. Chamberlain, and R. G. Baker. "Model Scale Experiments on Long Rod Penetration." *Proceedings of the Fourth International Symposium on Ballistics*, October 1978.
- [13] Silsby, G. F. "Penetration of Semi-infinite Steel Targets by Tungsten Long Rods at 1.3 to 4.5 km/s." *Proceedings of the Eighth International Symposium on Ballistics*, Orlando, FL, 23–25 October 1984.
- [14] Cuadros, J. H. Personal communication. Telephone conversation and correspondence on results of General Dynamics Pomona Division's in-house research on hypervelocity impact supporting their electromagnetic gun project for tank main armament, General Dynamics, 27 May 1987.
- [15] Wenning, C. J. http://www2.phy.ilstu.edu/~wenning/slh/How_Many_Data_Points.pdf from the *Student Laboratory Handbook, 2004–2014, Illinois State University* and available online at <https://sites.google.com/site/teachinghighschoolphysics/student-lab-handbook>, accessed 10 March 2016.
- [16] Lambert, J. P. and G. H. Jonas, "Towards Standardization in Terminal Ballistic Testing: Velocity Representation," BRL-R-1852, U.S. Army Ballistic Research Laboratory, Aberdeen Proving Ground, MD, January 1976.
- [17] Hohler, V. and A. Stilp. "Influence of Length-to-Diameter Ratio in the Range from 1 to 32 on the Penetration Performance of Rod Projectiles." *Proceedings of the Eighth International Symposium on Ballistics*, October 1984.
- [18] Hohler, V. and A. Stilp. "Penetration of Steel and High Density Rods in Semi-infinite Steel Targets." *Proceedings of the Third International Symposium on Ballistics*, March 1977.
- [19] Silsby, G. F., R. J. Roszak, and L. Giglio-Tos. "BRL's 50 mm High Pressure Powder Gun for Terminal Ballistic Testing - The First Years' Experience," ARBRL-03236, U.S. Army Ballistic Research Laboratory, Aberdeen Proving Ground, MD, January 1983, (ADA 123861).
- [20] Sun, G., J. Wu, G. Zhao, and J. Shi. *Acta Armamentarii*, Beijing, China, No. 4, pp. 1-8, Nov. 1981.
- [21] Small, L. *Hardness, Theory and Practice, Part I, Practice*, Service Diamond Tool Company, Ferndale MI, p. 8.26, 1960.
- [22] Roecker, E. and C. Grabarek, "The Effect of Yaw and Pitch on Long Rod Penetration into Rolled Homogeneous Armor at Various Obliquities." *Proceedings of the Ninth International Symposium on Ballistics*, Royal Military College of Science, Shrivenham, England, 29 April – 1 May 1986.
- [23] Wright, T. W. "A Survey of Penetration Mechanics for Long Rods." ARBRL-TR-02496, U.S. Army Ballistic Research Laboratory, Aberdeen Proving Ground, MD, June 1983, ADA131152.
- [24] Bruchey, W. J. and J. T. Glass. "Orthogonal Grid Technique for Studying Internal Deformation and Energy Absorption in Target Penetration." BRL-MR-3415, U.S. Army Ballistic Research Laboratory, Aberdeen Proving Ground, MD 21005, December 1984, ADA149989.
- [25] Misesy, J. "Analysis of Ballistic Limit." ARBRL-MR-02815, U.S. Army Armament R&D Command, U.S. Army Ballistic Research Laboratory, Aberdeen Proving Ground, MD, March 1978, ADA054324.

- [26] Grubinskas, R. C. "A Review of the V₅₀ Ballistic Limit Requirements of MIL-A-46100." ARL-MR-095, U.S. Army Ballistic Research Laboratory, Aberdeen Proving Ground, MD, December 1993, ADA274927.
- [27] Zook, J. A., K. Frank, and G. F. Silsby. "Terminal Ballistics Test and Analysis Guidelines for the Penetration Mechanics Branch." BRL-MR-3960, U.S. Army Ballistic Research Laboratory, Aberdeen Proving Ground, MD, January 1992, ADA246922.
- [28] Grabarek, C. "Penetration of Armor by Steel and High Density Penetrators." BRL-MR-2134, U.S. Army Ballistic Research Laboratory, Aberdeen Proving Ground, MD, 1971, AD 518394L.
- [29] Wikimedia Commons. Public domain photo from Joker Island. **Israeli Merkava Mk I Tank at Lešany Military Technical Museum, Czech Republic**, 6th Tank Day, 30 August 2008. https://commons.wikimedia.org/w/index.php?title=File:Merkava_1_1-Lesany-1.jpg&oldid=331356446, 29 May 2020.
- [30] Vooris, J. J., LCPL. USMC Photo 050224-M-8205V-024, Saqlawiyah, Iraq.
- [31] Frank, K. "Armor-Penetrator Performance Measures." ARBRL-MR-03097, U.S. Army Ballistic Research Laboratory, Aberdeen Proving Ground, MD, March 1981, ADB058174.
- [32] HQ U.S. Army Reserves Europe. "Depleted Uranium." <http://www.per.hqusareur.army.mil/SERVICES/SAFETYDIVISION/radiation/Briefings%20and%20Training/HND-OUT%20ch04.doc>, accessed 27 March 2007, no author or date listed.
- [33] U.S. Army Research Laboratory. *Armor Plate, Steel, Wrought, Homogeneous (For use in Combat Vehicles and for Ammunition Testing)*. MIL-DTL-12560K, Aberdeen Proving Ground, MD, 7 September 2013.
- [34] ASTM International Subcommittee E28.06. *Standard Hardness Conversion Tables for Metals Relationship Among Brinell Hardness, Vickers Hardness, Rockwell Hardness, Superficial Hardness, Knoop Hardness, Scleroscope Hardness, and Leeb Hardness*. ASTM E140 – 12be1, Conshohocken, PA, 2012.
- [35] Meyer, L. W. and F. Pursche. "Modern High Strength Low Alloyed Steels." 1st International Conference about Recent Trends in Structural Materials, COMAT 2010 Conference Proceedings Primavera Hotel and Congress Center, 25–26 November 2010, Pilsen, Czech Republic.
- [36] Maalekian, M. "The Effects of Alloying Elements on Steels (I)." Christian Doppler Laboratory for Early Stages of Precipitation, Institut für Werkstoffkunde, Schweiß-technik und Spanlose Formgebungsverfahren, Technische Universität Graz, October 2007.
- [37] U.S. Army Research Laboratory. *Armor Plate, Steel, Wrought, High-Hardness*. MIL-DTL-46100E with Amendment 1, Notice 1, Aberdeen Proving Ground, MD, 11 February 2009.
- [38] U.S. Army Research Laboratory. *Armor Plate, Steel, Wrought, Ultra-High-Hardness*. MIL-DTL-32332, Aberdeen Proving Ground, MD, 24 July 2009.
- [39] Gooch, W., M. Burkins, D. Mackenzie, and S. Vodenicharov. "Ballistic Analysis of Bulgarian Dual Hard Steel Plate." 22nd International Symposium on Ballistics, Vancouver, BC Canada and Monterey, CA, 14–18 November 2005. (<http://www.dtic.mil/ndia/22ndISB2005/Friday/gooch.pdf>, accessed 3 September 2015).
- [40] Kleponis, D. S., A. L. Mihalcin, and G. L. Filbey, Jr. "Material Design Paradigms for Optimal Functional Gradient Armors." ARL-RP-92, U.S. Army Research Laboratory, Aberdeen Proving Ground MD, April 2005.
- [41] NobelClad Co., Broomfield, CO. Copyrighted figures used by permission April 2019.
- [42] Speedy Metals Online Industrial Metal Supply. "Fact Sheet on 17-4 PH Steel." <http://www.speedymetals.com/information/ Material2.html>, accessed 26 August 2015.
- [43] Doherty, K., R. Squillacioti, B. Cheeseman, B. Placzankis, and D. Gallardy. "Expanding the Availability of Lightweight Aluminum Alloy Armor Plate Procured from Detailed Military Specifications." ARL-RP-385, U.S. Army Ballistic Research Laboratory, Aberdeen Proving Ground, MD, July 2012, ADA-568648.
- [44] U.S. Army Research Laboratory. *Armor Plate, Aluminum Alloy, Weldable, 5083, 5456, and 5059*. MIL-DTL-46027J, Aberdeen Proving Ground, MD, 4 September 1998.
- [45] U.S. Army Research Laboratory. *Armor Plate, Aluminum Alloy, 7079*. MIL-DTL-46063H, Notice 1, (Inactive), Aberdeen Proving Ground, MD, 4 September 1998. (Last basic revision was MIL-DTL-46063H, 14 September 1998.)
- [46] U.S. Department of Defense. Department of Defense Index of Specifications and Standards. Part 1. Alphabetical Listing. Washington, DC. 1 July 1989, ADA-219610.
- [47] Jones, T. L. Personal communication. U.S. Army Research Laboratory, Aberdeen Proving Ground, MD, March 2007.
- [48] Wikipedia. "T-14 Armata." https://en.wikipedia.org/wiki/T-14_Armata, accessed 26 May 2016.
- [49] Magness, L., Jr. "The Ballistic Performance of Depleted Uranium Kinetic Energy Penetrators." Presented at the Core DUR IPT Meeting, Aberdeen Proving Ground, MD, 30-31 March 2000.
- [50] Wikimedia. "File:125mm_Bm15_APFSDS.JPG." https://commons.wikimedia.org/wiki/File:125mm_Bm15_APFSDS.JPG, accessed 3 April 2016.
- [51] Bharat Rakshak. Consortium of Indian Defense Websites. "Project BRF – Indian APFSDS Ammunition Scenario." <https://forums.bharat-rakshak.com/viewtopic.php?f=3&t=6668&start=40>, accessed 11 September 2015.

- [52] Kalinich, J. F., C. A. Emond, T. K. Dalton, S. R. Mog, G. D. Coleman, J. E. Kordell, A. C. Miller, and D. E. McClain. "Embedded Weapons-Grade Tungsten Alloy Shrapnel Rapidly Induces Metastatic High-Grade Rhabdomyoma-sarcomas in F344 Rats." *Environmental Health Perspectives*, Vol 113, No. 6, June 2005.
- [53] Hahn, F. F., R. A. Guilmette, and M. D. Hoover. "Implanted Depleted Uranium Fragments Cause Soft Tissue Sarcomas in the Muscles of Rats." *Environmental Health Perspectives*, Vol 110, No.1, Jan 2002.
- [54] Wikipedia. "Chapman-Jouget Condition." https://en.wikipedia.org/wiki/Chapman%E2%80%93Jouguet_condition, accessed 24 December 2013.
- [55] Wikipedia. "Explosive." <https://en.wikipedia.org/wiki/Explosive>, accessed 24 December 2013.
- [56] Wikipedia. "Sonoluminescence." <https://en.wikipedia.org/wiki/Sonoluminescence>, accessed 24 December 2013.
- [57] U.S. Department of the Interior. *Blaster's Training Modules - Module 1 – Explosives*. Prepared for the Office of Technology Transfer, Western Regional Office, Office of Surface Mining, Denver, Colorado, 2008, <https://www.osmre.gov/resources/blasting/btm/Module1.pdf>, accessed 29 July 2017.
- [58] Fowler, S. E. "Safety and Arming Device Design Principles." NAWCWD-TP-8431, Naval Air Warfare Center, Weapons Division, China Lake, CA, May 1999, ADA363924.
- [59] Colburn, N. L. "Chapman-Jouguet Pressures of Several Pure and Mixed Explosives." NOLTR-64-58, Naval Ordnance Laboratory, White Oak, MD, September 1964.
- [60] Wikipedia. "HMX." <https://en.wikipedia.org/wiki/HMX>, (accessed 13 August 2020).
- [61] Williams, H. "Contact Dermatitis within the Explosives Industry – A Case Report." *Current Allergy and Clinical Immunology*, Vol. 20, No. 3, pp. 151–154, August 2007.
- [62] Bouma, R. H. B., M. Stuijvinga, A. C. van der Steen, and H. J. Verbeek. "Physics of 1) Multiple Initiation Points in Fragmentation Warheads and 2) Explosive Forming of Metal Parts." *Proceedings, New Models and Hydrocodes for Shock Wave and Processes in Condensed Matter*, Edinburgh, Scotland, May 19–24, 2002, TP101, at <http://hsrlab.gatech.edu/AUTODYN/papers/paper132b.pdf>, accessed 23 December 2013.
- [63] Wikipedia. "Composition B." https://en.wikipedia.org/wiki/Composition_B, accessed 13 August 2020.
- [64] Wikipedia. "Plastic Explosive." https://en.wikipedia.org/wiki/Plastic_explosive, accessed 13 August 2020.
- [65] U. S. Department of Defense. Department of Defense Index of Specifications and Standards. Part 1. Alphabetical Listing. Washington, D.C. 1 November 2006.
- [66] Kennedy, J. E. "Gurney Energy of Explosives: Estimation of the Velocity and Impulse Imparted to Driven Metal." Sandia Laboratories Report SC-RR-7-790, Albuquerque, NM, 1970.
- [67] Predebon, W. W., W. G. Smothers, and C. E. Anderson. "Missile Warhead Modeling: Computations and Experiments." BRL-MR-2796, U.S. Army Ballistic Research Laboratory, Aberdeen Proving Ground, MD, October 1977, ADA047294.
- [68] Wilkins, M. L. "Calculation of Elastic-Plastic Flow," *Methods in Computational Physics*, Vol. 3, B. A. Alder, S. Fernbach, and M. Rotenberg, eds., Academic Press, N.Y., pp. 211–262, 1964.
- [69] U.S. Department of the Army. *Data Sheets for Guns, Howitzers, and Mortars: Interoperable Ammunition*. TM 43-0001-28-3, HQDA, Washington, DC, September 1986.
- [70] Breech, B. A. "Extension of the Gurney Equation to Two Dimensions for a Cylindrical Charge." ARL-TR-5467, U.S. Army Research Laboratory, Aberdeen Proving Ground, MD, March 2011.
- [71] Tie-peng, L., Q. Jian-ping, X. En-peng, and N. Gong-jie. "An Engineering Model for Calculating Axial-Preformed Fragments Driven by a Confined Explosive Charge," *Proceedings of the 25th International Symposium on Ballistics*, Beijing, China, 17–21 May 2010, China Science and Technology Press, Beijing, Volume 1, pp. 659–667.
- [72] Gilliam, J. "AMRDEC Technology as it Pertains to the Global War on Terror." *Presentation at the 39th Annual Gun and Ammunition/Missiles and Rockets Conference and Exhibition, 13–16 April 2004*, <http://www.dtic.mil/ndia/2004gun/wed/Gilliam.ppt> accessed 29 July 2017.
- [73] Altenau, E.-W. and W. Witt. "Warhead for Projectiles and Rockets." U.S. Patent 4,305,333, Rheinmetall GmbH, Dusseldorf, Germany, assignee, 15 December 1981.
- [74] Held, M. "Fragmentation Warhead." U.S. Patent 5,544,589, Daimler-Benz Aerospace, assignee, Munich, Germany, 13 August 1996.
- [75] Walker, E. H. "A Model of Antifratricide Shield Interaction with Jets Formed by Multiple Artillery Round Detonation." ARBRL-TR-02466, U.S. Army Ballistic Research Laboratory, Aberdeen Proving Ground, MD, January 1983.
- [76] Kennedy, D. R. *History of the Shaped Charge Effect: The First 100 Years – A Paper in Four Parts*. Copyright 1983 by Donald R. Kennedy, Mountain View, CA, for distribution at the DARPA/DOE Armor/Anti-armor Information Exchange Meeting, 6–8 March 1990, at the behest of Mr. Gordon Forman, Advanced Technology Assessment Center, Los Alamos National Laboratories, Los Alamos, NM, ADA220095.
- [77] Sandstrom, D. J. "Armor/Anti-Armor Materials by Design." Los Alamos National Laboratory Journal LA-UR-1000, *Los Alamos Sciences*, No. 17, Summer 1989, pp. 36–50, Los Alamos National Laboratories, Los Alamos, NM, available from the Federation of American Scientists, http://fas.org/sgp/othergov/doe/lanl/pubs/as_number17.htm.

- [78] Mah, R. and P. Martell. "ATAC and the Armor/Anti-Armor Program." Los Alamos National Laboratory Journal LA-UR-1000, *Los Alamos Science*, No. 17, Summer 1989, pp. 51–67. Available from the Federation of American Scientists, <http://fas.org/sgp/othergov/doe/lanl/pubs/number17.htm>.
- [79] U.S. Department of the Army. *Army Ammunition Data Sheets for Land Mines (FSC 1345), Technical Manual 43-0001-36*. Headquarters, U.S. Department of the Army, Washington, D.C., 15 September 1997.
- [80] Smit, D. "CSIR Defencetekes Landwards Defence Programme – Technobrief – April 2002." Council for Scientific and Industrial Research (South Africa), www.csir.co.za, accessed February 2007.
- [81] Chou, P. C., W. P. Walters, R. D. Ciccarelli, and O. W. Weaver. "Jet Formation Mechanics of Hemispherical Warheads." BRL-CR-545, U.S. Army Ballistic Research Laboratory, Aberdeen Proving Ground, MD, 1985.
- [82] Walters, W. P. and S. K. Golaski. "Hemispherical and Conical Shaped-Charge Liner Collapse and Jet Formation." BRL-TR-2781, U.S. Army Ballistic Research Laboratory, Aberdeen Proving Ground, MD, February 1987, ADA179735.
- [83] Summers, R. L., W. P. Walters, and R. D. Dick. "The Behavior of Shaped Charges with Open-Poled Hemispherical Liners." BRL-TR-3169, U.S. Army Ballistic Research Laboratory, Aberdeen Proving Ground, MD, November 1990, ADA229151.
- [84] Pugh, E., R. Eichelberger, and N. Rostoker. "Theory of Jet Formation by Charges with Lined Conical Cavities." *Journal of Applied Physics*, 23, 532–536, 1952.
- [85] Von Holle, W. G. and J. J. Trimble. "Temperature Measurement of Copper and Eutectic Metal Shaped Charge Jets." BRL-R-2007, U.S. Army Research Laboratory, Aberdeen Proving Ground, MD, August 1977.
- [86] Uhlig, W. C. and C. R. Hummer. "In-flight Conductivity and Temperature Measurements of Hypervelocity Projectiles." Presented at the 12th Hypervelocity Impact Symposium, Published in *Procedia Engineering*, Volume 58, 2013.
- [87] Flis, W. J. and P. C. Chou. "Penetration of Compressible Materials by Shaped Charge Jets." Seventh International Symposium on Ballistics, The Hague, Netherlands, 19–21 April 1983.
- [88] Walters, W. P. "Introduction to Shaped Charges." ARL-SR-150, U.S. Army Research Laboratory, Aberdeen Proving Ground, MD, March 2007, ADA 469696.
- [89] Walters, W. P. "The Shaped Charge Concept Part I. Introduction." BRL-TR-3142, U.S. Army Ballistic Research Laboratory, Aberdeen Proving Ground, MD, August 1990.
- [90] Walter, K. "Shaped Charges Pierce the Toughest Targets." Lawrence Livermore National Laboratory's *Science and Technology Review*. Research Highlights, June 1998. http://www.llnl.gov/str/pdfs/06_98.3.pdf, accessed 2 March 2007.
- [91] Simmons, B. "A Study of Shaped-Charge Collapse and Jet Formation Using the HEMP Code and a Comparison with Experimental Observations." BRL-MR-3417, U.S. Army Ballistic Research Laboratory, Aberdeen Proving Ground, MD, December 1984, ADA149472.
- [92] Morris, J. S., S. I. Jackson, and L. G. Hill. "A Simple Line Wave Generator Using Commercial Explosives." Shock and Detonation Physics, DE-9, Los Alamos National Laboratory, Los Alamos, NM. Preprint of <http://dx.doi.org/10.1063/1.3295158>, American Institute of Physics Conference, 28 June–3 July 2009, Nashville, TN, *Proceedings 1195, 408 (2009)* at <http://public.lanl.gov/~sjackson/> (accessed 4 August 2015).
- [93] Baker, E. L., J. D. Pham, and A. S. Daniels. "Low Reaction Rate, High Blast Shaped Charge Waveshaper," U.S. Patent 7,752,972, 13 July 2010.
- [94] Hasenberg, D. "Consequences of Coaxial Jet Penetration Performance and Shaped Charge Design Criteria." NPS-PH-10-001, U.S. Naval Postgraduate School, Monterey, CA, April 2010.
- [95] U.S. Army Joint Munitions Command. "Hall of Fame – Dr. R. J. Eichelberger." <http://www.jmc.army.mil/Docs/History/2012%20AHOF%20Inductee%20-%20Eichelberger.pdf> (accessed 4 March 2015).
- [96] Wikipedia. Monniaux, D., Photo of sectioned cannon-launched shaped charge round at the Journées Nation Défense, Paris, 24–25 September 2005. Used by permission under the terms of the GNU Free Documentation License, Version 1.2 or any later version. https://en.wikipedia.org/wiki/High-explosive_anti-tank_warhead (accessed 14 August 2020).
- [97] Seifert, K. and A. Crispino. "Feasibility Study of Explosively Driven Hypervelocity Projectiles." PIFR-559, Physics International Company, San Leandro, CA, 1974.
- [98] Massey, M. F. "Impact Fuze for Projectiles." U.S. Patent 2,764,092, 25 September 1956, assigned to the U.S.A. (Secretary of War).
- [99] Pugh, E. M. and R. J. Eichelberger. "Fluted Liners for Shaped Charges," U.S. Patent 3,726,224, 10 April 1973. Assigned to Giddings and Lewis, Inc., Fond du Lac, Wisconsin.
- [100] Chawla, M. S., J. D. Simich, S. W. Henderson, and R. K. Bethel. "Shaped Charge for Producing Large Perforations." U.S. Patent 5,753,850 A, 19 May 1998, assigned to Western Atlas International, Inc.
- [101] Barker, J. M. "Method and System for Packing Explosive Products for Transportation." U.S. Patent 6,454,085 B1, 24 September 2002, assigned to Halliburton Energy Services, Inc.
- [102] De Klerck, W. P. C.; M. A. Schrader; and A. C. der Steen. "Compatibility Testing of Energetic Materials, Which Technique?" *Journal of Thermal Analysis and Calorimetry*, Vol. 56 (1999; 1123–1131) Copyright 1999, Akadémiai Kiadó, Budapest, Kluwer Academic Publishers, Dordrecht, at <http://link.springer.com/article/10.1023%2FA%3A1010152911477#Page-1>, (accessed 16 February 2015).

[103] North Atlantic Treaty Organization. "Chemical Compatibility of Ammunition Components with Explosives (Non-nuclear Applications) – Ed. 2," Standardization Agreement STANAG 4147, June 5, 2001.

[104] Walker, E. H.; G. Gibbons; and Bowers, G. A. "Ammunition Rack for Vehicles," U.S. Patent 4,484,678, United States of America as represented by the Secretary of the Army, Washington, D.C., assignee, (27 November 1984).

16. BIBLIOGRAPHY

- Acton, F. S. *The Analysis of Straight Line Data*. John Wiley and Sons, New York, 1959.
- Baker, W. E., P. S. Westine, and F. T. Dodge. *Similarity Methods in Engineering Dynamics*. Spartan Books. Distributed by Hayde Book Company, Inc., Rochelle Park, NJ 07662, 1973. A revised edition of 2 December 2012 is available from Elsevier.
- Friedman, J. H. "Data Analysis Techniques for High Energy Particle Physics." SLAC-R-176 UC-34d, Stanford Linear Accelerator Laboratory, Stanford University, Stanford, CA 94305, September 1974.
- Polya, G. *Mathematics and Plausible Reasoning Volume I: Induction and Analogy in Mathematics*. Princeton University Press, Princeton, NJ, 1954.
- Polya, G. *Mathematics and Plausible Reasoning Volume II: Patterns of Plausible Inference*. Princeton University Press, Princeton, NJ, 1954.
- Tufte, E. R. *The Visual Display of Quantitative Information*. Graphics Press, Cheshire, CT, 1983.
- Walters, W. P. "The Shaped Charge Concept, Part I. Introduction." U.S. Army Ballistic Research Laboratory Technical Report BRL-TR-3142, Aberdeen Proving Ground, MD, August 1990.

APPENDIX A. HISTORICAL OVERVIEW OF FIGHTING VEHICLE ARMOR AND ANTIARMOR TECHNOLOGY

The organized presentation of a body of knowledge suggests that it somehow sprang into being overnight from first principles. This is certainly not the case in ordnance and armor development. While a few discoveries were made by accident, many resulted from narrowly focused efforts driven by dire need. There is little financial support for theoretical work in armament development. The elucidation of theoretical principles often follows many years of the practical work, the result of interpreting seemingly unrelated fragments of empirical knowledge. It is only the continual need to improve the armor on fighting vehicles in response to improvements in antiarmor munitions that has led to the current state of U.S. armor technology. The constant shift in advantage in military technology from offense to defense and then back to offense, etc. is ongoing.

Before armor design begins, guidelines for necessary armor protection levels and armament performance are established, based on experience with the current tank family, the expected future threats, which in turn are based on current intelligence and extrapolated from historical trends. The theaters of operation are postulated, setting constraints on transportation, deployment, and maneuverability. Economic, political, and even intangible psychological factors often have more influence on the final design than technical factors, life-cycle costs, and battlefield performance. Battlefields become battle spaces, deployment philosophy evolves, and there is a constant flux of resources available. All of these factors influence the final design of any weapon

system that finally gets committed to production. In particular, the tank is a vehicle, so the armor designer must work with vehicle designers to achieve maximum **mobility for the vehicle's allowed weight and the weight's disposition on the vehicle.** For example, some of the Mine-Resistant Ambush-Protected family of vehicles are constrained to relatively low cross-slope angle because of a high center of gravity, reducing effective mobility. Usually, as production begins on an item, changes in the world suggest the need for further modifications.

Design would begin with the customer specifying a prioritized list of performance targets. Most nations prioritize crew survivability, particularly smaller nations such as Israel. They put the engine up front to serve to further armor the crew and have full-width rear doors to give the crew the best chance to escape if needed. For most nations, the tank would be seen as a shock weapon, so that maximum speed over expected terrain would be very important. Given that most areas in the world have old, narrow roads constrained by buildings and impassable terrain, as well as bridges, roads, and railroads that have significant weight restrictions, the ideal tank should stay under 50 tons. Hasty engineering work to reinforce a 50-ton bridge would immediately inform the enemy facing a force with 70-ton tanks. **Similarly, it doesn't take much over-weight traffic to break up a road's paving, reducing mobility.**

The level of threat varies with the azimuth and elevation around the vehicle, so the amount of armor needed varies with location. The customer may want the bottom of the tank armored against specific mine threats. The rest of the tank must, at least, resist credible fragment and small arms threats. The roof may require additional armor against attack by aircraft and other overhead threats.

The difference in armor protection around a tank has produced deceiving statistics. Some people have concluded that the armor needs to be redistributed on tanks because of studies suggesting that a large percentage of the killing shots hit the sides and rear. Overlooked in these statistics are ineffective hits on the frontal armor resulting from its high degree of protection. If you know your weapon will not kill a tank from the front, it is far better not to shoot at the tank at all to avoid exposing yourself to counter fire. The only way to ensure a kill on a tank when using an undersized weapon is to ambush it from the sides or rear.

The load-bearing capacity of the soil, roads, and bridges will dictate a maximum weight. Assuming that the allowed weight goal has not yet been reached, the balance is allotted to frontal armor, since the main threat to a tank is an opposing tank firing close to head-on. As possible, the frontal armor is disposed to meet the main gun threat to some reasonable azimuth, say 30°. The vulnerable area presented to an opposing tank should be minimized. The size of highway and railroad tunnels and other obstructions constrains the overall height, width, and to some extent, the length of the vehicle. The number, size, and disposition of the crew determine the shape of the interior of the fighting compartment to be armored, so that the armor designer is limited in the line-of-sight thickness available for armor. Refer back to the comments on the Russian Armata tank in Chapter 14.

Because defense resources are limited, the economics of production are critical, and an efficient industrial base is key during wartime. Each side produces all the materiel it can as rapidly as it can and rushes it to the front, while the other side is at work destroying the materiel, its production base, its distribution network, and its users as rapidly as possible. The side that fails to deliver replacements faster than the attrition rate will be defeated. Figure A-1 illustrates the telling effect of a negative attrition rate. Unreplaced losses at a rate of 2%

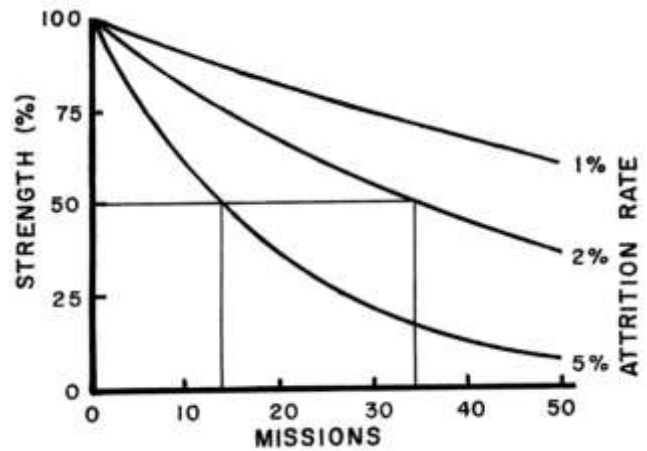


Figure A-1. The Toll of Attrition (Source: Silsby [1]).

per sortie will bring a unit to 50% of strength in about 35 sorties, while only about 15 sorties will have the same effect at a 5% rate of attrition. Careful attention to producibility, maintainability, repairability, and cost effectiveness in the design stages frees up capital for other critical applications.

As long as there are perceived threats to a nation, a war of sorts still rages as adversaries expend capital on weapons that could go to strengthening their economies. Once bankrupted, a nation is unable to wage a war, no matter how well prepared it is otherwise.

A.1 EARLY EVOLUTION OF THE TANK AND ANTITANK (AT) WEAPONS

In the Western world, at approximately the turn of the 20th century, the machine gun had transformed the nature of battle from maneuver to stagnation. In World War I (WWI), the romanticized tableaux of massive attacks by troops on foot, cavalry charges, and counterattacks had degenerated into the grinding nightmare of trench warfare. The spectacular culmination of the slow and silent subterranean warfare of the sapper, who tunneled in and destroyed defensive

works with explosives, broke the monotony of endless artillery barrages and massive assaults over short stretches of heavily defended land.

A.1.1 The Tank as Mobile Machine-Gun Nest

The tank was developed to swing the tide of warfare back to the offense. It was an assault vehicle conceived to neutralize the machine-gun nest (Figure A-2). First designs fulfilled three requirements. First, the need to deliver small-arms fire at a high cyclic fire rate dictated a machine gun as its main armament. Second, the need to negotiate the cratered and trenched battlefield was met by a long and wide track-laying suspension with an inclined forward end. Third, about 12 mm (a half an inch) of good-quality steel plate was the maximum armor thickness, sufficient to protect against all the small-arms ammunition used at the time. Since the armor was impregnable, high speed was not critical.



The British Mark II tank of WWI, mounting five Hotchkiss 0.303 light machine guns: two fired from each side and one from the front. No tank since has had such a commodious interior!

Figure A-2. The Tank as Mobile Machine-Gun Nest (Source: Silsby [1]).

A.1.2 AT Guns

To counter the tank threat, the first AT weapon was developed. The first purpose-built, AT rifle was introduced in 1918, the German Tank Abwehr Gewehr M1918 [2]. It was a large, Mauser-type, bolt-action rifle chambered for the 13.2 × 92mm semirimmed, bottleneck cartridge and could penetrate around 20 mm of armor at 200 m and 15 mm at 300 m, when striking at 90°.* By the time this rifle was fielded, the war was essentially over, though apparently not for the Germans. The next step was the 20 mm AT rifle. Because of its size and weight, it was usually handled by a two-man crew.

A.1.3 The Tank as AT Weapon

The armor thickness of the next generation of tanks, and hence their weight, was increased sharply by this simple, cheap, and ubiquitous gun. Power train and suspension improvements proceeded apace. With **the tank's heavy** load-bearing capability and its maneuverability on the battlefield, it was not long before the advantage of the tank as a highly mobile AT gun platform was realized (Figure A-3). The recoil system and the mechanism



U.S. Model A (1922).

Figure A-3. Early AT Tank (Source: Silsby [1]).

* Note that the British define obliquity (as in this Appendix) as the minimum angle between the shot line and plate plane, not between the shot line and target normal as the U.S. does.

needed to elevate and depress the gun were no problem to implement in the tank, but a turret was needed to train (point) the gun in azimuth. Fire-control system components were integrated into the vehicle, as well as auxiliary weapons. The tank assumed the role it has maintained to this date. Aircraft evolved to hunt aircraft, ships evolved to hunt ships, and tanks now hunt tanks.

A.1.4 Armor-Piercing (AP) Shot and the Towed AT Gun

Armor and antiarmor weapons did not appear out of a vacuum. From well before WWI, every nation that could afford to was revamping its navy. At that time, all naval capital ships were surface combatants. The primary armament consisted of many large naval rifles that used AP shot, and the primary defense was heavy armor. Armor, antiarmor shot and shell, and fuzing were all developing rapidly, which would immediately benefit armies. Meanwhile, the demand for smaller, rapid-fire guns, for example, for use against motor torpedo boats as well as land targets, resulted in a number of promising designs.

It appears that well before 1935, the various soon-to-be combatants were developing designs for a quick-fire (QF), single-shot, AT gun firing full-bore, AP shot that could be mounted in a tank and/or a towed gun. Most of these guns were quite effective until the armor on the next generation of tanks was thickened again. In World War II (WWII), there was a continuing evolution of gun calibers and tank armor, ending with an AT cannon of roughly 90 mm bore. Since then, the West has fielded only two more iterations, the 105mm rifled gun and the 120mm smooth bore, while the Soviets have developed a 125mm smooth bore. Advances in the carriage and recoil system design were not as significant as was the QF breech.

To this day, the QF breech mechanism design is an accepted standard world-wide in both antiarmor and

antiaircraft guns (Figure A-4). The gun is readied for action by opening the breech block against a stiff spring using an operating lever or other means. The breech block can travel horizontally or vertically. During the **block's travel, a number of** mechanisms are activated. The firing pin in the breech block cocks. The extractor fingers are an integral part of the breech mechanism. They cock to the rear and then lock the breech block in its fully open position. When fully open, the breech block clears a U-shaped slot in the breech ring, forming a guide for the cartridge.

With the gun laid (aimed), all that is needed to fire the gun is to throw a cartridge into the chamber. The cartridge case rim trips the extractors forward, releasing the breech block to close fully under heavy spring force against a mechanical stop. Just as the breech block fully closes, a mechanism releases the firing pin to fire the gun. As the shot starts up the barrel, the gun goes into recoil. A linkage pulls the breech block open, cocking the firing mechanism, and a cam surface on the breech block snaps the extractors rearward at the end of recoil travel, extracting and ejecting the spent shell casing. The breech block is locked open ready for the next shot.

Rates of fire can exceed 10 rounds a minute. Mechanical interposers prevent or interrupt firing under a number of conditions, e.g., the breech ring not fully screwed onto the barrel threads. The breech can be closed on a round manually, and the gun can be fired by lanyard if so desired. Loading the first round and closing the breech ready to fire is called charging the gun.

It was natural to use magazines to feed a QF gun. Firing ceased when releasing the trigger temporarily removed an interposer from one of the mechanical trains needed to keep the gun firing. A natural evolution was to feed from several magazines to allow selective fire, as between proximity and point-detonating fuzed antiaircraft ammunition. The evolution of a fuze that

communicates wirelessly with the gun console and appropriate ammunition makes this refinement unnecessary today.



From the Skoda works, produced in the interbellum. At the bottom is a QF breech from a 76mm German tank cannon.

Figure A-4. Czechoslovakian Towed AT Gun (Source: Silsby [1]).

A.2 THE DEVELOPMENT OF HEAVY FRONTAL ARMOR AND THE SC

The introduction of heavy frontal armor marked the transition to the modern tank. However, a weapon that could defeat it was quickly developed in WWII—the SC, necessitating further increase in the weight of armor needed.

Prior to WWII, V-shaped grooves in a sheet of explosive, detonated in contact with a thick, strong, ductile metal witness plate, had been observed to leave an impression, in what is named the Monroe effect, after its discoverer. Rather by accident, it was found that a liner on the explosive in the groove greatly increased the penetration. This discovery could not have come at a better time. Tanks had become effective threats on the battlefield. A lightweight explosive device that could perforate a significant thickness of armor was needed to defeat these threats.

Soon all of the combatants were working on the SC. There were already many techniques to launch explosive devices from guns and detonate them under just about any set of conditions. Rocketry was out of its infancy, too, providing another means of long-range delivery. SC warhead lethality increased rapidly. By the end of WWII, the SC was, next to the atomic bomb, the most effective AT munition. The spectacular explosion, the burned appearance of the hole it makes, and the munition's acronym, HEAT, all contributed to the popular misconception that the hole is burned through the armor by an incandescent jet of hot gases. The principles that make the SC lethal were discussed in Section 2.3, and the physics needed to design an effective lined-cavity charge warhead was discussed in Chapter 11. The formation of a jet from the Viper SC warhead is shown in Figure A-5.

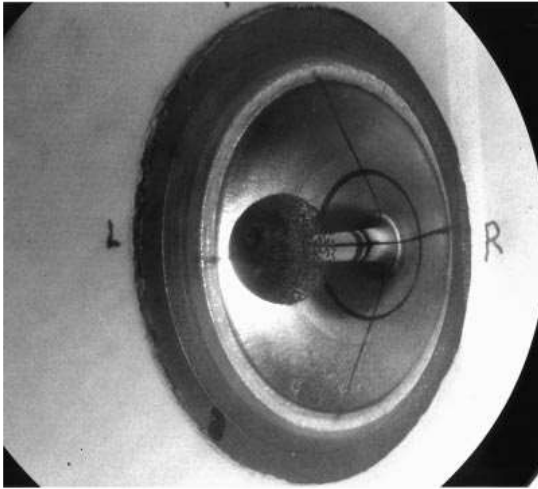


Figure A-5. Viper Warhead SC Jet Forming (Source: Walter [3]).

A.3 THE HIGH-EXPLOSIVE PLASTIC (HEP) ROUND

The HEP round was originally intended as a bunker buster [4]. Its performance against monolithic metallic armor was noted, and rounds were designed specifically for that purpose. The spin-stabilized, full-bore, bullet-shaped projectile consisted of a deformable, plasticized explosive fill in a thin, ductile shell, with a base-detonating fuze with a slight delay. When it strikes the armor plate, it deforms to contact the plate and then detonates. The extreme shock wave from the detonation sweeps through the steel or other material leaving the material behind the shock wave moving down-range in a compressed and heated state. When the shock wave encounters the rear surface, the material there is free to move to the rear without having to push on adjacent material. This reaction is much like the desktop novelty, **Newton's Cradle**, a series of largish, hanging ball bearings in contact. When the first one is pulled up and released (projectile), the individual balls in the train remain motionless, but the last one flies off the stack (spall).

Armor usually has a lot of tensile strength, so the rearward moving material has to have sufficient inertia to

tear off a spall, but it is easily done with current rounds hitting monolithic armor. When the spalled disk of the material at the target rear face is projected into the fighting compartment, it can have lethal effect without the armor being perforated.

Spallation failure is one of pure tension, and the failed surface of the material looks like the surface of a sponge, as opposed to a shearing failure normally encountered in ductile materials, which display striated marks from the relative motion of one side of the failure on the other. In the U.S., the M393 HEP round was standard for the 105 mm M68 tank cannon in 1985 [5]. The M393A3 HEP with tracer version is now type classified for use in the M68 cannon on the Stryker Mobile Gun System [6].

HEP rounds are easily countered. As in electromagnetic wave propagation, the medium can absorb energy propagating through it if a lossy deformation process is available. When a wave-front passes from one medium to another, the amount and direction of transmitted and reflected energy are partitioned based on the geometry of incidence and the shock impedances of the adjoining materials, which in turn depend on their stiffnesses and densities. Dual layers of armor plate with a bit of an air gap are quite effective, as the explosive shock wave couples only into the first plate, and the second plate must only stop a slow-moving spall. Of course, the two-plate system must be sufficiently robust to stop all the other threats expected. A second, less effective approach is to put a soft, thick liner in contact with the primary armor plate to reduce the strength of the tensile forces trying to fail-off the spall. The HEP round is no longer used as an antiarmor concept in most nations, although it continues to be used as an antibunker munition [4].

The British, however, continue to use the High-Explosive Squash Head (HESH) round, initially because of its effectiveness in defeating a Soviet T-55. In combat, tanks

travel with a round in the chamber, ready to fire. A lot of discussion goes into deciding what type of round should be chambered to maximize the survival of the tank in an unexpected confrontation. The British like the HESH round because it can accurately hit an opposing vehicle at extreme ranges. They feel that even if it **doesn't** kill the opposing vehicle, the concussion, flash, and smoke would surprise and confound the opposing crew. This effect would give the British tank the time to select the round of choice and fire a second and probably lethal shot before being spotted.

Cementing their favorable perceptions of the HESH round, which continues to this day, a blue-on-blue accident completely destroyed one of their Challenger 2 MBTs with an unlucky hit on its driver's hatch.

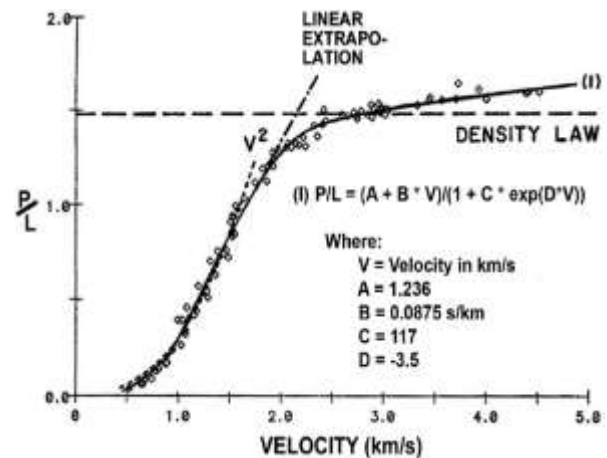
"Fortunately, in 2009, a new HESH round manufactured in Belgium has been trialed. This means that the Challenger 2 now has available a [sic] new tungsten FIN and HESH rounds, if and when required, which secures a line of ammunition for its calibre Length 55 rifled main gun, the L30, when required in the future [7]." (The 120 mm cannon tubes on the Challenger are rifled. FIN refers to a fin-stabilized, long-rod penetrator [LRP] round.)

A.4 THE HYPERVELOCITY ARMOR-PIERCING (HVAP) ROUND AND THE LRP

Two concepts integral to the success of the HVAP round enabled the introduction of the LRP. First, by saboting a subcaliber, high-density projectile, the gun's performance was improved, as was also the case with the discarding sabot AT round. Second, the HVAP round worked better than AP shot. This improvement was attributed to increased energy on a smaller footprint when attacking the target (energy density). Then, lengthening the penetrator and reducing its cross-sectional area further produced even higher energy densities. Added benefits accrued: The total inbore mass was further reduced, as was the retardation in

flight, so that striking velocities were increased. The very effective antiarmor LRP was developed, known militarily by various acronyms and abbreviations such as the Hypervelocity Armor-Piercing Fin-Stabilized Discarding Sabot with Tracer (HVAPFSDS-T).

In the lower end of the tank cannon velocity regime, the penetration continued to increase smoothly and rapidly with velocity, suggesting the rising limb of an upwardly directed parabola, so that the older equations relating penetration to energy continued to be adequate. This helped to hide from the researchers at the time the significance of the change in regime from rigid to eroding-rod penetration. Without the researchers realizing it, the de Marre equation and their energy-dependent equations were rendered inoperative. As velocities continued to increase, the performance lagged a bit, suggesting a linear relationship. A few people understood this linear relationship to mean that by doubling striking velocity, penetration could be doubled. However, a broader perspective is needed to model with reasonable confidence the performance of long rods fired from postulated, practical, increased-velocity launchers. Figure A-6 highlights this fact using



Curves fit to a large number of WA long-rod data spanning the velocity range to 5 km/s. (Ordnance velocity is 1-2 km/s.)

Figure A-6. P/L Versus Velocity, Showing Various Approximations (Source: Silsby [1]).

experimentally determined P/L versus velocity data for tungsten alloy (WA) long rods versus RHA.

A.5 WEIGHT-EFFICIENT TANK ARMOR

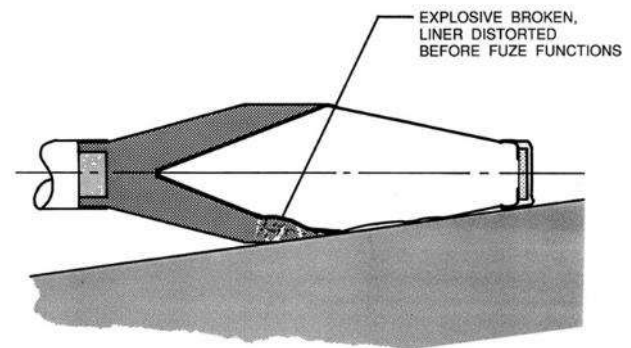
In the U.S., the cast ballistic hull remained the standard well after welding technology had become quite mature. The M60 tank, many of which now are serving to improve fishing in the Atlantic Ocean, was the last of its line. In the early 1970s, the jointly developed MBT 70, though never fielded, displayed many of the features found in today's tanks (Figure A-7). Like the M1, the MBT 70 had planar surfaces, skirting plates, and a high-obliquity upper glacis. Armor thickness in cast tanks was smoothly graded around the ballistic hull and turret. In a welded design, armor geometry and makeup can be tailored to provide varying protection levels needed to meet the threats from different directions just as well. And hardened and tempered rolled armor plate provides better protection on a weight-for-weight basis than the cast armor of earlier days.

The bulk of the presented frontal area of the tank hull is divided into two separate areas: the upper and the lower



Figure A-7. The M60, MBT 70, and M1 Tanks (Source: Silsby [1]).

glacis. (Armor names are often borrowed from those used to describe fortifications, as here, or the personal armor of the mounted knight.) The location and field of view required by the driver dictates that the upper glacis be sloped down in the forward direction, so it was implemented on the MBT 70 as a high-obliquity casting. This design tends to ricochet AP shot. Also, grazing contact greatly increased the probability of a fuzing failure on some earlier types of SC fuze. (Of course, the fuzes were rapidly improved.) At high enough angles of striking obliquity, the armor can engage the casing of an SC round before detonation, distorting and breaking the explosive, resulting in asymmetric collapse of the liner and serious degradation of warhead performance (Figure A-8).



Cost considerations doomed the MBT 70, not its armor. Techniques had even been worked out to repair shot-up armor by flame-cutting open the damaged cells, replacing the tile, and welding on a new cover plate.

Figure A-8. A Nonballistic Bonus of Obliquity (Source: Silsby [1]).

A.5.1 Weight-Efficient Frontal Armor

The lower glacis on the MBT 70 was the first weight-efficient SC defeating armor. It consisted of a series of cells containing glass tile embedded between heavy armor plate. Under extremely high pressure, the loosely packed molecular structure of glass is suddenly rearranged into a more compact form. As a result of this phase change, the cavity in the glass expands

significantly, which relieves the contact pressure momentarily. The jet advances without resistance a short distance, and then the cavity closes in on the jet again and the process repeats. The oscillating channel profile is thought to cause the everted jet debris to repeatedly turn back and impinge on the attacking jet self-destructively (Figure A-9).

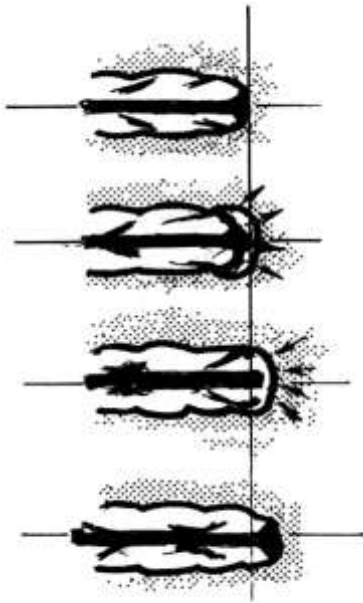


Figure shown is speculative.

Figure A-9. Confined Glass as an SC-Defeating Armor (Source: Silsby [1]).

A.5.2 The Skirting Plate as Weight-Efficient Armor

LRPs were the coming KE threat and even though the mechanism was not understood, experimental results showed spaced armor to be very weight-efficient against them. In retrospect, several things were happening.

The MBT 70's skirting plate was a high-hard steel plate. Because of its thinness and strength, the hole size created by an LRP was small, enhancing the sensitivity of an attacking LRP to yaw regardless of striking obliquity. When the attack occurred at high obliquity, as most would, the skirting plate was very effective against LRP.

The WA from which the first rods were made was not a very good ballistic material, and the oblique force on the rod nose and the asymmetric engagement of the tail fins as the skirting plate was perforated helped to break up the rod and yaw it. The shorter HVAP or AP shot would also pick up a yawing rate as it perforated the skirt, attacking the hull-side armor yawed, reducing its effectiveness. The skirting plate also served to detonate SC and HEP rounds far away from the hull-side armor, reducing their effectiveness.

A.6 THE EVOLUTION OF THE SC

The performance of the SC scales geometrically, so that the rapid increase in tank cannon bore diameter during and immediately following WWII resulted in concomitant increases in penetration performance. But there were other design improvements derived from increasingly sophisticated understanding of the principles behind the SC.

A.6.1 Eliminating SC Performance Degradation

The SC jet arises from everting part of the liner. People recognized that the characteristic tulip-shaped leading particles seen in radiographs resulted from the first part of the liner to be launched moving slower than later parts. This phenomenon is suggested by the umbrella-shaped spray of tip material in the photograph of the early stages of jet formation of the Viper warhead that was shown in Figure A-5. The jet is penetrating itself, reducing effective length. The cure was to round the liner apex. Likewise, the sensor, fuze, and other parts **that couldn't be moved out of the way of the jet** were made as insubstantial as possible.

The geometric scaling of SC jet performance implied that jet length and hence warhead performance were dictated by the warhead diameter. However, a liner does

not *have* to be a cone; it just always *had* been a cone. Someone realized that by conceptually stretching the cone nonlinearly so that it looks like the bell of a trumpet and tailoring the geometry of the explosive charge appropriately, the jet could be lengthened without increasing warhead diameter.

A.6.2 Threats to Technological Leads

No technological lead will be held for long. To be useful, **a technology must actually be employed.** “A ship in harbor is safe, but that is not what ships are built for [8].” A number of people must understand how it works. Details eventually leak out and security becomes less of a help than a hindrance. At some point the security classification is dropped. This is standard U.S. doctrine in the case of developmental ammunition, which is often declassified when first issued to the troops. Fortunately, with armor, much of the technology is safely hidden from casual observers. The thermal-mechanical treatment and the resulting mechanical properties of the armor material are not shared. It is very difficult to clandestinely obtain samples for analysis as the plate is welded up into a massive structure or tucked away in welded-shut compartments. The M1 has been in the field for perhaps 40 years and the armor technology is still classified.

As is the case with much of the technology discussed in this monograph, the trumpet-shaped liner was originally a very secret concept. When Dr. Eichelberger, a world-renowned SC researcher, retired as the U.S. Army Ballistic **Research Laboratory's (BRL's)** Director, the BRL SC developers were scandalized by the new portrait of him standing in front of a chalkboard on which were written the equations describing the physics behind the trumpet liner.

Where technologies originate in a broad arena and many nations are working to develop a useful product, usually

someone involved in its development will unilaterally decide to reveal the technology, often for commercial gain. This was the case with explosive reactive armor (ERA). Alternatively, one can lose the lead to espionage, as was the case early in the U.S. development of the atomic bomb.

In addition, technology arises from scientific principles, and there is no way to hide basic physics. Some people can determine what is inside a box from the simplest clues, e.g., from what constraints the offeror of a proprietary design puts on the firing trials and smelling the air in the range after a shot. In some cases, a careless word can reveal a guarded technology. In the late 1950s, people in the U.S. Patent Office were convinced that drug companies were illegally fixing prices. A drug company lawyer at the Patent Office inadvertently mentioned to a Patent Office lawyer that this price fixing was true but **that** “no one will be able to figure out the **formula.**” Now knowing that there was a formula, the Patent Office lawyer gathered historic pricing data and figured out the price fixing. She took the information to the Justice Department, and they hired her away from the Patent Office to successfully prosecute the case.

Sometimes, practicalities prevail. With the Global Positioning System (GPS), its operator, the military, wanted to keep the accuracy poor for those outside the inner circle, to avoid it being used by opponents for targeting in the U.S. (The Soviet Union was famous for locating cities 5 miles up or down the wrong side of a river in their published maps for just such a reason.) Many U.S. commercial operations felt that the benefits of an accurate system far outweighed the potential costs but could not prevail. Soon, someone realized that the miniscule timing error intentionally introduced in the satellite signals could be managed. All that was needed was to accurately determine the position of a fixed location and compare that with the position determined from the GPS satellite signals to back out an error

correction applicable to a broad surrounding area. This correction could be applied at key locations, and private transmitters could be installed to track moving trucks or other vehicles to within a few feet. With this practice spreading, albeit at considerable cost to private enterprise, the military dropped the practice of intentionally degrading the signal used by the public.

Two common ways to lose a lead are bragging and politics. Typical of the former was when someone wanted to appear smart and announced that they could track enemy **cell phones**. **It didn't take long for the enemy to switch critical communications to sneaker mail.** Then there is the general whose favorite weapon system is about to have its funding cut. A good way to influence such a decision is to tell the world about the weaknesses of the competing systems or the strengths of his own system, as was the case with DU armor. Probably one-quarter of the material that can be discussed in this monograph would still be secret were it not for such careless disclosures.

A.6.3 Evolution vs. Revolution

While management periodically mandates revolutionary improvements, most advances come from evolutionary changes. In the case of the SC, better metallurgy and tighter tolerancing resulted in better performance as did spin compensation for spin-stabilized warheads. Many advances in the design and fabrication of the explosive charge bought small performance improvements as well. One typical advance was the induction of a gradient in the fraction of the two-component explosives along the cast charge axis, better tailoring the detonation velocity and improving SC performance with no increase in weight. Another was the adoption of the wave shaper from nuclear warhead technology. The wave shaper is now used world-wide, which is not a good sign for nuclear nonproliferation.

A.7 ARMOR EVOLUTION

Warheads shot from existing portable launchers and from guns on existing tanks could perforate increasingly thicker armor. Armor development became one of the **highest priorities among the world's ground forces, and** considerable money and labor-hours were spent on this priority. In the U.S., the result was the special armor on the M1 tank, which is found on the hull, turret, and skirting plates.

In the mid-1980s, the new standard for the MBT reflected the thinking of the day. Adequate armor protection all around protected against artillery fragments and mine blast. Since the battle was to be across a well-defined front, heavy armor was wrapped around the front of the hull and turret to protect against SC and LRP threats from the main gun of opposing tanks to a bit over 30° off the front. Skirting plates boosted the protection to the hull side likewise. The fighting weight **of each nation's heavy tanks exceeds the desired value of 50 tons by an amount that reflects each nation's priority of protection over** mobility. The M1 weighs about 70 tons! Practical limitations dictate that this is about as heavy as a tank can get.

Compared to the earlier generation of tanks and their monolithic armor, the armor protection on the new generation has increased disproportionately to the weight. One gain in protection comes from including plenty of air space in the armor. As in the case of the skirting plate, air space allows an initial disturbance to grow, without any weight penalty. Compare the exterior of the M1 tank with that of the M60, with its monolithic hull. The volumes of the fighting compartments of the two are about the same, while the exterior of the M1 is much larger, showing the bulkiness of the modern armor.

The proponent of the M1 tank used an “armor in a box” fast-tracking concept as a way to allow the maximum time for the armor research community to improve their armor designs before they had to be committed to production. It is also a concession to the constant improvements foreseen in threat munitions. Rather than being an integral part of the vehicle armor, the M1 tank’s special armor is contained in compartments. The areas requiring heavy armor are covered with a series of armor steel boxes. The actual special armor package is dropped into this compartment, which is then welded shut. As improvements in armor technology are realized, only the design of the armor package is changed. Already-fielded tanks have been retrofitted to improve their protection. Repair of combat-damaged armor is simplified as well. The box containing the damaged armor section is burned open, the package is repaired or replaced, the hole in the box is patched, and the box is welded shut.

Historically, tanks are almost worthless without accompanying dismounted troops to keep opposing dismounted personnel with hand-held HEAT weapons away. Troops are transported to the battlefield in an armored personnel carrier that can keep up with the tanks. This vehicle protects them from artillery fragments and small-arms fire. However, now rather than an enemy that shells the Bradley from behind the forward line of troops, the Bradley is facing rocket-propelled grenades (RPGs) fired at close range. Fortunately, the concept of RA was developed, and like the concept of the SC, it spread quickly throughout the world. Relatively simple and relatively light, RA was effective.

A.8 RA

RA consists of a pair of armor plates set at obliquity with something solid sandwiched in between. First conceived to be single pairs of oblique parallel plates covering a large presented area, in practice the areas are protected

by a large number of small modules so as to limit protection loss to only a limited area when hit. Figure A-10 shows a Bradley Infantry Fighting Vehicle (IFV) outfitted with RA modules intended to defeat SC jets.



Figure A-10. Bradley IFV with RA Modules (Source: DoD [9]).

The initial RA concept was for the filler to be the typical HEs of that time. As an incoming round starts to perforate the first plate, the explosive detonates, driving the two plates apart. The plate velocities are approximated using the Gurney equations for metal plate acceleration by explosives. It was subsequently discovered that one could use a nonenergetic filler, and the energy from an SC jet impact alone could still impart significant plate motion. However, it can be challenging to compute plate velocities from first principles. Today RA includes ERA and Non-Energetic Reactive Armor (NERA).

By changing one’s viewpoint from fixed relative to the strike point to fixed relative to the moving plate, it can be seen that the vector addition of the plate motion to that of the jet results in the penetrator striking with significant yaw. The devastating effect of yaw on an LRP attacking a thick target was discussed in Chapter 7. The thinner the flyer plate relative to the jet diameter, the less its effect on the jet. So the plate thickness is reduced to where it is as thin as practical while still retaining

considerable effectiveness, so as to keep down armor weight [10].

The moving oblique plates destroy some length of the jet, the leading higher velocity material. This material would have created the largest hole diameter when attacking the primary hull-side armor, in the absence of the RA package. The RA reduces the diameter of the hole in the primary armor through which the rest of the jet must pass to continue the penetration. At the same time, the leading part of the jet usually penetrates as a continuous jet, while the trailing part of the jet may be particulated and less effective [10].

In detail, the jet blows a hole in the uprange plate, wasting some of its length. This admits the following part of the jet until plate motion results in reestablishing jet consumption and again some of the jet is wasted blowing another hole in the plate. Again, some of the jet gets through. This process is repeated as long as the plates are moving. These admitted lengths then have to blow holes in the moving rear plate. The overall effect on the primary hull-side armor of the RA applique chopping sections out of the jet is two-fold. There is less jet length presented to the primary hull-side armor, and the process of repeatedly stopping and resuming jet penetration in the primary armor eats up a lot more jet than would continuous penetration [10].

The lower-speed LRP will barely make a hole larger than itself, so that the two separating plates in ERA ride on the top and bottom of an LRP. If sufficiently thick relative to the rod diameter and adequately strong, the plates will bend, break, and scatter the resultant pieces of the rod, so that they are scattered significantly and no longer in train [10]. See Figure A-11.

The variables affecting the interactions between rod or jet (penetrator) and the two moving plates can be simplified by normalizing in terms of plate thickness to

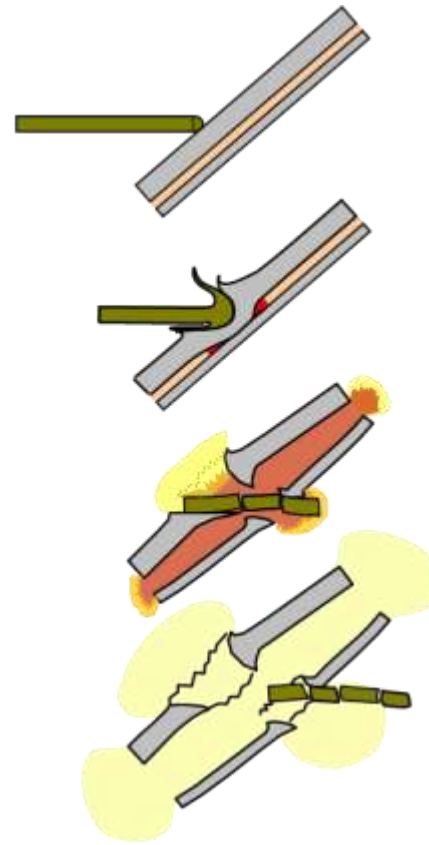


Figure A-11. ERA Plates Ride First One Side Then the Other of the Rod (Source: Silsby [1]).

penetrator diameter (T/D) ratio and plate strength to penetrator strength (KE) or impact pressure (SC). Then geometry and velocities at strike imply effective yaw and kinematics determines the amount of materials involved in the interaction. The plates in RA for the defeat of LRPs must have a considerably larger T/D than are needed for SC defeat because of the much lower impact pressures. Different nations have different emphases on how the two primary antiarmor threats (KE vs. SC) are perceived, and hence reactive armor (RA) packages may vary considerably among designs [10].

Quite small amounts of explosives can really toss around large plates. Initially we would frequently find a 2-ft × 4-ft piece of plate several hundred feet behind the target stand, stuck edge-on nearly full length into the mucky ground. This violent response would not be acceptable

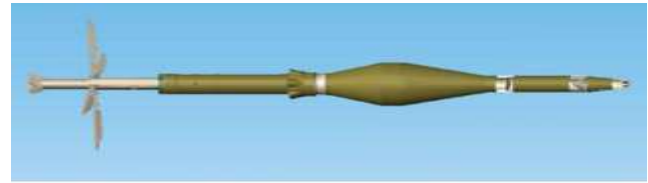
in a real application, so the recipe was changed to keep the flyer plates confined inside the module when hit. Once the RA flyer plates strike something such as the cover or rear of the box, their travel is arrested and the RA loses its weight effectiveness [10].

The practicalities of current RA design are to select an appropriately insensitive energetic material (or inert material) and optimize the explosive thickness and the plate thicknesses and obliquity based on expected plate velocity and geometry available for the module, given a threat velocity and diameter. The plates or explosives do not have to be of uniform thickness. According to McLeod, the Russians in particular have offered several generations of their own ERA designs effective against LRPs, at least one of which has a variable thickness charge that causes favorable plate rotation [10].

Note that when a detonation sweeps a plate sandwich, the passing detonation front imparts an impulse to the plates, after which the trapped gases accelerate them further. While it looks like the plate deforms in bending along a plastic hinge moving with the detonation front, it is really bent in shear to the Gurney fly-off angle (See Chapter 9). Furthermore, due to venting explosive gases at the edges, the edges of the plate do not accelerate up to their full Gurney velocity [10].

A.9 THE TANDEM SC

The tandem SC warhead obviates the need for a gun system so accurate and so sophisticated that it could hit the same spot on a target within fractions of a second to defeat RA. In this warhead, a small tickler charge is mounted well ahead of the main charge or slightly off axis. The main charge is shielded from the blast and fragments of the tickler charge and the timing is adjusted (Figure A-12).



Solidworks™ rendition shown in flight configuration. Tip fuze, tip charge liner, and shield are shown in cutaway sections.

Figure A-12. Typical Tandem SC RPG (Source: Silsby [1]).

Actually, the real development was not much more complex than that. Some tandem rounds for the RPG launcher look as if the designer replaced the forward aerodynamic fairing that provided the standoff for the main charge with an adapter that mounted a long hollow spike out front and put a small SC warhead in it a bit back from a piezoelectric impact fuze on the tip of the round.

There are only a few clues that real engineering was involved. In one instance, there is a blunt conical disc between the tip charge and the main charge (rear-most cutaway). It is thick enough that it cannot be perforated by debris from the tip charge. It is in such a location that the rearward velocity that it picks up from the detonation of the tip charge causes it to hit a second piezoelectric fuze (not visible) that sets off the main charge at the appropriate delay time.

A.10 OTHER ARMOR CONCEPTS

There are several fielded or promising armor concepts that can be discussed, for instance, active protection systems. Active protection systems work by detecting, classifying, tracking, and targeting incoming threats, which in the case of AFVs are AT guided or unguided missiles and gun-launched AT LRPs. It was the rapid evolution of the personal computer that enabled this technology. Success is still limited by the time needed, so that faster threats such as LRPs may still be able to slip

through. There are some open-literature works on electromagnetic armor, primarily Russian. In this concept, a pair of well-separated conductive plates is connected to a suitable capacitor bank. When an SC jet shorts the plates, current flows, heating the jet and softening it, while the induced magnetic field tends to burst the jet radially, dispersing it. This technology has the added advantage of being passive.

A.11 OTHER AMMUNITION CONCEPTS

Of course, evolving armor drives advances in the suite of antiarmor ammunition carried by a tank. As well, the evolving antiarmor threat spectrum has given rise to several other rounds for the tank main gun. Currently, the U.S. stocks a number of rounds for the 120 mm cannon on the M1 tank. The M830A1 Multi-Purpose AT (HEAT) round is a variant of the German DM12 round (HEAT with a fragmenting casing) fuzed for a multipurpose (MP) role, including counter-helicopter [11]. With the MP fuze replaced by a hardened nose and time-delay fuzing, the M830A1 HEAT round becomes the M908 obstacle-defeating round. The M829 is a DU KE LRP round. The M1028 canister round provides a good antimateriel/antipersonnel capability. A HEAT-TP-T and a KE-TP-T training round complete the inventory. Several other (smart) rounds are in various stages of development. Some foreign systems now or in the past might include antimateriel (flechette) or HE rounds and possibly a white phosphorous round, which have also been used as antipersonnel rounds.

A.12 CONCLUSION

The increasing understanding of the physics of penetration mechanics and the application of that understanding to design have resulted in advances in more weight-efficient armors. Mass, momentum, and energy are still conserved, however, so that one should

not lose track of where the spent material is headed after any particular penetrator-armor interaction, to avoid such embarrassments as successfully ricocheting an LRP off of an upper glacis, only to have it drive deep into the turret ring, destroying the tank. It is always cheaper and easier to apply new technology to threat munitions than to their targets, so that modern tanks and other AFVs still remain ponderous and not well-suited for evolving threat conditions. Computational methods have evolved to the point where they can be routinely used to eliminate a lot of testing, providing that the analyst periodically performs reality checks. Testing will always remain necessary to expose new physical phenomenon and to verify intended performance.

Cost is always a driver, so steel will remain the primary material selected for armor elements. Where performance is at a premium, as in personal protection, continued advances in materials technology will result in the introduction of tougher ceramics, better properties for lighter metals such as alloys of aluminum, titanium, and magnesium, and cheaper and better-performing composites. Wherever possible, the armor function should be built into the **vehicle's structural components**, and components such as engines, transmissions, and fuel should be used as armor.

A.13 APPENDIX A REFERENCES

- [1] Silsby, G. F. "Penetration Mechanics of Anti-Armor Kinetic Energy Penetrators." Self-published lecture hand-outs primarily for Baldini Resource Associates, 1987, 2004, and 2010.
- [2] Wikipedia. "Anti-Tank Rifles." https://en.wikipedia.org/Anti-tank_rifle, accessed 24 September 2020.
- [3] Walter, K. "Shaped Charges Pierce the Toughest Targets." Lawrence Livermore National Laboratory's *Science and Technology Review*, Research Highlights, June 1998. http://www.llnl.gov/str/pdfs/06_98.3.pdf, accessed 2 March 2007.
- [4] Wikipedia. "High-Explosive Squash Head." https://en.wikipedia.org/wiki/High-explosive_squash_head, accessed 7 November 2013.
- [5] U.S. Army Material Command. *Logistics. Complete Round Charts. Artillery Ammunition*. AMC Pamphlet AMC-P-700-3-3, Alexandria, VA, 30 November 1985. From Federation of American Scientists' archived copy at http://www.fas.org/man/dod-01/sys/land/docs/p700_3_3.pdf, accessed 7 December 2013.
- [6] MECAR, Inc. http://www.mecar.be/content.php?langue=english&cle_menus=11568-56627, © 2015, MECAR Inc., accessed 28 January 2015.
- [7] Wikipedia. "Challenger 2." https://en.wikipedia.org/wiki/Challenger_2, accessed 7 November 2013.
- [8] Shedd, J. A. *Salt From My Attic*. Mosher Press, 1928.
- [9] Department of Defense. <http://www.defenselink.mil/photos/newsphoto.aspx?newsphotoid=5657>, 30 October 2004 by Staff Sgt. Shane A. Cuomo, U.S. Air Force, accessed 23 April 2015.
- [10] McLeod, R. *Modern Explosive Reactive Armours*, © 1998 by Robb McLeod, reproduced in an abridged form by permission in <http://armor.kiev.ua/fofanov/Tanks/EQP/era.html>, accessed 30 March 2007.
- [11] Wikipedia. "Rheinmetall Rh-12." https://en.wikipedia.org/wiki/Rheinmetall_120_mm_gun, accessed 12 December 2013.

APPENDIX B. ACRONYMS AND ABBREVIATIONS

ACRONYM/ ABBREVIATION	DEFINITION	ACRONYM/ ABBREVIATION	DEFINITION
2-D	Two-Dimensional	HVAP	Hypervelocity Armor-Piercing
AAV	Amphibious Assault Vehicle	HVAPDS	Hypervelocity Armor-Piercing Discarding Sabot
AFV	Armored Fighting Vehicle	IAC	Information Analysis Center
AISI	American Iron and Steel Institute	ITLX	Initiating Thin Layer Explosive
AP	Armor-Piercing	KE	Kinetic Energy
APC	Armored Personnel Carrier	LANL	Los Alamos National Laboratory
APFSDS	Armor-Piercing Fin-Stabilized Discarding Sabot	LOS	Line-of-Sight
APG	Aberdeen Proving Ground	LRP	Long-Rod Penetrator
ARL	U.S. Army Research Laboratory	MBT	Main Battle Tank
AT	Antitank	NC	Nitrocellulose
ATGM	Antitank Guided Missile	NG	Nitroglycerine
BRL	Ballistic Research Laboratory	PHERMEX	Pulsed High-Energy Radiographic Machine Emitting X-Rays
CE	Chemical Energy	RA	Reactive Armor
DoD	Department of Defense	RDX	Cyclotrimethylenetrinitramine
DoE	Department of Energy	RHA	Rolled Homogeneous Armor
DSIAC	Defense Systems Information Analysis Center	SC	Shaped Charge
DU	Depleted Uranium	SCC	Stress Corrosion Cracking
EFP	Explosively Formed Penetrator	TLX	Thin Layer Explosive
HE	High Explosive	TNT	Trinitrotoluene
HEAT	High-Explosive Antitank	WA	Tungsten Alloy
HELP	Hydrodynamic Elastic-Plastic	WHA	Tungsten Heavy Alloy
HEP	High-Explosive Plastic	WMRD	Weapons and Materials Research Directorate
HHA	High-Hard Armor	WWI	World War I
HMMWV	High-Mobility Multipurpose Wheeled Vehicle	WWII	World War II
HMX	Cyclotetramethylene-tetranitramine		

FIGHTING VEHICLE ARMOR AND ANTIARMOR MUNITIONS

By Graham F. Silsby and Dr. Andrew Dietrich



Defense Systems
Information Analysis Center

DSIAC MONOGRAPH 2021-1340

DISTRIBUTION STATEMENT A

*Approved for public release:
distribution unlimited.*